

**Microplastics in the Aquatic Environment: Developing a  
Reliable and Rapid Holistic Analytical Process for  
Monitoring Microplastics in Wastewater Treatment Plant  
Effluents**

Mohammed Salih Mahdi Al-Azzawi

Vollständiger Abdruck der von der TUM School of Engineering and Design der Technischen Universität München zur Erlangung eines Doktors der Ingenieurwissenschaften genehmigten Dissertation.

Vorsitz: *Prof. Dr.-Ing. Markus Disse*

Prüfer\*innen der Dissertation:

1. Prof. Dr.-Ing. Jörg E. Drewes
2. Prof. Dr.-Ing. Martin Jekel
3. apl. Prof. Dr. rer. nat. habil. Brigitte Helmreich

Die Dissertation wurde am 12.07.2022 bei der Technischen Universität München eingereicht und durch die TUM School of Engineering and Design am 25.11.2022 angenommen.

## *Abstract*

Due to the continuing accumulation of microplastics in the environment, as well as their potential health risks, the monitoring of microplastics in various environmental samples is an area of rapidly growing interest. There are three main steps associated with any microplastic monitoring effort: Sampling, sample preparation, and sample analysis. Due to the lack of standardized or harmonized procedures, a comparison of results from different studies is very difficult or often impossible to carry out. The objective of this dissertation was to validate and standardize all three steps for monitoring microplastics in wastewater treatment plants (WWTPs) effluents. First, different sampling methods were explored and a field study regarding sampling secondary and tertiary effluents from three wastewater treatment plants using a pressure driven cascade filtration system was employed and its advantages investigated. Moreover, sample preparation methods were optimized and validated for microplastics with sizes  $\geq 80 \mu\text{m}$  first, and later validated further for small microplastics ( $\leq 10 \mu\text{m}$ ). Sample analysis with a focus on the benefits and limitations as well as the synergies of thermoanalytical and spectroscopic methods were also investigated in a second field study. Finally, an optimized, fluorescence-based sample analysis method was proposed. This technique can either be used as standalone method or as a rapid screening/complementary tool for spectroscopic or thermoanalytical methods, depending on the information and accuracy required. The utilization of a cascade filtration system for sampling enabled the successful collection of representative samples consisting of multiple cubic meters of water. This, when coupled with Thermal extraction - desorption gas chromatography coupled with mass spectrometry (TED-GC/MS), provided a fast and accurate mass concentration for microplastics in WWTPs effluents that can be used to provide mass balance applications for modeling and regulatory purposes. Moreover, Fenton and hydrogen peroxide-based protocols for sample preparation were successfully developed and validated. Both protocols led to a near complete removal of the organic matrix contained in wastewater, while not having significant adverse effect on microplastics, down to  $1 \mu\text{m}$ . When sample preparation was combined with a spectroscopic analysis like Micro-Fourier-transform infrared spectroscopy ( $\mu\text{FTIR}$ ) or Raman micro-spectroscopy ( $\mu\text{Raman}$ ), it provided clean samples with low interference from the environmental matrix. Further, a best

practice guideline regarding all three steps was successfully developed, based on considering field experience and a comprehensive literature review. This also outlined the synergies and limitations of spectroscopic and thermoanalytical analytical methods. Finally, the development of the Nile red fluorescence-based analysis showed very low interference potential down to 40  $\mu\text{m}$  in a sludge sample with 95% of the natural particles falling below that size. To summarize, a holistic approach for the analytical process for monitoring microplastics in WWTPs effluents was discussed in this study, with guidelines for a standardized and effective workflow for the three steps required as part of the monitoring process of microplastics in the environment: sampling, sample preparation and sample analysis.

## *Acknowledgement*

This PhD project would not be possible without the help and support of many, many people. I especially would like to thank my direct supervisor Prof. Dr.-Ing. Jörg E. Drewes for his continuing support as well as the brilliant management of the project. I also like to extend my gratitude to the other members of my scientific committee, namely Prof. Dr.-Ing. Martin Jekel and Prof. Dr. Brigitte Helmreich, who took the time to support me and provided valuable critique when I needed it most.

I especially want to express my gratitude to my mentor, Dr. Oliver Knoop whom without his constant support, both scientifically and emotionally, I would not be finishing this PhD with any sort of success. Another person who deserves high praise is Dr. Christian Wurzbacher who always welcomed my strange microscopy and filtration related questions with open arms and helped me massively.

I also would like to thank the assortment of students I had throughout these 3.5 years long journey; Mohammad Javad Ahmadi, Nwankwo Joseph Nnamdi, Sami Fanger, Simran Chauhan, Jonas Schmidt, and Kristina Mraz. You guys made many of the experiments possible and helped me finish the PhD on time.

My deepest gratitude goes to all of the co-authors who helped me with the publications, Matin Funck, Simone Kefer, Julia Reichel, Jana Weißer, Christoph Schwaller, Aylin Yildirim, Elisabeth Von der Esch, Kristina Mraz, Oliver Jacob, Dr. Korbinian P. Freier, Dr. Marco Kunaschk, Dr. Karl Glas, Dr. Jochen Tuerk, Dr. Oliver Knop, Dr. Natalia P. Ivleva, Prof. Dr. Martin Elsner, Prof. Dr.-Ing. Jörg E. Drewes, and Prof. Dr. Torsten C. Schmidt. The work we together did on those publications would not have been possible, or half as engaging and fulfilling, if it wasn't for your contributions and support.

For funding and supporting the projects I took parts in, I would like to express my gratitude to the Federal Ministry of Education and Research (BMBF) within the framework of the project 'SubµTrack: Tracking of (Sub)Microplastics of Different Identities - Innovative Analysis Tools for Toxicological and Process Evaluation'. Also, the Bavarian research foundation as part of the project (MiPAq: Microparticles in the aquatic environment and in food - are biodegradable polymers a possible solution to the "microplastic problem"?). I would also like to thank all the project partners from both of these projects for the valuable insights and the interesting work they presented to advance the state of knowledge in such a short time in this relatively new field.

My time at the chair has been wonderful thanks to the great work atmosphere and the friendliness of everyone at the chair, Dr. Konrad Koch, Dr. Uwe Hübner, and Prof. Dr. Brigitte Helmreich all deserve special thanks for all their advice and support throughout the past 6.5 years cross both my Master and PhD studies.

Another large piece of thanks goes to the wonderful staff at the chair, Myriam Reif, Wolfgang Schröder, Susanne Petz, Andrea Vogel, Heidrun Mayrhofer, Ursula

Wallentits, Klaus Lindenblatt and Hubert Moosrainer. Also, a special thanks to Susanne Weißler and Marianne Lochner for their constant help to all my administrative questions.

A big special thank you to Dr. Daphne Keilmann-Gondhalekar who is the gentlest soul I have ever met and has helped me a lot to believe in myself and improve throughout both the master and PhD.

Finally, a word of thanks to my friends and colleagues at the chair who made the PhD journey a lot more tolerable, especially in those all too familiar phases of self-doubt and desperation that every PhD student inevitably gets! Special shoutout to Katrin Stür-Patowsky, Millaray Sierra Olea, Nebojša Ilić, Julia Reichel, and Carolina Feickert Fenske.

## Contents

1. Introduction and state-of-the-art .....	1
1.1. Background and problem definition.....	1
1.1.1. Sampling.....	2
1.1.2. Sample preparation .....	4
1.1.3. Sample analysis.....	7
1.1.4. Examples .....	9
1.2. State-of-the-art.....	12
1.2.1. Sampling.....	12
1.2.2. Sample preparation .....	13
1.2.3. Sample analysis.....	17
2. Research objectives and hypotheses.....	25
3. State-of-the-art sampling of tertiary sand filter effluents .....	30
3.1. Introduction .....	31
3.2. Materials and Methods.....	32
3.2.1. Sample collection system and sampling procedure .....	32
3.2.2. Investigated wastewater treatment plants (WWTP) .....	34
3.2.3. Sample preparation and contamination prevention.....	35
3.2.3. Analytical Method .....	36
3.2.4. Polymer Calibration and process blanks.....	37
3.3. Results and Discussions .....	37
3.3.1. Polymer concentration reduction by sand filters .....	37
3.3.2. Comparison of polymer retention at the three WWTPs.....	40
3.4. Conclusion .....	42
4. Sample preparation methods .....	44
4.1. Sample preparation for microplastic particles .....	44
4.1.1. Introduction .....	45

4.1.2. Materials and Methods.....	50
4.1.3. Results and discussion .....	59
4.1.4. Conclusion .....	71
4.2. Sample preparation for sub-microplastics .....	73
4.2.1. Introduction .....	74
4.2.2. Methodology .....	76
4.2.3. Results and discussion .....	81
4.2.4. Conclusion .....	85
5. Sample analysis .....	87
5.1. Microplastic analysis methods and development of state-of-the-art protocols	87
5.1.1. Introduction .....	89
5.1.2. Materials and methods of the case study: Microplastics in Tertiary Sand Filter Effluents.....	94
5.1.3. Results and discussion .....	98
5.1.4. Conclusion .....	106
5.2 Developing a rapid microplastic analysis technique inside wastewater samples using fluorescence staining.....	108
5.2.1. Introduction .....	109
5.2.2. Materials and Methods.....	110
5.2.3. Results and Discussion.....	120
5.2.4. Conclusion .....	127
6. Research outcome and discussion.....	129
7. Research outlook .....	136
8. References .....	139
9. Appendix .....	157
9.1. Supplementary Material for Chapter 3 .....	157
9.1.1. <i>Sampling Volumes</i> .....	157
9.1.2. <i>Volumes extracted from basket filters and aliquots</i> .....	158

9.1.3. <i>Polymer calibrations</i> .....	160
9.1.4. <i>Sample filtration and processing</i> .....	162
9.2. <i>Appendix A (Appendix for Chapter 4.1)</i> .....	166
9.3. <i>Supplementary Material for Chapter 4.1</i> .....	175
9.3.1. <i>Protocols investigated in the study</i> .....	175
9.3.2. <i>Polymers investigated and their characteristics</i> .....	181
9.3.3. <i>Results from TD-Pyr-GC-MS</i> .....	182
9.3.4. <i>Images from microscopy</i> .....	184
9.3.5. <i><math>\mu</math>FTIR spectra before and after chemical treatments</i> .....	188
9.3.6. <i>Size distribution analysis</i> .....	191
9.3.7. <i>Pre-experiments of Organic matter removal efficiency</i> .....	195
9.4. <i>Supplementary material for Chapter 4.2</i> .....	196
9.4.1. <i>Fenton Protocol</i> .....	196
9.4.2. <i>Exposure times used for fluorescence microscopy</i> .....	196
9.4.3. <i>Thresholding the grey values for segmentation</i> .....	197
9.4.4. <i>Fluorescence spectroscopy images and resulting size distributions</i> .....	198
9.5. <i>Supplementary Material for Chapter 5.1</i> .....	204
9.5.1. <i>Sampling campaign information</i> .....	204
9.5.2. <i>Aliquot information</i> .....	205
9.5.3. <i>Sample preparation for spectroscopic analysis: Fenton</i> .....	207
9.5.4. <i><math>\mu</math>FTIR analysis</i> .....	208
9.5.5. <i><math>\mu</math>Raman analysis</i> .....	209
9.5.6. <i>Sample preparation for TED-GC-MS</i> .....	210
9.5.7. <i>TED-GC-MS analysis</i> .....	210
9.5.8. <i>TED-GC-MS calibration and quality control samples</i> .....	211
9.5.9. <i>Polymer identification</i> .....	213
9.5.10. <i>Basket filter sieve integrity evaluation</i> .....	218



9.5.11. <i>Picture of algae in extracted samples</i> .....	219
9.5.12. <i>Reduced flow sampling campaign</i> .....	219
9.5.13. <i>Complementary results from spectroscopic analyses</i> .....	220
9.6. <i>Supplementary material for Chapter 5.2</i> .....	222
9.6.1. <i>Staining protocol development</i> .....	222
9.6.2. <i>Workflow protocol optimizations</i> .....	224
9.6.3. <i>Code used to analyze the brightness of particles using ImageJ</i> .....	228
9.6.4. <i>Image of polymer controls using the final workflow</i> .....	228
9.6.5. <i>Examples of <math>\mu</math>FTIR spectra</i> .....	232

### List of figures

Figure 1. Overview of the main analytical techniques used in this study and the information and limitations of each. ....	24
Figure 2. Overview of the research objectives, the associated hypotheses, tasks, and papers. ....	29
Figure 3. A: Scheme of the cascadic microplastic sampling system B: Picture of the cascadic microplastic sampling system onsite. ....	33
Figure 4: TED-GC-MS results of PE, PS, PP and PET concentration in samples before the sand filter (B.SF.) and after the sand filter (A.SF.).....	38
Figure 5: TED-GC-MS results of PE, PS, PP and PET obtained from WWTP B. The bar plots show the respective polymer concentration in samples before the sand filter (B.SF.) and after the sand filter (A.SF.).....	39
Figure 6. Left: The normalized emitted annual polymer load ( $\text{mg yr}^{-1} \text{ P.E.}^{-1}$ ) for each WWTP. Right: Total annual emitted polymer load.....	40
Figure 7. Workflows of the three selected protocols for processing microplastics from wastewater sludge samples. ....	51
Figure 8. The workflow used in this study for investigating the organic matter removal efficiency. ....	58
Figure 9. Visual difference between type I & II Fenton reactions (end of reaction). A: type II that failed to initialize boiling. B: type II which initialized boiling. C: type I. ....	62
Figure 10. Differences between type I Fenton reaction and a type II Fenton reaction that failed to initialize boiling when digesting a piece of tissue paper. A, C: type II before and after reaction. B, D: type I before and after reaction.....	62
Figure 11. Size distribution analysis for PLA, the green area represents the smallest 10 <sup>th</sup> percent (d10).....	65
Figure 12. Relative particle size changes after treatment compared to the controls (for weighted average sizes & 10 <sup>th</sup> percentiles (d10)).....	65
Figure 13. Relative particle size changes after temperature treatments compared to controls (for weighted average sizes & 10 <sup>th</sup> percentiles (d10)).....	66

Figure 14. Normalized FTIR spectra of reference PET particles. Top: measured in reflectance mode on FTIR microscope; bottom: measured in ATR mode .....	68
Figure 15. The end result of the gravimetric analysis done on 2 mL of sludge. A: dried sludge (surrogate) B: dried retentate and filter after hydrogen peroxide treatment, C: dried retentate and filter after Fenton treatment. ....	71
Figure 16. The relative changes of the average sizes compared to the respective control samples. ....	83
Figure 17. Size distribution of PLA for the three sample types. The values are presented as a ratio to circumvent the difference in particle count between the samples. ....	84
Figure 18. Three samples of PP under the fluorescence microscope with x400 magnification. ....	85
Figure 19. Process flow chart for microplastic sampling and analysis with the most important considerations and recommendations for every step. ....	90
Figure 20: Schematic and picture of the cascadic filtration .....	95
Figure 21. Results of the analysis for a WWTP. The influent for the sand filter was taken before an operational abnormality occurred, whereas the effluents of the sand filter were taken during the abnormality. ....	100
Figure 22. FTIR and TED-GC-MS results for an 8-hour volume proportional sampling at a WWTP in 2020. ....	102
Figure 23. Size distribution of the detected particles (100 $\mu\text{m}$ , 50 $\mu\text{m}$ via $\mu\text{FTIR}$ and 10 $\mu\text{m}$ via $\mu\text{Raman}$ ) from the sieve fractioning. ....	103
Figure 24. Schematic of the experimental plan to develop a final workflow to detect microplastics within environmental samples. ....	117
Figure 25. Non-spiked sludge sample image of the background fluorescence brightness for the workflows: A. No post-treatment: Sample $\rightarrow$ Fenton $\rightarrow$ NR staining, and B. with post-treatment using the best performing workflow: Sample $\rightarrow$ Fenton $\rightarrow$ NR staining $\rightarrow$ NaClO (30 minutes). ....	122
Figure 26. Comparison of microplastic brightness after applying NR staining (MP+NR) and after applying the final workflow (MP+NR+NaClO). Particle brightness are sorted	

from largest to smallest. Note that Fenton is not included in the workflow here as discussed above. .... 123

Figure 27. Comparison of controls, mixed samples and sludge blanks for particles >40  $\mu\text{m}$  (left side), >25  $\mu\text{m}$  (middle), and >10  $\mu\text{m}$  (right side). .... 124

Figure 28. Comparison images of A: non-spike sludge (blank), B: polymer mix (Control), and C: Spiked sludge samples. All samples were treated with the same workflow (Sample  $\rightarrow$  Fenton  $\rightarrow$  NR  $\rightarrow$  NaClO 30 min). .... 125

Figure 29. Comparison of PE-spiked samples and blanks for particles >40  $\mu\text{m}$  (left side), >25  $\mu\text{m}$  (middle), and >10  $\mu\text{m}$  (right side). .... 126

Figure 30. Comparison images of A: non-spike sludge (blank) and B: PE-spiked sludge sample. All samples were treated with the final workflow 'Sample  $\rightarrow$  Fenton  $\rightarrow$  NR  $\rightarrow$  NaClO 30 min'. .... 126

Figure 31. Micrograph of PS particles of different sizes (100 nm, 750 nm, and 1.4  $\mu\text{m}$ ). A. Control, B. after Fenton, C. after hydrogen peroxide. Micrograph courtesy of M.Sc. Kevin Guerrero from IUTA..... 137

## List of tables

Table 1. Overview of the methods used to sample WWTP effluents and the potential pitfalls. Text marked in red represent a potential error source. ....	10
Table 2. Protocols investigated in this study .....	50
Table 3. Protocols that were investigated for their effects on the polymers.....	54
Table 4. The reaction differences for the five batches of hydrogen peroxide when using 100 mL Erlenmeyer flasks on the rubberized bench. T <sub>max</sub> : maximum temperature. .	60
Table 5. The reaction difference for type I and II Fenton reaction when using 100 mL Erlenmeyer flasks on the aluminum bench for heat dissipation.....	60
Table 6. Influence on the partial pyrolysis of thermal desorption (TD) products at 200 °C for both PA und PS.....	69
Table 7. Average total and corresponding organic removal efficiencies for the investigated protocols.....	70
Table 8. The sample preparation protocols used in this study. For further details, refer to Al-Azzawi et al. [57].....	78
Table 9. The observed values from eight retention evaluations of tertiary sand filters using $\mu$ FTIR and $\mu$ Raman spectroscopy. $\mu$ FTIR results are the sum of the 100 $\mu$ m and 50 $\mu$ m filter, whereas $\mu$ Raman results are from the 10 $\mu$ m filter. The samples marked with (*) were single sand filter cells with a common influent. The influent samples were sampled the day before the effluents could be sampled. This might explain the presence of larger number of smaller particles in the effluents of the cells. For the purposes of using surrogates, however, this should be irrelevant.....	106
Table 10. Workflow development to increase the remaining brightness on PE particles after treatment. RT: room temperature.....	114

## *Abbreviations*

ATR	Attenuated Total Reflection
EM-CCD	Electron Multiplying Charge Coupled Device
FL	Fluorescence
FPA	Focal Plane Array
FTIR	Fourier Transform Infrared
GC/MS	Gas Chromatography Coupled with Mass Spectrometry
HPLC	High Performance Liquid Chromatography
LDPE	Low Density Polyethylene
LWWTP	Laboratory Scale Wastewater Treatment Plant
MALDI-ToF/MS	Matrix-Assisted Laser Desorption/Ionization Time-Of-Flight Mass Spectrometry
NB	Nile Blue
NIR	Near IR Spectroscopy
NR	Nile Red
PA	Polyamide
PC	Polycarbonate
PE	Polyethylene
PET	Polyethylene Terephthalate
PLA	Polylactic Acid
PLE	Pressured Liquid Extraction
PP	Polypropylene
PS	Polystyrene
PVC	Polyvinyl Chloride
Py-GC/MS	Pyrolysis Gas Chromatography Coupled with Mass Spectrometry

SEC	Size Exclusion Chromatography
TD-PTR/MS	Thermal Desorption-Proton Transfer Reaction-Mass Spectrometry
TD-Pyr-GC/MS	Thermal Desorption Pyrolysis Gas Chromatography Coupled with Mass Spectrometry
TDU	Thermal Desorption Unit
TED-GC/MS	Thermal Extraction - Desorption Gas Chromatography Coupled with Mass Spectrometry
TGA	Thermogravimetric Analyzer
UPW	Ultrapure Water
WWTPs	Wastewater Treatment Plants
$\mu$ FTIR	Micro-Fourier-Transform Infrared Spectroscopy
$\mu$ Raman	Raman Micro-Spectroscopy

# 1. Introduction and state-of-the-art

## 1.1. Background and problem definition

According to plastics Europe, in 2020, around ten million tons or 33% of the European post-consumer plastic waste was sent to recycling, with another 40% being incinerated for energy recovery, leaving around seven million tons or 23% of all plastic waste to reach landfills [1]. Globally, the recycling rates are even lower at around 14% [2]. However, the aforementioned numbers deal only with collected consumer waste and not the total plastic produced [3]. For example, the total production of plastics in 2020 in Europe was estimated to be 55 million tons [1]. Which means that the fraction of recycled to produced plastics in Europe is 19% rather than the aforementioned 33%. This could be an indication that the majority of the 367 million tons of globally produced plastics eventually end up in the environment over a longer time period [1]. This low recycling rate, coupled with large production and low environmental degradability for plastics has been leading to plastic waste accumulating in various environments for many decades [4]. There it is subsequently weathered down and broken into smaller and smaller pieces [5]. These small plastic particles formed directly by degradation of larger plastic pieces are referred to as secondary microplastics, whereas microplastics manufactured directly as such are termed primary microplastics [6]. The first studies mentioning marine microplastic contamination in the aquatic environment appeared in the literature in the 1970s. The term microplastic itself appeared for the first time in a study by Thompson et al. in 2004 [7] and is now generally defined as plastic particles which are smaller than 5 mm in size, further classification defines microplastics between 1 – 5 mm as large microplastics and plastic particles smaller than 1 mm as microplastics [8–12]. Due to the continuing accumulation of plastic debris in the environment and the resulting potential toxicity and various health risks to both animal and human life, the subject has gained traction, both in the scientific community and in the public eye, In particular during the last few years [8, 13–16].

Microplastic contamination of aquatic environments can occur via different pathways such as atmospheric deposition and terrestrial discharges, especially from coastal regions as a result of improper plastic disposal [17]. Pabortsava et al. recently shed a light on massive amounts of microplastics hidden deep beneath the ocean surface, which were previously not accounted for and was sometimes referred to in the



literature and the media as the missing plastic debris or missing ocean plastics [17, 18].

One potential point sources for microplastic contamination of aquatic systems are wastewater treatment plants (WWTPs), which despite their high efficiency to remove particulate matter from liquid waste, including microplastics, can still be a significant source for microplastics due to the large quantity of discharged wastewater effluents (secondary or tertiary) as well as the relatively high suspended solids content which might be similar to or higher than natural streams, especially for secondary effluents [19–22].

In order to achieve a holistic protocol for the analytical process of monitoring microplastics in the environment, three steps need to be carried out in sequence: Sampling, sample preparation, and finally sample analysis [22, 23]. Any error introduced in any of these steps, will adversely impact downstream steps, thereby compromising results and preventing comparability within a study or between different studies.

The objective of this dissertation was to investigate and outline the best practices for each of those three steps, which can be used for standardization.

### 1.1.1. Sampling

The first step in the analytical process begins with sampling. Sampling can be seen as a process of mass or volume reduction in order to obtain a manageable amount that can be handled for analysis [24]. A representative sample needs to reflect the characteristics of the entire batch (or in this case, the effluents) as closely as possible. The representativeness of a sample is a question of the total amount collected as well as sampling technique. Sampling errors can be multiple orders of magnitude larger than analytical errors, but this essential part is often overlooked, which can lead to non-representative samples being the cause of erroneous results later, regardless of the kind of analytical techniques used [24].

The main challenge with representative sampling from aqueous samples is the need to simultaneously capture both high sample volumes and smaller sized microplastics to create representative samples [22, 25]. Larger particles are less prevalent in samples when compared to smaller particles, which are much more abundant [26].

Therefore, large sample volumes are needed to capture a representative sample for larger particles, but this often comes at the expense of the minimum sampled particle size. This simultaneous requirement for capturing large volumes and small particles presents challenges for sampling systems. For example, bucket grab samples can only sample a few liters at best, making them unsuitable for representative sampling, whereas meshes and sieves can suffer from cake filtration buildup if the mesh size is too small so as to capture smaller particles, which then limits the total amount of water that can be sampled, thereby inducing over/under-estimation errors for larger particles. Further, different analytical methods require different sampling techniques. Thermoanalytical methods require the concentration of samples in order to detect smaller particles, which possess very little mass despite their abundance [25]. On the other hand, spectroscopic analysis can only analyze a small sub-sample and can suffer from misrepresentation of the sample, depending on the distribution of particles in that sub-sample [23]. Since larger microplastics are less abundant, a sufficiently concentrated sample for the larger particles is necessary when analyzing samples using spectroscopic methods to avoid over or underestimating the microplastic content, thus requiring greater volumes to be collected.

The type and frequency of sampling plays an important role in determining the reliability and replicability of the results. For example, batch or spot sampling is the most common type, but it can be susceptible to misrepresentation due to the heterogeneous nature of wastewater, operational abnormalities or even sampling errors which might render the obtained results non-reproducible [27]. Continuous or composite sampling over longer periods of time (up to 24 hours) can be used instead, usually intermittently over regular intervals of 1-2 hours to give a temporal representative sample [27–29]. However, continuous sampling can be more complicated and difficult to implement than a simple grab sample which typically is collected over 1-3 hours [22, 30]. An alternative solution could be to utilize several random batch samplings at different temporal points to account for heterogeneity as well as outlier events.

Another crucial aspect of sampling is generating field blank samples to quantify the degree of contamination during sampling [26]. Several studies initiated open to atmosphere field blanks in parallel to the main sampling method [23, 31]. However, a

standardized and representative blank sampling protocol is yet to be adopted in literature for microplastic field sampling.

To summarize, sampling is the most crucial step, as nothing can be done to amend a non-representative sample in the next two steps of the analytical process. The main challenge during sampling is the requirement to capture large volumes to collect enough larger microplastics, which occur less frequently than smaller microplastics, as well as the simultaneous capturing of very small microplastics. This can be approached with a sealed cartridge cascade filtration system with various mesh sizes [22, 30, 32]. This filtration system, as well as the need to harmonize the workflow in the field, are still not fully investigated and represent a knowledge gap.

### 1.1.2. Sample preparation

Environmental samples contain many natural constituents which can be either organic or inorganic in nature. Both types of natural constituents can interfere with the analysis of microplastics, either by covering the particles, or interfering with their identifying spectra or pyrograms [26, 33]. Therefore, it is essential in most cases to remove or reduce the organic and inorganic content of complex environmental samples before the analytical step. Sample preparation helps to avoid interference which may lead to under or overestimation of the microplastic content in the sample. This kind of interference occurs even when employing cutting-edge analysis like micro-Fourier-transform infrared spectroscopy ( $\mu$ FTIR) and Raman micro-spectroscopy ( $\mu$ Raman). Both of which can identify microplastics via their spectral fingerprints, a process which can be difficult when there is significant interference from the natural matrix in the sample [26]. Due to the low microplastic content in most environmental samples (<1% wt), removing the natural matrix as much as possible also increases the plastic to non-plastic ratio in the sample [26]. This would aid in increasing the sensitivity of measurements and the statistical significance as a result of being able to analyze larger subsamples due to matrix removal [23, 26, 34].

Unfortunately, there are no standardized sample preparation methods yet, and this is sometimes a completely overlooked aspect of analytical processes for monitoring microplastics in the environment. Due to the lack of standardized and properly validated sample preparation methods, a wide variety of sample preparation protocols

were used in countless studies, making a comparability of their results very difficult or even impossible [33, 35–49].

The natural matrix can be split into two categories: First, natural inorganic constituents, which can be separated from microplastics gravimetrically via density separation by using concentrated salt solutions [33, 42, 50–52]. Second, a matrix like wastewater is rich in natural organic matter, which has a very similar density to microplastics and cannot be effectively removed gravimetrically. Therefore, such organic rich matrices need to be chemically or enzymatically digested, which entails the application of harsh reagents like oxidants (hydrogen peroxide or Fenton reactions), bases (NaOH, KOH), and acids (HCL, H<sub>2</sub>SO<sub>4</sub>, HNO<sub>3</sub>) [33, 35–50]. These chemical reagents might inadvertently alter microplastic particles by affecting important characteristics such as size or functional surface groups, thus undermining the accuracy of the analysis [33].

Studies attempted to validate sample preparation methods to avoid these issues, but those study contained some disadvantages in their methodology, which were specifically avoided in this dissertation. These disadvantages included:

(1) Working exclusively with larger particle sizes (>500 µm), which might not represent the fate of smaller particles, especially size categories which are rapidly growing in importance like small microplastics (≤10 µm) due to the increased surface area to volume ratios [33, 35, 36, 38].

(2) Validating only a small number of particles, thereby reducing the statistical significance of their findings [33, 36, 38, 43, 44].

(3) When validating surface changes via Fourier-transform infrared spectroscopy (FTIR), studies utilized the attenuated total reflection (ATR) mode to document the effects of sample preparation on polymers, as well as to create reference spectra for identifying unknown particles in environmental samples. However, those environmental samples are usually analyzed via µFTIR [33, 35, 43, 50]. These two analysis modes can present different results if the beam penetration depth is not mathematically corrected for and might lead to different results during analysis [53].

(4) Studies lacked harmonization and consistency, especially when it comes to oxidative digestions using Fenton reactions, which have been described very differently between studies. Whereas some studies actively cooled the reaction,

others heated it up [33, 35, 42, 43, 54, 55]. Reaction times for Fenton were also described very differently, ranging from a few minutes to 24 hours [33, 43, 55]. Some of these contradictions are surprising when one considers that Fenton is an exothermic reaction with a diffusion limited reaction rate [56]. Thus, it should be a rapid reaction that does not require external heating. Cooling, when done, is usually to avoid exceeding the thermal threshold of polymers [33]. However, reaction kinetics are known to increase with increasing temperatures. Thus, if the cooling requirements are removed, there might be an opportunity to reduce the required reaction times, while keeping or increasing the organic matter digestion efficiency of the reaction. However, the effects of short-term microplastics exposure to high temperatures under extreme conditions, such as those encountered during a Fenton reaction, have not yet been investigated. Thus, both the inconsistencies and the need for cooling need to be investigated.

Further considerations for sample preparation are the requirements for the analysis technique to be performed, as analytical methods like  $\mu$ FTIR and  $\mu$ Raman or Pyrolysis-Gas Chromatography-Mass Spectrometry (Py-GC/MS) are more susceptible to organic interference than a method like Thermal Extraction-Desorption Gas Chromatography Mass Spectrometry (TED-GC/MS), thereby requiring more strict chemical digestion procedures as part of their sample preparation than the latter [26, 57, 58].

To summarize, some form of sample preparation is necessary for the majority of environmental samples and analytical techniques. However, care must be taken to avoid adversely impacting the microplastic analysis when utilizing chemical digestion methods. This aspect has not yet been harmonized in literature or practice, which can lead to over or under estimation of the microplastic content during the analysis step, as different sample preparation methods have different effectiveness at removing the natural environmental matrix, as well as different tendencies to affect the microplastics being investigated. Also, a method for very small microplastics ( $\leq 10 \mu\text{m}$ ) needs to be developed and validated, as this size range is of growing concerns in the last few years. These are knowledge gaps that need to be addressed and investigated.

### 1.1.3. Sample analysis

Sample analysis is a vital step that is used to analyze the content of microplastic in the processed samples. Sample analysis can be done in several ways, which will be discussed in more details in the next subchapter (1.2.3. Sample analysis). However, each of them provides unique advantages and has their own limitations.

For example, visual sorting can work either by eye for larger microplastic particles, or via optical microscopy, either in transmission or incidence modes, for smaller microplastics. The issue with both of those approaches is the large underlying risk of over or underestimation and the completely different results obtained from the same sample by different operators (operator bias) [26]. This is due to the difficulty in differentiating microplastics from natural particles, even after sample preparation.

To alleviate this limitation, spectroscopic methods like  $\mu$ FTIR and  $\mu$ Raman are used. These methods not only provide a microscopic image of the sample like the previous case, thereby providing information about the size and shape of particles, they additionally provide a chemical identification of the polymers via comparing the measured spectra of particles in the sample against a known database of materials and polymers. This process can also be automated, thereby removing operator bias. The downside to these methods are the cost of the equipment and the long analysis times, as well as the minimum particle size based on the minimum spatial resolution employed [26, 59–62].

Another approach that can identify and quantify microplastics in environmental samples in a somewhat faster fashion is a thermoanalytical approach like Py-GC/MS and TED-GC/MS. These methods do not provide an image of the particles, thus no information regarding size distribution or shape of particles such as the case with microscopic and spectroscopic methods. However, thermoanalytical techniques can provide mass concentrations for each polymer based on the pyrograms obtained from the degradation byproducts of the sample during pyrolysis which are then separated in the gas chromatography (GC) column and analyzed via mass spectrometry (MS) [26]. Thermoanalytical methods can measure particles regardless of minimum size. This does not mean, however, that thermoanalytical analysis can easily measure even nanoplastics, as smaller particles possess a smaller mass according to the cubic law, which makes detecting them nearly impossible without a suitable method to

concentrate the small particles from the sample. Thermoanalytical methods are also affected by the fact that the existence of several larger, heavier particles can easily overshadow the presence of many smaller, lighter particles [26]. Furthermore, thermoanalytical methods, unlike microscopic and spectroscopic methods, are destructive [63].

Due to the different kind of information that can be obtained via spectroscopic and thermoanalytical methods, their results are not directly comparable. Several studies attempted workarounds to facilitate this comparison. Such workarounds included estimating the mass of the polymers based on spectroscopic images of the sample [64, 65]. Estimating mass using spectroscopic images has been tested and validated in literature and is prone to large errors due to estimating a mass (3-D) based on a 2-D image of the particles [64–67]. The resulting error ranged from overestimation by a factor of 6 or underestimation by a factor of 10 [67]. Even finely optimized estimation methods still had an error factor of 3 when compared directly to the Py-GC/MS results [67]. Similarly, attempting to approximate the size of analyzed microplastics by using a cascade filtration sampling device with a thermoanalytical method is proposed [22, 68, 69]. However, this workaround is likely only a very rough estimate but has not yet been validated for its accuracy.

There are more workarounds that are used to overcome the practical challenges during sample analysis. For instance, spectroscopic techniques such as  $\mu$ FTIR and  $\mu$ Raman require relatively long analysis times, ranging from hours for  $\mu$ FTIR to days with  $\mu$ Raman when scanning environmental samples [61, 62]. This forces researchers to utilize time saving measures such as smaller sample aliquots and partial filter scans, or even using regular microscopy plus selective particle scan with spectroscopic techniques to identify what is considered suspect particles [19, 60, 70–72]. Both workarounds might deliver non-representative data; partial filter scans could misrepresent the sample due to inhomogenous distribution of particles, whereas selective spectroscopic scans of suspicious particles are subject to operator bias and a large over- or underestimation of the results [26, 68].

As a possible alternative to costly and time consuming spectroscopic methods, some studies investigated the potential to tag microplastic particles with selective fluorescence dyes such as Nile Red (NR), both as isolated particles as well as mixed in sediments and biological samples [51, 73–82]. This should in theory have a higher

reliability than regular microscopy due to the use of selectively absorbing dyes, while at the same time being faster and more affordable than spectroscopic methods. However, almost no study attempted this for wastewater samples, which are very complex due to the variable nature of their natural organic matrix. Shim et al. [76] even mentioned how fluorescence dyeing of environmental samples that contain organic matter can be challenging due to the accidental co-dyeing of the natural organic matter, causing interferences and impeding analysis. Only a recent study by Nguyen et al. [83] investigated wastewater samples using several analytical techniques including fluorescence spectroscopy. However, this study was not focused on fluorescence analysis, thus, no comprehensive fluorescence results were presented there.

To summarize, only reliable analytical techniques that can identify the polymers' chemical signatures should ideally be used. This is then coupled with automation to remove operator bias as much as possible. Furthermore, the differences between the analytical techniques in terms of obtained information (particle number, size, mass...etc.), as well as the sampling and sample preparation requirements make comparing results from different studies very difficult. The inherent differences also necessitates that the analytical technique must be carefully selected and planned beforehand as part of the research question [26]. The workarounds proposed in literature to circumvent these differences also need to be investigated and if possible, validated. Finally, there is the possibility to utilize cost-effective alternatives such as selective dyeing and fluorescence microscopy to identify microplastics within environmental samples. However, this has not been thoroughly tested and it can be prone to similar pitfalls as regular microscopy if not properly validated for the intended environmental matrix type. There are currently no studies that have validated fluorescence microscopy-based techniques for wastewater matrices, which needs to be addressed and investigated.

#### 1.1.4. Examples

To provide concrete examples on aforementioned challenges and errors during sampling, sample preparation and sample analysis, an overview of studies that attempted to monitor secondary and tertiary effluents from WWTP and their utilized methods is provided in Table 1. Potential sources of errors are highlighted in bold red.



Table 1. Overview of the methods used to sample WWTP effluents and the potential pitfalls. Text marked in red represent a potential error source.

Study	Mp conc. In secondary/tertiary effluents	Sampling		Sample preparation	Sample analysis
		Sampled method & volumes [l]	Mesh size [µm]		
Carr et al. 2016 [19]	0.0002 MP/L Secondary	Stacked sieves 5680 L	180 - 480	Density separation	Optical microscopy
Ziajahromi et al. 2017 [20]	0.48 MP/L Secondary	Stacked sieves 27 – 150 L	25 - 500	Density separation + H <sub>2</sub> O <sub>2</sub> (30%)	Optical microscopy + selective FTIR
Marlies et al. 2016 [21]	5.9 MP/L Secondary	Stacked sieves 10 – 20 L	20- 4750	None	Optical microscopy
Liu et al. 2019 [84]	28.4 MP/L Secondary	Single sieve 3 x 10 L	47	H <sub>2</sub> O <sub>2</sub> (30%)	Optical microscopy + selective Raman
Hidayaturrahman-et al (2019) [85]	164-1444 MP/L secondary 33-297 MP/L tertiary	Grab sample 2 L	None	H <sub>2</sub> O <sub>2</sub> (30%)	Optical microscopy
Talvite et al. (2017) [86]	0.7 MP/L Secondary 0.02 MP/L tertiary	Stacked sieves 4 – 1000 L	20 - 330	None	Optical microscopy + selective FTIR
Bayo et al. (2020) [87]	1.08 MP/L tertiary	Grab 72 L	None	None	Optical microscopy + selective FTIR
Mason et al. (2016) [88]	0.05 MP/L secondary	Stacked sieves 500-21000 L	125, 355	Fenton	Optical microscopy

Ben-david et al. (2020) [89]	7.3 MP/L Tertiary	Stacked sieves <b>10-100 L</b>	0.45 - 425	Fenton	<b>Optical microscopy + select particles with SEM and Raman</b>
Michielssen et al. (2016) [21]	2.6 MP/L	Grab <b>≤38 L</b>	<b>None</b>	<b>None</b>	<b>Optical microscopy</b>
Simon et al (2018) [65]	19-447 MP/L <b>0.5 - 12 µg/L</b>	<b>Single sieve 4 - 82 L</b>	10 µm	Fenton	µFTIR

The common mistakes made during the investigations are noted in Table 1; some studies gathered too little sample volume to gain representative results [20, 21, 65, 84, 85, 87]. Other studies utilized large mesh sieves, which for the most part do not collect the smaller fractions of microplastics which represent the majority of microplastics in terms of numbers [19, 84, 88]. Several of these studies listed ignored the requirement to remove the organic matrix via a proper sample preparation method. This will severely limit the provision of a proper sample for WWTP effluents, especially when employing microscopic and spectroscopic analytical techniques [19, 21, 86, 87].

Moreover, the vast majority of those studies relied solely either on optical microscopy or utilized optical microscopy with selective spectroscopic analysis (µFTIR, µRaman) for selected suspect particles that the operator could not confidently identify [19–21, 84–89]. This approach is very prone to error and should be avoided, as microscopy does not provide any information on the chemical composition. The reliance on human operator for determination of microplastic from an environmental matrix or which particles to analyze via spectroscopy is also an inherent weakness of this method, made only worse if the sample was not properly treated with a digestive sample preparation protocol. Finally, Simon et al. presented mass estimations for microplastic emissions from Danish WWTP to be around 0.56 g/PE, despite using only µFTIR for the analysis, which is a highly error prone workaround as discussed previously [65].

## 1.2. State-of-the-art

### 1.2.1. Sampling

For microplastic investigations in the aquatic environments, there is a lack of harmonized sampling techniques. Especially for aqueous samples, where a wide variety of different sampling techniques were implemented and tested. The focus in this dissertation was placed on aqueous samples, specifically treated WWTPs effluents. The main factors to be considered are the desired sample volume and expected microplastic content, particle size of interest and particular matrix composition. Due to the lack of standardization, many studies exist that established their own sampling devices and protocols [19–22, 84, 85, 87–93]. For example, studies dealing with limnic and marine systems down to a maximum water depth of 0.5 m used various types of nets (manta, plankton, neuston and bongo nets) [22, 52, 94]. The nets concentrate microplastics in-situ, leading to more accurate and representative results [95]. Mesh openings used were usually 333  $\mu\text{m}$  but studies have used a variety of meshes ranging from 50 to 3,000  $\mu\text{m}$  [22, 52, 96–100]. The reason to use larger mesh sizes is to avoid rapid net clogging [52]. However, this could lead to a large underestimation of microplastic content as smaller particles are vastly more abundant than larger particles [101]. For the surface layer, NG et al. collected the upper micro-layer of surface water via using a rotating drum and surface tension [102].

Similarly for studies dealing with wastewater sampling, a variety of sampling devices were used, ranging from a grab sample using a bucket [21, 85], to a pump driven system with a single mesh with defined opening [90], or a stack of filters with decreasing mesh sizes [19, 88, 93]. Another method which is used to increase the amount of collected water, is to employ a sealed system of cartridge filters under pressures, either as a single cartridge filter [91], or a multistage cascade filtration assembly with decreasing mesh sizes [94]. The benefit of this method is the simultaneous gathering of large sampling volumes on the larger sieves while still collecting the smallest particles on the small sieves in a relatively short time due to the pressure which is usually driven via a pump [52]. This method has also been recently utilized to sample WWTP effluents [32].

Different sampling methods have their strengths and weaknesses. However, each of them delivers different results [19, 22, 85, 93]. As is discussed in studies covering

sampling theories and representative sampling, sampling errors can be much higher than the analytical errors [24, 103]. Thus, the lack of harmonization and standardization might induce erroneous sampling techniques and prevents the comparability of the results between a single and different studies.

### 1.2.2. Sample preparation

Studies utilized a variety of methods for sample treatment. Some studies even showed a valuable insight into the effects of sample preparation both on the natural matrix as well as the microplastic particles [33, 46, 50]. Below is an overview of the most common sample preparation methods in literature and their effects on microplastics.

**Density separation** is a technique where a variety of salts are used to increase the density of solutions so that microplastics would float to the surface and be separated by density difference. Commonly used salts are sodium chloride, sodium iodine, lithium meta-tungstate, and zinc chloride [42, 51, 52]. However, this is only effective for the removal of inorganic matter. Microplastics have densities between 0.8 – 1.1 g/ml, whereas most inorganic matter is much denser than that. Organic matter on the other hand tend to have very similar densities to microplastic and as such cannot be effectively separated by gravity [33, 50]. This means that density separation techniques are not very effective for organic rich matrices like wastewater and sludge samples [33], but essential for inorganic rich sample matrices, such as soils and sediments.

**Alkaline digestion** techniques are commonplace for studies dealing with biological tissues. However, there are many reported adverse side effects in literature. For example, Karami et al. tested KOH (10%) at different temperatures and exposure times and reported discoloration of PA and a reduction of PVC and PET recovery that became worse with higher temperatures [44]. The same issue was reported by Munno et al. at room temperature for 2 weeks who reported discoloration of PE [38]. On the other hand, Herrera et al. as well as Dehaut et al. both reported no adverse effects when using 10% KOH at 60 °C and 24 hours [36, 40]. Similarly, Hurley et al. reported only a small weight decrease for PC under the same conditions [33].

This could indicate that 10% KOH (or 2 M) at 60 °C and 24 hours could be a viable candidate for a method development as it does not seem to impact any of the major plastics tested by those studies.

Similarly for NaOH, studies investigated potential adverse effects between 1 and 10 M, at various temperatures (room temperature to 60 °C), and contact times (overnight to a week) and most of them reported degradation of some common polymers, especially PET [33, 36, 40, 41]. On the other hand, Catarino et al. reported no significant effect on any of the tested polymers (PET, PE, PVC, PA) when treated with 1 M (or 4%) of NaOH at 60 °C overnight. These findings indicate that NaOH might be slightly more aggressive to the polymers than KOH digestion.

**Acidic digestions** like HNO<sub>3</sub> were reported by several studies at different concentrations, temperatures and contact times to be very damaging to microplastics, often completely destroying sensitive polymers like PA, but also causing notable effects on less sensitive polymers like PS and PE [36, 37, 44, 45, 48, 49].

Similarly for HCL where Karami et al. reported loss of PA and melting of PET when utilizing 37% of HCL at 25 °C for 96 hours [44].

**Oxidative digestions** are one of the most common methods to remove organic matter from samples in literature. However, the reported effects on microplastic particles vary wildly. For example, Hurley et al. showed that hydrogen peroxide (30%) at 70 °C for 24 hours caused discoloration of PA, PP and PS [33]. Karami et al. observed similar behavior for hydrogen peroxide (35%) at 50 °C and 96 hours with PET and they reported a loss of PA [44]. Nuelle et al. also reported on discoloration for a range of plastics including PA, PC, PP, PET, LLDPE, PVC, PUR, and LDPE when treated via 30% hydrogen peroxide at room temperature overnight. The effect increased to include size reduction of PP and PE when the concentration of peroxide was increased to 35% at the same conditions [46]. On the other hand, Avio et al. reported no adverse effects from 30% hydrogen peroxide at 50 °C overnight [45]. Likewise, Sujathan et al. also reported no effects when PE was treated with 30% hydrogen peroxide at 70 °C overnight [47]. Overall, this could indicate that the effects on microplastics are regulated by the concentration of the hydrogen peroxide, as well as the temperature and contact times. Thereby necessitating a balance between the three factors in order

to find the optimum removal of the organic matrix and the minimal effects onto microplastics.

Fenton reaction is another common oxidation reaction that uses hydrogen peroxide with an iron catalyst to achieve higher removal rates [104]. This reaction faired even more favorably with less reported effects on microplastics than regular hydrogen peroxide, with multiple papers reporting no observed effects on the microplastic particles after treatment [33, 35, 42, 43]. However, as discussed previously, those methods utilized completely different reaction dynamics, temperatures and contact times. Some studies like Hurley at al. cooled the reaction with an ice bath to keep it under 40 °C, whereas others like Masura et al. actually heated the reaction to get it to start [33, 42]. These completely different reaction behaviors between studies need to be investigated, standardized and validated.

Based on these reports, oxidation techniques appear to be the most promising for sample preparation of wastewater samples. They first need to be harmonized and standardized for their effects on microplastics over a wide range of sizes.

**Enzymatic digestion** has been proposed as an alternative to harsh chemical reagents in order to be gentler on the polymers. However, this works best on biological tissues [37, 41]. According to Hurley et al. enzymatic digestion is not very effective on wastewater and sludge samples due to the complex nature of the matrix, requiring long treatment times with expensive reagents and often incomplete digestion [33]. Indeed, enzymatic digestion was combined with chemical treatment methods in order to obtain sufficient removal of the wastewater matrix [91].

**Surfactants** have been rarely implemented in the sample preparation process. However, Schymanski et al. proposed that fats and stearic acids might be a source of interference for spectroscopic as well as thermoanalytical methods [105]. A surfactant might be able to dissolve those fats in a sample to then be subsequently removed via filtering and rinsing the sample. Thorough rinsing is important as some surfactants can create interference for spectroscopic analysis like  $\mu$ FTIR [106]. A further theoretical advantage of using surfactants as a secondary step during sample preparation is the suspendability of microplastic particles which might be improved and prevented from sticking to surfaces or debris. However, no study investigated this so far and it needs further investigation before it can be recommended.

To correlate the findings mentioned above, an overview of the solutions as well as the knowledge gaps are needed. Li et al. recently performed a principal component analysis and discovered that alkaline treatments showed the greatest effect on microplastics, followed by high and low concentration acids, and that oxidative treatments like Fenton and hydrogen peroxide had the least impact [107]. They also ranked the changes to microplastic and showed that PET, PA and PMMA were most affected by chemical treatment, followed by PS, then PE, and finally PP as the least affected polymers [107]. However, their study proposed that acidic treatments were less harmful than alkaline treatments, which goes against what previous studies have shown so far. Nevertheless, it agreed with the observation that oxidative digestion seems to cause the least impact on polymers.

Furthermore, alkaline and acidic digestions seem to be most effective at removing biogenic matrices such as animal tissues, but not as effective against sludge and sediments [33, 36, 39, 44, 48, 49]. However, this effectiveness will not be very useful if the adverse effects on the investigated microplastics are significant, which still needs to be investigated further, especially regarding potential impacts on small microplastics.

On the other hand, oxidative digestions like Fenton and hydrogen peroxide seem to be highly effective at removing the organic matter from sludge, wastewater samples and sediments, while at the same time providing decent removal of biogenic matter [33, 35, 43–47]. Although further validation of their adverse effects on microplastics, as well as harmonization are needed before these sample preparation methods can be recommended.

Finally, the validation of sample preparation methods for microplastics does not necessarily translate directly to a valid method for smaller microplastics, especially sizes  $\leq 10 \mu\text{m}$ . These smaller particles possess a much larger surface area to volume ratio compared to larger particles. This can amplify the rather minor effects that were observed in the previous investigations targeting larger microplastic particles. Thus, applying the sample preparation methods, which are validated for larger microplastics, directly to small microplastics could lead to erroneous results. Small microplastics and nanoplastics are becoming more and more the focus of studies recently. Therefore, it is necessary to validate and, if necessary, optimize the sample preparation methods for small microplastics in order to ensure they do not cause unexpected effects.

There seems to be a gap in literature regarding this subject and a severe lack of studies validating sample preparation methods for very small particles. Possible reasons are the difficulty in obtaining microplastics in such small sizes as they are not commercially available, except for PS and PE usually. Further, as discussed previously, the detection of such small particles using regular spectroscopic methods is either not possible due to minimum spatial resolution, in the case of  $\mu$ FTIR, or would also take unfeasibly long time, in the case of  $\mu$ Raman spectroscopy. This might constitute another hurdle in designing a study that can validate the effects on very small microplastics and nanoplastics.

### 1.2.3. Sample analysis

The majority of current studies, especially those that investigate environmental samples, utilize the cutting-edge spectroscopic methods like  $\mu$ FTIR and  $\mu$ Raman and thermo-analytical approaches like TED-GC/MS and Pyr-GC/MS [26, 108]. Vibrational spectroscopic methods like FTIR and Raman are based on the radiation-molecular interactions and the resulting molecular vibrations [26]. Therefore, they can effectively identify and quantify microplastics and even nanoplastics in environmental samples.

**Fourier transform infrared (FTIR) spectroscopy** is a non-destructive method which relies on IR spectroscopy and utilizes the mid-infrared region of the spectrum ( $400 - 4000 \text{ cm}^{-1}$ ) to excite the molecules and causes them to vibrate in unique patterns which can be then be interpreted as specific fingerprints to identify them in a sample [26]. Aside from natural organics in the sample matrix, which can interfere with the spectroscopic analysis, water is the largest interference source for IR spectroscopy, requiring the sample to be completely dried first [26]. There are generally two types of common FTIR analysis. The first one is Attenuated Total Reflection (ATR) which utilizes a germanium, diamond or zinc selenide crystal to interact directly with the particle surface [26]. Pimpke et al. reported that 58% of studies which used FTIR, utilized some sort of ATR for their analysis due to the low cost of analysis [71]. However, ATR is not really suitable for particles smaller than  $500 \mu\text{m}$  or environmental particles due to its interaction with a single particle at a time [26, 33, 35, 43, 50]. For those samples with smaller particles or for environmental samples,  $\mu$ FTIR is usually used. This method is comprised of an FTIR spectrometer



which is then coupled with an optical microscope. This means that the spatial resolution is governed by the limit of diffraction [26]. According to Salzer et al. the theoretical resolution limit is around  $1.7 \mu\text{m}$  at  $4,000 \text{ cm}^{-1}$  to  $13 \mu\text{m}$  at  $500 \text{ cm}^{-1}$  [109]. Studies place the actual theoretical limit for current  $\mu\text{FTIR}$  techniques between  $10 - 20 \mu\text{m}$  [60, 65, 91, 110–112]. However the suggested actual limit for  $\mu\text{FTIR}$  in environmental samples can be as high as  $50 \mu\text{m}$ , with smaller particles being analyzed via  $\mu\text{Raman}$  [113]. To increase measurement speeds for  $\mu\text{FTIR}$ , Focal Plane Array (FPA) detectors can be used. They are comprised of a grid or an array of detectors and can analyze a larger filter area [26]. Current state-of-the-art FPA detectors are capable of scanning an area of  $14 \times 14 \text{ mm}^2$  within 4 hours using a  $128 \times 128$  or  $64 \times 64$  array of detectors [71]. This enabled recent studies to detect microplastics in various environmental samples such as marine ice, wastewater, storm water, and drinking water [70, 91, 112, 114–117]. There are two measurement methods for FPA  $\mu\text{FTIR}$ . The first is the transmission mode, in which the IR beam is first passed through the sample and detects the absorbed amount which is not very suitable for thick particles or particles with strong colors [26]. Transmission mode is commonly used with aluminum oxide filters (Anodisc). Those filters are inexpensive and can be easily obtained but due to absorption, they do limit the spectral range that can be obtained. For more broad spectral analysis, silicon filters can be used, which allows the entire mid-infrared region to pass through [118]. The second mode is reflectance where the IR beam is reflected from the surface of the particles, but this needs to account for scattering corrections [26]. The most common filter type to be used with reflectance mode is a gold plated polycarbonate (PC) filter [60, 119].

**Raman spectroscopy** is another non-destructive vibrational spectroscopic technique based on the concept of Raman light scattering [120]. It excites and vibrates the molecules, providing a similar spectral fingerprint as with IR spectroscopy. The advantage that Raman offers is the ability to be coupled with microscopy  $\mu\text{Raman}$  to detect much smaller particles than what  $\mu\text{FTIR}$  is capable of [26]; down to approximately  $300 \text{ nm} - 1 \mu\text{m}$  of spatial resolution compared to  $10 \mu\text{m}$  for  $\mu\text{FTIR}$  [26, 61, 121]. It has been successfully used to detect microplastic in various environmental samples such as surface waters, waste- and drinking water as well as sediments [60, 122–124]. Raman was even successfully used to detect nanoplastics in some cases [125, 126]. Unfortunately, an arrangement like FPA for  $\mu\text{FTIR}$ , where several thousand

spectra are obtained simultaneously, is not possible to implement for Raman as it must operate in the visible region [26]. Instead, Raman can utilize an Electron Multiplying Charge Coupled Device (EM-CCD), which helps speed up acquisition but is not as effective as FPA [59]. Therefore, Raman spectroscopy requires significantly longer analysis time than FTIR (hours vs days) [59, 61, 62].

Therefore, it is recommended to utilize  $\mu$ Raman for smaller particles (10 – 20  $\mu\text{m}$ ) and  $\mu$ FTIR for larger ones [61, 121]. Kumar et al. even suggested analyzing all microplastic particles  $>50 \mu\text{m}$  with  $\mu$ FTIR and particles  $<50 \mu\text{m}$  with  $\mu$ Raman [113]. A further advantage to Raman spectroscopy is the lack of water interference, thus the ability to investigate aqueous and biota matrices [26]. However, it is very susceptible to auto-fluorescence in samples, therefore the removal of the organic and inorganic matrix is of utmost importance [26]. The Raman laser can have several wavelengths that need to be optimized to avoid interference [121]. Common lasers are 442 nm, 455 nm, 514.5 nm, 532 nm, 633 nm, and 785 nm [78, 127–131]. Another aspect to consider is the appropriate laser power and avoiding very high powers that would lead to thermal decomposition of the polymers [26].

The standard measurement mode of  $\mu$ Raman is the imaging mode, which like  $\mu$ FTIR, scans the entire surface area. This requires long analysis times as well as generates massive amount of data in the form of Raman spectra [26]. An alternative that was developed is a particle scan mode, where Raman is first preceded by optical microscopy and an image analysis software capable of detecting all particles on the filter area. Afterwards, an automated scan is done using  $\mu$ Raman to scan only the particles, thus saving time and processing power [26, 132]. Currently, several commercial and even open source libraries for automated microplastic scanning exist such as GEPARD and TUM-ParticleTyper [133, 134]. Despite utilizing image recognition to reduce analysis time, the lack of FPA still means that Raman analysis is time consuming, therefore it is not possible to scan the entire filter, especially when particles in the low  $\mu\text{m}$  range are to be detected. This is because of the inverse relationship between particle size and their abundance in a sample in an exponential fashion [26]. For example, Cabernard et al. measured only 19  $\text{mm}^2$  (5%) of the filter area when measuring particles down to 1  $\mu\text{m}$  [60].

This very small area can induce over or under estimations when extrapolating the results, as the particles land in random patterns on the filter surface. Several random

selection criteria for representative subsampling were investigated; Anger et al. applied a random sampling approach to determine what an effective particle count would be for different samples [121]. They discovered that if a sample contained around 0.5% microplastic content then 5% of the total particles needed to be scanned to achieve an error margin of 10% or less. This also signifies the importance of sample preparation in order to increase the microplastic content in the sample via removing organic and inorganic matter [26]. Several other investigations to determine best subsampling strategy were discussed recently by Schwaferts et al. and Brandt et al. [135, 136].

**Pyrolysis gas chromatography coupled with mass spectrometry (Py-GC/MS)** is a thermoanalytical method based on the analysis of pyrolysis degradation products of the polymers in the form of pyrograms. The pyrograms are then used as unique fingerprints to identify the original polymers that produced them via the use of commercial or self-made libraries [26]. While it is a destructive method, the resulting pyrograms can be reanalyzed later if new library elements are present [26, 71]. The ability to identify additives is also possible, though it requires expertise and the appropriate libraries [71]. The analysis can be operated in several modes, depending on the sample type to be analyzed; single shot and multi-shot analysis, evolved gas analysis and thermochemolysis [137]. The downsides of Py-GC/MS is the very small amount of sample that can be analyzed (<1 mg) and the contamination potential of the system via surface interactions with the organic matrix [26, 32]. This makes it necessary to perform proper sample preparation to remove as much of the natural matrix as possible and to concentrate the microplastics in order to successfully analyze the sample [26]. Despite these limitations, Py-GC/MS has been shown to detect nanoplastics in environmental samples [138, 139]. Such an analysis is possible depending on the concentration of polymers in the sample and the matrix composition, and is aided by sample preparation [32, 140]. Pressured liquid extraction (PLE) and solvent extraction techniques can also be applied to extract and concentrate the polymers from an environmental sample for further analysis [141, 142]. In some cases, microplastics can be detected directly in complex samples without removing the organic matrix. For example, Funck et al. detected microplastics in WWTP effluents using only sample extraction and drying [32]. Finally, an advantage of Py-GC/MS is

the ability to differentiate between car and truck tire wear as they differ in the amount of natural rubber utilized [143].

**Thermal extraction - desorption gas chromatography coupled with mass Spectrometry (TED-GC/MS)** offers a similar approach to Py-GC/MS but utilizes a Thermogravimetric Analyzer (TGA) during the pyrolysis step. The pyrolysis products are then purged and adsorbed to a solid-phase extraction stir bar. This adsorber bar is then transferred to a Thermal Desorption Unit (TDU) where the decomposition products of the polymers are desorbed and separated by a GC-column then analyzed via MS [26, 144]. Dümichen et al. was the first to utilize the technology to detect microplastics in environmental samples in 2015 [34]. Currently TED-GC/MS has been established as a viable method to analyze microplastics in complex environmental samples such as WWTP effluents, and tire wear in street runoff as well as food and sediment samples [22, 25, 26, 144–146]. TED-GC/MS has a major advantage over Py-GC/MS in terms of sample amount, which can reach up to 100 mg, or 200 times larger than what is possible with Py-GC/MS [26]. This enables TED-GC/MS to analyze environmental samples with minimal sample preparation requirements and offers an advantage in terms of sensitivity and representative sampling compared to all other discussed methods so far [26, 57, 58]. One downside of TED-GC/MS compared to Py-GC/MS is the inability to detect the natural rubber in truck tire wear particles due to interference with plant matter that is difficult to separate from the matrix [26, 144].

### **Alternative methods**

There are alternative analytical methods that have been adapted to detect microplastics such as Pressurized Fluid Extraction (PFE), liquid extraction and analysis using High Performance Liquid Chromatography (HPLC), size exclusion chromatography (SEC), Matrix-Assisted Laser Desorption/Ionization Time-Of-Flight Mass Spectrometry (MALDI-ToF/MS), or Near IR spectroscopy (NIR), but these were either only applied to solid matrices such as sediments (PFE and liquid extraction) [68, 147, 148], or are not practical for environmental samples due to the miniscule sample size allowed (MALDI-ToF/MS) [26], or the insufficient minimum spatial resolution ( $\geq 200 \mu\text{m}$  in the case of NIR) [149]. Finally, Materić et al. utilized Thermal Desorption-Proton Transfer Reaction-Mass Spectrometry (TD-PTR/MS) for high

resolution detection of trace amounts of microplastics in snow cores [150]. However, the reported recovery rates for PS were only estimated to be 15% and interference with organic matter should be taken into account [26, 150].

### **Fluorescence microscopy**

As previously shown, microplastic quantification usually requires the utilization of costly equipment like  $\mu$ FTIR,  $\mu$ Raman, TED-GC-MS and Py-GC/MS. The analysis times required can also be very long (hours to days depending on the sample and analysis) [68, 151]. This can limit the scale with which microplastic monitoring campaigns can be performed. Thus, it was desirable to develop a reliable analytical method that is simple, relatively quick, and cost effective to serve as an alternative analysis, or at least to complement more complex analytical methods. A viable candidate for this analysis is fluorescence microscopy, using lipophilic dyes like Nile red (NR) and Nile blue (NB). For example, it is shown that utilizing fluorescence staining with NR can aid in pre-selecting particles to be chemically analyzed by FTIR in order to reduce operator bias and selection error [51, 76, 152–154].

This technique can also be used standalone to quantify microplastics in a sample. However, only a handful of studies already investigated dyeing microplastics inside environmental samples directly (e.g., sediments and biological tissues) [51, 78–80, 82]. Nguyen et al. even attempted the application of various analytical techniques on wastewater samples, including fluorescence microscopy [83]. Though, that study provided no explicit results for fluorescence analysis nor a validation for their methodology. Furthermore, most of these studies were limited to particle sizes above 100  $\mu\text{m}$  [51, 76, 77, 82].

Since environmental samples like wastewater samples contain a high amount of organic content, any fluorescence dyeing technique for wastewater samples must be developed further in combination with an effective sample preparation method. This is to remove the organic content beforehand and minimize false positives during subsequent fluorescence analysis. Studies attempted this in the past, but each had certain disadvantages. For example, Erni-Cassola et al. [78] investigated smaller microplastic particles down to 20  $\mu\text{m}$  in sediment samples using Nile red, but they utilized hydrogen peroxide at high temperatures (100°C), which exceeds the continuous operational temperatures of several polymers and can be detrimental to

microplastics [33]. Similarly, Dowarah et al. [80] used Nile red to report the presence of microplastic particles down to 22  $\mu\text{m}$  in bivalves. However, they utilized KOH for sample preparation, which can degrade PET and PLA particles, so there might have been a certain loss of particles in their case. Finally, Vermeiren et al. [82] utilized Fenton digestion and Nile red to quantify microplastics in organic rich sediment samples. However, the microplastic particles in that study were only quantifiable down to 125  $\mu\text{m}$  with a detection limit of 62.5  $\mu\text{m}$ . Furthermore, the Fenton reaction used in that study utilized long reaction times (24 hours) and 2.5% (v/v) sulfuric acid. This led to size changes in PE and PET [82].

If developed and validated properly to avoid the aforementioned disadvantages, this combined sample preparation and staining technique would represent the possibility for a quick and affordable quantification method for microplastics in WWTP effluents. This can subsequently be used as a bulk monitoring method of microplastic particles when the exact knowledge of polymer composition or mass is not required. Thus, enabling monitoring campaigns on wider scales than what was possible thus far. This kind of rapid quantification could also serve as a screening step to determine which samples warrant a more detailed analysis using  $\mu\text{FTIR}$  or  $\mu\text{Raman}$  spectroscopy for example

### **Summary and synergies between the different analytical methods**

As discussed above, the conditions, shortcoming and information for each analytical method is different. For example, spectroscopic analysis techniques obtain information regarding particle number, size, morphology, and identity but not the mass. On the other hand, thermoanalytical techniques can obtain mass concentrations and identity, which make them indispensable for mass balance and modelling applications [26, 62]. However, they do not provide any information about particle number or size, which are useful parameters for tracking particles in the environment. Examples are toxicity related studies in organisms [26].

Furthermore, thermoanalytical methods are somewhat fast and not limited by particle size, given enough preconcentration of the sample [67], whereas spectroscopic analysis methods require no preconcentration but are limited by analysis speed and the minimum spatial resolution, as well as over/underestimation of the sample depending on the analyzed sub-aliquot [91, 118, 155].

Finally, alternative methods like fluorescence microscopy are inexpensive and readily available, very fast and can be automated with ease. But they can only provide information about particle size and numbers with no identification of the particles, thus it can be prone to over and under estimation of microplastic content. This might be overcome by adding sample preparation to the workflow, but it needs to be properly validated before a recommendation can be made.

Given the wide range of obtained information, the advantages, and disadvantages of each method, it might be beneficial to combine two or more of them to obtain a bigger picture depending on the sample and desired information. An overview of the main methods and the information they provide is presented in Figure 1. All of these aspects need to be clearly discussed in order to lay out guidelines for best practices when attempting to detect microplastic in wastewater samples.

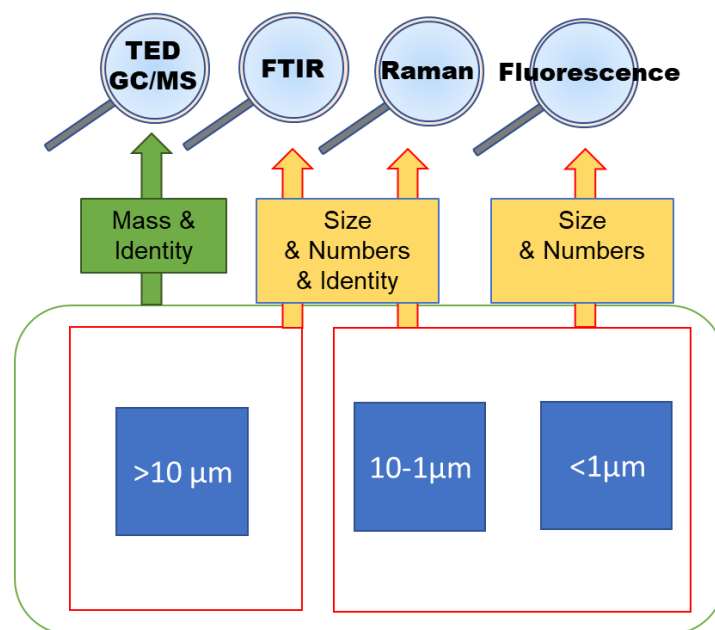


Figure 1. Overview of the main analytical techniques used in this study and the information and limitations of each.

## 2. Research objectives and hypotheses

The objective for this doctoral thesis was to present and optimize a holistic analytical process for the monitoring of microplastics in WWTP effluents. This included investigating the three main steps involved in microplastic monitoring: **Sampling, sample preparation and sample analysis**.

Therefore, this dissertation began by demonstrating and testing a previously established cartridge-based cascade sampling system during a field sampling campaign at different WWTPs (chapter 3). Then sample preparation methods for both microplastics (chapter 4.1) and small microplastics (chapter 4.2) were investigated. Further, the state-of-the art sample analysis methods, their synergies and the best practices for monitoring microplastics in WWTP effluents were discussed (chapter 5.1). Finally, the possibility to develop a fast and affordable microplastic quantification method based on fluorescence dyes and fluorescence microscopy (chapter 5.2) was investigated. An overview of the chapters, tasks as well as hypotheses associated with them is provided in Figure 2.

### **Hypotheses:**

**Hypothesis (1a): “A sample preparation method can be developed that will not reduce the size of microplastic particle which are  $\geq 200 \mu\text{m}$  by more than 10% while also not compromising the identification of microplastics using FTIR spectroscopy or TD-Pyr-GC-MS”. (Chapter 4.1).**

The reagents used in sample preparation can be harsh on the polymers. Those reagents include acids, bases and oxidants [33]. Polymers are usually resilient, but not all polymers can withstand all treatments, especially smaller particles which possess larger surface area to volume ratios, thereby increasing their reactivity. Hence, it was necessary to validate sample preparation methods for a wide variety of microplastics in common sizes (80 - 330  $\mu\text{m}$ ), while also avoiding the disadvantages from earlier studies, which were discussed previously. The two main criteria investigated were surface and functional group changes to the microplastics that might hinder identification, as well as the reduction of the average size of particles, which might indicate losses and under-reporting of particles. An increase in the average size can be expected as well, but that can be the result of particle agglomeration and does not necessarily constitute a loss of material.



Due to the significant time and effort to establish reproducible particle aging protocols, this dissertation did not cover aged polymers which would add an extra layer of variables such as oxidized, weakened chains on the polymer surfaces, and increased surface area for reaction due to nano cracks, which might make the polymers even more susceptible to common pre-treatment procedures.

The expected outcome of this part was the development and validation of one or more sample preparation methods that do not significantly affect the size distribution or identifiability of microplastic particles occurring in environmental samples, while removing the majority of organic matter from a wastewater sample.

**Hypothesis (1b): “Fenton reactions can be used without cooling to rapidly reduce organic matter content in sludge samples (>90%), without compromising the identification of microplastics using FTIR spectroscopy or TD-Pyr-GC-MS or the size distribution of microplastics by more than 10%”. (Chapter 4.1).**

One suitable sample preparation method often reported in literature is the Fenton oxidation. This reaction is usually used in studies in conjunction with an ice bath in order to maintain the temperatures below 40 °C to prevent thermal damage to the polymers [33, 43]. However, chemical reactions double in rate for each temperature increase of about 10 °C. Therefore, the Fenton reaction could theoretically be performed during a very short time (minutes) and still be very effective at removing organic matter if the temperatures are allowed to increase. Consequently, this method needed to be first optimized and validated for both safety aspects as well as any adverse effects on polymers. This hypothesis was validated using the same procedure established for testing hypothesis 1a.

**Hypothesis (2): “The size distribution of sub-microplastics ( $\leq 10 \mu\text{m}$ ) is reduced by more than 10% after directly applying the selected sample preparation methods based on hydrogen peroxide and Fenton as specified for Hypothesis 1”. (Chapter 4.2).**

As discussed in the previous chapter, the smaller the plastic particles are, the larger their surface area is compared to their volume. Since alterations of the particles happen at the surface of the polymer, the reactivity of smaller particles to sample

preparation will increase [156]. Thus, the protocols which are safe for preparing samples of larger microplastics might not be so for samples containing very small microplastics ( $\leq 10 \mu\text{m}$ ). Therefore, the selected sample preparation protocols from hypothesis 1 were re-validated and those small microplastics to avoid misrepresenting the analysis.

**Hypothesis (3): “Hydrophobic fluorescence dyes can be used in conjunction with sample preparation to establish an affordable, rapid quantitative analysis for microplastic particles larger than  $40 \mu\text{m}$  in WWTP effluents. This approach can quantify microplastics with an accuracy of  $\geq 70\%$  compared to  $\mu\text{FTIR}$ ”. (Chapter 5.2).**

Hydrophobic fluorescence dyes such as Nile red were previously investigated as a method of staining microplastic particles [73, 75, 76]. Some papers even attempted to dye environmental samples directly by relying on the difference in hydrophobicity between the natural matrix and the microplastics, in order to selectively dye only the microplastic particles and not the organic and inorganic constituents [51, 77]. To the best of the author’s knowledge, no previously reported study focused on fluorescence microscopy in wastewater effluent samples, which typically contain a large number of different organic matter fractions that can result in severe interferences. Further, studies mostly investigated particles larger than  $100 \mu\text{m}$  [51, 76, 77, 82].

Therefore, a validated sample preparation protocol that does not affect the targeted microplastics needed to be combined with a staining procedure in order to detect and quantify microplastics below  $100 \mu\text{m}$  in size. Initial investigations done in the frame of this dissertation showed that it was not at all feasible for WWTP effluents to be dyed without prior sample treatment. This is to be expected due to the excessive background fluorescence resulting from the organic matter content, especially for particle sizes  $< 40 \mu\text{m}$ , as many particles seemed to light up in wastewater samples below that size. Thus, it can be stipulated that combining an effective, validated sample preparation method with a fluorescence dying protocol for wastewater samples could provide a rapid quantification for microplastics down to  $40 \mu\text{m}$ . This could be used to complement expensive, lengthy analysis via spectroscopic as well as thermoanalytical techniques. Fluorescence microscopy would only provide information

about the size as well as the number of particles with no identification. Although, it would provide this information relatively rapidly and at low cost to enable larger scale monitoring programs. Should the need arise to perform a more detailed analysis to identify the polymers in samples, then the proposed fluorescence technique can be used as a screening step to select only samples of interest, thus saving time and resources when performing more complex analysis techniques.

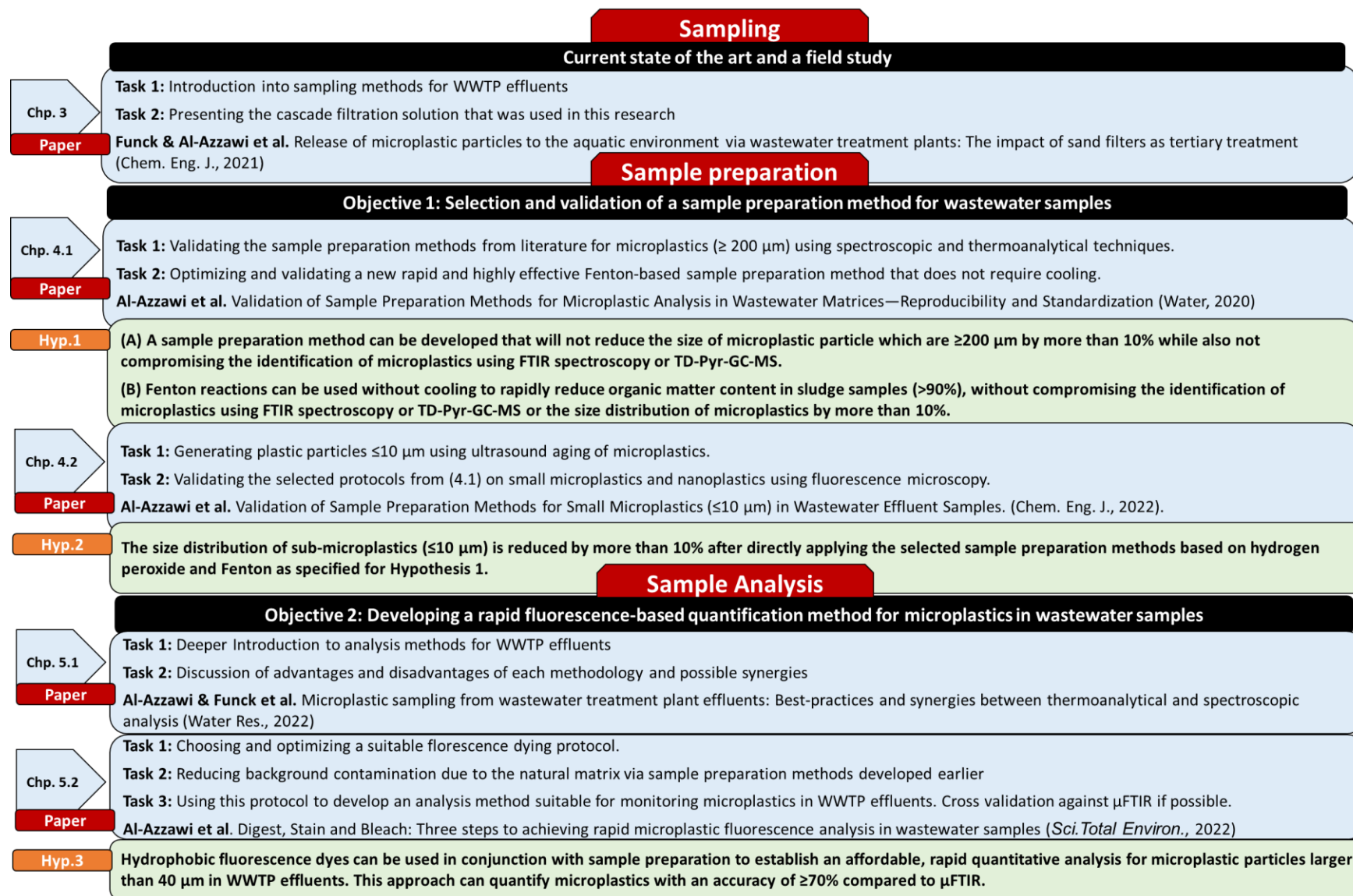


Figure 2. Overview of the research objectives, the associated hypotheses, tasks, and papers.

### 3. State-of-the-art sampling of tertiary sand filter effluents

This chapter serves to introduce state-of-the-art cascade sampling method coupled with a TED-GC/MS thermoanalytical method for fast mass estimation of microplastics in wastewater streams. There are **no hypotheses** associated with this chapter.

This chapter has been published as follows:

Funck, M., Al-Azzawi, M.S.M., Yildirim, A., Knoop, O., Schmidt, T.C.T.C., Drewes, J.E., Tuerk, J., 2021. Release of microplastic particles to the aquatic environment via wastewater treatment plants: The impact of sand filters as tertiary treatment. *Chemical Engineering Journal*. 426, 130933.

<https://doi.org/10.1016/J.CEJ.2021.130933> - Reproduced by permission of the respective journal

**Author contributions:** Shared first authorship between **Matin Funck** and **Mohammed S.M. Al-Azzawi**

**Matin Funck:** Conceptualization, Methodology, Field Performance, Sample Analysis, Formal Analysis and Writing Original Draft Preparation. **Mohammed S.M. Al-Azzawi:** Conceptualization, Methodology, Field Performance, Formal Analysis and Writing Original Draft. Aylin Yildirim: Methodology, Sample Analysis, Reviewing and Editing. **Oliver Knoop:** Conceptualization, Supervision, Reviewing and Editing. **Torsten C. Schmidt:** Conceptualization, Supervision, Reviewing and Editing. **Jörg E. Drewes:** Conceptualization, Supervision, Project Administration, Funding Acquisition, Reviewing and Editing. Jochen Tuerk: Conceptualization, Supervision, Funding Acquisition, Reviewing and Editing.

#### *Abstract*

Monitoring of microplastics (MP) release into the aquatic environment is an important topic and proposed point sources for microplastics are wastewater treatment plants (WWTPs). Three full-scale WWTPs (A, B, C) were investigated to compare the effect of continuously and discontinuously backwashed sand filters to retain microplastics from secondary treated wastewater effluents. A cascade filtration unit using steel

basket filters with mesh sizes of 100  $\mu\text{m}$ , 50  $\mu\text{m}$  and 10  $\mu\text{m}$  was employed for sampling. The subsequent analysis used thermal extraction desorption gas chromatography mass spectrometry (TED-GC-MS). This combined analytical approach offered the benefit of sampling multiple cubic meters of WWTP effluent and using a robust quantification analytical method for microplastic without the need for an additional chemical-based sample preparation step. Due to the different capacities of the three WWTPs, the results were normalized based on population equivalents (P.E.). Four common polymers were targeted in this study (i.e., PE, PS, PP, and PET). PE was the most common polymer detected in secondary effluents, with normalized annual loads ranging between 2.8  $\text{mg yr}^{-1} \text{ P.E.}^{-1}$  and 8.4  $\text{mg yr}^{-1} \text{ P.E.}^{-1}$ . Results showed that sand filters offered additional efficient MP retention capabilities, with the sand filters offering, on average, an extra 79%  $\pm$  11% of MP retention when compared to secondary treatment. Finally, one filter cell with aged and one with restored granular media were compared. The aged cell did not indicate lower retention of microplastic while using granular media that was already in operation for seven years.

### 3.1. Introduction

In the last century, synthetic polymers became widespread in industrial processes and society. As the properties of such materials can be altered with additives to enhance physical properties such as flame retardation, plastics can be uniquely designed according to the specific use [157]. Since the start of industrial-scale plastic production in 1950, the global production increased yearly to 359 million tons in 2018 worldwide [158]. Due to high consumption, improper disposal and low recycling rates, plastic debris has become a ubiquitous pollutant in the environment worldwide [159]. Microplastics (MP) are defined differently in the literature, either as plastic particles smaller than 5 mm, or smaller than 1 mm [8–11], and their investigations have gained importance in recent years [31, 108, 157, 160–164]. There is a debate about whether or not microplastic particles possess potential adverse effects on the aquatic and terrestrial organisms [30, 159, 165]. Studies indicated that wastewater treatment plants (WWTPs) usually release low numbers of microplastic particles per cubic meter as part of their final effluents [30, 166–171]. However, due to the large annual effluent volumes, WWTPs might still be a considerable potential point source for microplastic release to the aquatic environment. And recent studies discussed WWTP's as a point

source for MP [22, 172–175]. Therefore, the role of WWTP's in microplastic emission is still debatable.

In order to reduce pathogens, suspended matter and nutrients prior to discharge to the aquatic environment, some WWTPs have implemented tertiary treatment [11]. Tertiary treatments, such as media or membrane filtration, commonly involve physicochemical processes such as coagulant addition and filtration [176]. Although these tertiary treatment steps are not designed to specifically retain MP [30, 86, 177], MP particles could be retained due to the various retention mechanisms that occur during filtration. For example filtration through porous media induces mechanisms like straining, sedimentation, impaction, interception and diffusion [30, 170, 178, 179]. The efficiency of MP retention within sand filtration has been previously investigated with stereoscopic microscopy as the main detection method [19, 86, 173, 176, 177]. However, this optical method does not allow for microplastic identification and it has been reported to have significant biases [11]. Ben-David et al. (2021) employed spectroscopic methods including FTIR and  $\mu$ Raman as detection methods to investigate the removal of MP through a sand filter, as these techniques are capable of identifying microplastic types [87, 89]. They reported a decrease of 72% of particles of a secondary effluent by tertiary sand filtration at a single WWTP, which can be influenced by the state of that specific WWTP during sampling, reducing reliability of the results.

Furthermore, the focus of these studies was on emitted particle numbers as particles per volume [21, 85–87, 89]. The current study aimed to quantitatively investigate the MP mass load in secondary and tertiary WWTP effluents and the retention of MP in continuously and discontinuously back washed sand filters used in tertiary treatment. Finally, the annual normalized MP emission load for WWTPs of different capacities was compared.

## 3.2. Materials and Methods

### 3.2.1. Sample collection system and sampling procedure

The cascadic microplastic filtration device used for sampling was utilized as described previously [32]. It consists of a 5 mm pre-filtration steel sieve (Hornbach Baumarkt AG, Duisburg, Germany), a SG 40 pump (Victor Pumpen GmbH, Munich, Germany)

maintaining a high flowrate (up to  $18 \text{ m}^3 \text{ h}^{-1}$ ) coupled with three basket sieves of decreasing cut-offs (i.e.,  $100 \mu\text{m}$ ,  $50 \mu\text{m}$ ,  $10 \mu\text{m}$ ) (Krone Filter GmbH, Oyten, Germany), and a flowmeter (ESSKA.de GmbH, Hamburg, Germany). Online pressure gauges (ESSKA.de GmbH, Hamburg, Germany) are installed upstream of the  $50 \mu\text{m}$  and  $10 \mu\text{m}$  sieves to monitor the pressure drop at the inlet of these sieves as a function of cake formation build-up due to accumulating particulate matter present in secondary effluent [32]. The  $100 \mu\text{m}$  sieve was not monitored in the final assembly as it was shown to reach cake filtration condition only after the  $50 \mu\text{m}$  sieve has reached that state. Individual sieves can then be specifically removed when a back pressure of 1 bar is reached to minimize cake filtration conditions. Usually, the backpressure of the  $10 \mu\text{m}$  sieve reaches a terminal pressure of 1 bar first and therefore is delivering the smallest sampling volumes, whereas the larger sieves can continue to operate after swapping out the  $10 \mu\text{m}$  filter module. Typical sampling volumes for the  $10 \mu\text{m}$  filter were around 200 L before reaching terminal backpressure, whereas for the  $100 \mu\text{m}$  and  $50 \mu\text{m}$  filters, several cubic meters of secondary and tertiary effluents could be sampled. The exact volumes filtered during the multiple sampling campaigns at the respective WWTPs are summarized in Table\_3\_Sl. 1.

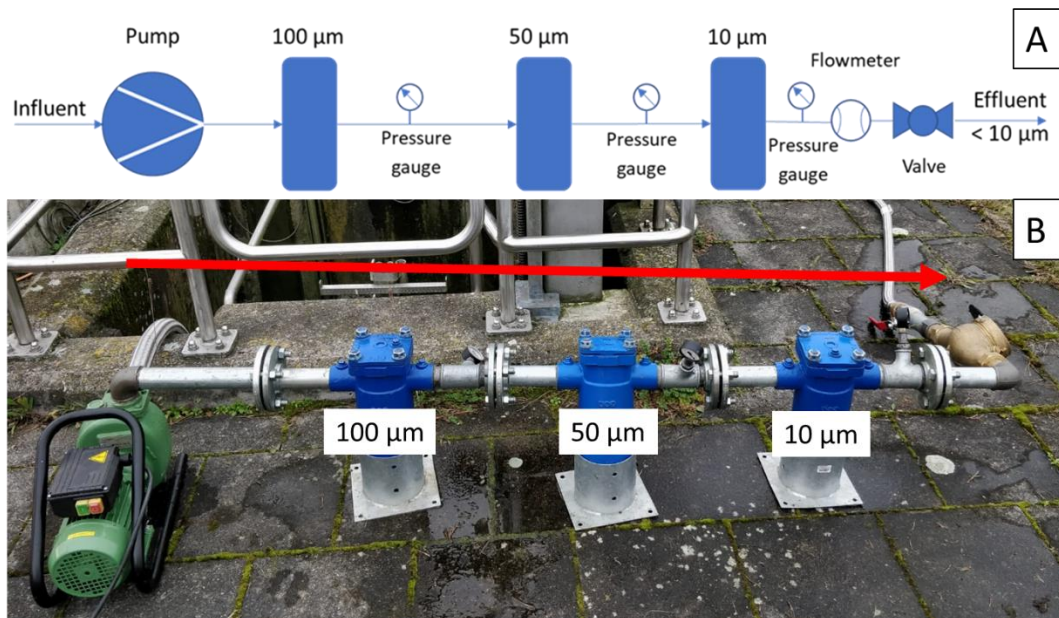


Figure 3. A: Scheme of the cascadic microplastic sampling system  
 B: Picture of the cascadic microplastic sampling system onsite.



### 3.2.2. Investigated wastewater treatment plants (WWTP)

The sampling campaigns took place between February 2020 and January 2021. Sampling was performed during dry and mild weather conditions. Three full-scale municipal WWTPs with varying capacities and tertiary treatment trains in Germany were sampled, to allow a broader assessment of MP emissions by WWTPs.

WWTP A had a capacity of one million P.E. during dry weather conditions at an influent flow rate of  $1.63 \text{ m}^3 \text{ s}^{-1}$ . Around 21% of the influent originated from various commercial and industrial sources, whereas the remainder of the influent originated from residential sources. The final tertiary treatment step utilizes a discontinuously backwashed sand filter consisting of 24 sand filter cells with a shared intake and effluent of all sand filter cells. The sampling campaigns were carried out to monitor MP content both before and after the entire sand filter assembly (mixed effluent of all active cells).

Furthermore, the WWTP was in the process of restoring the granular media and replacing the backwash nozzles in the sand filter cells successively. This allowed to sample the individual effluents of a cell employing sand in operation for 7 years and a cell utilizing restored sand just two weeks after the intense cleaning procedure to investigate the potential difference in retention efficiency. From WWTP A three individual samples were collected for both secondary and tertiary effluents. Additionally, one sample each for the old and renewed cells were taken (See SI, chapter 9.1).

WWTP B had a capacity of 120,000 P.E. with an influent flowrate of  $0.12 \text{ m}^3 \text{ s}^{-1}$ , where one third of the influent originated from industrial and commercial sources. The WWTP employed 24 continuously backwashed sand filters that were divided in 3 parallel trains, which could be switched on or off based on influent load. As was the case with WWTP A, samples were taken before and after the entire sand filter unit. Two samples were collected from WWTP B.

Finally, WWTP C had a capacity of 92,000 P.E with an influent flowrate of  $0.10 \text{ m}^3 \text{ s}^{-1}$ . The influent mainly consisted of municipal wastewater. The WWTP employed only conventional primary and secondary treatment, with no additional tertiary steps; thus, at WWTP C only the secondary effluent was sampled. Finally, three samples were collected from WWTP C.

Based on the dry weather influent flow rates of each WWTP and their corresponding average discharged mass of MP per cubic meter, the total MP mass emissions per year were calculated.

### 3.2.3. Sample preparation and contamination prevention

To avoid contaminations, any plastic was avoided in all parts of this work. The sampling system was sealed during operation and constructed completely from metal parts including the tubing. The sampling system was flushed at the full flow rate of the pump for 30 seconds before each sampling started. The steel basket filters were always covered with aluminum foil till insertion in their sealed modules, avoiding airborne contamination.

After sampling concluded, the sieves were removed and wrapped again in aluminum foil. The sieves were then transported to the lab where they were placed in a laminar flow box (Laminar Flow Module FMS series SuSi, Spetec, Erding, Germany). Gloves were avoided during further sample processing and only cotton lab coats were worn. Glassware was properly rinsed with ultrapure water (UPW, Arium pro VF, Satorius AG, Göttingen, Germany) and additive-free detergent before use. The retained solids on each sieve were extracted into a glass flask with the aid of a wire brush made of iron and ultrapure water. These concentrated aliquots were then transferred into sealed glass flasks and the suspension volume was noted (200 - 300 mL). Exact sampling volumes and aliquots used for microplastic analysis are summarized in Table\_3\_SI. 1, 2 and 3.

An aliquot (Table\_3\_SI. 3) from these flasks was then filtered through a 0.2 µm cellulose-nitrate filter membrane with 45 mm diameter (General Electric, Boston, Massachusetts, U.S.A.). The residue on the filter was transferred into a glass vial with 60 µL of a 1 g L<sup>-1</sup> Tween 20 (Merck KGaA, Darmstadt, Germany) solution. The recovery of this process was gravimetrically validated, and the recovery determined to be 90 wt% ± 1wt%. A detailed description of the validation process is provided in the SI section *sample filtration and processing*.

### 3.2.3. Analytical Method

The analytical method was adapted in accordance to Eisentraut et al. (2018) using a different adsorbent [144]. The decomposition products were then sorbed at 40 °C on a 20 mm x 0.5 mm solid phase stir bar adsorber (Twister, Gerstel GmbH & Co KG, Mülheim an der Ruhr, Germany) consisting of polydimethylsiloxane instead of a Sorb-Star PDMS bar. 70 µm alumina crucibles were used to hold samples during thermal extraction at the thermo gravimetric analyzer unit with a TGA2 autosampler (Mettler-Toledo, Gießen, Germany). Each sample was weighted by the TGA and heated from 25 °C to 600 °C, with a heating rate of 10 °C min<sup>-1</sup> and nitrogen (N<sub>2</sub>) purge gas flow at 50 mL min<sup>-1</sup>. The software used was the STARe Software V16.10. (Mettler-Toledo Gießen, Germany). The decomposition products were purged with the N<sub>2</sub> from the TGA through a 240 °C heated coupling unit (Gerstel GmbH & Co KG, Mülheim an der Ruhr, Germany).

The adsorber was then transferred via the autosampler robot (MultiPurposeSampler, Gerstel GmbH & Co KG, Mülheim an der Ruhr, Germany) to the thermal desorption unit 3.5+ (TDU3.5+) (Gerstel GmbH & Co KG, Mülheim an der Ruhr, Germany). Prior to thermal desorption 3 µL of a styrene-d<sub>8</sub> (98% purity, Sigma-Aldrich Chemie GmbH; Taufkirchen, Germany) in ethanol (≥99.5% purity, Carl Roth GmbH + Co. KG, Karlsruhe, Germany) solution with a concentration of 10 ng µL<sup>-1</sup> was added by the autosampler robot to the twister by liquid injection for quality control. Within the TDU3.5+ unit, the decomposition products are mobilized from 50 - 200 °C with a heating rate of 40 °C min<sup>-1</sup>, using split-less mode and helium (He) with 99.999 mol% purity (Air Liquide Deutschland GmbH, Düsseldorf, Germany) and a flow of 24 mL min<sup>-1</sup> as a carrier. This desorbs the decomposition products from the solid phase and into the cooling injection system (CIS4, Gerstel GmbH & Co KG, Mülheim an der Ruhr, Germany) to be cryo-focused at -120 °C for 8.75 min and are subsequently released at -120 °C to 270 °C with a heating rate of 12 °C sec<sup>-1</sup>.

The decomposition products are then introduced into the gas chromatograph (GC7890, Agilent, Santa Clara, California, USA) equipped with a capillary column (HP 5ms Ultra Inert 30 m x 250 µm x 0.25 µm, Hewlett Packard, Palo Alto, California, USA). The chromatographic separation was achieved with a temperature program of 40 - 300 °C at a rate of 5 °C min<sup>-1</sup>, 4 min isothermal at 300 °C with a 1 mL min<sup>-1</sup> He flow. The separated products enter the mass spectrometer (5977 B MSD, Agilent) with

the GC-MS coupling interface heated to 300 °C, an ion source temperature of 230 °C, a quadrupole temperature of 150 °C and an electron ionization at 70 eV. Scan mode with a range of  $m/z$  35 - 440 was used. The acquisition software was MassHunter GC/MS Acquisition B.07.06.2704 18-Jul-2017 (Agilent, Santa Clara, California, USA) coupled with Maestro1 Version 1.5.3.83 / 3.5 (Gerstel GmbH & Co KG, Mülheim a.d.R., Germany). For data evaluation, MassHunter Qualitative Analysis Version 10.0 Build 10.0.10305.0 (Agilent, Santa Clara, California, USA) was used.

#### 3.2.4. Polymer Calibration and process blanks

For calibration of the commonly produced polymers polystyrene (PS) (BS-Partikel GmbH; Mainz, Germany), polyethylene (PE) (Celanese Services Germany GmbH; Sulzbach, Germany), polypropylene (PP), polyethylene terephthalate (PET) (Bundesanstalt für Materialforschung und –prüfung, Berlin, Germany) were chosen. These four polymers represented around 67% of the European plastic demand in 2018 [158]. Calibrations used and results for quality control samples and their description are provided in the SI (*chapter: 9.1.3. Polymer calibrations*) for reference. Characteristic pyrolysis products are documented in Table\_3\_SI. 5. whereas Table\_3\_SI. 6 shows the calculated absolute LODs and LOQs.

Field process blanks for all sampling campaigns were conducted as described previously [32], and did not show positive findings using TED-GC-MS for any polymer and WWTP.

### 3.3. Results and Discussions

#### 3.3.1. Polymer concentration reduction by sand filters

Thermogravimetric analysis provides only information about composition and mass, but no information about particle size distribution and numbers. However, due to the utilization of the cascade filtration, it was possible to operationally define the detected microplastic polymers as particles between 5 mm - 100  $\mu\text{m}$ , 100  $\mu\text{m}$  - 50  $\mu\text{m}$ , and 50  $\mu\text{m}$  - 10  $\mu\text{m}$ .

The four targeted polymers PE, PS, PP, and PET were detected in the effluents of all WWTPs. The results for WWTP A suggest a correlation between the mass

concentrations of the polymers and each filter fraction (Figure 4). Figure 5 shows the results of WWTP B. The mass concentration of particles decreased with decreasing filter fraction size, i.e., particles found on the 100  $\mu\text{m}$  sieve before the sand filter (B.SF.) and after the sand filter (A.SF.) had a higher mass concentration compared to the particles found on the 50  $\mu\text{m}$  and 10  $\mu\text{m}$  sieves. This was expected, as the particle size decreases, the overall mass of the particles decreases as well .

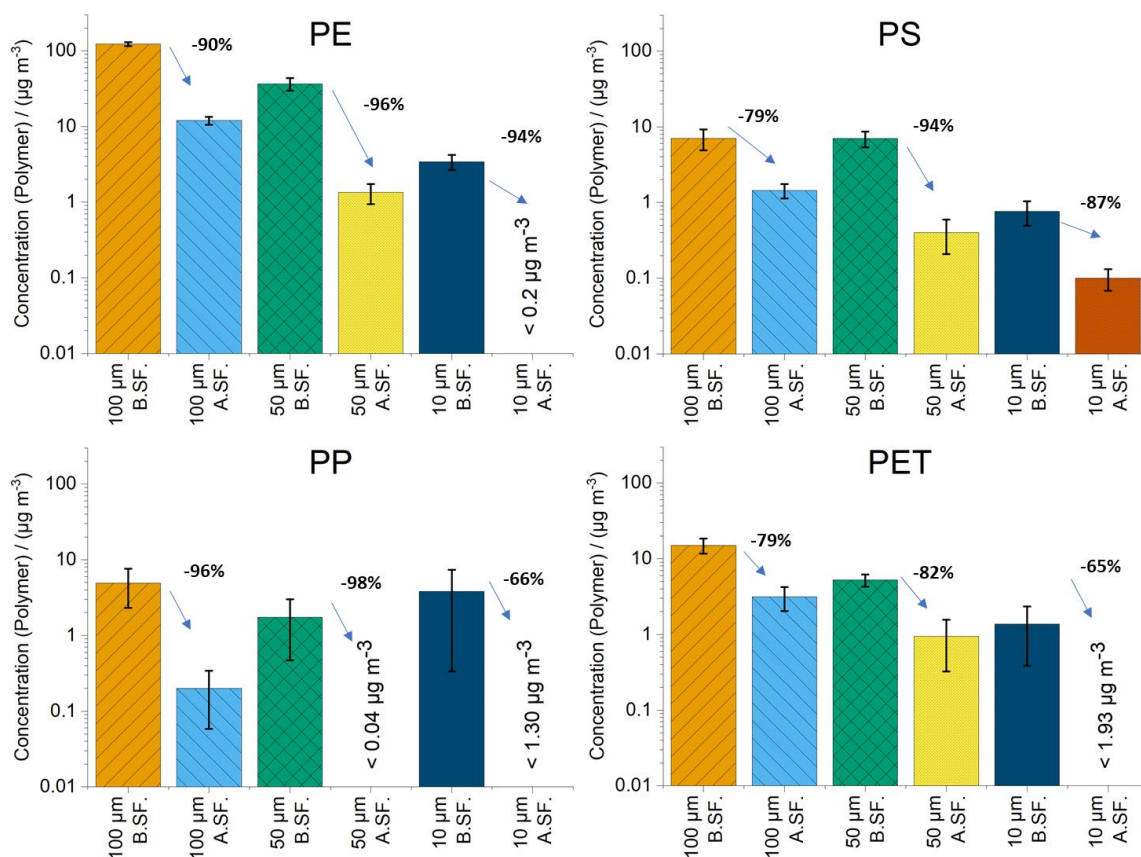


Figure 4: TED-GC-MS results of PE, PS, PP and PET concentration in samples before the sand filter (B.SF.) and after the sand filter (A.SF.) are presented as bar plots for WWTP A, given in  $\mu\text{g m}^{-3}$  on a logarithmic scale for 100  $\mu\text{m}$ , 50  $\mu\text{m}$  and 10  $\mu\text{m}$  sieve fractions. In the bar plot the standard deviations between the three sample campaigns at WWTP A are given. Polymers which were below the limit of detection (LOD) are marked as such with the respective value for each respective fraction. The LOD concentration was calculated by dividing the absolute LOD (Table\_3\_Sl. 6) by the respective average sampling volume taken from Table\_3\_Sl. 1. An arrow with a negative percentage value shows the retention based on the mean mass concentration of each respective polymer B.SF. and A.SF. The retention of MP for polymers below the LOD was calculated by using half of the LOD.

Comparing the concentrations found before and after the sand filter in Figure 4, a high reduction of all polymer concentrations can be observed. The average retentions were  $94\% \pm 3\%$  for PE,  $87\% \pm 6\%$  for PS,  $87\% \pm 15\%$  for PP, and  $75\% \pm 8\%$  for PET (exact concentrations are given in Table\_3\_Sl. 7). Additionally, the polymer PE exhibited

concentrations one magnitude higher in all samples when compared to the other polymers.

The sampling results of the effluents from the sand filter cells using old and restored media are presented in Figure\_3\_Sl. 1. Due to the renewal of the old sand filter cell the data is based on one sampling.

The concentration reduction efficiency of the MP during sand filtration in WWTP B was comparable to that of WWTP A (Figure 5).

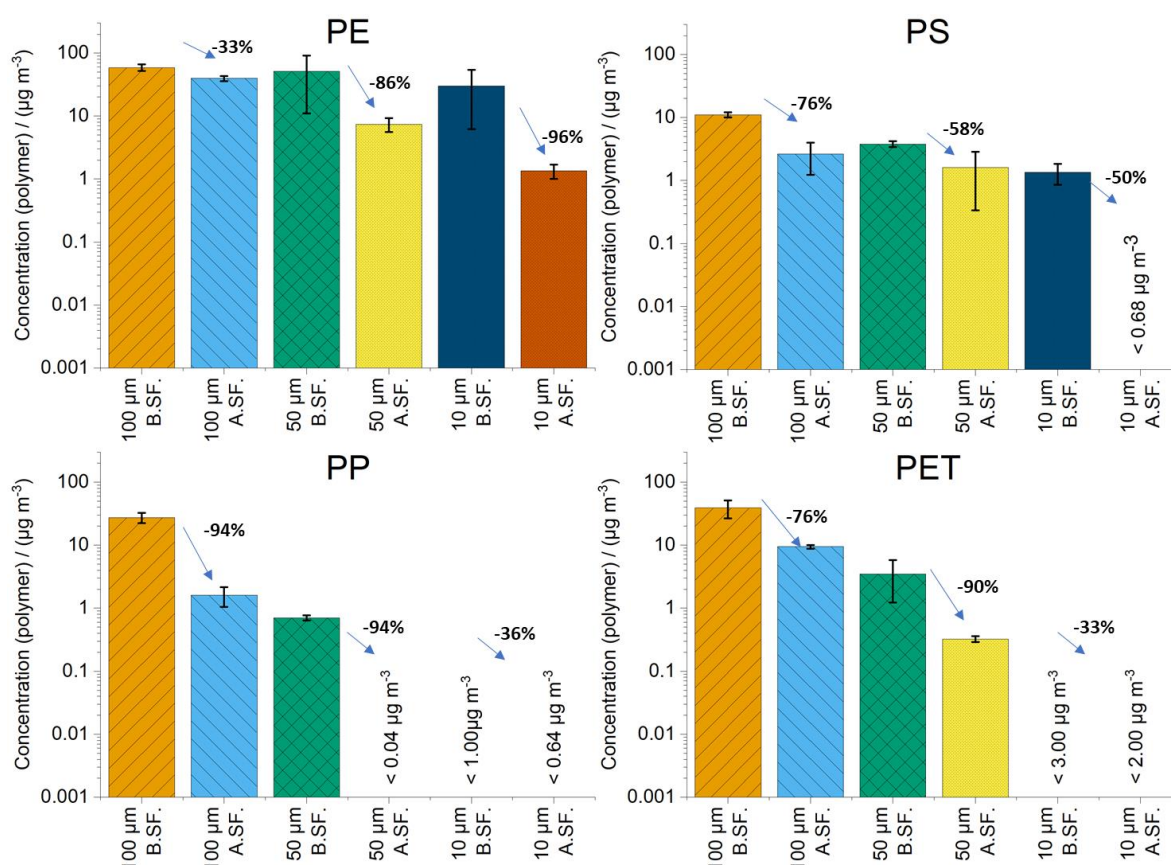


Figure 5: TED-GC-MS results of PE, PS, PP and PET obtained from WWTP B. The bar plots show the respective polymer concentration in samples before the sand filter (B.SF.) and after the sand filter (A.SF.). Polymer concentration is given on a logarithmic scale in  $\mu\text{g m}^{-3}$  for 100 $\mu\text{m}$ , 50 $\mu\text{m}$  and 10 $\mu\text{m}$  sieve fractions. Error bars represent the standard deviations between the two sampling campaigns at WWTP B. For concentrations below the LOD, the values are indicated as such. The LOD concentrations were calculated by dividing the absolute LOD-values (Table\_3\_Sl. 6) by the corresponding average sampling volume taken from Table\_3\_Sl. 1. An arrow with a negative percentage value shows the retention based on the mean mass concentration of each respective polymer B.SF. and A.SF. The retention of MP for polymers below the LOD were calculated by using half of the LOD.

The sand filter in WWTP B retained on average  $71\% \pm 28\%$  of PE,  $61\% \pm 11\%$  of PS,  $75\% \pm 27\%$  of PP and  $67\% \pm 24\%$  of PET (exact concentrations are given in Table\_3\_Sl. 8). The results shown in Figure 6 indicate a high retention of all targeted polymers.

Both WWTP A and B have different types of sand filters with the same number of 24 sand filter cells. With WWTP A's sand filter being discontinuously backwashed and the sand filter of WWTP B being continuously backwashed. The retention of microplastic concentrations is similar in both sand filters. Therefore, the backwashing mode is not influencing the MP retention. It is notable that PP and PET were below LOD for both WWTP A and B in the smaller size fractions of their final effluents.

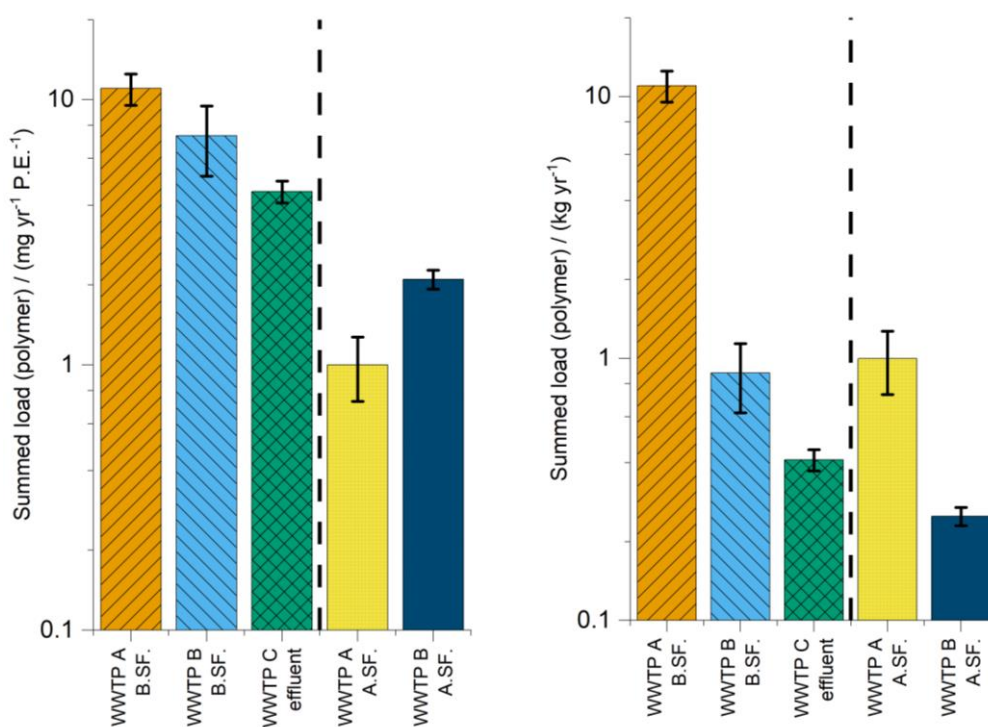


Figure 6. Left: The normalized emitted annual polymer load ( $\text{mg yr}^{-1} \text{P.E.}^{-1}$ ) for each WWTP. Right: Total annual emitted polymer load. Values were calculated based on the observed concentrations and dry weather influent volume. The emitted PE, PS, PP, and PET load for each WWTP was summed. Results are given for before and after Sand filter (B.SF. and A.SF.). For WWTP A and B, results are presented alongside with the effluent WWTP C (without tertiary sand filter).

Though WWTP B contained in general less PP and PET even before the sand filter. However, the difference between the two was not drastic as can be seen from Figure 4 & Figure 6 and it might indicate normal differences in the influent quality or variations in the secondary treatment efficiency.

### 3.3.2. Comparison of polymer retention at the three WWTPs

A normalized comparison among the three WWTPs based on the estimated released and accumulated annual load of the different polymers PE, PS, PP and PET is

presented in Figure 6. Sand filtration at WWTP A significantly reduced the annual secondary effluent MP emissions from  $11.0 \text{ mg yr}^{-1} \text{ P.E.}^{-1}$  to  $1.2 \text{ mg yr}^{-1} \text{ P.E.}^{-1}$ .

At WWTP B, the sand filtration was able to reduce the annual load from  $7.3 \text{ mg yr}^{-1} \text{ P.E.}^{-1}$  to  $2.1 \text{ mg yr}^{-1} \text{ P.E.}^{-1}$ . Thus, the total removal efficiency for all polymers across all sizes was found to be  $89\% \pm 18\%$  and  $71\% \pm 7\%$  for the sand filters at WWTP A and B, respectively. WWTP C was the lowest capacity plant and did not employ tertiary treatment. It emitted  $4.1 \text{ mg yr}^{-1} \text{ P.E.}^{-1}$ . When taking the different capacities of the plants into account, the estimated total annual polymer emissions from WWTP A, B and C differ only slightly at  $1.2 \text{ kg yr}^{-1}$ ,  $0.3 \text{ kg yr}^{-1}$ , and  $0.4 \text{ kg yr}^{-1}$ , respectively. Therefore, WWTP C, due to its smaller capacity, might have low annual emissions when compared to larger scale plants, even without tertiary treatment. However, this aspect should be further investigated.

Mass loads as presented in this study can be used to assess the overall point source contributions by WWTPs, which could be beneficial for regulatory and targeted monitoring purposes.

In literature most studies present mass estimations based on size of the MP particles as determined by spectroscopic analysis, and the density of the corresponding polymers [64, 65] Thus the findings are not well comparable, as this approach includes uncertainties since a two-dimensional particle recording is used to estimate the particle mass [66, 67].

One of the few studies which investigated the mass concentrations of MP directly was Bannick et al., where MP emissions from secondary treated effluent of a WWTP with a capacity of  $2.86 \text{ m}^3 \text{ s}^{-1}$  were investigated [22]. They analysed PS and PE via three sampling campaigns on consecutive days with a cascadic filtration and TED-GC-MS. Concentrations found in the secondary effluent were in the  $\text{mg m}^{-3}$  range. For PE the combined mean concentration in the  $100 \mu\text{m}$  and  $50 \mu\text{m}$  sieve fractions was  $83.6 \text{ mg m}^{-3} \pm 26.8 \text{ mg m}^{-3}$ . For PS, the combined mean concentration was  $1.5 \text{ mg m}^{-3} \pm 0.9 \text{ mg m}^{-3}$ . This corresponds to an estimated normalized annual emission of  $4.80 \text{ g yr}^{-1} \text{ P.E.}^{-1}$ , which is very high and amounts to  $7.7 \text{ tons yr}^{-1}$  in total. This might be explained by the fact that the sampling took place over 3 consecutive



days. Therefore, abnormal operational conditions were possibly included and is not representative of the normal operation. Thus, the data should not be extrapolated for the entire year. These concentrations are much higher than what was observed in the current study with the focus on four polymers, giving a maximum of  $11.0 \text{ mg yr}^{-1} \text{ P.E.}^{-1}$  for WWTP A at B.SF. Since these results are normalized, these three orders of magnitude difference in mass concentration between the studies cannot be explained by the difference in plant capacity. Therefore, further studies are required, focusing on mass loads in WWTP effluents while analysing multiple polymers. This would give more data concerning MP load emissions from WWTP, where mass balances for WWTPs and their respective processes could be attained. This would further inform assessments on their toxicological relevance for receiving environments and ultimately the need for regulatory actions.

### 3.4. Conclusion

The high-volume sampling system in combination with the nondiscriminatory mass-based analysis technique using an automated TED-GC-MS method allowed for a rough MP size classification and estimating the annual mass emissions of MP in the secondary and tertiary treated effluents in a statistically robust fashion. This approach indicates its suitability for monitoring programs of MP as the method combination allows a sample analysis within hours.

The estimated total emitted annual loads and the normalized emitted annual loads for the tertiary effluents were at most  $2.1 \text{ mg yr}^{-1} \text{ P.E.}^{-1}$  ( $0.3 \text{ kg yr}^{-1}$ , WWTP B). To confirm these emission ranges and consider this method combination for a standard monitoring program, more studies employing mass-based detection methods to investigate MP in WWTP effluents are required. This study clearly shows the high MP removal efficiency during tertiary sand filtration. Finally, PE was the polymer with the highest abundance in all the sampled WWTP stages, mirroring its status as one of the polymers with the highest demand in today's society and maybe requiring more optimized waste recycling.

### *Acknowledgment*

The presented scientific work was funded by the Federal Ministry of Education and Research (BMBF) within the framework of the project 'Sub $\mu$ Track: Tracking of (Sub)Microplastics of Different Identities - Innovative Analysis Tools for Toxicological and Process Evaluation', award number 02WPL1443A-G.

## 4. Sample preparation methods

This chapter deals with the validation of sample preparation methods and is divided into two sub-chapters:

### 4.1. Sample preparation for microplastic particles

This sub-chapter deals with the intimal method development and validation for microplastics ( $\geq 80 \mu\text{m}$ ) and the testing of **hypotheses 1a & 1b**.

**“Hypothesis (1a)** *A sample preparation method can be developed that will not reduce the size of microplastic particle which are  $\geq 200 \mu\text{m}$  by more than 10% while also not compromising the identification of microplastics using FTIR spectroscopy or TD-Pyr-GC-MS”*

**“Hypothesis (1b)** *Fenton reactions can be used without cooling to rapidly reduce organic matter content in sludge samples (>90%), without compromising the identification of microplastics using FTIR spectroscopy or TD-Pyr-GC-MS or the size distribution of microplastics by more than 10%”*

This sub-chapter has been published as follows:

Al-Azzawi, M.S.M., Kefer, S., Weißer, J., Reichel, J., Schwaller, C., Glas, K., Knoop, O., Drewes, J.E., 2020. Validation of Sample Preparation Methods for Microplastic Analysis in Wastewater Matrices—Reproducibility and Standardization. **Water**, 12, 2445. <https://doi.org/10.3390/w12092445>- Reproduced by permission of the respective journal

#### **Author Contributions:**

Conceptualization, Mohammed S. M. Al-Azzawi, Christoph Schwaller, Jörg E. Drewes, Oliver Knoop; methodology & data analysis: Size Analysis: Mohammed S. M. Al-Azzawi, Simone Kefer; FTIR: Mohammed S. M. Al-Azzawi, Jana Weißer; Pyr-GC/MS: Mohammed S. M. Al-Azzawi, Julia Reichel; writing—review and editing, Mohammed S. M. Al-Azzawi, Oliver Knoop, Jana Weißer, Simone Kefer, Julia Reichel, Christoph Schwaller and Jörg E. Drewes; supervision, Jörg E. Drewes, Oliver Knoop, and Karl Glas.

## Abstract

There is a growing interest to monitor microplastics in the environment, corresponding to increased public concerns regarding potential adverse effects on ecosystems. Monitoring microplastics in the environment is difficult due to the complex matrices that can prevent reliable analysis if samples are not properly prepared first. Unfortunately, sample preparation methods are not yet standardized, and the various efforts to validate them overlook key aspects. The goal of this study was to develop a sample preparation method for wastewater samples, which removes natural organic matter without altering the properties of microplastics. Three protocols, based on KOH, H<sub>2</sub>O<sub>2</sub>, and Fenton reactions, were chosen out of ten protocols after a literature review and pre-experiments. In order to investigate the effects of these reagents on seven polymers (PS, PE, PET, PP, PA, PVC and PLA), this study employed  $\mu$ FTIR, laser diffraction-based particle size analysis, as well as TD-Pyr-GC/MS. Furthermore, the study discussed issues and inconsistencies with the Fenton reactions reported in literature in previous validation efforts. Findings of this study suggest that both H<sub>2</sub>O<sub>2</sub> and Fenton reactions are most effective in terms of organic matter removal from microplastic samples while not affecting the tested polymers, whereas KOH dissolved most PLA and PET particles.

### 4.1.1. Introduction

The first studies regarding microplastic contamination in oceans appeared in the 1970s and since then interest in the topic has been rapidly growing, especially in recent years [8, 13]. Microplastics are defined differently in literature, either as plastic particles smaller than 5 mm, or smaller than 1 mm [8–11]. Due to the difficulty of monitoring microplastics in the environment, even decades later there is still not enough data to get a full picture of microplastic contamination [13]. The difficulty in assessing microplastics in the environment lies in distinguishing microplastics from the complex mixture of natural organic and inorganic particles in any given environmental matrix. These can be for example inorganic particles like sand and silt, but also organic particles originating from biofilms, plant and animal debris [61]. Even with the advent of modern analytical methods such as Fourier-transform infrared spectroscopy (FTIR) and Raman spectroscopy, a natural matrix can still hinder the detection of

microplastics or at least increase the error factor considerably. Therefore, appropriate sample preparation steps are necessary.

Inorganic matter is usually separated from microplastics by using density differences. Common microplastics have a density close to that of water (0.83-1.1 g/cm<sup>3</sup>), whereas most inorganic constituents have higher densities. Using a concentrated salt solution, such as sodium chloride (NaCl) or sodium iodine (NaI) solutions (with density of 1.2 and 1.8 g/cm<sup>3</sup>, respectively), microplastics and inorganics can be separated based on the difference of their respective densities [33, 50].

On the other hand, organic matter has a similar density to microplastics and cannot be separated based on density differences [28, 50]. Thus, a matrix rich in organic matter, such as biosolids, wastewater effluents or streambed sediments, needs to be treated via chemical digestion protocols such as oxidative, acidic, alkaline, as well as enzymatic digestions [50]. However, the use of strong chemical reagents can inadvertently affect the characteristics of the microplastics being analyzed [33, 180]. Whereas enzymatic digestion protocols are usually safe for microplastics, they require long digestion times, which limits their applicability [33]. To this date, there are no standardized sample preparation methods. This is one of the main factors limiting the comparability between various efforts to monitor microplastics in the environment [33].

#### *4.1.1.1. Sample preparation methods for removing organic matter*

Oxidative digestion methods are common in literature, most of which are protocols utilizing hydrogen peroxide (H<sub>2</sub>O<sub>2</sub>). It was utilized under various conditions with different concentrations (15 – 35 %), temperatures (room temperature up to 70 °C), and reaction times (a few hours to a week) [33, 44–47].

Table\_4.1\_A. 1 summarizes some hydrogen peroxide protocols used in microplastic studies and the effects on both organics as well as polymers [33, 44–47]. In general, it can be observed that hydrogen peroxide provided effective digestion and little degradation in polymers when using lower temperatures (up to 60 °C) and/or shorter reaction times (up to 24 hours). Therefore, hydrogen peroxide was identified as a viable candidate to be investigated in this study.

Fenton reaction is a viable alternative to hydrogen peroxide, as it usually requires lower reaction times [35, 42, 43]. Similar to the situation with hydrogen peroxide, Fenton reactions were applied differently in literature. The utilized reaction times varied from 20 minutes to 24 hours, depending on the applied protocols [43, 54, 55].

Table\_4.1\_A. 2 summarizes some of the Fenton protocols used in microplastic studies [33, 35, 42, 43]. There it can be observed that Fenton can provide effective digestion, while causing minimal effects on the investigated microplastics. Therefore, Fenton was considered as a candidate to be investigated in this study.

Acid based digestion methods, such as hydrochloric acid (HCl) and nitric acid (HNO<sub>3</sub>), have been traditionally used to digest biological samples such as fish tissues [44, 48, 49]. Studies reported that some polymers are sensitive to acids and might be affected or dissolved during treatment [36, 37, 45, 46, 49, 181, 182]. Table\_4.1\_A. 3 summarizes some of the acid-based protocols used in literature [36, 37, 44–46, 48, 49]. Some acid digestions were tested in pre-experiments in this study (SI section 1.1) where they were found to result in microplastics deterioration. Based on this and reports from literature about degradation of several polymers, acid-based digestions were excluded from this study.

Alkaline treatments such as potassium hydroxide (KOH) and sodium hydroxide (NaOH) were also often used for biological samples [36–39, 41, 44, 46]. Some studies reported that alkaline digestion might cause discoloration or damage to the investigated microplastics, especially NaOH [40, 41]. On the other hand, Hurley et al. [33] tested a digestion method with 10 % of KOH at 60 °C, and achieved around 57 % removal of organic matter from sludge, while observing minimal changes of the microplastics tested. Table\_4.1\_A. 4 summarizes some of the alkaline based protocols used in literature [33, 36–41, 44, 46]. Alkaline digestions were tested in the pre-experiments performed in this study (SI section 1.1), and a protocol based on KOH (10%) was selected as a possible candidate to be investigated further.

Finally, enzymatic digestions can be an alternative to chemical digestions, especially for biological tissues such as those from fish or plankton [37, 41]. It has also been used in conjunction with other treatment methods to treat wastewater samples [91]. The problem with such protocols is usually the long period of time (days) required for complete digestion. In addition, applying this digestion can be expensive or might be

incomplete, especially for wastewater samples, which can require a follow-up application of other chemical reagents for a complete digestion [33]. For this reason, enzymatic digestions were excluded from this study, as a rapid reaction and efficiency were key attributes desired in the protocol selection.

#### *4.1.1.2 Parameters used in microplastic monitoring*

An important goal when analyzing microplastic particles found in environmental samples is the determination of size and abundance [183–185]. Chemical digestion methods might dissolve microplastic particles and cause a general decrease in their size or a loss of particles under a certain size range. This would cause an underestimation of the microplastics and represent serious consequences for the conclusions of some studies. Furthermore, identifying polymer types is also desirable during microplastic monitoring and often involves specific pyrograms from gas chromatography coupled with mass spectrometry (GC-MS), or spectra from Fourier-transform infrared spectroscopy (FTIR). An improper digestion method might interfere with these specific pyrograms/spectra and hinder unambiguous microplastic identification. Therefore, it is important that the selected chemical digestion method neither alters the size of the investigated particles, nor interfere with their identification.

#### *4.1.1.3. Research objectives and state-of-the-art*

The objective of this study was to investigate the most common sample preparation methods for isolating microplastic particles from organic matrices, as well as to discuss the inconsistencies that have been identified in different studies. Then this knowledge was used to develop and validate sample preparation methods to extract microplastics from wastewater samples, without affecting the important identifying parameters for microplastics that were discussed in the previous section.

Several recent studies have already attempted to validate sample preparation methods for microplastics [33, 35, 36, 38, 43, 44, 50]. However, these studies contained one or more of the following shortcomings: **(A)** working with larger microplastic particles (> 500 µm) due to easier handling and analysis [33, 35, 36, 38]. Smaller particles have a larger surface area to volume ratio and might be far more susceptible to unintended effects from the chemical reagents used in sample

preparation. **(B)** Using a small number of microplastic particles, which can limit the statistical significance of the findings [33, 36, 38, 43, 44]. **(C)** When using FTIR to compare the IR spectra of microplastic particles before and after exposure to the chemical treatment. It is common to compare the spectra of treated particles against their reference spectra to observe any changes. However, due to easy handling, reference spectra are often obtained in attenuated total reflection (ATR) mode, while for environmental samples, usually FTIR microscopy ( $\mu$ FTIR) spectra are used [33, 35, 43, 50]. These modes of analysis do not always yield the exact same result, thus cannot be used interchangeably. Some FTIR researchers mentioned that ATR and  $\mu$ FTIR spectra differ from one another due to different beam penetration depths [53]. However, this has never been addressed in studies concerning microplastics, where the practice of obtaining reference spectra using ATR and comparing it to  $\mu$ FTIR spectra of the treated environmental sample is very common. This can lead to confusion in spectra interpretation if not addressed. **(D)** For studies implementing a digestion protocol based on the Fenton reaction, handling of the large amounts of precipitated iron (III) particles usually is not mentioned. This phenomenon can negatively affect microplastic detection by covering the entire sample with a layer of iron (III) particles. **(E)** Finally, studies reported completely different behaviors and contact times for the Fenton reaction [33, 35, 42, 43, 54, 55]. Some studies even reported reaction times up to 24 hours [55], which seems unlikely in terms of reaction kinetics, as the Fenton reaction forms hydroxyl radicals, which result in diffusion limited reaction rates. Thus, the process should be rapid. Finally, studies like Masura et al. [42] heated the reactants to 75 °C, which is surprising as the Fenton reaction is exothermic and sometimes cooling is recommended to protect polymers from excessive temperatures [33].

To allow a comprehensive validation and to consider the shortcomings of the mentioned previous validation efforts, the experimental design in this study was adapted accordingly: **(A)** Microplastic particles with sizes between 80 – 330  $\mu$ m were selected. **(B)** For size distribution analysis, depending on the microplastic type, approximately  $4 \times 10^3$  –  $2 \times 10^5$  particles were investigated. **(C)**  $\mu$ FTIR analysis was applied to both the reference and treated microplastic particles in order to minimize bias in interpretation. **(D)** The Fenton reaction as possible digestion method for microplastics was further investigated by adapting the protocol from Tagg et al. [43]



and refining it to address the issues associated with the precipitation of iron (III). **(E)** Finally, an experimental setup was dedicated to investigating Fenton reaction kinetics. This was intended to elucidate the reasons behind the discrepancies and long reaction times required for the Fenton reaction as reported in some studies [35, 55].

## 4.1.2. Materials and Methods

### 4.1.2.1. Selection of sample preparation protocols

Ten feasible sample preparation protocols were selected based on a comprehensive review of the peer-reviewed literature [19, 33, 41, 43, 47, 49, 155, 186]. They were then investigated in pre-experiments using 250  $\mu\text{m}$  PS-particles (BS-Partikel, Germany) and an optical microscope (Axioplan 2, Carl Zeiss AG, Germany) to assess visual changes to the particles' surface. For further details refer to SI section 1.1.

Furthermore, questionnaires were sent to the project partners within the research consortium 'Plastic in the Environment' sponsored by the German Federal Ministry of Education and Research, to gather more information about the most common methods utilized to digest environmental samples. Findings from these reviews along with observations from the pre-experiments resulted in a final selection of three methods for further testing. An overview of the selected protocols is provided in Table 2. Furthermore, a workflow for applying the protocols to real sludge/wastewater samples is provided in Figure 7.

*Table 2. Protocols investigated in this study*

<b>Protocols</b>	<b>Temperature</b>	<b>Time</b>
Fenton (30% $\text{H}_2\text{O}_2$ + 20 g/L $\text{FeSO}_4$ ) [43]	Unregulated	10 min + 10 min cooling
KOH (10%) [36]	60 °C	24 hr.
$\text{H}_2\text{O}_2$ (30%) [33]	60 °C	24 hr.

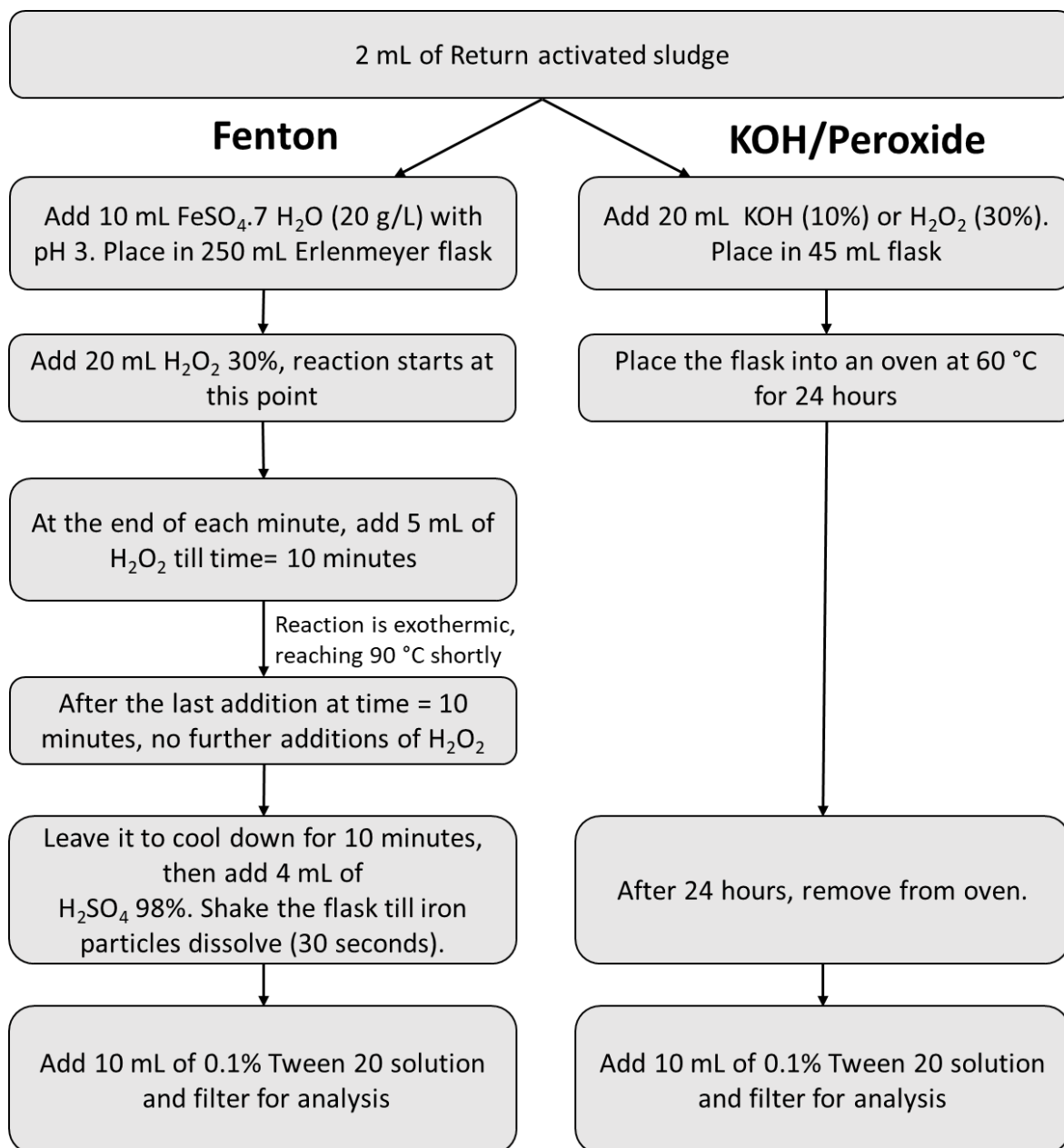


Figure 7. Workflows of the three selected protocols for processing microplastics from wastewater sludge samples.

In case other sample volumes are used than what is specified in Figure 7, the ratios of reactants should be kept the same. For KOH and hydrogen peroxide protocols, the ratio of reagent to sample is 10:1. As for Fenton, the ratios can be back calculated from the procedure described in Figure 7. Alternatively, a scaling factor (K) is utilized to achieve this goal, complete explanation is given in the SI (section 1.2).

#### *4.1.2.2. Materials*

Seven different polymers were used in this study: Polystyrene (PS), low density polyethylene (LDPE), polyvinyl chloride (PVC) (Ineos, London, UK), polypropylene (PP) (Borealis, Vienna, Austria), polyethylene terephthalate (PET) (TPL, Zurich, Switzerland), polyamide (PA) (Lanxess, Cologne, Germany), and polylactic acid (PLA) (Nature Works, Minnetonka, MN, USA). The particle sizes for all polymers were between 80 – 330 µm (detailed information in SI, Table 2).

Ultra-pure water (UPW) was produced using an arium® pro VF (Sartorius, Germany) with an ultra-filter and used for all steps. Hydrogen peroxide (H<sub>2</sub>O<sub>2</sub>) (30 %) was purchased from Merck, Germany and Carl Roth, Germany. Different batches were tested (ISO/ Ph.Eur. stabilized; for synthesis, stabilized, Carl Roth, Germany & VWR, Germany) to observe the impact of the different manufacturing standards of hydrogen peroxide quality on Fenton reaction kinetics. The ferric sulfate (FeSO<sub>4</sub>) catalyst was prepared using FeSO<sub>4</sub> 7H<sub>2</sub>O (Merck, Germany), which was weighed and dissolved in UPW and the pH was subsequently adjusted to 3 using sulfuric acid (H<sub>2</sub>SO<sub>4</sub>, 0.5 M; VWR, Germany). Potassium hydroxide (KOH, 10 wt%) was prepared from dissolving pure KOH pellets (Merck, Germany) in UPW. To minimize contamination by foreign particles, all reagents were filtered prior to application, using 0.2 µm syringe filters.

Sample filtration was performed using a vacuum filtration unit made of glass (DURAN, Germany). Filters used were 25 mm in diameter with a pore size of 0.2 µm track etched polycarbonate filters (PCTE, unsterile, Carl Roth, Germany). For rinsing glass apparatuses and producing stable microplastic suspensions, 0.1 % (V/V) of the surfactant Tween 20 (Merck, Germany) in UPW was utilized (SI, section 1.5).

#### *4.1.2.3. Contamination mitigation and quality assurance*

To ensure minimal air-borne microparticle cross-contamination, all experiments were conducted in a laminar flow box (Laminar Flow Module FMS series SuSi, Spetec, Germany). The samples were handled outside of this setup only when weighing the microplastics. During this process the samples were always covered with aluminum foil to prevent cross-contamination. Lab coats made only out of cotton were worn at all times to avoid plastic fibers contaminating the samples.

#### 4.1.2.4. Investigating the discrepancies in Fenton reactions

The authors of the current study were perplexed by the widely different Fenton reaction kinetics and behaviors reported in literature, and the lack of discussion thereof [33, 35, 42, 43, 54, 55]. The Fenton reaction is exothermic and should not require any external heating to exceed temperatures of 40 °C [56]. This was in accordance with the pre-experiments performed in this study, as well as reactions described by Hurley et al. [33] and Tagg et al. [43], where the digestion reactions with organic matrices were quick, needing merely 20 minutes to complete, and required cooling to prevent them from exceeding 40 °C. On the other hand, some studies mentioned reaction times up to 24 hours, or described heating the reactants externally to 75 °C [42, 55].

To investigate if the source of those discrepancies is somehow related to the various manufacturing processes used to produce hydrogen peroxide, identical H<sub>2</sub>O<sub>2</sub> concentrations (30 %) were used, albeit from five different commercially available batches **(i)** Hydrogen peroxide 30 %, stabilized, (Perhydrol®) EMSURE® ISO analytical reagent, Supelco® (Merck, Germany), **(ii)** Hydrogen peroxide 30 % ROTIPURAN® p.a., ISO, stabilized (Carl Roth, Germany), **(iii)** Hydrogen peroxide 30 %, Ph. Eur, stabilized (Carl Roth, Germany), **(iv)** Hydrogen peroxide 30 % for synthesis, stabilized (Carl Roth, Germany), as well as **(v)** Hydrogen peroxide 30 % stabilized, EMPROVE® ESSENTIAL Ph. Eur., BP, USP, SAFC® (Merck, Germany).

The Fenton protocol was performed identically with each one of these batches of hydrogen peroxide. No microplastics were used in these experiments, as the investigation was concerned merely with the kinetics and general behavior of the Fenton reaction itself. Thus, samples comprised only the filtered reagents (hydrogen peroxide and iron sulfate), no additional particles or organic matter were added to prevent any unforeseen implications. The reaction was performed as explained in Figure 7 and the SI, chapter 9.3.1, with a scaling factor (K) of 2 mL (SI, section 1.2), or simply (2 mL of FeSO<sub>4</sub> 7H<sub>2</sub>O<sub>2</sub> and 4 mL of H<sub>2</sub>O<sub>2</sub> as starting volumes (Figure 7)), resulting in a final total reagents volume of 16 mL. The experiments were performed in duplicates in 100 mL Erlenmeyer flasks. The temperature and pH of the reactions were recorded over time. To understand the effects of thermal dissipation/insulation on reaction kinetics, additional experiments for the selected hydrogen peroxide batches were performed by placing the 100 mL Erlenmeyer flasks on an aluminum

bench to simulate a larger heat dissipation condition, whereas plastic centrifugal tubes (50 mL) were used to simulate heat insulation.

Subsequently, the experiments with the 100 mL Erlenmeyer flasks were repeated but a 1.5x1.5 cm piece of paper tissue was placed inside each flask and allowed to react as before in order to observe the effects of different reaction kinetics on the removal of organic matter.

#### 4.1.2.5. Investigating the effects of sample preparation on microplastics

To ensure that sample preparation protocols do not interfere with the characterization of microplastic parameters as mentioned in (section 4.1.1.2 Parameters used in microplastic monitoring), they were investigated for changes in their size distributions as well as their characterization by  $\mu$ FTIR and Thermal Desorption-Gas Chromatography coupled with mass spectrometry (TD-Pyr-GC/MS), before and after applying the digestion protocols. Table 3 shows the samples that were prepared for these investigations. The samples were prepared in 50 mL glass flasks for Fenton samples, and 10 mL glass tubes for the rest. Polymers were each made as individual samples for all the tests listed below in order to assess the changes to each of them individually.

Table 3. Protocols that were investigated for their effects on the polymers.

Protocols	Description
Control	5 mL UPW @ Room Temperature
Fenton	As described in Figure 7 (2 mL FeSO <sub>4</sub> as a starting volume)
H <sub>2</sub> O <sub>2</sub>	As described in Figure 7 (5 mL H <sub>2</sub> O <sub>2</sub> )
KOH	As described in Figure 7 (5 mL KOH)
**Temperature control 60 °C	5 mL UPW @ 60 °C and 24 hours
**Temperature control 90 °C	5 mL UPW @ 90 °C and 20 Minutes

\*\*Only performed for size distribution analysis in order to isolate melting or agglomerating effects of the elevated temperature from the effect of the chemical reagents.

The temperature controls simulated maximum temperatures and durations encountered in each of the protocols (60 C° and 90 C° for H<sub>2</sub>O<sub>2</sub>/KOH and Fenton protocols, respectively, and were made for the same exposure times (24 hours and 20 minutes, respectively).

#### 4.1.2.5.1. Size distribution analysis by laser diffraction

Laser diffraction measurements for particle size distribution analysis were conducted using a Malvern “Mastersizer S long bed”, a small volume sample dispersion unit (SVSDU), and a sample disperser, all manufactured by Malvern Panalytical (UK). In the optical unit, a 2 mW He-Ne-laser with 633 nm wavelength, 18 mm beam width, and 2.4 mm beam length, was sent through a 300 RF lens, whose measurement range is 0.05-900 µm. The wet standard scattering model was applied. The refractive index of water was used as the refractive index of the medium. The refractive indices applied were 1.5295 (real) and 0.1 (imaginary) in 1.33 (medium). All measurements were carried out according to ISO 13320:2009-10 [187].

Duplicate samples and controls, each consisting of 200 ± 50 mg for PS, PE, PET, PA, PLA, and PVC as well as 60 ± 15 mg for PP were used as per Table 3. Each sample was further subdivided into two repetitions to improve the reliability of the analysis. All samples were suspended in 10 mL UPW containing a concentration of 0.1 % (V/V) of the surfactant Tween 20, vortexed for 40 seconds @2,500 RPM prior to analysis and then poured into the wet dispersion unit. Measurements were only made after waiting for 2 minutes to ensure full dispersion. The laser was aligned at the beginning of each measuring session. The background scattering was determined before adding the sample aliquots into the SVSDU, which was pre-filled with deionized water and then stirred for 2 min to ensure proper dispersion in the system. After each measurement the SVSDU was cleaned with a 0.1 % (V/V) Tween 20 solution. The weighted average of each size distribution was calculated to compare the treated samples against their corresponding control samples. Further, the smallest 10<sup>th</sup> percentile of the size distribution was also compared in order to observe if the smallest particles in the size distribution exhibited more size changes than the average size particles. Finally, to test the statistical significance, the frequency tables from the Mastersizer measurements were transformed to raw data by using the Real Statistics Resource

Pack add-in for Microsoft Excel, after which the data was exported to IBM's SPSS® Statistics package, where a Kruskal-Wallis 1-way analysis of variance (ANOVA) was performed for each polymer type across all treatment methods. These results were subsequently compared against their respective controls with a post hoc analysis. The differences were only considered significant if the probability (p) of the null hypothesis being true was smaller than 0.05.

#### 4.1.2.5.2. FTIR analysis

Samples and controls were prepared according to the protocols listed in Table 3, by weighing 2.5 mg of each of the microplastic types (PS, PE, PET, PP, PVC, PA, and PLA). Samples were then filtered through a gold-coated polycarbonate membrane (diameter 25 mm, pore size 0.8  $\mu\text{m}$ , Analytische Produktions-, Steuerungs- und Kontrollgeräte GmbH, Germany) and measured by  $\mu\text{FTIR}$  spectroscopy on Agilent Cary 620 spectrometer coupled to Agilent Cary 670 FTIR microscope, equipped with a 128 x 128 pixel Focal Plane Array detector. IR images were measured in reflectance mode at a spectral resolution of 8  $\text{cm}^{-1}$  within a spectral range from 3,750 to 800  $\text{cm}^{-1}$  and a number of 30 scans. Before IR imaging, a mosaic photograph of the samples was taken in order to visualize any changes of particle surface morphology. For each polymer type and treatment, spectra from ten particles were extracted from the IR image and their average spectra was calculated and normalized to values from 0 to 1. Additionally, further control particles were measured in ATR mode (Germanium crystal) in order to illustrate the differences between ATR and reflectance  $\mu\text{FTIR}$  analysis modes.

#### 4.1.2.5.3. Thermal analysis by TD-Pyr-GC/MS

The TD-Pyr-GC/MS analysis was conducted with a thermal desorption unit (TDU) equipped with a TDU Pyrolysis module, a Multipurpose sampler (MPS) robotic<sup>PRO</sup>, a Cooled Injections System CIS 4 with C506 (all by Gerstel, Germany) and an 7890B gas chromatograph equipped with an DB-5MS Ultra Inert column in combination with an 5977B MSD mass spectrometer (all by Agilent, USA). In the first step, the samples were thermodesorbed to analyze volatile compounds at a final thermo-desorption (TD) temperature of 200 °C. The sample was then cryofocused in the cooled injection system (CIS) at -50 °C. The desorption mode was split-less. The GC/MS method for

the TD step was adopted from Ochiai et al., 2005. [188]. However, the cryo-focusing was conducted at -50 °C instead of -150 °C. In the second step, the sample was pyrolyzed with a final temperature of 800 °C, followed by a GC/MS analysis. The mass spectrometer was operated in full-scan mode (m/z range 40 to 550) with electron impact ionization (70eV). For further details, refer to Reichel et al. (submitted).

Duplicate samples were prepared as per Table 3, by weighing 2.5 mg of each of the microplastic types. The reference particles of the polymers PS, PE, PLA, PET, PA and PP were analyzed using TD-Pyr-GC/MS; once without treatment (control) and once after applying the sample preparation method. The chromatograms of the TD and pyrograms were compared in order to detect possible changes for the untreated and treated polymers regarding the characteristic pyrolysis products. PVC analysis could not be conducted due to the limitation of the TD-Pyr-GC/MS.

#### *4.1.2.6. Determination of the organic matter removal efficiency from sludge samples*

Thickened sludge samples were collected from the return activated sludge (RAS) at a local wastewater treatment plant in the city of Freising, Germany. The organic content of the sludge was first determined via loss on ignition (LOI) by placing it in a furnace at 550 C° according to DIN 38409-1:1987-01 [189].

To gravimetrically determine the effectiveness of the three selected protocols, papers like Hurley et al. [33] used a procedure where sludge was first dried at 105 °C for 24 hours to establish the starting dry weight of the sludge before treatment. Digestion protocols were applied to the dried sludge, and what remained was then filtered, dried and weighed. The difference in weight between the starting dry weight and the final weight was assumed to correspond directly to the removal of organic matter.

This seemingly logical approach proved to be insufficient and error prone. The pre-experiments in this study revealed that following the aforementioned approach resulted in dried and hardened clay like material that clumped and did not readily digest via the applied protocols (SI, chapter 9.3.7). Therefore, a new approach was created where the sludge was not dried before treatment, instead its starting dry weight would be based on a control sample (surrogate). The process was performed in parallel as shown below in Figure 8.



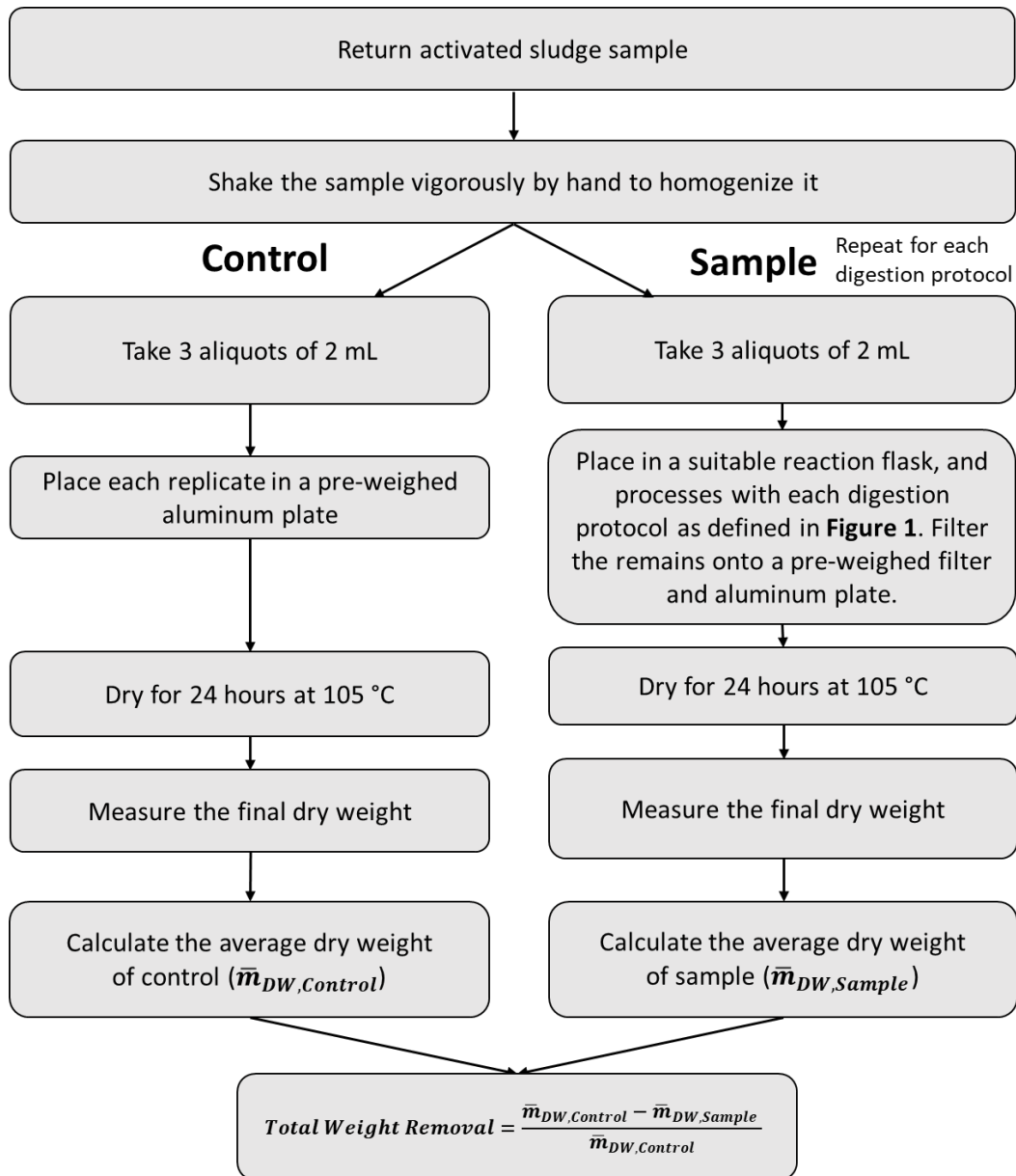


Figure 8. The workflow used in this study for investigating the organic matter removal efficiency.

Finally, studies assumed that all weight loss from digestion protocols corresponded directly to organic matter removal [33], even though there is a certain number of inorganic and organic constituents that will dissolve during digestion, thus presenting additional weight loss that could be misconstrued as organic matter removal. This might explain findings of some studies like Hurley et al. [33] who reported organic matter removal efficiencies over 100 %. To showcase that the total weight loss after digestion may not entirely be due to the organic matter removal, ultrapure water was added to 2 mL sludge aliquots. They were then left for 2 hours to dissolve readily solvable inorganic and organic fractions, filtered and subsequently dried for weight

determination. This was done in duplicates, following the workflow described in Figure 8.

### 4.1.3. Results and discussion

#### 4.1.3.1. *Discrepancies in Fenton reactions*

The reasons behind the aforementioned surprising descriptions of Fenton reactions in the literature can finally be understood based on the experiments of this study, as two general behaviors for the Fenton reaction were observed, when testing the five aforementioned batches of hydrogen peroxide. These differences occurred despite employing identical protocols and concentrations. To the best of the authors' knowledge, these different reaction behaviors have not been discussed in the literature before. Thus, it is important to understand the mechanism behind these behaviors. This is important to assure reproducible Fenton based sample preparation methods. These two general behaviors of the Fenton reaction are subsequently referred to as type I and type II Fenton reactions:

**Type I Fenton reaction:** This reaction type has been used and validated in this study and can be reproduced when using batches i, ii, iv & v. Its typical behavior was to start fizzing immediately after mixing the reactants, accompanied by a rapid temperature increase, which peaks at the range of 82 – 90 °C within 2 – 4 minutes, depending on the flask's thermal insulation, as the reaction reaches its maximum intensity. This can be described as a boiling-like behavior and a change in color from an initial dark color to orange due to formation of iron precipitates. The reaction kinetic showed some variation but it was largely consistent between runs as well as between different hydrogen peroxide batches as can be seen by the similar maximum temperatures and low standard deviation for the four batches presented in Table 4.

**Type II Fenton reaction:** This type was observed only when using batch iii of hydrogen peroxide. It typically exhibited a slower reaction kinetic than type I reactions. The initial fizzing was either very weak or missing. Temperatures increased at a lower rate than type I reactions and a critical temperature of 55 °C was needed in order to initialize boiling, which when occurred, would reach 82 – 90 °C within 7-10 minutes. However, the reaction was erratic as can be seen in the elevated standard deviation values of batch iii compared to the remaining batches in Table 4. Identical parallel

tests were performing differently, some reaching the boiling phase and others staying below 55 °C and failing to initialize boiling. This was especially true when the Erlenmeyer flasks were placed on the aluminum bench to simulate larger heat dissipation (Table 5). The experiments were repeated with two different bottles of batch iii to ensure that it was not a coincidence.

*Table 4. The reaction differences for the five batches of hydrogen peroxide when using 100 mL Erlenmeyer flasks on the rubberized bench. T<sub>max</sub>: maximum temperature.*

<b>H<sub>2</sub>O<sub>2</sub> Batches</b>	<b>T<sub>max</sub> [°C]</b>	<b>pH @ T<sub>max</sub> [-]</b>	<b>Time till T<sub>max</sub> [sec]</b>
(i)	86.9 ± 0.9	1.62 ± 0.03	157 ± 4
(ii)	87.2 ± 0.2	1.67 ± 0.06	167 ± 19
(iii)	70.4 ± 23	1.72 ± 0.23	510 ± 127
(iv)	85 ± 0.4	1.67 ± 0.05	173 ± 11
(v)	84.9 ± 1.7	1.69 ± 0.04	192 ± 5

Surprisingly, type II reactions exhibited much more consistent results when using the more thermally insulating 50 mL centrifugal tubes, consistently reaching 90 ± 0.5 °C within 3 – 4 minutes, very similar to the kinetics of type I when performing the same test. This indicates that heat insulation plays a much larger role for type II reactions than it does for type I, which had a very consistent behavior, regardless of heat insulation of the used reaction flask. The color change still occurred as was the case with type I, albeit the end color is a light yellow instead of orange, indicating that different iron species could be involved. The reactions that failed to initialize boiling had even less precipitation of iron (III), as shown in (Figure 9).

*Table 5. The reaction difference for type I and II Fenton reaction when using 100 mL Erlenmeyer flasks on the aluminum bench for heat dissipation.*

<b>Reaction type</b>	<b>T<sub>max</sub> [°C]</b>	<b>pH @ T<sub>max</sub> [-]</b>	<b>Time to T<sub>max</sub> [sec]</b>
Type (I) (batch (ii))	84.1 ± 3.4	1.65 ± 0.09	228 ± 3
Type (II) (batch (iii))	60.8 ± 29.3	1.7 ± 0.25	554 ± 190

Finally, when using 100 mL Erlenmeyer flasks with tissue papers; type I consistently visually digested the paper at the end of the reaction, a similar result was observed on the tests where type II would initialize boiling. However, when type II failed to reach

the critical temperature needed for the boiling phase, the paper tissue was still visibly floating at the end of the reaction (Figure 10). Since the reaction of type II is very unpredictable, it was excluded from this study and was not further validated.

Based on the observations revealed in this study, it is assumed that type II reactions were used in works like Masura et al. [42], where they needed to heat the reactants to 75 °C to exceed the critical temperature discussed above and thereby initializing the boiling phase of the reaction. It can also be seen in the study of Prata et al. [35], who heated the reaction at 50 °C for 1 hour. The slower kinetics of type II could also explain the long reaction times in studies like Prata et al. and Flotron et al. [35, 55]. Whereas type I might be the one used in investigations such as Hurley et al. and Tagg et al. [33, 43] where no additional heat was needed to start the reaction and reaction times were short.

The formation of iron precipitates during Fenton reactions was not mentioned in microplastic related studies. This might cause problems during filtration when not addressed (especially for type I), as iron precipitates tended to remain on the filters and covered the microplastics, which would have prevented particle identification. This was solved in this study by adding 5 % (v/v) of 98 % sulfuric acid at the end of the reaction, which quickly reacted with the precipitating iron species and dissolved them within 30 seconds (Figure 7).

It became obvious that the reaction behavior of Fenton is influenced by the employed batch of hydrogen peroxide. It can be assumed that the stabilization agents added to the hydrogen peroxide is the critical factor for differentiation of the type I and type II reaction behaviors. However, the stabilization agents are not stated by the manufacturers directly and were not further investigated within this study.

The validations performed in this study followed type I Fenton reaction by using batch (ii) of the hydrogen peroxide for all subsequent validation experiments.

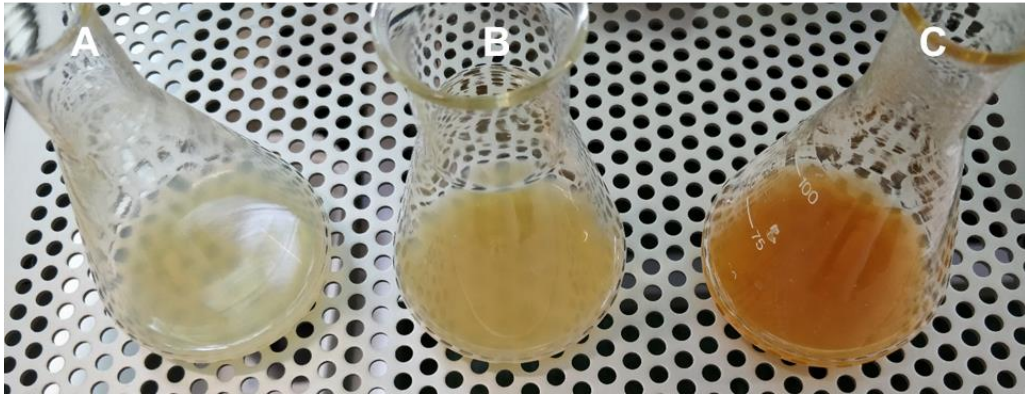


Figure 9. Visual difference between type I & II Fenton reactions (end of reaction). A: type II that failed to initialize boiling. B: type II which initialized boiling. C: type I.

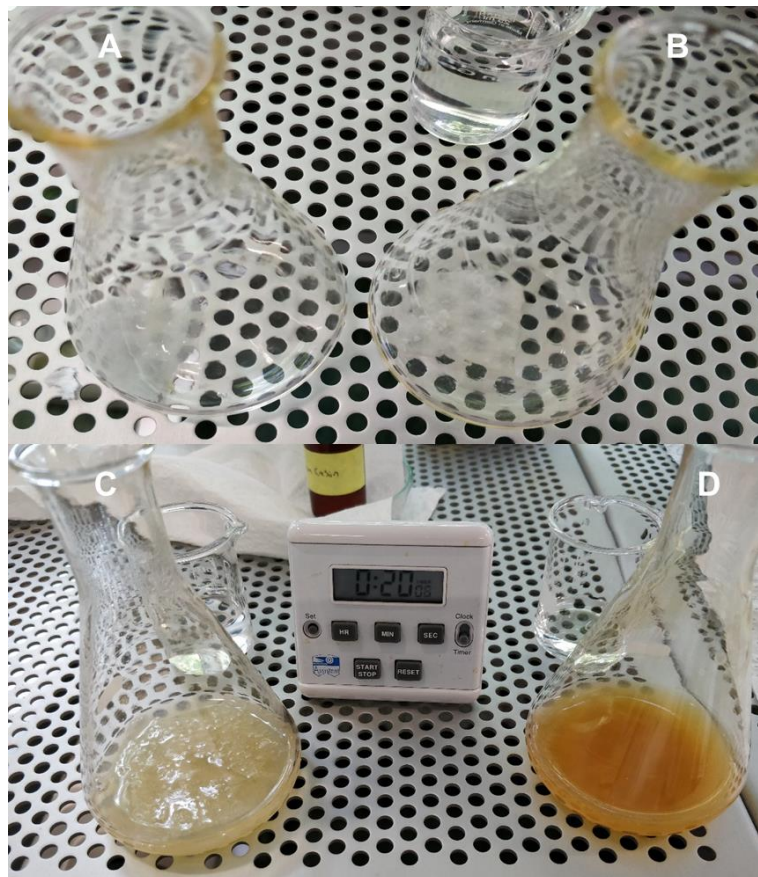


Figure 10. Differences between type I Fenton reaction and a type II Fenton reaction that failed to initialize boiling when digesting a piece of tissue paper. A, C: type II before and after reaction. B, D: type I before and after reaction.

#### 4.1.3.2. Investigating the effects of sample preparation on microplastics

##### 4.1.3.2.1. Variation in size distribution (Laser diffraction)

Some polymers such as PLA and PET did not tolerate the KOH protocol. Hence, the majority of PET and PLA particles were dissolved after the KOH digestion. The

remaining few particles in the suspension after digestion did not produce enough signal to be reliably detected. Nevertheless, the resulting signal for PLA still showed a significant reduction in the size of the surviving particles as can be seen in Figure 11 for PLA. On the other hand, PS exhibited a slight size increase which indicated the formation of a few small agglomerates or swelling. The rest of the polymers showed little to no change after being exposed to KOH. The effect of KOH on PLA, PET and PS can clearly be seen in Figure 12. The changes were statistically significant after using Kruskal-Wallis post hoc pair tests, with ( $p = 0.00$ ) for both PLA and PET and ( $p = 0.006$ ) for PS, both of which are well below the significance value ( $p > 0.05$ ).

Using a 1 and 10 M NaOH and 60 °C for 24 hours, Hurley et al. [33] observed a degradation of PET. They attributed it to the saponification of ester bonds on the polymer's surface. However, they observed no such effect when using KOH (10%) with the same conditions. Other studies also observed no adverse effect on PET particles when using different KOH protocols [36, 40, 190]. This might be because the aforementioned studies utilized larger microplastics ( $> 500\mu\text{m}$ ) which possessed lower surface area to volume ratios, making them potentially less susceptible to the digestion reagents than the microplastics used in this current study. This issue, when coupled with the very small number of particles used in the aforementioned studies, can severely reduce the reliability of their results. As for PLA, no study was found that tested it specifically with the protocols chosen in the current study. However, Kühn et al. [190] tested six biodegradable microplastic particles with 1 M KOH at room temperature for 2 days. The authors observed that PLA particles, derived from biodegradable bags, were completely dissolved after applying the treatment. This agrees with the results found in the current study.

Fenton and hydrogen peroxide protocols both showed no significant changes regarding the size distribution of the tested polymers (Figure 12), with the exception of PLA, which exhibited slight agglomeration tendencies with increased temperatures, especially during Fenton reactions, which can briefly reach 90 °C. This manifested itself as an average size increase for PLA of 8.6 % and 16.9 % for hydrogen peroxide and Fenton, respectively (Figure 11 and Figure 12). These changes were statistically significant only for Fenton though ( $p=0.04$ ). The temperature controls showed a more extreme case with 9.4 % and 28.9 % size increase for 60 °C and 90 °C, respectively (Figure 13). The temperature controls for 90 °C even showed a larger statistical

significance when compared to the Fenton samples ( $p=0$ ). This indicated that indeed, the forming of agglomerates was caused by increased temperatures. Possibly by making the particle's surface sticky, which caused some of the particles to randomly adhere to each other. This is supported by the fact that PLA has a glass transition temperature of around 60 °C, which would cause it to become sticky past this temperature [191]. Still, the changes were not disastrous, and the information about the particles was not lost as a result of melting. Although, when accurate size assessments for PLA are needed, when using these Fenton or hydrogen peroxide protocols, it is recommended to apply a correction to the average sizes to account for these results. This was also the main reason for suspending the particles after treatment in 0.1 % Tween 20 solution and vortexing for 40 seconds before an analysis was made, as it helped to break some of the agglomerates.

In order to understand the effect on smaller particles, the changes to the smallest 10<sup>th</sup> percentile of the size distribution ( $D(v,0.1)$ , abbreviated here as  $d_{10}$ ), were investigated. Figure 11 provides a visual representation of  $d_{10}$  (green highlight). The smaller particles can be more susceptible to degradation during treatment because of their larger surface area to volume ratios. Based on the  $d_{10}$  fractions, the tendency for severer size changes on smaller particles could be observed, although the accuracy of the measurement degraded when measuring the smallest 10<sup>th</sup> percentile. This can be seen in Figure 12 and Figure 13 by the larger standard deviations for  $d_{10}$ , compared to the mean size measurements. This might be attributed to the reduction of accuracy in light scattering techniques when larger and smaller particles are present in the same sample, as larger particles scatter the light at larger angles than smaller particles and might cover them.

It can be further inferred from the results presented in Figure 12 and Figure 13, that there are more statistically significant size changes for  $d_{10}$  than when testing the larger particles. However, due to the reduced measuring accuracy of the Mastersizer under these conditions, concrete conclusions cannot be drawn, other than there is probably an increased tendency for smaller particles to be affected by the applied treatments.

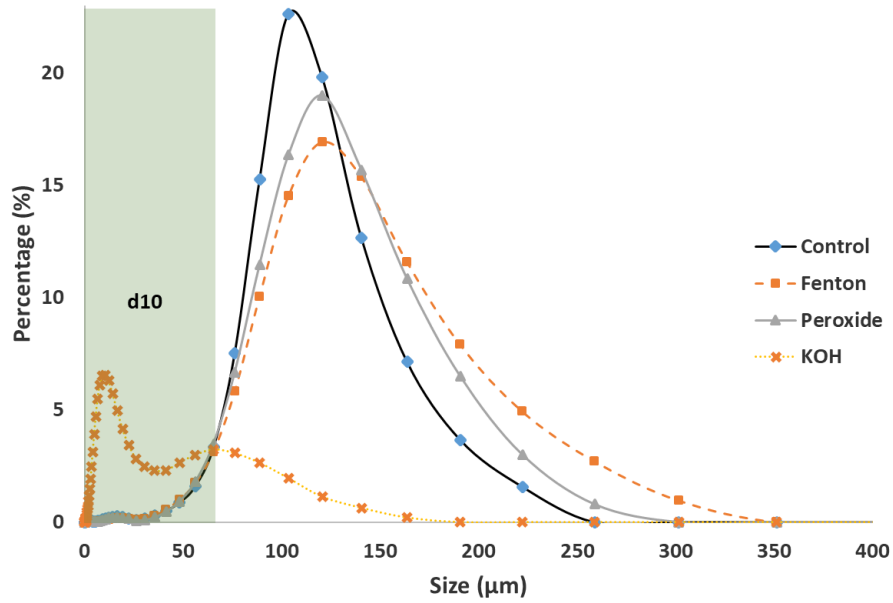


Figure 11. Size distribution analysis for PLA, the green area represents the smallest 10<sup>th</sup> percent (d10).

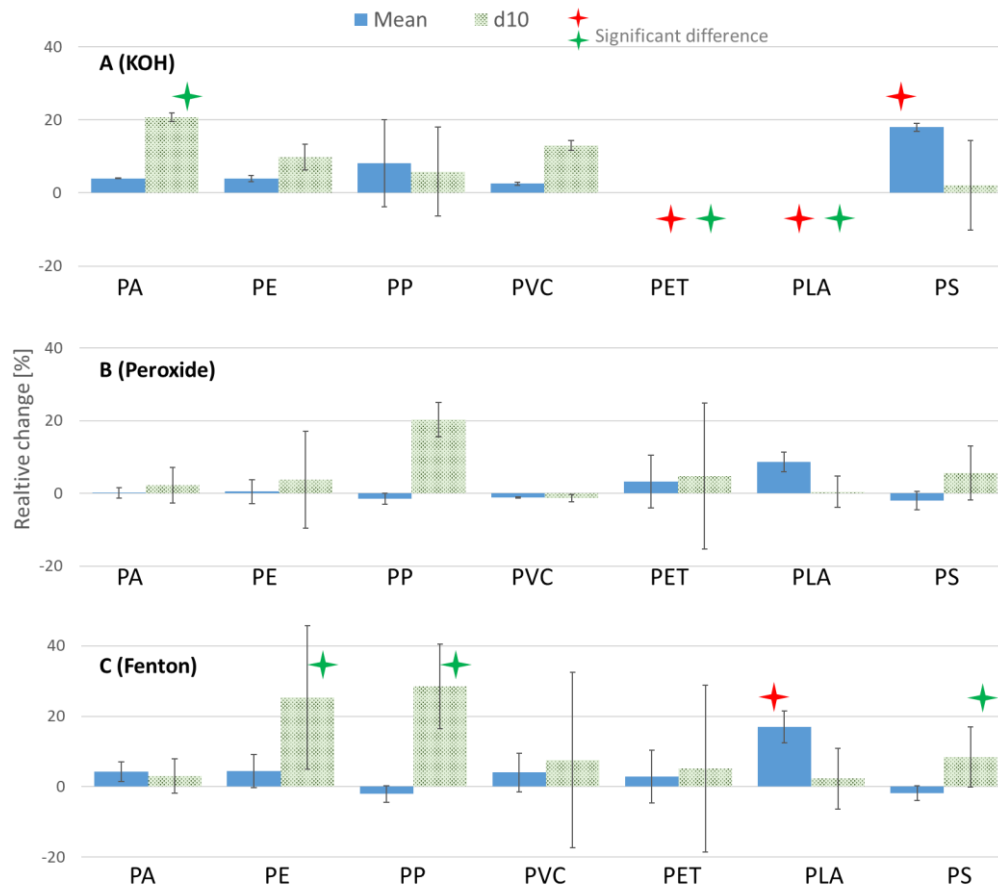


Figure 12. Relative particle size changes after treatment compared to the controls (for weighted average sizes & 10<sup>th</sup> percentiles (d10)). The error bars represent the standard deviations. PLA and PET in fig (A) were completely destroyed. The red and green stars indicate statistical significance for the entire distribution, as well as d10, respectively.



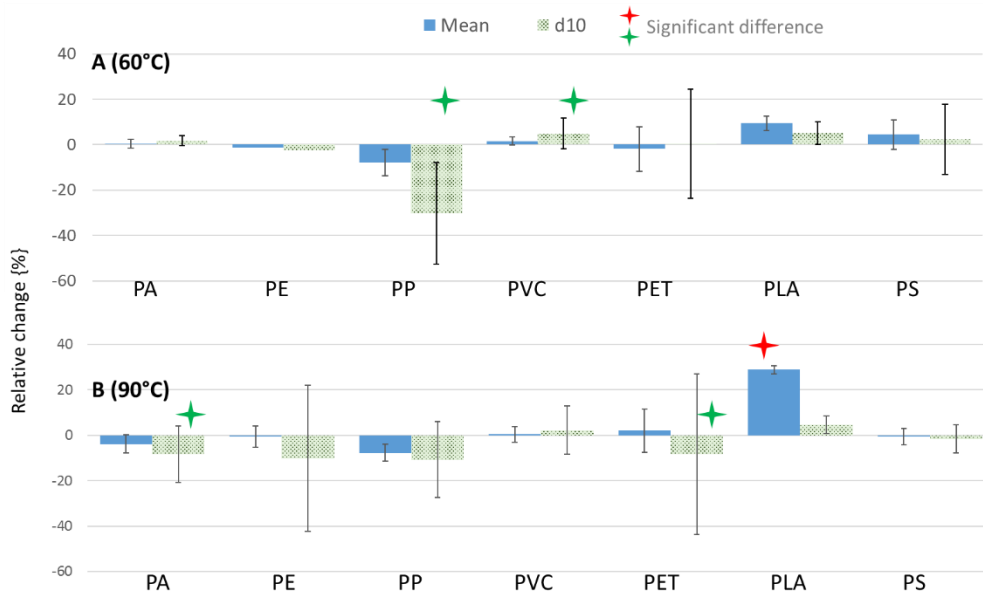


Figure 13. Relative particle size changes after temperature treatments compared to controls (for weighted average sizes & 10<sup>th</sup> percentiles (d10)). The error bars represent the standard deviations. A: 60 °C for 24 hr, B: 90 °C for 20 min. The red and green stars indicate statistical significance for the entire distribution, as well as d10, respectively.

#### 4.1.3.2.2. Variation in infrared spectra (FTIR)

$\mu$ FTIR spectra of the treated microplastic particles in general revealed only few alterations compared to untreated (reference) particle spectra (SI, Figures 9-15). Most of the modifications were small and are not suspected to hamper polymer identification.

As discussed for the size distribution experiments, the majority of PLA and PET microparticles were dissolved after the KOH treatment and consequently their spectra were expected to be altered severely. However, only small changes were observed in the spectra of the few remaining particles after KOH treatment (Figure\_4.1\_A. 1 and Figure\_4.1\_A. 2). All treated PLA particles exhibited a relatively narrow band of intermediate strength at 3,500  $\text{cm}^{-1}$  (Figure\_4.1\_A. 2). This band was a lot broader in untreated PLA particles. Spectra of KOH treatment induced a weak band at 3,650  $\text{cm}^{-1}$  to the PLA spectrum. Both bands indicate that OH groups were formed during sample treatment. Such OH groups were described by Zhang et al. [192] when investigating infrared spectra of PET.

The spectra of the KOH-treated PET particles (Figure\_4.1\_A. 1) lacked the shoulder present in untreated particles at the C=O band at 1,720  $\text{cm}^{-1}$ . Additionally, the band at

1,945  $\text{cm}^{-1}$ , an aromatic C-H bending overtone, was weaker compared to the other samples. This is in accordance with the fact that alkaline hydrolysis can be used in the recycling process of PET [193]. Nevertheless, these changes were quite small and are not suspected to hamper polymer identification.

In PVC, all digestion protocols induced a band at 3,300  $\text{cm}^{-1}$ , representing the formation of OH groups by the oxidative reagents, indicating a hydroxylation at the surface (Figure\_4.1\_A. 3) In general, the spectral changes observed were small, however, they may lead to confusion of inexperienced users during spectra interpretation. If the spectral range above 3,000  $\text{cm}^{-1}$  is considered for polymer identification in a database search, it is recommended to include an altered PVC spectrum into the database. The rest of the microplastics exhibited no changes after the digestion protocols.

It can be concluded that if PLA and PET are among the target polymers for microplastic analysis, samples should not be treated with KOH. It is very likely that the few PLA and PET particles detected in the KOH samples investigated in this study were outliers that used to be much larger prior to the KOH digestion, whereas the vast majority of the particles were too small and dissolved during KOH digestion.

As was mentioned earlier, due to the easy handling, usually attenuated total reflection (ATR) mode is used for validation by researchers. However, ATR is suitable only for clean isolated particles that are big enough to be placed on the ATR crystal individually and therefore, this mode is not applicable for small microplastic particles ( $< 500 \mu\text{m}$ ) from environmental samples. This is where FTIR microscopy ( $\mu\text{FTIR}$ ) is used instead. The usage of focal plane array (FPA) detectors enables the generation of FTIR images across a big sample area and therefore reduces measurement time for real samples. Often, studies would use ATR spectra of reference particles to identify the spectra of a sample, regardless if the latter were obtained using ATR or  $\mu\text{FTIR}$ . But the spectra obtained with the two methods are not perfectly comparable without mathematical correction to account for the wavelength-dependent differences in penetration depth. Because penetration depth decreases with increasing wavenumbers for ATR measurements, the C-H stretch region around 2,900  $\text{cm}^{-1}$  exhibits very weak absorption bands. These bands are significantly larger for  $\mu\text{FTIR}$  spectra. That is why in this study, particle alterations due to chemical treatment were examined by

comparing treated and untreated  $\mu$ FTIR spectra with each other to reduce bias caused by different spectral acquisition modes.

In Figure 14, a  $\mu$ FTIR reflectance mode spectrum of an untreated PET particle is shown in comparison to an ATR spectrum of the same material. Both spectra were normalized. The ATR spectrum is not ATR-corrected, thus, the differences between the spectra are fairly substantial, especially at higher wavenumbers. As was already discussed by von der Esch et al. [119], ATR spectra represent mostly the particle surface because of the low penetration depth compared to  $\mu$ FTIR spectra which in the lower wavenumbers penetrate more deeply into the material and therefore represent the bulk properties of the particle. In manual data evaluation as well as in automated approaches, this can lead to confusion and misinterpretation. It is therefore recommended to establish a reference database comprising of  $\mu$ FTIR spectra in transmission and/or reflection mode, depending on the sample measurement method.

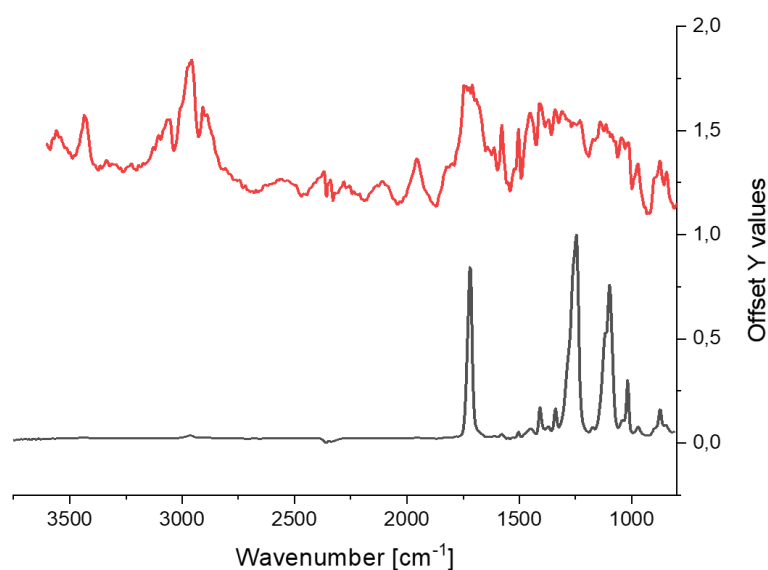


Figure 14. Normalized FTIR spectra of reference PET particles. Top: measured in reflectance mode on FTIR microscope; bottom: measured in ATR mode

#### 4.1.3.2.3. Variations in Pyr-GC/MS chromatograms

As KOH resulted in significant degradation of PLA and PET particles, it was excluded from this analysis. The characteristic substances of the polymers PE, PLA, PET and PP were completely decomposed during pyrolysis. However, in the case of the polymers PA and PS, treatment with Fenton and  $H_2O_2$  had an influence on their thermal stability. The ratio of the volatile pyrolysis products observed during the

thermal desorption step at 200 °C to the stable pyrolysis products at 800 °C was decreased after treatment, especially PA (Table 6). This means that the amount of pyrolysis products that were volatile at 200 °C was reduced after applying the treatments, and more of the pyrolysis products were remaining stable until the second pyrolysis step at 800 °C. Nevertheless, all of the polymers were still clearly identifiable in all cases. The pyrolysis products of the individual polymers are shown in (SI, Table 3).

*Table 6. Influence on the partial pyrolysis of thermal desorption (TD) products at 200 °C for both PA und PS.*

<b>Polymer type</b>	<b>Particle treatment</b>	<b>Pyrolysis Products in TD [%] / Standard deviation [%]</b>
PA	untreated	74.5 / 19.0
	Fenton	17.1 / 12.65
	H <sub>2</sub> O <sub>2</sub>	3.0 / 3.67
PS	untreated	79.3 / 12.5
	Fenton	78.8 / 16.9
	H <sub>2</sub> O <sub>2</sub>	71.9 / 10.9

#### *4.1.3.3. Organic matter removal efficiency*

Since the KOH protocol degraded PLA and PET, only H<sub>2</sub>O<sub>2</sub> and Fenton protocols were considered for further investigations. First, the dry weights of the sludge control aliquots (surrogates) were established as was described in Figure 8. The triplicates exhibited highly consistent results with a standard deviation of < 5 % (average dry weight was 75.17 ± 3.55 mg). Therefore, implementing the dry weight of the controls as reference for the removal efficiency, as was described in Figure 8, can be seen as a better alternative to the reported method of drying the sludge of each sample before digestion to establish its dry-weight. As explained in the methods chapter, this would have had a far greater impact on the results, due to the hardening and clumping of dried sludge, thus reducing the efficacy of the digestion. This could in fact explain the higher removal efficiency compared to Hurley et al. [33]. As they used similar protocols but dried each sludge sample before applying digestion.

As indicated before, usually the lost weight is taken to correspond directly to the loss of organic matter. However, the organic content of the dry sludge was determined to

be 70.5% via loss on ignition (LOI). Based on this, organic removal efficiencies > 100 % were obtained (Table 7). This clearly cannot be the case. This can be explained by the dissolution of some inorganic salts and inorganic carbon, which would pass through during the filtration process and be observed as extra lost weight. Hence, extra samples were investigated, where sludge aliquots were mixed with UPW as described in the previous chapter. The results revealed that dissolution of the readily solvable organic and inorganic compartments in ultrapure water had a weight reduction of around 5.9 % ± 2.3 %. This is far from negligible and indicates that some organic and inorganic content was dissolved and registered as extra weight loss. This phenomenon is expected to intensify for lower pH values and higher temperatures, such as the ones encountered during the Fenton and hydrogen peroxide protocols. However, this wasn't necessary for the scope of this paper, as the comparison between protocols did not require exact knowledge of the removed inorganic components. This side experiment was only intended as a proof of concept to clarify the reported removal percentages which are sometimes larger than 100 % in literature. In fact a study by Karami et al. [44] did not dry the biological samples beforehand, which compromised the absolute removal values they reported, but as a comparative tool between the investigated protocols, it was still a valid result, as all samples were treated equally. Thus, no further investigations regarding this were perused.

*Table 7. Average total and corresponding organic removal efficiencies for the investigated protocols.*

<b>Protocol</b>	<b>Total weight removal</b>	<b>Corresponding organic matter removal**</b>
Fenton	83.5 % ± 1.8 %	118.4 % ± 2.6 %
H <sub>2</sub> O <sub>2</sub>	71.3 % ± 1.2 %	101.1% ± 1.6 %

\*Results represent the average and standard deviation for the three sample repetitions.

\*\* The results were not adjusted to account for the loss of inorganic matter, hence removal efficiencies over 100 % are present.

Finally, Figure 15 shows a visual comparison of the filtered results from the hydrogen peroxide and Fenton protocol for the gravimetric analysis. Even though the weight difference between the sludge treated with Fenton and hydrogen peroxide protocols was not large, the characteristic of the remaining material differed between the two. Whereas the hydrogen peroxide treated sample showed visible particulate matter after digestion, Fenton showed only coloration of the filter with no visible organic particles.

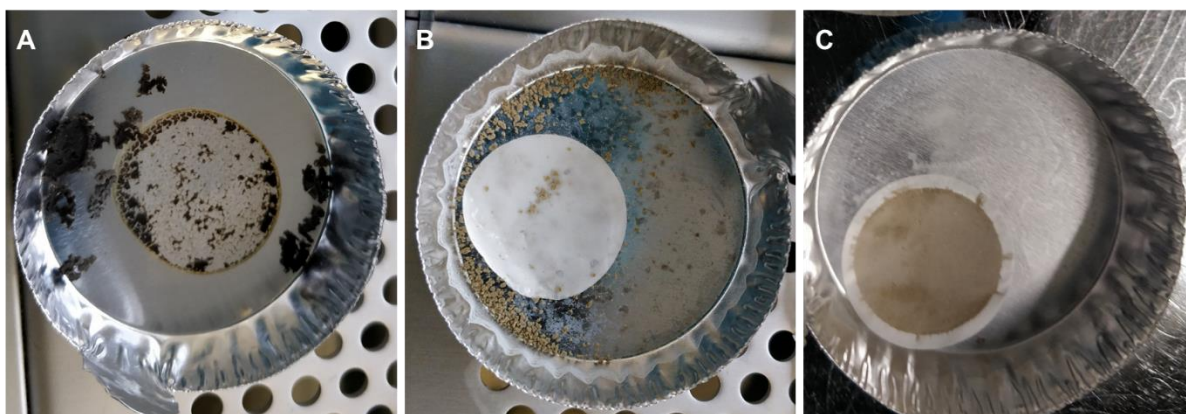


Figure 15. The end result of the gravimetric analysis done on 2 mL of sludge. A: dried sludge (surrogate) B: dried retentate and filter after hydrogen peroxide treatment, C: dried retentate and filter after Fenton treatment.

#### 4.1.4. Conclusion

If one sentence could summarize the findings of this paper, it would be: “the devil is in the details”. The initial intention of the authors was to screen through sample preparation methods in the literature and adapt and validate the most suitable methods for microplastic monitoring in wastewater samples. It was soon clear however, that large variations existed between the reported results in the peer-reviewed literature. Further, it was not always possible to simply replicate the results due to seemingly insignificant missing details, which turned out to be basic but essential to take into account when replicating someone’s work. Therefore, this study tried to consider even the smaller details in order to clarify the reasons behind the different results in literature. Along the journey, surprising but important discoveries were made regarding the different types of Fenton reactions that exist, even when one is seemingly using identical chemical reagents and protocols. The study recommends using the Fenton reaction as described in Figure 7 as well as the SI, section 1.2. It provided excellent organic matter removal efficiency from wastewater samples in a very short amount of time and had very little adverse effects on the seven investigated microplastic types. However, it is of utmost importance that the used sort of hydrogen peroxide has to be tested beforehand to ensure that it provides a type I Fenton reaction as was defined in this study. Type II Fenton reactions were explored and defined in this study, but they were not validated and are not recommended for this application due to their much slower reaction kinetics. The use of hydrogen peroxide also provided similar results to

Fenton, but the much longer reaction times (24 hours as opposed to 20 minutes) limits the rapid throughput potential of the latter when compared to Fenton. Additionally, the remaining organic particles after the hydrogen peroxide digestion (Figure 15), could constrain particle counting and identification.

### *Acknowledgment*

This research was funded by the Bayerische Forschungsförderung, grant number 1258-16 and by the German Federal Ministry of Education and Research (BMBF), grant number 02WPL1443A.

## 4.2. Sample preparation for sub-microplastics

This sub-chapter deals with the further validation of the developed protocols (from chapter 4.1) for small microplastic particles ( $\leq 10 \mu\text{m}$ ) as well as nanoplastics. This subchapter deals with testing **hypothesis 2**.

*“**Hypothesis (2)** The size distribution of sub-microplastics ( $\leq 10 \mu\text{m}$ ) is reduced by more than 10% after directly applying the selected sample preparation methods based on hydrogen peroxide and Fenton as specified for Hypothesis 1”*

This sub-chapter has already been published as follows:

Mohammed S.M. Al-Azzawi, Oliver Knoop, Jörg E. Drewes. Validation of sample preparation methods for small microplastics ( $\leq 10 \mu\text{m}$ ) in wastewater effluents, **Chemical Engineering Journal**, Volume 446, Part 1, 2022, 137082, <https://doi.org/10.1016/j.cej.2022.137082>. - Reproduced by permission of the respective journal.

### **Author contribution:**

**Mohammed S. M. Al-Azzawi:** Conceptualization, methodology, sample analysis, writing; **Oliver Knoop:** Supervision, Project Administration, Reviewing and Editing.; **Jörg E. Drewes:** Supervision, Project Administration, Funding Acquisition, Reviewing and Editing.

### *Abstract*

The interest to monitor microplastics in various environmental matrices has grown substantially in recent years. However, monitoring microplastics remains a challenge due to interactions with complex environmental matrices, especially those rich in natural organic matter (NOM) like wastewater effluents. Therefore, sample preparation methods are needed to remove NOM and ensure minimal interference during analysis. So far, there have been only a few attempts to standardize and validate the effects of sample preparation methods on microplastics. However, no efforts exist that validated the impacts of sample preparation methods on small microplastic particles ( $\leq 10 \mu\text{m}$ ). Those smaller particles might be more susceptible to adverse effects after chemical digestion as a result of the increased surface area to mass ratio, compared to their larger counterparts. In this study, pellets from six polymers were successfully tagged



with a fluorescent dye and subsequently fractured using ultrasound treatment to produce small particles of tagged microplastic. The generated microplastics ( $\leq 10 \mu\text{m}$ ) were then subjected to two sample preparation methods that were previously validated for wastewater effluents, namely Fenton and hydrogen peroxide oxidation. The effects on microplastics were assessed using size distribution changes, which were measured via fluorescence microscopy. Results revealed some large changes in the size distribution of microplastics ( $\leq 10 \mu\text{m}$ ) after applying Fenton and hydrogen peroxide. However, these changes were largely reduced when excluding particles  $< 1 \mu\text{m}$ . The results indicated that, for the most part, both sample preparation methods can be used for small microplastic particles (1 - 10  $\mu\text{m}$ ), whereas hydrogen peroxide is more suitable if nanoplastics ( $< 1 \mu\text{m}$ ) are to be investigated.

### **Keywords**

Fluorescence microscopy; Nile red; oxidation digestion; nanoplastics; small microplastics; Fenton

#### **4.2.1. Introduction**

Interest in microplastic research has been steadily increasing in the last few years. Microplastics are generally defined as plastic particles less than 5 mm in size, though microplastics between 1 – 5 mm are referred to as large microplastics, whereas plastic particles smaller than 1 mm are called microplastics [8–12, 23, 62, 69, 123]. However, recently there is increasing interest to also study small microplastic particles in the low micrometer range since these particles might result in adverse health effects [194]. Analyzing environmental samples containing such small microplastics is constrained by interference resulting from natural organic and inorganic matter. Examples of those would be animal and plant debris, sand and silt [61]. These constituents need to be separated before a proper analysis can take place. Inorganic particles are often denser than microplastics and as such, gravity separation techniques might be used to remove them using various salt solutions [33, 50]. On the other hand, many organic particles possess a density very similar to plastics and cannot be effectively removed via gravity separation [28, 50]. Thus, organic matrices are commonly removed by chemical digestion by applying acids, bases, oxidation, or enzymatic reagents [33, 36–41, 44–49, 91]. Wastewater treatment plants (WWTPs) represent a potential point

source of microplastic emissions to the aquatic environment. Several studies exist that have quantified microplastic emissions from WWTPs but reported widely varying results [19–22]. This can be due to the inherent differences between the performance of WWTPs, but also due to the different analytical techniques utilized [20, 22, 32, 84, 89]. The concern for this study was the validation of sample preparation methods as part of the analytical process. Many studies have shown that these reagents can inadvertently impact microplastic particles [33, 36, 37, 40, 180–182]. Several studies attempted to validate sample preparation methods and to quantify their effects on microplastics. However, these studies were limited to microplastics  $>10\ \mu\text{m}$  [33, 35, 38, 43, 44].

Due to their larger surface to volume ratios, smaller microplastics are more susceptible to chemical treatment when compared to larger microplastic particles. In a previous study by the authors, some evidence was reported that small particles could be more affected by sample preparation methods, but the analytical data did not allow a conclusive assessment for this size range ( $\leq 10\ \mu\text{m}$ ) [57].

The lack of data for those small microplastics is also due to the challenge in manufacturing microplastics at this small size range. PE and PS are available in various sizes as micro- and even nano-spheres that are manufactured and sold directly for research and commercial purposes. Other types of microplastics, however, could not be commercially obtained this way.

Von der Esch et al. discussed the manufacturing of nanoplastic suspensions using large plastic fragments exposed to ultrasound treatment (@35 kHz) in a 0.25 M KOH solution for 15 hours [119]. This can prove to be a useful method, if modified to generate small microplastics instead of nanoplastics. Moreover, the presence of KOH was reported by the authors in a previous study to be detrimental to several polymer types such as PET and PLA [57]. For example, KOH has been shown to induce an alkaline hydrolysis in PET which causes chain scission at the ester group which reduces the molecular mass [195]. PLA suffers from the same weakness where the ester group can be a weak link and open to cleaving via hydrolysis [196]. Therefore, a method based on ultrasound treatment that is intended to generate small microplastics ( $\leq 10\ \mu\text{m}$ ) for a validation study must eliminate exposure to KOH and optimize the ultrasound power and contact time in order to render the required particle sizes without inducing unnecessary stress on the polymers.

The aim of this study was to validate the two previously investigated sample preparation methods (Fenton and hydrogen peroxide oxidations) to not adversely affect small microplastics ( $\leq 10 \mu\text{m}$ ).

## 4.2.2. Methodology

### 4.2.2.1. Materials

The following different polymers were purchased either as larger fragments or pellets ( $>5 \text{ mm}$ ): low density polyethylene (LDPE), polyvinyl chloride (PVC), fluorescent polystyrene (PS) (Ineos, London, UK), polypropylene (PP) (Borealis, Vienna, Austria), polyethylene terephthalate (PET) (TPL, Zurich, Switzerland), polylactic acid (PLA) (Nature Works, Minnetonka, MN, USA), and polyamide (PA) (Lanxess, Cologne, Germany).

Hydrogen peroxide (30%) (Carl Roth, Germany) was used for both Fenton and hydrogen peroxide oxidation protocols. Ferric sulfate solution for the Fenton reaction was prepared from a hydrated salt (Merck, Germany). The pH value was then adjusted using 0.5 M sulfuric acid (98%, VWR, Germany). The filters used for separating larger particles were  $10 \mu\text{m}$  and  $5 \mu\text{m}$  nylon membrane filters (Carl Roth, Germany). Filters used for microscopic analysis were track etched polycarbonate filters ( $0.2 \mu\text{m}$ , Carl Roth, Germany). Nile red dye was obtained from Carl Roth, Germany. An ultrasound homogenizer was used to generate the small microplastics (Sonsoplus HD70, Bandelin, Germany). Samples were analyzed using an LMD7 Laser Microdissection Microscope (Leica, Germany) in confocal fluorescence mode and an automated stage with a stitching function, providing an overview over a larger filter area in mere minutes using Leica Application Suite X (LAS X) software.

### 4.2.2.2. Plastic tagging using fluorescence

In order to facilitate accurate analysis of the size distribution of microplastics using microscopy, fluorescence tagging was utilized. Using fluorescence staining as a first step helped with identifying and excluding the subsequent contamination from smaller particles resulting from unavoidable degradation of the walls of the tubes, which were used to contain the target plastic pellets during ultrasonication.

PS particles were obtained directly as fluorescent pellets; thus, they did not require Nile red dye, but for all other polymers, the following method was used.

First, the various pellets and fragments were rinsed with ultrapure water to remove any contaminations that might have occurred during shipping. Then around 1 g of each polymer pellets/fragments were placed separately in a 50 mL dark brown PP centrifugal test tube (VWR, Germany). The dark tubes helped to protect the Nile red dye from photo bleaching during storage and processing. Nile red working solution was made by first preparing a 100 mg/L stock solution in acetonitrile, which was then diluted by a factor of 10 with ultrapure water to produce 10 mg/L Nile red working solution in 10% acetonitrile. This working solution was then added to the test tubes containing the pellets/fragments and filled to the 50 mL mark. After which, the tubes were sealed and shaken using a vortex mixer for 1 minutes each and subsequently placed in an oven for 2 hours at 60 °C. Tubes were then removed from the oven and filtered on a metal sieve with a 500 µm mesh size (Carl Roth, Germany). Finally, the pellets were rinsed with methanol to remove any precipitated Nile red particles that were attached to the plastic pellets. The original centrifugal tubes were also dyed in the process. Hence, these were discarded, and the pellets were transported into new dark centrifugal tubes (made of non-stained PP that did not fluoresce) and prepared for the next step.

#### *4.2.2.3. Generation of smaller microplastic particles*

This method was adopted from Von der Esch et al. [119] and modified to eliminate the usage of potassium hydroxide solution as well as adjust the ultrasonication parameters to produce microplastics rather than nanoplastics. The final experimental setup was as follows.

The tubes containing the dyed pellets/fragments were filled with 25 mL 0.1% Tween 20 solution. Tween 20 solutions aided in preventing particle agglomeration during storage and facilitated the propagation of ultrasound waves through the sample. The samples were then brought in contact with the micro-tip of a Sonos HD70 ultrasound homogenizer. Sonication took place for 12 hours @ 20 kHz and 60 W. The procedure was paused for 20 minutes every 3 hours to allow the samples to cool down and additional 0.1% Tween 20 solution was added to compensate for evaporative losses.

The resulting 25 mL suspensions were vortexed for 1 minute and filtered through a metal sieve with a 500 µm mesh size (Carl Roth, Germany) to remove the original pellets. The pellets were then rinsed with an additional 25 mL of 0.1% Tween 20 solution to extract smaller particles that were attached to the pellets. The filtrate containing only microplastics of less than 500 µm was then filtered consecutively through a 10 µm followed by a 5 µm nylon membrane filter to further reduce the size of the particles in the final suspension. This consecutive filtration was found to be more effective than directly filtering through a 10 µm or even a 5 µm filter, where a significant breakthrough of larger (>10 µm) particles was observed. The final volume of 50 mL suspension containing mostly only the smaller microplastic (≤10 µm) were then transferred to a new dark centrifugal tube and stored pending further treatment and analysis.

#### 4.2.2.4. Sample preparation

Two sample preparation methods were investigated in this study: Fenton reaction as well as hydrogen peroxide oxidation. In a previous study, both methods were optimized and validated for larger microplastics by the authors [57]. A summary of the conditions of these methods is summarized in Table 8.

Table 8. The sample preparation protocols used in this study. For further details, refer to Al-Azzawi et al. [57].

Sample preparation protocols	Temperature	Reaction time
Control (ultrapure water)	Room temperature	24 hr.
Fenton (30% H <sub>2</sub> O <sub>2</sub> + catalyst 20 g/L FeSO <sub>4</sub> )	Unregulated (max 90 °C)	10 min + 10 min cooling
H <sub>2</sub> O <sub>2</sub> (30%)	60 °C	24 hr.

Triplicates of each sample and controls were prepared. To ensure that the fluorescence particles are indeed the tagged plastics and not contaminants from the containing vessels or ambient air, blank samples using 25 mL of 0.1% Tween 20 in a dark centrifugal tube were prepared without Nile red dye and processed like the other samples.

All lab work was performed in a laminar flow box (FMS series SuSi, Spetec, Germany) as much as possible to avoid air contamination. Blue nitrile gloves were worn to avoid skin contact to the particles or the equipment, as skin flakes were determined to be

fluorescent in a similar fashion to the dyed microplastic particles. Furthermore, as mentioned previously microplastics were stained as a first step and stored in new, non-stained PP containers in order to ensure that any contamination taking place, would not be able to fluoresce unless it possessed autofluorescence properties like the aforementioned skin flakes. The prepared microplastic suspensions from the previous step were each vortexed for 1 min and subsequently 0.2 mL was withdrawn for each sample and control.

For the hydrogen peroxide protocol, 10 mL of 30% hydrogen peroxide was added to the samples in 50 mL dark tubes, which were subsequently vortexed for 1 min and subsequently placed in an oven for 24 hours at 60 °C. Similarly, for Fenton reactions, 2 mL of the FeSO<sub>4</sub> catalyst was added to the samples in 100 mL conical flasks. Then 4 mL of hydrogen peroxide was added on top of that to start the reaction. Subsequently, 1 mL of H<sub>2</sub>O<sub>2</sub> was added each minute for 10 minutes. Afterwards, the reaction was left to cool for 10 minutes. Finally, 0.8 mL of concentrated sulfuric acid (98%) was added to dissolve the precipitated iron particles. The details for the reactions are described by Al-Azzawi et al. [57]. A short summary is documented in the Supplemental Information (SI, section 1). After completion of all reactions, the samples were filtered via a 0.2 µm track etched polycarbonate membrane filter (Carl Roth, Germany) and rinsed with 100 mL of ultrapure water to remove any traces of the reagents.

Microscopy slides were pre-wetted with a smeared drop of ultrapure water, the filters were then carefully placed on top using tweezers. This wetting process helped in making the hydrophilic membrane filters stick uniformly to the glass slides. Finally, a cover slip was placed on top of the filter and affixed with clear tape on the sides to prevent air contamination. These two steps combined helped to flatten the filter and reduce waviness, thereby producing clearer, sharper images by the microscope.

#### *4.2.2.5. Size distribution analysis*

The slides were analyzed with an LMD7 Laser Microdissection Microscope (Leica, Germany) using 40X objective and DFC700 GT black and white camera. Acquisition and post-analysis were made using the Leica Application Suite X (LAS X) software. Due to the different brightness levels of polymers after dying, as well as the reduction of brightness after treatment due to partial oxidation of the dye, control samples from

each polymer were first analyzed to determine the minimum image exposure time that would lead to a dark background and bright particles without overblown highlights for that particular polymer. Such highlights tended to interfere with the autofocusing mechanism of the microscope and produced larger out of focus rings around brighter particles, leading to an overestimation of their size, whereas under exposure tended to lose the smallest particles. Subsequently, the Fenton and hydrogen peroxide treated samples were analyzed with a compensated exposure time that gave a similar visual look in terms of background and particle brightness to the respective control samples analyzed earlier. As expected, the required exposure times for samples were higher in all instances due to the aforementioned reduction in polymer brightness after treatment.

The parameters for image acquisition were as follows: Excitation wavelength was 557 - 583 nm, emission wavelength was 602 – 658 nm, sensor binning was adjusted to 2x2 at a resolution of 960x720 pixels, sensor sensitivity was set to 10, and image exposure times were between 5 and 150 ms depending on the polymer and the sample brightness as discussed above (for details, please see Table\_4.2.\_SI. 1). The membrane filter was partially scanned with 169 tiles which equated to a surface area of 4.8 x 3.8 mm. Those were then automatically stitched together via the LAS X software. The autofocus adjustment was set to reacquire for every tile with a Z-movement threshold of 80  $\mu\text{m}$  and 15 steps of accuracy. Threshold values for segmentation based on brightness were selected to be constant for each polymer type across all its samples (details are reported in the Table\_4.2.\_SI. 2). This limited the variability to only the exposure times, making it easier to estimate the measurement error. A 'fill holes' algorithm was then applied to the resulting image to reduce noise induced false positives during post-analysis. The minimum resolution was set at 0.517  $\mu\text{m}$ . The results of each set of sample triplicates were then averaged and compared against the triplicate set of the respective controls.

To calculate the exposure compensation error for each polymer, three samples per polymer were scanned with two different exposures at the exact same coordinates. One was optimally exposed according to visual observation, then another scan was performed with either twice or half of the chosen optimal exposure time. Finally, the averages from both sets were compared for each polymer. This accounted for a 'worst-case scenario' regarding instrumental inaccuracies and the human factor when selecting the exposure times for samples.

Another error factor was the presence of a few particles which were much larger and have managed to break through the two filtration steps. Those particles, being the largest and brightest on the filter, also had a negative impact on both the autofocus as well as the average size calculations as they tended to blur the images causing the small particles to be difficult to detect. Moreover, those largest particles, especially the ones over 50  $\mu\text{m}$ , tended to skew the average size calculation significantly. Thus, a cutoff point for particles  $>10 \mu\text{m}$  needed to be selected to avoid overestimation of the average sizes of the particles in the analyzed filter area. They represented a mere  $5 \pm 3\%$  of the number of detected particles across all samples, yet they caused an increase of the average size distribution of  $49 \pm 38\%$ . This also had the added benefit of reducing the average measurement errors due to exposure normalization (worst case scenario) from 15 % to 11 % across the six polymer types. The average size of controls was  $2 \pm 0.35 \mu\text{m}$  across all polymers when only particles  $\leq 10 \mu\text{m}$  were considered.

### 4.2.3. Results and discussion

#### 4.2.3.1. Fluorescence dying

Following the proposed sample preparation procedures, PE was the only polymer that could not be dyed successfully for this study. Larger PE fragments did readily adsorb the Nile red dye and become bright under the microscope, however, after ultrasonication only a small number of particles would light up distinctly, making an accurate detection impossible. Therefore, experiments with PE could not be carried out further. Based on previous experience, PE at least when treating larger particles is not susceptible to significant changes when applying Fenton and hydrogen peroxide [57]. This might also be true for PE particles  $\leq 10 \mu\text{m}$  in size. All other polymers (PS, PA, PLA, PET, PP and PVC) could be dyed successfully and were easy to distinguish under the microscope both before and after treatment.

#### 4.2.3.2. Observed changes in small microplastics ( $\leq 10 \mu\text{m}$ ) after sample preparation

To increase statistical significance, several thousand particles were analyzed for each single sample; on average  $7,182 \pm 4,979$  fluorescence particles were detected per set of triplicates, across all polymer types, whereas no particles could be detected in the



blank samples. As expected, due to the different number of particles between samples, which depended on the scanned filter coordinate as well as the sample, no loss criteria based on particle numbers could be derived.

Thus, the method applied in this study was to investigate the changes in the average size of the particles. An increase in the average diameter is associated with a loss of the smallest fractions and/or agglomeration of particles due to excessive heat. However, it was unclear in some cases if the smallest particles were completely lost or if simply the dye has been oxidized on the smallest particles due to their large surface area to volume ratios, thereby preventing them from lighting up. Thereby making the findings of this study a conservative assessment. On the other hand, significant decrease in the average size was only observed with PLA and PS and it was associated with dissolution of a cluster of larger particles into smaller ones. This was observed as a distinct increase in the ratio of the nanoplastic particles in the distributions ( $<1 \mu\text{m}$ ) when compared to control samples (all images and results are presented in SI, section 4). Ratios were used instead of absolute numbers in order to be able to normalize each distribution by the total number of particles to compare samples of widely differing total particle numbers as a result of randomness of particle distribution on the filter surface.

Due to the various analysis parameters, error sources needed to be included as part of the assessment. Thus, results were only considered significant if, for the triplicate runs for any specific polymer, the average size change was larger than both the average exposure compensation error and the average standard deviation.

For the fractions  $\leq 10 \mu\text{m}$ , taking significance into account as defined above, Fenton showed a size decrease for PS and PLA by  $33\% \pm 22\%$  and  $46\% \pm 15\%$ , respectively, and a size increase for PA by  $19\% \pm 7\%$ . Whereas hydrogen peroxide showed a size decrease for PS and PLA by  $19\% \pm 3\%$ ,  $37\% \pm 4\%$ , respectively, and a size increase for PP by  $21\% \pm 7\%$ . Details regarding all the polymers in the  $\leq 10 \mu\text{m}$  are presented in Figure 16.

#### *4.2.3.3. Observed changes in small microplastics (1 - 10 $\mu\text{m}$ ) after sample preparation*

Limiting the results to only the size fraction of 1 - 10  $\mu\text{m}$  showed less significant changes than the previous case ( $\leq 10 \mu\text{m}$ ). The 1 - 10  $\mu\text{m}$  size fraction might be more realistic, as it eliminated overestimation of particles resulting from image noise at the

nanoscale (<1  $\mu\text{m}$ ). This noise reduction had the benefit of yielding lower standard deviation between runs compared to the previous case ( $\leq 10 \mu\text{m}$ ). Moreover, detecting nanoplastics <1  $\mu\text{m}$  in environmental matrices with the current technology is not feasible [12, 59, 197].

When limiting the results to the size fraction (1 – 10  $\mu\text{m}$ ) and taking significance into account as defined above, Fenton showed an average size increase for PA, PET and PVC by 20%  $\pm$  4%, 8%  $\pm$  4% and 14%  $\pm$  8% respectively, whereas hydrogen peroxide showed a size increase for PA by 9%  $\pm$  4% and a size decrease for PET and PLA by 5%  $\pm$  4% and 11%  $\pm$  2%, respectively. Details of the average size changes when compared to the controls for each polymer are presented in Figure 16.

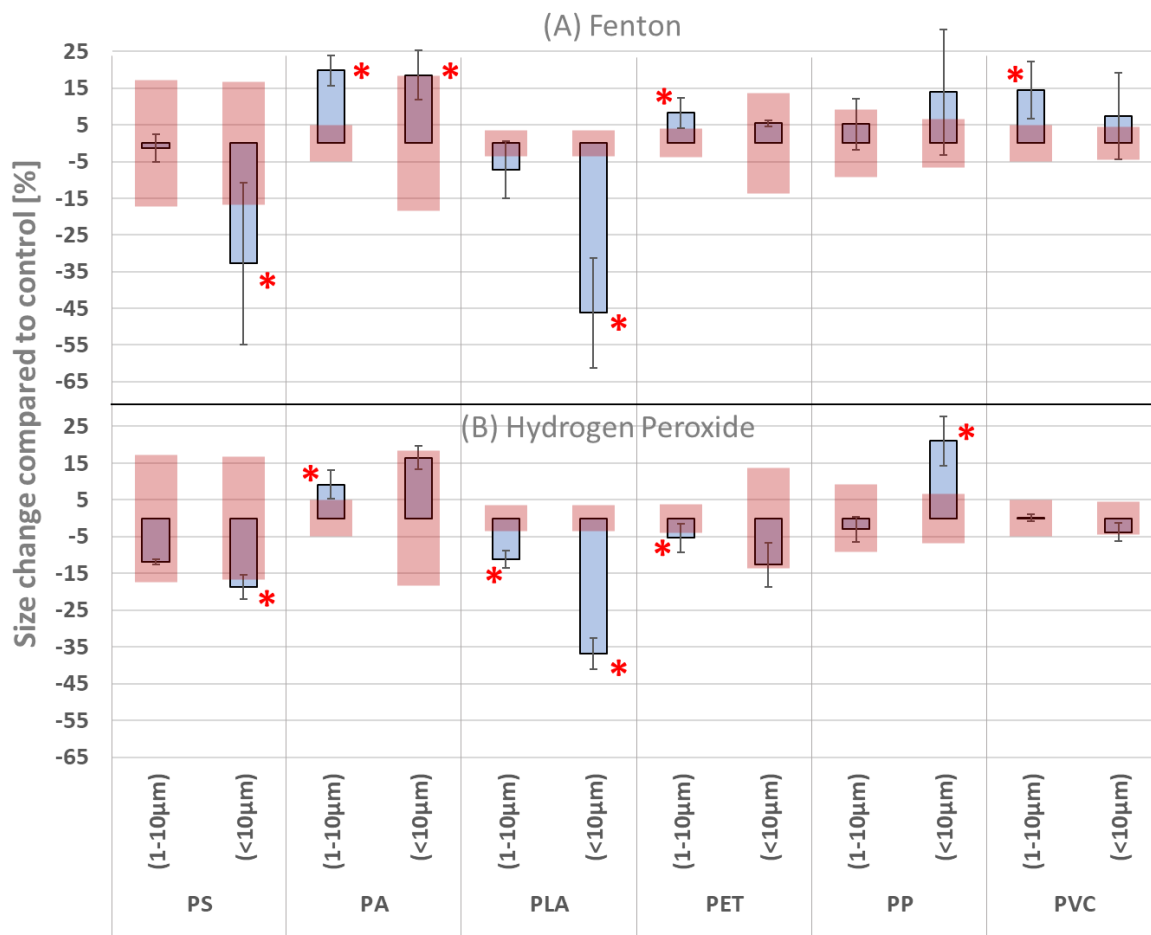


Figure 16. The relative changes of the average sizes compared to the respective control samples. Samples are divided into two groups: <10  $\mu\text{m}$  and 1-10  $\mu\text{m}$ . The transparent red areas represent the measurement error due to exposure normalization (worst case scenario); the solid lines represent the standard deviation of the triplicate measurements. Columns marked with a red (\*) indicate a significant change that is larger than both the measurement error as well as the standard deviation.

The effects on particle size distributions were as expected; samples that exhibited a decrease in size distribution showed a larger ratio of smaller particles ( $\leq 1 \mu\text{m}$ ) and hence a reduction of particles in the larger fractions ( $> 1 \mu\text{m}$ ). As an example, this is

shown for PLA in Figure 17. The opposite was true when the average size increased; there was a decrease in the smaller fractions and an increase in the larger fractions.

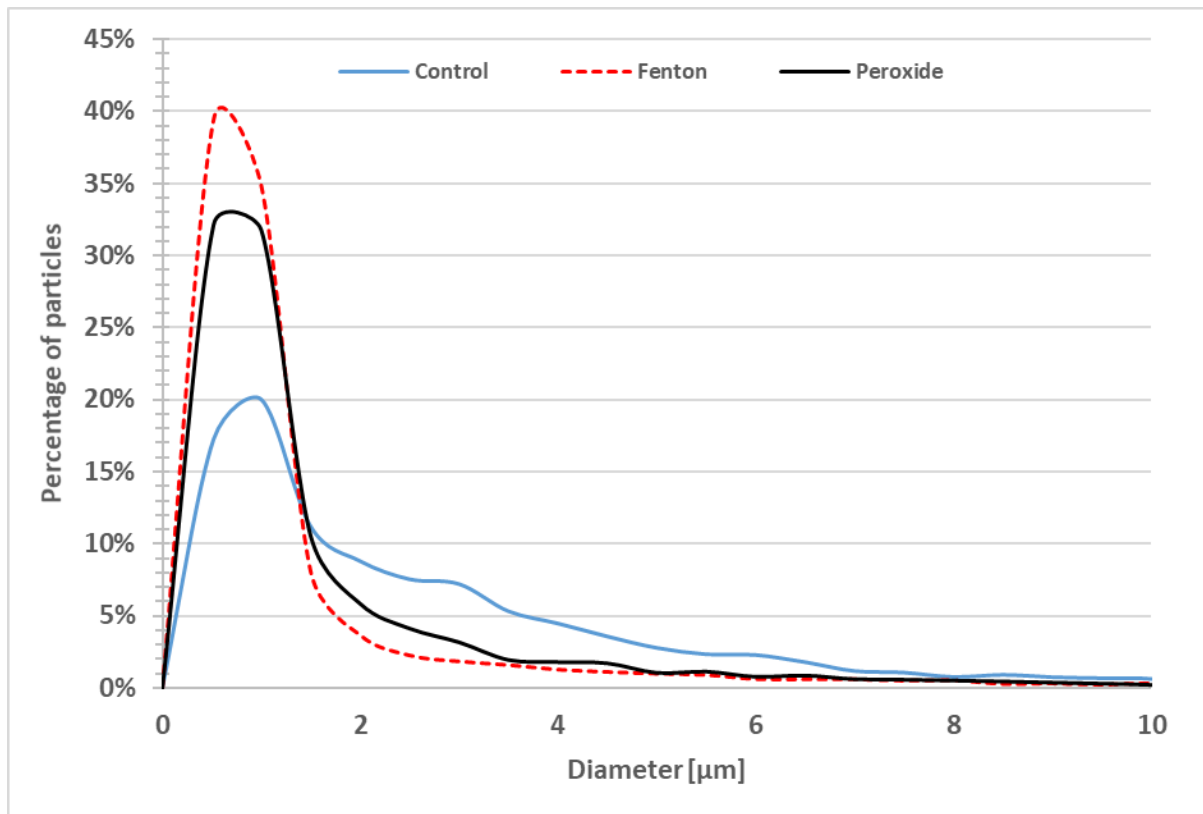
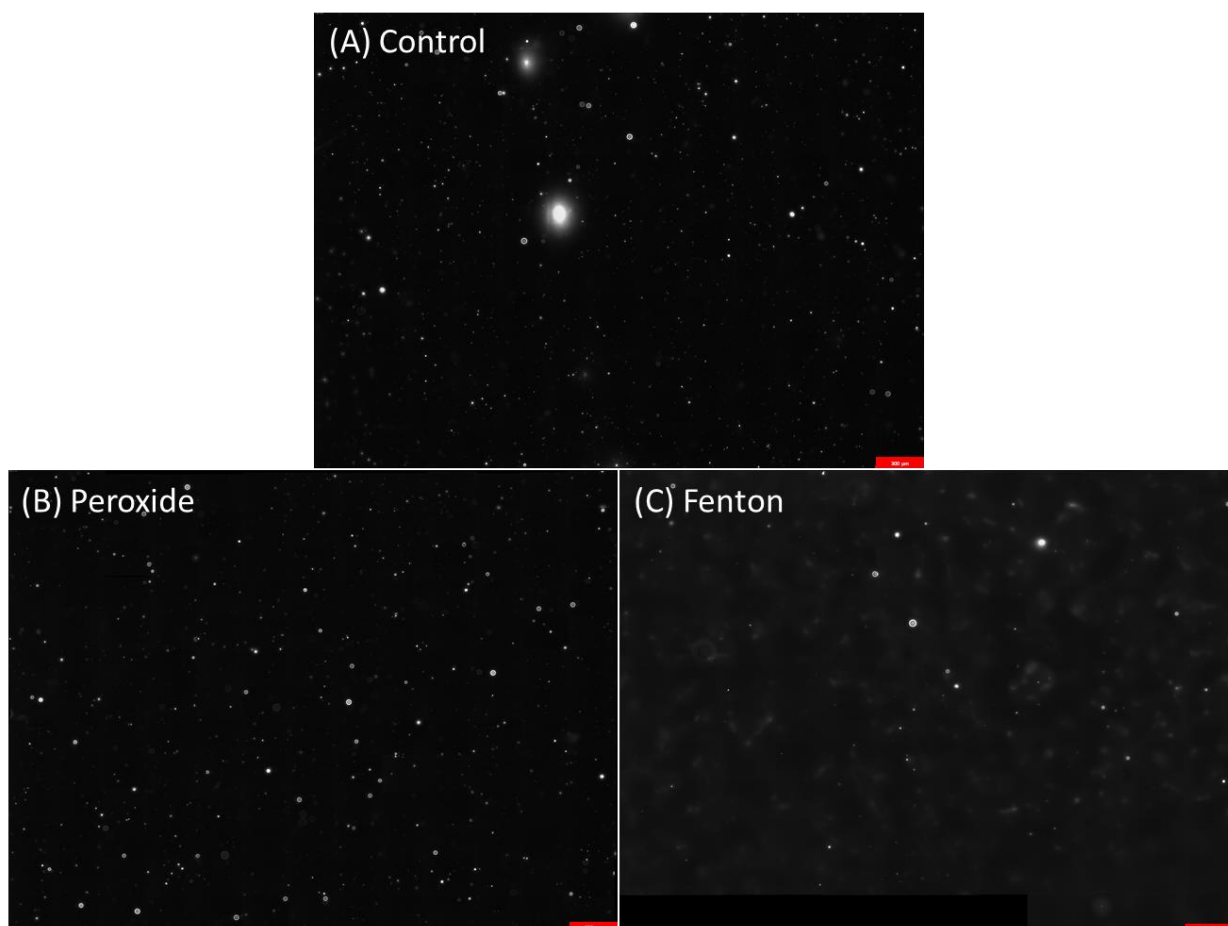


Figure 17. Size distribution of PLA for the three sample types. The values are presented as a ratio to circumvent the difference in particle count between the samples.

However, as stated it was unclear if the reduction in particle size at the smallest fraction was due to a loss of dye, a loss of the smallest particles, or due to particle agglomeration as a result of high temperatures. Examples of this were PP and PA, where the number of small particles dropped significantly after treatment with Fenton (Figure\_4.2\_Sl. 1 & Figure\_4.2\_Sl. 2), either due to loss of dye or actual loss of particles. In the case of PP, there was a cloudy appearance on the filter (Figure 18 (C)), where the small particles were so dim that the microscope could not focus on them. Therefore, the actual results for some of the samples might represent less change than what is reported here. Thereby making this study a conservative assessment.



*Figure 18. Three samples of PP under the fluorescence microscope with x400 magnification. Fenton samples were so dim that the autofocus function of the microscope could not focus on small particles. Hence the cloudy appearance. The red scale bars represent 300  $\mu\text{m}$  in length.*

#### 4.2.4. Conclusion

This study aimed to validate the suitability of using Fenton and hydrogen peroxide for microplastic samples of  $\leq 10 \mu\text{m}$  in size. Results suggest that both types of sample pre-treatment seem suitable for microplastic particles in the size range of 1 – 10  $\mu\text{m}$ .

The majority of observed changes occurred in the range of nanoplastics ( $< 1 \mu\text{m}$ ). This was confirmed when excluding particles  $< 1 \mu\text{m}$ , where both Fenton and hydrogen peroxide exhibited a much lower impact on the size of the microplastic particles. Although, there were exceptions that showed changes over 10% in the size range of 1 - 10  $\mu\text{m}$ , such as PA and PVC in the case of Fenton and PLA in the case of hydrogen peroxide. Nevertheless, those changes were still much lower than if nanoplastics are to be taken into account and were also not severe enough to hamper the detection of the particles in any way.

In a previous study, Fenton and hydrogen peroxide protocols were optimized and validated for larger microplastics (80 – 330  $\mu\text{m}$ ) in wastewater sludge samples [57]. Combining this knowledge with the results of the current study revealed that both methods are suitable for a wide range of microplastic sizes (1 – 330  $\mu\text{m}$ ) and can be recommended for studies investigating microplastics in environmental samples and especially wastewater effluent samples.

However, when nanoplastics (<1  $\mu\text{m}$ ) are of interest, findings of this study suggest following the hydrogen peroxide protocol. Samples prepared with hydrogen peroxide exhibited less significant size changes as the ones prepared with Fenton.

Finally, due to the reliance on an oxidizable fluorescent dye and the uncertainty in some case if the decrease of smallest particles (<1 $\mu\text{m}$ ) is indeed a result of particle loss or merely dye degradation, the results of this study represent a conservative assessment. If the microplastics/nanoplastics were to be analyzed via Raman microspectroscopy instead, the results could be even more favorable.

#### *Acknowledgement*

The following students at the Chair of Urban Water Systems Engineering, Technical University of Munich, provided valuable help by performing the experiments for developing the Nile red dye protocol: Sami Fanger, Simran Chauhan and Kristina Mraz.

#### *Funding sources*

The presented scientific work was funded by the German Federal Ministry of Education and Research (BMBF) [grant number 02WPL1443A] and the Bavarian Research Foundation [grant number: 1258-16].

## 5. Sample analysis

This chapter deals with state-of-the-art microplastic analysis methods and the development and optimization of a fluorescence based analytical approach.

The Chapter is divided into two sub-chapters:

### 5.1. Microplastic analysis methods and development of state-of-the-art protocols

This sub-chapter deals with the state-of-the-art sample analysis methods, their benefits and limitations, as well as synergies. However, the subchapter deals not only with sample analysis, but also partly with sampling, and sample preparation. It lays in best practices for monitoring microplastic emissions from WWTPs. This sub-chapter has **no hypothesis** associated with it.

This sub-chapter has been published as:

Mohammed S.M. Al-Azzawi, Matin Funck, Marco Kunaschk, Elisabeth Von der Esch, Oliver Jacob, Korbinian P. Freier, Torsten C. Schmidt, Martin Elsner, Natalia P. Ivleva, Jochen Tuerk, Oliver Knoop, Jörg E. Drewes. Microplastic sampling from wastewater treatment plant effluents: Best-practices and synergies between thermoanalytical and spectroscopic analysis. **Water Research**, Volume 219, 2022, 118549, <https://doi.org/10.1016/j.watres.2022.118549> - Reproduced by permission of the respective journal.

**Author contribution:** Shared first authorship between Mohammed S.M Al-Azzawi and Matin Funck.

**Mohammed S. M. Al-Azzawi:** Conceptualization, Methodology, Field Performance, Formal Analysis and Writing Original Draft. **Matin Funck:** Conceptualization, Methodology, Field Performance, Sample Analysis, and Writing Original Draft. **Marco Kunaschk:** Sample Analysis, Formal Analysis, Conceptualization, Reviewing. **Elisabeth Von der Esch:** Sample Analysis, Formal Analysis, Conceptualization, Reviewing. **Oliver Jacob:** Sample Analysis, Formal Analysis, Conceptualization, Reviewing. **Korbinian P. Freier:** Sample Analysis, Formal Analysis, Conceptualization, Reviewing.

Torsten C. Schmidt: Conceptualization, Supervision, Reviewing and Editing. **Martin Elsner**: Reviewing and Editing. **Natalia P. Ivleva**: Reviewing and Editing. **Jochen Tuerk**: Conceptualization, Supervision, Funding Acquisition, Reviewing and Editing. **Oliver Knoop**: Conceptualization, Supervision, Project Administration, Reviewing and Editing. **Jörg E. Drewes**: Conceptualization, Supervision, Project Administration, Funding Acquisition, Reviewing and Editing.

### *Abstract*

Wastewater treatment plants (WWTPs) may represent point sources for microplastic discharge into the environment. Quantification of microplastic in effluents of WWTPs has been targeted by several studies although standardized methods are missing to enable a comparability of results. This study discusses theoretical and practical perspectives on best practices for microplastic sampling campaigns of WWTPs. One focus of the study was the potential for synergies between thermoanalytical and spectroscopic analyses to gain more representative sampling using the complementary information provided by the different analytical techniques. Samples were obtained before and after sand filtration from two WWTPs in Germany using cascade filtration with size classes of 5,000 – 100  $\mu\text{m}$ , 100 – 50  $\mu\text{m}$ , and 50 – 10  $\mu\text{m}$ . For spectroscopic methods samples were treated by a Fenton process to remove natural organic matter, whereas TED-GC-MS required only sample extraction from the filter cascade.  $\mu\text{FTIR}$  spectroscopy was used for the 100  $\mu\text{m}$  and 50  $\mu\text{m}$  basket filters and  $\mu\text{Raman}$  spectroscopy was applied to analyze particles on the smallest basket filter (10  $\mu\text{m}$ ). TED-GC-MS was used for all size classes as it is size independent. All techniques showed a similar trend, where PE was consistently the most prominent polymer in WWTP effluents. Based on this insight, PE was chosen as a surrogate polymer to investigate whether it can describe the total polymer removal efficiency of tertiary sand filters. The results revealed no significant difference (ANOVA) between retention efficiencies of tertiary sand filtration obtained using only PE and by analyzing all possible polymers with  $\mu\text{FTIR}$  and  $\mu\text{Raman}$  spectroscopy. Findings from this study provide valuable insights on advantages and limitations of cascade filtration, the benefit of complementary analyses, a suitable design for future experimental approaches, and recommendations for future investigations.

KEYWORDS: TED-GC-MS;  $\mu$ FTIR spectroscopy;  $\mu$ Raman spectroscopy; granular media filtration; microplastic emissions; surrogate polymer.

### 5.1.1. Introduction

According to Plastics Europe (2019), plastic production has been steadily increasing since the first introduction of a fully synthetic polymer in 1907 to production rates as high as 359 million tons per year reported for 2018 [158]. Low global recycling rates for plastics lead to accumulation of plastic waste in the environment [159]. First studies investigating the presence of microplastics in the environment appeared in the 1970s and the interest has been growing since [198]. Microplastics are defined as plastic particles and fibers in the size range 1  $\mu$ m – 1mm, fragments in the size range 1 – 5 mm can be referred as large microplastics [23].

Despite removing a significant amount of microplastic particles from wastewater, various studies show that conventional wastewater treatment plants (WWTPs) might still be potential point sources of microplastics to the aquatic environment [30]. However, the process of sampling and analyzing microplastics is yet to be standardized, despite studies having attempted to harmonize the applied methodologies [31, 199]. In most cases, the definitions of the processes, from the research question to the analysis of microplastics, as well as the problems and pitfalls faced during these steps, are not being addressed.

In this study, best practices regarding microplastic sampling and analysis are addressed, based on field and laboratory experience by the authors in the context of sampling secondary and tertiary treated wastewater effluents from two WWTPs with tertiary sand filters. Analysis was performed with thermal extraction desorption-gas chromatography-mass spectrometry (TED-GC-MS), micro-Fourier-transform infrared spectroscopy ( $\mu$ FTIR) and Raman microspectroscopy ( $\mu$ Raman). Therefore, the strategies, challenges, pitfalls, possible synergies and limitations of the analytical methods in the application to wastewater effluent samples are presented.

For this purpose, the discussion clusters into four main aspects as summarized in Figure 19: general considerations (research question), sampling, sample preparation, and sample analysis. Each aspect is treated in further detail in the following chapters.



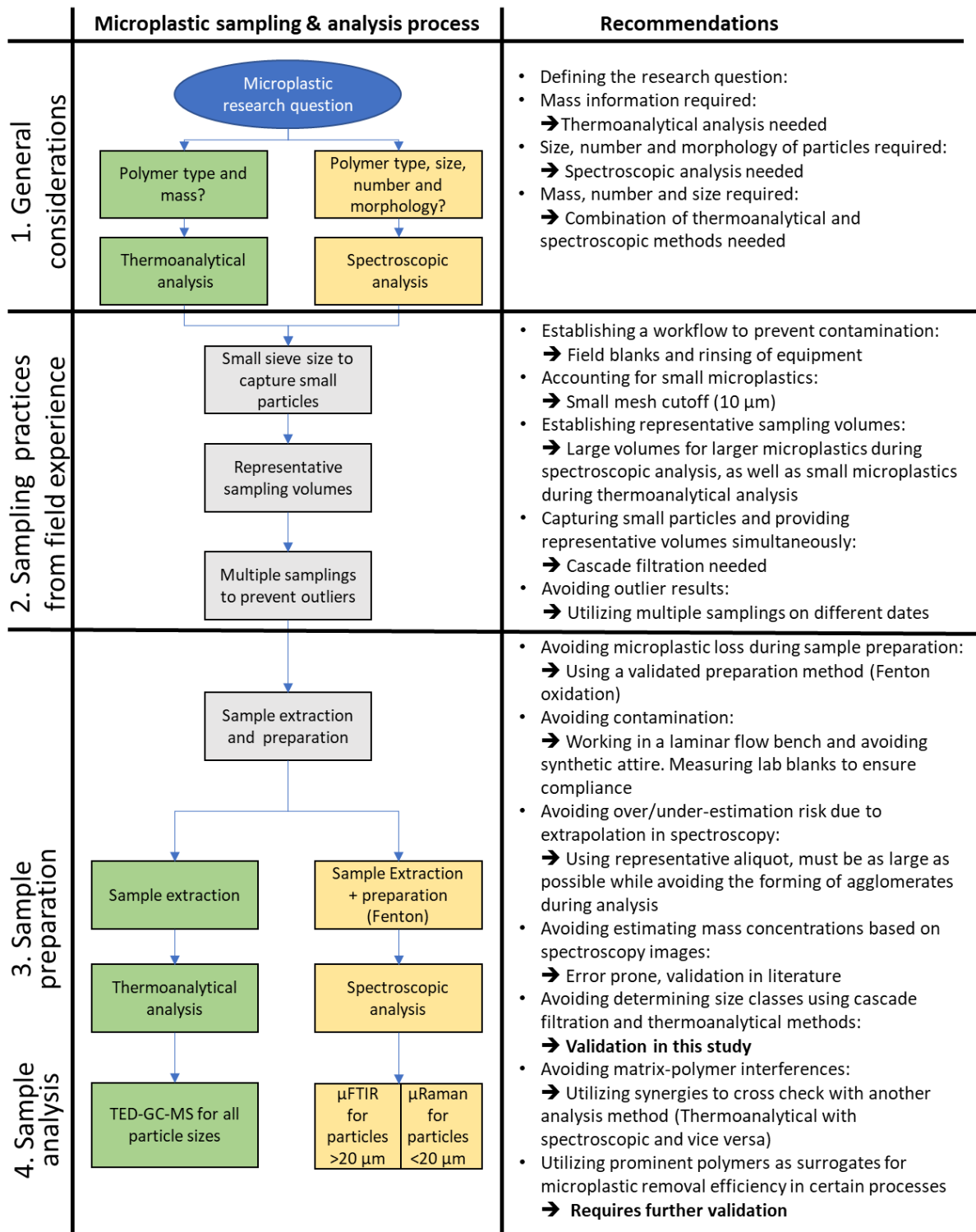


Figure 19. Process flow chart for microplastic sampling and analysis with the most important considerations and recommendations for every step.

#### *5.1.1.1. General considerations*

Studies investigating the release of microplastics from WWTPs can utilize spectroscopic analysis methods, such as  $\mu$ FTIR and  $\mu$ Raman, or thermoanalytical techniques like TED-GC-MS [25, 89, 92]. However, due to time and cost constraints, most studies are forced to quantify microplastics using only one of those analytical techniques, restricting them to either certain particle size ranges or masses, thus limiting the type of information obtained. The results obtained by both types of analytical methods differ from each other in the following key areas: Spectroscopic methods reveal information regarding the morphology (particles and fibers can be distinguished), size, number and identity of the particles but masses cannot be quantified directly [62]. Thermoanalytical methods provide information only on mass and identity but not about particle morphology, size or numbers [62]. Shortcoming regarding particle size information might be partially alleviated via sieve fractioning using cascade filtration [22], but this should be handled cautiously as it might be prone to error. Finally, different analytical techniques require tailored sample preparation methods. Thus, depending on whether number, size, morphology, polymer type and/or mass of microplastic particles need to be determined for answering the specific research question, the analytical technique must be selected in advanced, as sampling and sample preparation methods need to be adjusted accordingly.

#### *5.1.1.2. Sampling considerations*

The main challenge when sampling wastewater streams is the ability to sample representative volumes and to simultaneously capture small and large microplastics [22]. Multiple sampling approaches are reported in literature, such as grab sampling using buckets or pumping through a single sieve, or a stack of sieves [19, 85, 88]. However, those methods may lack the ability to sample large representative volumes. These volumes are especially required for thermoanalytical methods; bucket grab samples are usually limited to a few liters and only suited for dissolved analytes. Sieves can suffer from cake filtration and rapid pressure drops, if the mesh sizes are small enough for capturing smaller particles. A possible solution to both problems is the use of pressurized cartridges with a stack of sieves [32, 200, 201]. This technique

employs a pressurized housing with a cascade of filters or sieves of decreasing sizes, for example, 100  $\mu\text{m}$ , 50  $\mu\text{m}$  and 10  $\mu\text{m}$ . A pump then forces wastewater under pressure through the sieves, allowing filtration of multiple cubic meters using larger sieves (50 – 100  $\mu\text{m}$ ), where cake filtration build-up is slower to occur. This simultaneously allows processing multiple hundreds of liters over the smallest sieve (10  $\mu\text{m}$ ). This would still allow a representative volume for the smaller microplastics as they require less sampling volumes (hundreds of liters vs thousands of liters for larger fractions), due to their abundance compared to larger microplastics [23, 32]. Since TED-GC-MS,  $\mu\text{FTIR}$  and  $\mu\text{Raman}$  require different representative sampling amounts, the specific sampling volume for the analytical method is paramount: Small microplastics, despite their abundance, have a low mass, thereby requiring higher volumes to be concentrated when analyzed via TED-GC-MS [25]. In contrast, larger microplastics, despite their high mass, occur less frequently. Thus, spectroscopic methods might require a higher sampling volume to avoid analysis errors such as over or under estimation of the microplastic content in larger size fractions. This is exacerbated by the fact that spectroscopic methods can usually only analyze a small aliquot of the sample compared to TED-GC-MS [23].

#### *5.1.1.3. Sample preparation*

The entire sample preparation process must be carried out in a clean room or in a laminar flow box alongside lab and field blanks to minimize contamination.

Both  $\mu\text{FTIR}$  and  $\mu\text{Raman}$  are very sensitive to interference from the organic environmental matrix due to similar spectra of microplastics and natural organics. Thus, requiring targeted matrix removal during sample preparation beforehand to avoid analytical artifacts [57]. An interference for  $\mu\text{FTIR}$ ,  $\mu\text{Raman}$  and TED-GC-MS are stearic acids and fats, which could be interpreted as a false positive detection of PE [105]. Using a surfactant/emulsifier might help remove these compounds from the sample, as they can be dissolved and subsequently removed via filtration. However, the surfactant needs to be thoroughly rinsed to remove any traces as it can lead to interferences with  $\mu\text{FTIR}$  [106]. Furthermore, digestion-based sample preparation helps in removing traces of such interferences from the treated samples by digesting the organic compounds. Multiple methods such as acidic or alkaline digestion and

enzymatic methods are employed. Here, a promising method for removing organic matter without adversely affecting polymers from wastewater samples is an oxidative digestion using the Fenton reaction [33, 57]. In contrast to sample treatment for  $\mu$ FTIR and  $\mu$ Raman, sample preparation for TED-GC-MS usually does not require chemical digestion. However, they still require sample extraction from the filter cascade [58].

#### *5.1.1.4. Sample analysis*

$\mu$ FTIR and  $\mu$ Raman both require relative long analysis times, whereas TED-GC-MS is comparatively faster [62]. To circumvent long analysis times for spectroscopic methods, some studies attempted either scanning a small percentage of the filter, or utilizing microscopy for pre-screening and only analyzed selected particles via spectroscopy [19, 72]. Unfortunately, both approaches might reduce the quality of the statistical data obtained [68].

Whereas  $\mu$ FTIR spectroscopy is not reliable for particles  $<10\ \mu\text{m}$  in size,  $\mu$ Raman spectroscopy is able to quantify these particles reliably. Studies worked out that  $\mu$ Raman spectroscopy can detect up to 35% more particles in the range of  $500\ \mu\text{m}$  to  $50\ \mu\text{m}$  compared to  $\mu$ FTIR spectroscopy [59, 60]. K ppler et al. (2016) reported a  $\mu$ Raman spectroscopy analysis duration of 38 h, which is significantly longer compared to  $\mu$ FTIR spectroscopy (20 min) [59]. Shortening the  $\mu$ Raman spectroscopy analysis time to 90 min by changing scan parameters led to a loss of information and the detected particle number was comparable to  $\mu$ FTIR spectroscopy [59]. Therefore the authors recommended that due to lengthy analysis times, particles in the size range of  $500\ \mu\text{m}$  to  $50\ \mu\text{m}$  should be analyzed by  $\mu$ FTIR, while particles in the size range of  $50\ \mu\text{m}$  to  $1\ \mu\text{m}$  should be analyzed by  $\mu$ Raman [59]. The proposed size division at  $50\ \mu\text{m}$  has been recently applied for  $\mu$ FTIR and  $\mu$ Raman analysis of microplastics down to a size of  $3\ \mu\text{m}$  in commercially important mussels [26].

Finally, TED-GC-MS can be used for all size classes with the caveat that a sample of sufficient mass concentration is required. Especially for smaller sizes, it is critical to concentrate the sample to reach the limits of detection and quantification (LOD and LOQ) of this method [25]. To benefit from the synergies of these analytical methods while avoiding their shortcomings, these three methods may be combined when analyzing a sample which has been subdivided via size fractioning, as recommended

by K ppler et al. (2016), and adequately processed in sample preparation [59]. However, due to cost and time constraints, or lack of access to all analytical methods, a combination has not always been feasible.

Thus, for the first time, best practices for  $\mu$ FTIR,  $\mu$ Raman and TED-GC-MS are presented in literature based on real world samples and analysis. Alongside novel findings from these analyses, such as the feasibility of using surrogate polymers during evaluation of process efficiency, a focus on the synergies among the methods are presented.

## 5.1.2. Materials and methods

### of the case study: Microplastics in Tertiary Sand Filter Effluents

#### *5.1.2.1. General considerations*

The study's objective was to assess synergies between thermoanalytical and spectroscopic analytical methods in real samples. This comparison was performed by co-analyzing samples using TED-GC-MS,  $\mu$ FTIR- and  $\mu$ Raman spectroscopy. However, due to time constraints, not all samples were analyzed via  $\mu$ FTIR and  $\mu$ Raman, when compared to TED-GC-MS samples (for more information on aliquots, see SI section 2). As discussed in the results, despite this limitation, the synergies between the three analytical methods could be clearly elucidated.

#### *5.1.2.2. Sampling protocol*

Two WWTPs were investigated by performing sampling campaigns from 2019 until 2021. Sampling was performed for the secondary treated effluents and the tertiary sand filter effluents. The detailed information regarding the WWTP, the configuration and removal efficiency of the sand filters were published as part of a separate study by the authors [25]. The sampling unit consisted of a high-volume pump (SG 40 Victor Pumpen GmbH, Munich, Germany) and three basket filters (Krone Filter GmbH, Oyten Germany) configured in a cascade with different cut-off values (100  $\mu$ m, 50  $\mu$ m, 10  $\mu$ m). The sampling unit is further described in [32]. A schematic as well as a photo of the cascade system can be seen in Figure 20.

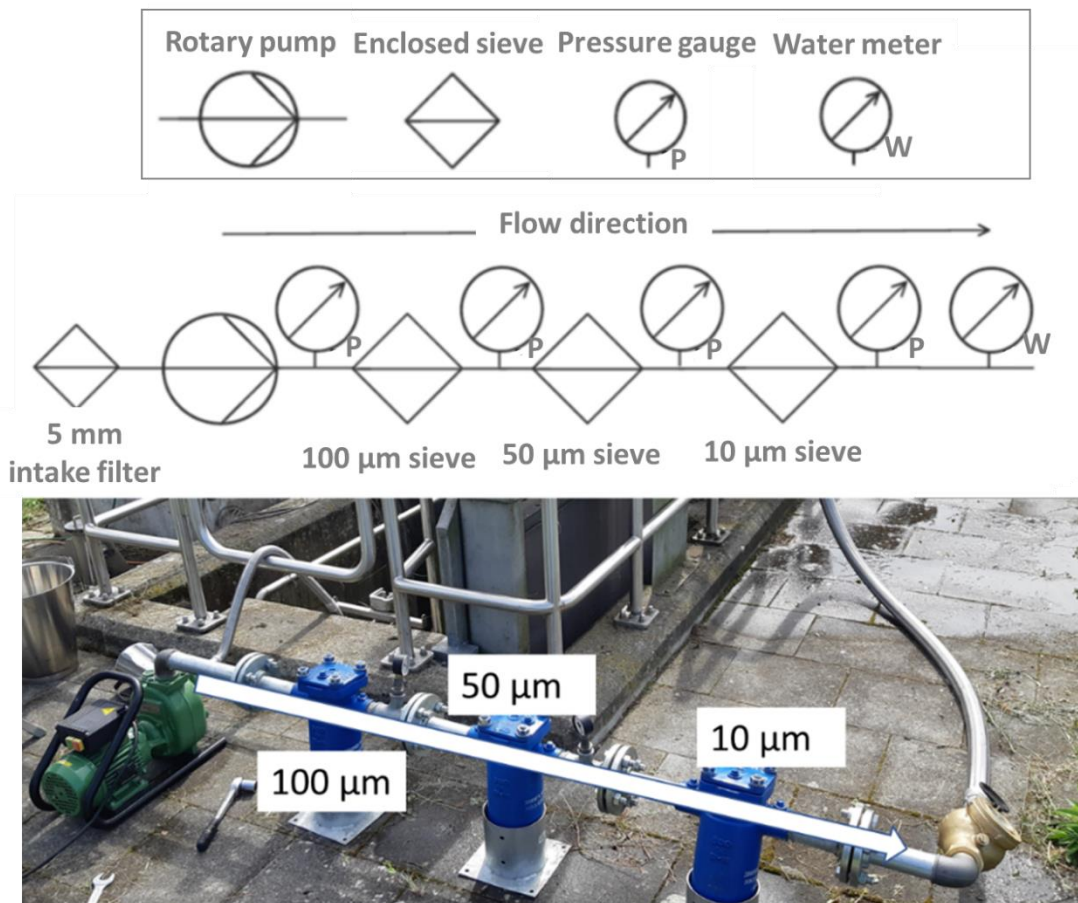


Figure 20: Schematic and picture of the cascading filtration

Cake filtration was avoided by monitoring pressure changes at the sieve inlets. Approximately 200 - 400 L of wastewater effluent could be filtered through the smallest 10 µm sieve. At an inlet pressure of 0.8 bar, the 10 µm sieve was removed from its modular housing and the larger two sieves (100 µm, 50 µm) could resume sampling and processing volumes of up to 7 m<sup>3</sup> [32]. A method for in-situ rinsing of the cascade filtration system was also investigated and the following protocol was developed:

- (1) The empty cascade filtration system was rinsed by pumping through 150 - 200 L of feed stream. This ensured that only the feed stream was present and homogenized inside of the sealed system. Washing was always done at the maximum performance of the pump (up to 18 m<sup>3</sup>/h), to flush all contamination and debris from the system.
- (2) The pump was stopped, the module for the 100 µm filter sieve was opened and the filter was placed inside. The system was then rinsed again with 20 - 30 L. This allowed the positioning of the 50 µm sieve into the effluent of the 100 µm sieve, which is upstream from it, without danger of contamination with larger particles.

(3) The same process was then repeated for the 10  $\mu\text{m}$  sieve as it was inserted into its corresponding module downstream of the 50  $\mu\text{m}$  filter sieve and sampling could be started.

Three types of blank samples were investigated to ensure contamination-free processing of collected samples:

(1) Laboratory blanks were investigated by applying the Fenton protocol to ultrapure water (UPW) samples as described by Al-Azzawi et al. (2020) [57].

(2) Process blanks were investigated by cleaning and rinsing the sieves after sampling, then immediately performing a sample extraction on those clean sieves as is described in the next section. The purpose of this was to measure the effect of potential contamination from sieves on the next sampling event.

(3) Field blanks were also investigated, where a sieve was placed in a parallel blank sampling unit for the duration of the sampling to quantify air contamination at the sampling site.

#### *5.1.2.3. Sample preparation*

Sieves were wrapped in aluminum foils before and after sampling. All rinsing and filtration steps took place inside a laminar flow box (Laminar Flow Module FMS series SuSi, Spetec, Germany) to avoid airborne contamination.

Particles were rinsed from each filter into a glass beaker using UPW and a metal brush [32]. Aliquots were then filtered via Whatman<sup>TM</sup> cellulose nitrate membrane filter (45 mm diameter, 0.2  $\mu\text{m}$  pore size, GE Healthcare Life Sciences, Chalfont ST Giles, GB). The filtered material was transferred into another glass beaker with 1 mL of a 0.1% (V/V) Tween 20 surfactant solution (Merck KGaA, Darmstadt, Germany) to aid in removing particles from the filter. Subsequent sample preparation for spectroscopic analysis was then conducted using a slightly modified version of the Fenton protocol, which was described by Al-Azzawi et al. (2020) [57], for details see SI, chapter 9.5.3. Thermoanalytical analysis via TED-GC-MS did not require Fenton treatment, because the low amount of organic matter (< 1 mg total mass) did not interfere with quantification and identification of the polymers. A possible exception could be fats and stearic acid which can cause interference in TED-GC-MS, but those were not

observed in the samples. Further studies concerning this topic are required for finding a threshold value in dependence of the sample. Samples were filtered via cellulose nitrate membrane filter and then transferred into glass vials via 600  $\mu\text{L}$  of a  $1 \text{ g L}^{-1}$  solution of 0.1% (V/V) Tween 20. The technique used is described in Funck et al. (2021) [25].

#### 5.1.2.4. Analysis

##### 5.1.2.4.1. $\mu\text{FTIR}$ spectroscopy analysis

Fenton treated aliquots (10 – 30 % of the total sample volume) from the 100  $\mu\text{m}$  and 50  $\mu\text{m}$  sieves were filtered on 25 mm Anodiscs<sup>TM</sup> (Whatman<sup>TM</sup>, PP-supported, 0.2  $\mu\text{m}$  pore size) and subsequently analyzed via focal plane array (FPA-)  $\mu\text{FTIR}$  spectroscopy. Further details of the analytical method are described in chapter 9.5.4.

##### 5.1.2.4.2. $\mu\text{Raman}$ spectroscopy analysis

Fenton treated aliquots (10 – 20 % of the total sample volume) from the 10  $\mu\text{m}$  sieves were measured via Raman microspectroscopy according to the protocol brought forward by Von Der Esch et al. (2020) [133]. The morphological characterization software *TUM-ParticleTyper* [119, 133, 202] was used. The method is described in detail within chapter 9.5.5.

##### 5.1.2.4.3. TED-GC-MS analysis

The analytical method was published previously by Funck et al. (2020) [32]. For each WWTP sample an aliquot (30%-100% of the total sample volume) was taken. Details including quality control samples are in chapter 9.5 in sections 6 to 8.



### 5.1.3. Results and discussion

#### *5.1.3.1. General considerations*

Using the data from multiple methods coupled with cascade filtration allowed for a complementary understanding of their synergies and limitations. Further, a validation of workarounds was possible, like the use of cascade fractioning to estimate size fractions utilizing only thermoanalytical methods. Finally, it enabled using a common surrogate polymer to assess the removal efficiency of microplastics in sand filter rather than relying on the total polymers according to each method's identification library.

#### *5.1.3.2. Sampling best practices based on lessons learnt from literature and field experiences*

This section conveys the lessons and best practices learnt from literature reviews as well as two years of investigations made during the sampling campaigns conducted by the authors. Sampling was performed using the cascade filtration system and the sampling protocol presented in Section 2.2. This represented an optimized method established by the authors to prepare the system in the field and minimize contamination in-situ, due to its practicality and cost effectiveness when compared to rinsing the system with filtered UPW. This sampling protocol allowed at the same time to remove any previous contaminations from the system and to ensure that every filter sieve receives the correct size fraction of the particles. The process was fast, requiring only 5 minutes, and it can be applied to any cascade filtration system for any aquatic sample.

As recommended by previous studies [23, 31], initially field blanks were prepared in parallel by using a clean sieve that was exposed to the air. This may not be fully representative, however, the authors hypothesized that such open-air blanks dealt only with airborne contamination, whereas the sampling system used in this study was enclosed and samples were taken from one meter below the water surface from an effluent discharge trench, where the nature of light airborne particles makes them unlikely to sink to 1 m depth and to be sucked into the cascade filtration system.

Results obtained during the open-air blank field sampling agreed with this observation; All field blanks were measured using all three methods. Whereas spectroscopic

analyses showed a large number of particle pollution in most of the field blank samples, TED-GC-MS could not detect polymers in any field blank samples. This indicated that indeed, the particles detected via spectroscopic analyses were indeed very light and possessed little mass so that they could not be detected by TED-GC-MS despite high nominal particle counts. Therefore, open-air field blanks might not be suitable as a field blank when working with sealed systems and sampling from at least one meter below the surface.

#### *5.1.3.3. Sample preparation*

Using the surfactant Tween 20 (solution 0.1% V/V) to suspend the samples during extraction from the sieves aimed to reduce particle agglomeration and increase suspendability. Additionally, the surfactant aids the homogeneity when the sample is subdivided into aliquots. Tests on PS particles (90 – 125  $\mu\text{m}$ ) showed 97% uniformity in suspension when dividing tap water samples mixed with (0.1% V/V) Tween 20 solution.

Further, for spectroscopic analysis, Fenton reaction was used and little to no interference from residual natural organic matter particles for both  $\mu\text{FTIR}$  as well as  $\mu\text{Raman}$  was observed.

#### *5.1.3.4. Analysis*

##### *5.1.3.4.1. Synergies between the analytical methods*

With the main three analytical methods for microplastic analysis employed for the evaluation of the WWTP samples, the respective results can be compared, and synergies pointed out: An overall positive outcome is the general tendency that measurements from TED-GC-MS and  $\mu\text{FTIR}/\mu\text{Raman}$  showed an agreement. Samples with higher microplastic content (secondary effluents) show an elevated microplastic content across all three methods when compared to the tertiary effluents of the sand filters. Furthermore, all three methods agreed that PE was by far the most abundant polymer in all samples, both before and after sand filtration. Possibly the most compelling proof was provided by the identification of an outlier in the sampling campaign: at one time point all three methods agreed that there was a larger amount

of PE in the tertiary effluent compared to the secondary effluents (see Figure 21). In this case, using multiple methods provided the assurance that the outlier was not from the analytical methods used due to artifacts, but rather an abnormality in the operation of the investigated WWTP. Indeed, upon investigation, the WWTP reported an issue on that day with the flow feeding the sand filters. Although the effects of this flow irregularity remained a mystery as to why only PE was affected and not the rest of the polymers. Nevertheless, the event served to test the synergies between the three analytical techniques in the case of an outlier. This is an exemplifying case of using the synergies of different analysis methods to achieve higher reliability. Another indication of synergies was PP, which was detected in some spectroscopic samples where TED-GC-MS was not able to detect it. This also included several of the process blanks, demonstrating that spectroscopic analysis can detect small light-weight particles that are below the detection limits for mass-based approaches. In the case of the process blanks, it is suspected that the lining of the hydrogen peroxide bottle cap used in the Fenton reaction was the source of the PP particles in some of the samples. Since spectroscopic analyses could detect PP in the process blanks, PP was considered as a false positive only for spectroscopic samples in this study.

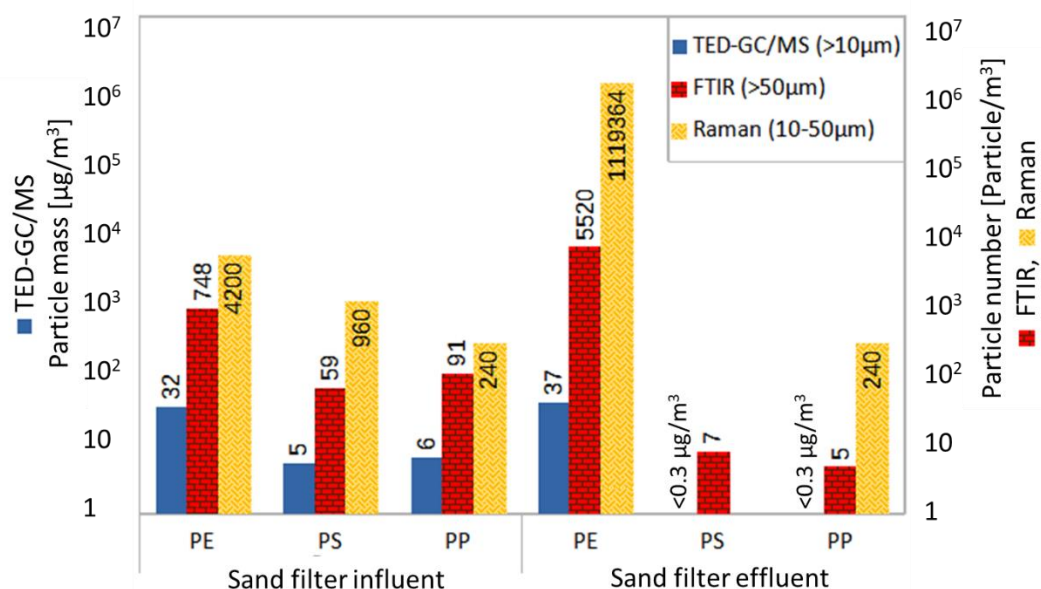


Figure 21. Results of the analysis for a WWTP. The influent for the sand filter was taken before an operational abnormality occurred, whereas the effluents of the sand filter were taken during the abnormality. The sampling for both influent and effluent were conducted on the same day in August of 2019 with only hours apart from each other. 100 µm, 50 µm filter sieves were analyzed by µFTIR, while the 10 µm filter sieves were analyzed by µRaman. TED-GC-MS was used across all filter sieves. The right y-axis represents particles/m³ for spectroscopic analyses, whereas the left axis shows the mass concentration of microplastic as analyzed via TED-GC-MS. For a complete breakdown of all polymers analyzed by spectroscopic approaches, kindly refer to Figure\_5.1\_Sl. 6 in the supporting materials.

However, it is worth mentioning that while the general trend is clear for all three types of methods, the degree of the increase observed by each analytical method varied substantially. For the example of Figure 21 and PE;  $\mu$ Raman samples exhibited an increase by a factor of 266.5, whereas  $\mu$ FTIR results increased by a factor of 7.4 and TED-GC-MS results revealed only an increase by a factor of 1.2. This can be explained by the fact that smaller particles are more prevalent in the samples as a rule, explaining the generally much larger number of particles detected by  $\mu$ Raman compared to  $\mu$ FTIR spectroscopy, as  $\mu$ FTIR spectroscopy is measuring only the particles down to 50  $\mu\text{m}$  whereas  $\mu$ Raman spectroscopy is used in this study to analyze only the smallest fraction (10  $\mu\text{m}$  – 50  $\mu\text{m}$ ) [59]. Furthermore, due to the cubic law, the smaller particles do not possess high mass, which can explain the modest increase in the mass determined by TED-GC-MS measurements.

Comparing the results of Figure 21 to literature, where the same methods were used for quantifying the MP effluent from sand filters, further indicates that the abnormality of the WWTP during operation is most likely responsible for the unexpected results. In a previous study by the authors, [25], the same WWTP exhibited lower amounts of all polymers in the sand filter effluent in multiple sampling campaigns. Analysis was conducted with TED-GC-MS only, but regardless of the method the results in Figure 21 differ significantly. In three sampling campaigns the average retention of PE was  $94\% \pm 3\%$ , whereas the presented results show an increase of PE in the sand filter effluent. Additionally, Ben-David et al. conducted an analysis of MP at a WWTP with a sand filter as tertiary treatment with  $\mu$ RAMAN [89]. Here also a significant retardation of polymers was observed after the sand filter, thus proving the results as non-representative for WWTP's.

The phenomenon of smaller particles not possessing a high mass, as previously described was observed during an 8-hour flow proportional sample, where the flow of the inlet pump to the filter cascade was restricted to achieve volumes similar to the normal grab samples (1 - 3 hours). This changed flow regime during sampling caused a change in the type of sampled microplastic particles; The sample included particles which were clearly detected via  $\mu$ FTIR, but no mass was detected when using TED-GC-MS indicating that those particles might be exclusively lighter/thinner because of the changed flow parameters to the cascade filter. The results for the 8-hour volume proportional sample are shown in Figure 22. This additionally indicates that the

resulting mixed and grab samples might not be comparable due to the different flow conditions required. This fact was proven by further sampling campaigns analyzed by TED-GC-MS. These results are shown in chapter 9.5.12.

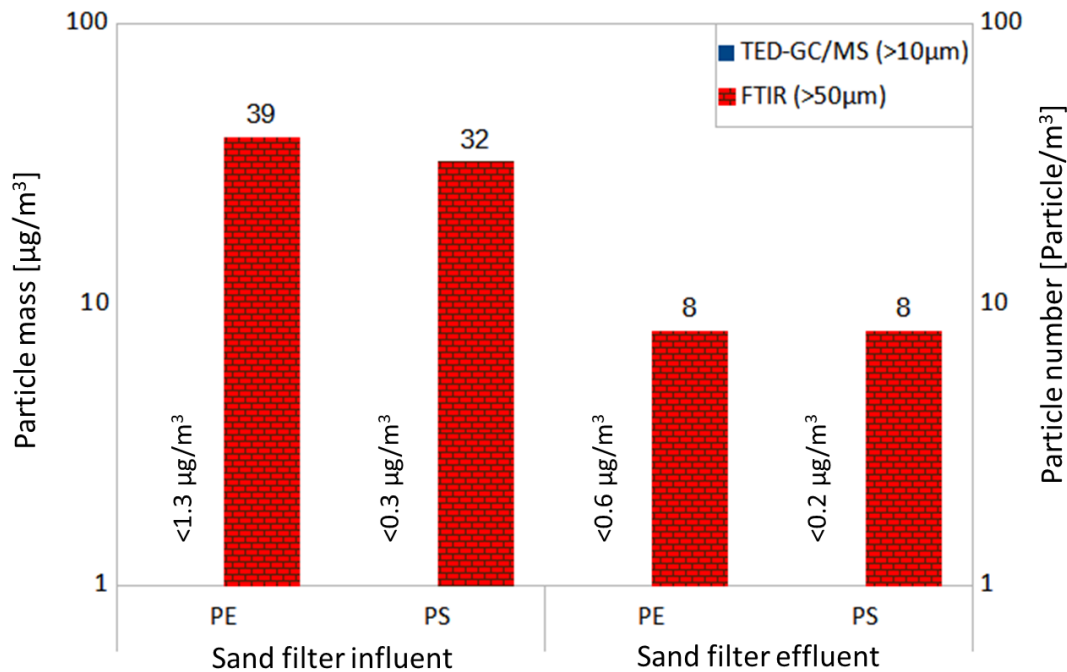


Figure 22. FTIR and TED-GC-MS results for an 8-hour volume proportional sampling at a WWTP in 2020. The results for the main polymers PE and PS are presented with particle number for  $\mu\text{FTIR}$  and masses in  $\mu\text{g m}^{-3}$  for TED-GC-MS. Corresponding LOQ for TED-GC-MS are shown additionally.

Based on this and as shown in the workflow of Figure 19, it is recommended to cross-check between analyses when a result does not follow expectations based on previous experiences from the sampling point/similar points or show interferences.

#### 5.1.3.4.2. Validating the estimation of size classification using cascade filtration and thermoanalytical analysis

The sampling system used consisted of three filters with decreasing sieve sizes (100  $\mu\text{m}$ , 50  $\mu\text{m}$ , 10  $\mu\text{m}$ ). This has been suggested to help in obtaining size fractions when using thermoanalytical methods [68]. The size distribution measurements via spectroscopic analysis after categorizing them by cascade filter and effluent type can be seen in Figure 23.

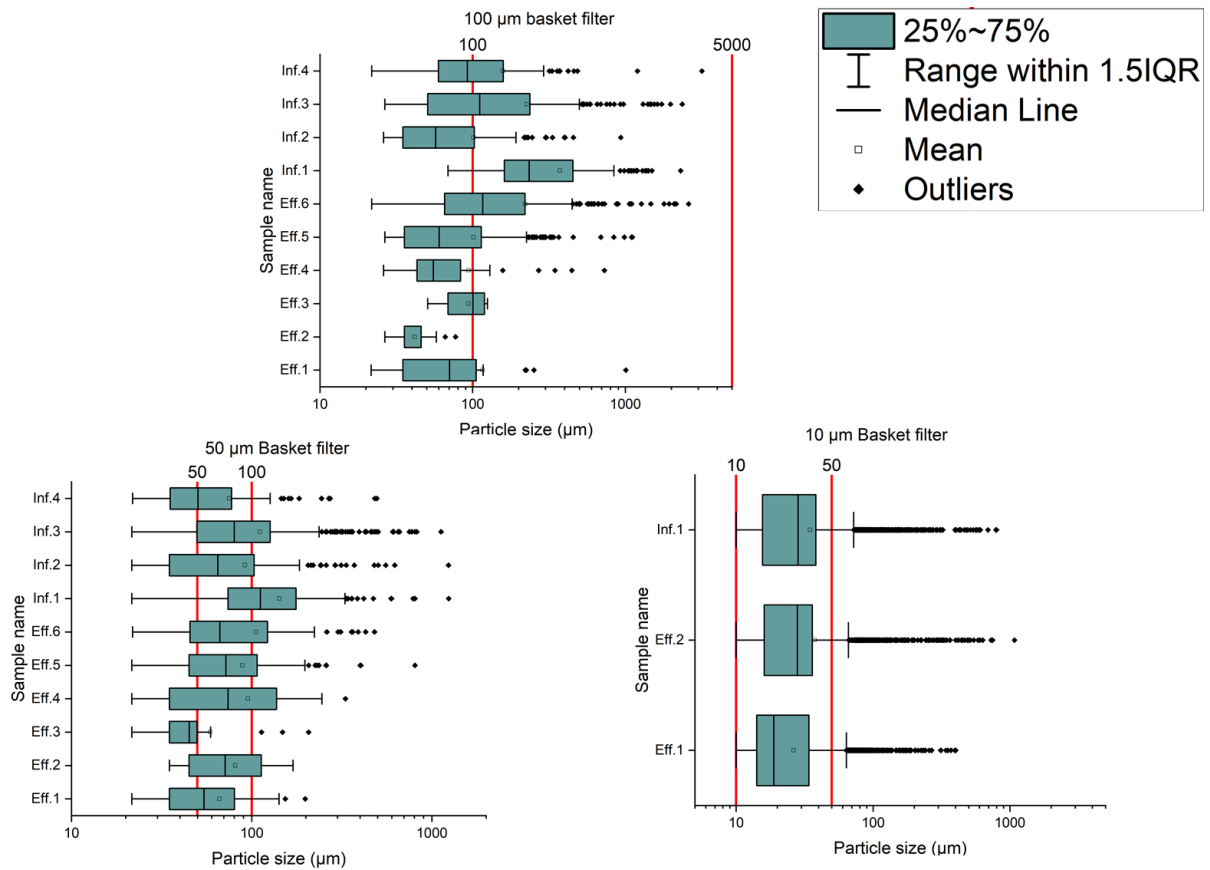


Figure 23. Size distribution of the detected particles (100 µm, 50 µm via µFTIR and 10 µm via µRaman) from the sieve fractioning. 100 µm, 50 µm filter sieves were analyzed by µFTIR, while the 10 µm filter sieves were analyzed by µRaman. The ideal range represented by the red bars refers to the theoretical ideal size range of the particles that should be found on the corresponding sieve.

It can be observed that for the 100 µm sieve, on average only  $57\% \pm 26\%$  and  $32\% \pm 18\%$  of the detected particles, in the influent and effluent of the sand filter, respectively, were in the expected ideal size range (i.e.,  $>100\ \mu\text{m}$ ). This can be attributed to cake filtration occurring, where particles including algae in the wastewater stream are clogging the filters. A picture of a sample extracted from the 100 µm basket filter is depicted in chapter 9.5.11.

From the particles detected on the 50 µm sieve, only  $34\% \pm 3\%$  and  $30\% \pm 12\%$  of the particles detected, in the influent and effluent of the sand filter, respectively, were in the ideal size range (50 µm – 100 µm).

Finally, the smallest sieve (10 µm) was analyzed via µRaman spectroscopy. It showed 87% (sand filter influent, single sample) and  $94\% \pm 6\%$  (sand filter effluent) of the particles detected, were in the ideal size range 10 µm -50 µm. However, it was not possible to know if particles smaller than 10 µm were also present on the 10 µm filter, since those are below the reliable detection range of the applied µRaman analysis.

This can be attributed to irregularities in pore sizes in the utilized steel filter meshes. This was investigated using optical microscopy and the results showed a damage (SI section 10) in the mesh already after three uses, with tears in the mesh corresponding to much larger sizes than the nominal pore size. This explains the presence of larger particles on the smaller filters.

Unfortunately, it is difficult to completely avoid this effect as the filters in a cascade are under pressure for multiple hours during sample filtration and afterwards the microplastic must be extracted from those filters with the use of brushes. Furthermore, the technique from Funck et al. (2020) was employed, where a metal wire brush was used to extract the samples from the filters with recovery rates of >80 % [32]. To avoid filter damage, a soft shoe brush made of horsehair instead of the established metal brush was investigated for sample extraction to reduce the damage to the filters without compromising the microplastic extraction efficiency (chapter 9.5.10.). In the light of these precautions, however, it is recommended to consider the particle size-related information obtained via thermoanalytical methods and cascade filters only as a very rough estimate. Additionally, the basket filters should be thoroughly investigated for damages after sample extraction. A more detailed investigation of size fractions requires the use of spectroscopic analysis such as  $\mu$ FITR and  $\mu$ Raman spectroscopy.

Nevertheless, the use of such a modular cascade filtration system instead of a single sieve is recommended, due to the combination of large volume sampling for the larger sieves with the ability to capture smaller particles, either via the small sieves early on, or via cake filtration on the larger sieves at later stages.

#### 5.1.3.4.3. Feasibility of using surrogate polymers during evaluation of process efficiency

When discussing the total amount of microplastic emissions, it is important to analyze as many polymer types as possible, or at least most of the common polymers, despite the effort and time required to establish identification libraries. For example, both thermoanalytical and spectroscopic techniques utilize either commercial, open source or self-created identification libraries. However, when attempting to evaluate the efficiency of various processes in WWTPs, it could be advantageous if there was a

single polymer that can be used as a surrogate to represent the behavior of all other microplastics inside a defined system boundary.

Results in this study suggest that if a study's objective is to evaluate the efficiency of microplastic removal inside of sand filters, then utilizing PE might achieve a representative result compared to taking all available polymers into account (Table 9). This may indicate that the behavior of PE during tertiary sand filtration at a WWTP seems to mimic well that of other polymers. PE was selected as it was the polymer found in the majority of collected samples and represented the single largest fraction of the polymers (25%  $\pm$  13% PE on average in all effluent and influent samples).

One-way analysis of variance (ANOVA) showed no significant difference ( $p \leq 0.05$ ) when the retention efficiencies obtained by analyzing all possible polymers (excluding PP due to the aforementioned blank issue: 10 polymers for  $\mu$ FTIR spectroscopy and 7 polymers for  $\mu$ Raman spectroscopy), was compared to the retention of the surrogate (PE). This indicated that PE could be a viable surrogate candidate in such similar cases, i.e., process evaluation in wastewater treatment, even though it makes up only a quarter of the total polymer fraction.

These results represent first insights into the usage of surrogates to assess process efficiency. The topic is not yet discussed in literature to the best knowledge of the authors. This is surprising as surrogate parameters are often used in water and wastewater engineering to simplify process evaluations, even when dealing with trace pollutants [203]. However, this topic would require a dedicated study to further validate these results and ensure statistical significance, as the amount of data (especially for  $\mu$ Raman spectroscopy) cannot be used for any definite statements. As can be seen in Table 9, for example, Raman analyses for the determination of removal efficiency were conducted by taking samples at the influent and effluent of the tertiary sand filters. This was not possible to do at exactly the same time with the equipment available and was in fact done 24 hours apart, which might explain the increase of the number of particles (<50  $\mu$ m) in the effluent, making these results non representative of the actual WWTP performance.

The same situation holds true for TED-GC-MS samples: while having a large number of samples, the analysis only included four polymers (PE, PS, PP and PET), and thus, not enough to make a statement about total polymers vs PE.



It is worth stressing again that such an approach might only be applicable for a process evaluation like removal efficiencies as this depends on the general behavior of microplastics across both sides of a process boundary (sand filter in this case). This surrogate method is not yet intended for use as a general estimator for the total amount of microplastic in a certain system.

*Table 9. The observed values from eight retention evaluations of tertiary sand filters using  $\mu$ FTIR and  $\mu$ Raman spectroscopy.  $\mu$ FTIR results are the sum of the 100 $\mu$ m and 50 $\mu$ m filter, whereas  $\mu$ Raman results are from the 10 $\mu$ m filter. The samples marked with (\*) were single sand filter cells with a common influent. The influent samples were sampled the day before the effluents could be sampled. This might explain the presence of larger number of smaller particles in the effluents of the cells. For the purposes of using surrogates, however, this should be irrelevant.*

<b>Sample</b>	<b>Total retention</b>	<b>Surrogate retention (PE)</b>
FTIR 1	84%	88%
FTIR 2	97%	79%
FTIR 3	69%	75%
FTIR 4	11%	83%
FTIR 5*	94%	94%
FTIR 6*	96%	94%
Raman 1*	-634%	-385%
Raman 2*	19%	-67%

#### 5.1.4. Conclusion

The presented process flow chart for microplastic sampling and analysis (Figure 19) allows to establish a workflow based on thermoanalytical and/or spectroscopic methods. The study presented pitfalls and considerations regarding sampling and analysis: For example, the need to harmonize sampling methods including representative volumes as well as sampling flow speeds since otherwise there can be no comparability between studies. Furthermore, due to high volume sampling combined with simultaneous capturing of large and small particles, the use of cascade filtration is highly recommended for microplastic grab samples at WWTP effluents. However, this recommendation does not extend to the use of cascade filtration to estimate the size distribution of microplastics when using a thermoanalytical analysis method.

The study highlighted the potential role of synergies between various analytical approaches to gain more complete information on the sample to determine outliers and interferences for example. However, even though the combination of analytical techniques helped to verify the observation of an operational outlier event, the reason behind the event could not be identified or explained.

This study was aimed at WWTP effluents. However, the considerations and procedures are transferable to other sample types or matrices, provided that the necessary adjustments to the sampling and sample preparation are to be made. Finally, the study recommends further investigations of the use of surrogate polymers for determining retention efficiency, as a time and cost saving measure.

### *Acknowledgment*

We are thankful for receiving funding by the Federal Ministry of Education and Research (BMBF) as part of the project (Sub $\mu$ Track: Tracking of (Sub)Microplastics of Different Identities - Innovative Analysis Tools for Toxicological and Process Evaluation), grant number 02WPL1443A-G and the Bavarian research foundation as part of the project (MiPAq: Microparticles in the aquatic environment and in food - are biodegradable polymers a possible solution to the "microplastic problem"?), grant number: 1258-16.

## 5.2 Developing a rapid microplastic analysis technique inside wastewater samples using fluorescence staining

This sub-chapter deals with the development and validation of a fluorescence based microscopic analysis for rapid and cost-effective microplastic analysis. This sub-chapter deals with the testing of **hypothesis 3**.

*“**Hypothesis (3)** Hydrophobic fluorescence dyes can be used in conjunction with sample preparation to establish an affordable, rapid quantitative analysis for microplastic particles larger than 40  $\mu\text{m}$  in WWTP effluents. This approach can quantify microplastics with an accuracy of  $\geq 70\%$  compared to  $\mu\text{FTIR}$ ”*

This sub-chapter is published as following:

Al-Azzawi, M. S. M.; Kunaschk, M.; Mraz, K.; Freier, K. P.; Knoop, O.; Drewes, J. E. Digest, Stain and Bleach: Three Steps to Achieving Rapid Microplastic Fluorescence Analysis in Wastewater Samples. *Sci. Total Environ.*, **2023**, 863, 160947. <https://doi.org/10.1016/J.SCITOTENV.2022.160947>.

### **Author contribution:**

**Mohammed S. M. Al-Azzawi:** Conceptual design, experimental work, data analysis, script writing, revisions; **M. Kunaschk:** conceptual design, experimental work, data analysis, script writing, revisions; **K. Mraz:** conceptual design, experimental work, data analysis, script writing, revisions; **K. P. Freier:** conceptual design, data analysis, script writing, revisions; **O. Knoop:** conceptual design, management, script writing, revisions; **J.E. Drewes:** conceptual design, management, script writing, revisions.

### *Abstract*

Efforts associated with common analytical techniques for microplastics including spectroscopic and thermo-analytical techniques are limiting the ability to perform large-scale monitoring of microplastics in the aquatic environment, because the analytical equipment required is costly and the analysis itself time consuming. Thus, there is a need to develop low cost, rapid alternative monitoring approaches. One possible alternative is the use of selective fluorescence staining of microplastic particles directly applied to environmental samples. However, to the best of our knowledge this has not yet been successfully implemented for wastewater samples.

In this study, sludge samples are used as surrogates for wastewater alongside six different polymers to develop a combined sample preparation and staining protocol that could selectively stain microplastics without significant interference from the natural constituents of the sludge. Results confirmed that using Fenton's reagent to remove the organic matter before staining the sample with Nile red (NR) and subsequently bleaching it by sodium hypochlorite resulted in the best workflow to selectively stain microplastics and then analyze them in wastewater samples using fluorescence microscopy.

### 5.2.1. Introduction

Microplastic quantification usually requires the utilization of costly equipment like  $\mu$ FTIR,  $\mu$ Raman spectroscopy or TED-GC-MS. The analysis time required for these techniques can be very long (i.e., hours to days depending on the sample and method of choice) [68, 151]. This can limit the scale with which microplastic monitoring campaigns can be performed. Thus, it is desirable to develop a reliable analytical method that is simple to perform, relatively fast, and cost-effective to serve as an alternative analytical method or at least to compliment more expensive analytical methods [51]. Optical microscopy is one such technique, however, it suffers from large error potential and operator's bias due to the lack of ability to distinguish natural particles from microplastics [204, 205]. A possible solution to improve the reliability of optical microscopy is the implementation of fluorescence which has been shown to increase the detection quota for microscopy, especially for smaller particles [204]. Andrady et al. suggested using lipophilic dyes to dye microplastics selectively, further enhancing the accuracy of fluorescence microscopy [206]. Examples of suitable dyes are Nile red (NR) or Nile blue (NB), which are lipophilic solvatochromic dyes. Their emission spectra (colors) are dependent on the polarity of the surrounding medium (increasing polarity red shifts their emission spectra) due to the twisted intramolecular charge transfer [51, 207, 208]. In the case of NR for example, intramolecular forces acting on the electrons due to medium polarity causes a twisting motion of the diethylamino group relative to the fixed aromatic groups which causes the solvatochromic behavior and color shifts [207]. NR and NB emission spectra are also susceptible to changes in the pH of the medium [209]. A handful of studies already investigated dyeing microplastics within environmental samples (e.g., sediments and

biological tissues) [51, 78–80, 82]. One study even attempted the application of various analytical techniques on wastewater samples, including fluorescence microscopy [83]. However, that study provided no explicit results for fluorescence analysis nor a validation for its methodology. Most of these studies were limited to particle sizes above 100  $\mu\text{m}$  [51, 76, 77, 82]. Nevertheless, these studies served as proof-of-concept for the targeted staining of microplastic within an environmental matrix.

Further, the use of staining within real environmental matrices, especially ones rich in organic matter like wastewater effluents, requires sample preparation to reduce the false detection and interference from matrix co-staining [204, 210, 211]. This has been investigated by studies before, but only for sediment and biological samples [51, 78–80, 82]. However, no study included a validated method for detecting microplastics within wastewater or sewage sludge samples.

This study builds upon previous studies to develop a rapid quantification method for wastewater effluent samples. A rapid quantification method can be utilized to facilitate larger-scale monitoring campaigns or to serve as an initial screening approach to identify relevant samples to be investigated later with more accurate but time intensive analytical techniques like  $\mu\text{FTIR}$  and  $\mu\text{Raman}$  spectroscopy. Alternatively, this approach can be used complementary to thermo-analytical techniques which cannot give information regarding size and number of particles within a sample [26]. In theory, the proposed staining method can detect plastic particles down to around 200 nm using regular fluorescence microscopes before the limit of diffraction makes it impossible to resolve objects without super-resolution techniques, such as Stimulated Emission Depletion (STED) microscopy [212].

### 5.2.2. Materials and Methods

The staining dyes Nile red (NR) (Carl Roth GmbH, Germany) and Nile blue (NB) (Alfa Aesar, United Kingdom) were acquired. The polymers used were polyamide (PA) (Lanxess, Cologne, Germany), polyethylene terephthalate (PET) (TPL, Zurich, Switzerland), polylactic acid (PLA) (Nature Works, Minnetonka, MN, USA), polystyrene (PS), low density polyethylene (LDPE), polyvinylchloride (PVC) (Ineos, London, UK), poly(methyl methacrylate) (PMMA) (Röhm, Germany), and

polypropylene (PP) (Borealis, Vienna, Austria), which were milled using a cryo-mill to provide defined sizes of 90 to 125  $\mu\text{m}$ . However, as the experimental results revealed, they also contained many smaller particles, therefore realistically the processed particles represented a size distribution smaller than 125  $\mu\text{m}$ . Additionally, spherical 40  $\mu\text{m}$  PS particles were tested (BS-Partikel, Germany). Due to the extended time period during which the experiments took place and shortages in some of the polymers, not all polymers were employed in all of the tests, especially the pre-experiments. This is noted for each subchapter.

The highest interferences for fluorescence microscopy can be expected due to the high organic carbon content within biosolids and effluents of wastewater treatment plants and therefore represents a worst-case scenario. Sludge can be adapted as a representative (surrogate) for wastewater samples. Sludge samples used were obtained from the return activated sludge of the WWTP in Freising, Germany. The sludge was characterized by a total solids (TS) content of 4.9% and volatile solids (VS) content of 3.24%.

#### *5.2.2.1. Initial staining protocol development*

Various fluorescence staining protocols using different solvents and dyes were investigated based on previous reports published in the peer-reviewed literature [51, 73, 75–78]. This was done to select suitable solvents that would not affect the size characteristic of the microplastics during the staining procedure. First, the effects of different solvents on microplastics in the size range of  $<125 \mu\text{m}$  (PS, PE, PET, PLA, PA, and PMMA) were validated after 10 minutes of exposure to various solvents (i.e., ethanol, n-hexane/ethanol (1:1), acetone, acetonitrile). The solvents were all diluted to 10% with ultrapure water (UPW), except for n-hexane/ethanol (1:1). They were subsequently tested for any induced change to the size distribution of the microplastics using laser diffraction analysis employing a Mastersizer long bed S (Malvern panalytical, UK).

The next step was to establish a basic staining protocol for the suitable solvents obtained from the previous step. Ten staining protocols using different solvents and Nile red concentrations were tested on PS, PE, PET, PLA, and PA fragments ( $<125 \mu\text{m}$ ). The specific protocols tested are summarized in Table\_5.2\_A.1. The

effectiveness of all staining protocols was evaluated using fluorescence microscopy (Axioplan 2, Carl Zeiss AG, Germany), whereby ten random particles were isolated and their grey values (brightness) were measured via ImageJ image analysis software (code in the Appendix, chapter 9.6.3). Afterwards, the protocols that provided the highest brightness values and could stain all tested polymers were chosen for further optimization.

#### *5.2.2.2. Optimizing staining resiliency*

Sample preparation is an essential step in processing wastewater samples to reduce the amount of natural organic matter content, thereby reducing interferences and improving analytical accuracy [57]. However, sample preparation methods might inadvertently oxidize staining dyes. Attempting to circumvent this by applying the staining step after sample preparation with no post treatment is also not possible, as the entire sample is then stained and no particles can be detected due to excessive interference. Therefore, a robust dying protocol needed to be developed and tested that could withstand a sample preparation step.

First, control samples each containing the individual polymers PS, PE, PET, PLA, and PA were stained with the best performing protocol from the previous step. Subsequently, a Fenton digestion protocol was applied to the pre-stained microplastics as proposed by Al-Azzawi et al. [57]. Fenton was selected as the first candidate due to the very effective sludge treatment performance observed by the authors in two previous studies as well as the minimal effects on microplastic particles down to 1  $\mu\text{m}$  in size [57, 213]. The difference in fluorescence intensity before and after applying Fenton was recorded by measuring the average intensity of random ten microplastic particles from each sample using ImageJ (code available in the Appendix, Chapter 9.6.3). Results will be discussed below but it is important to note that PE was the only polymer that lost all its fluorescence staining when exposed to Fenton and became completely invisible using fluorescence microscopy. Since PE is a very abundant polymer in WWTP effluent samples [25], a new staining protocol was needed to optimize the staining performance to improve microplastic dye retention after application of sample preparation. Thus, it was selected as a surrogate polymer to represent all polymers when optimizing the staining protocols further. During this

step, ten additional protocols were tested based on optimizing the best performing protocols from the first experiments, using the following parameters: 10 – 20% concentrations of acetonitrile and ethanol as a carrier solvent with either Nile red or Nile blue (1 – 10 mg/L) as a dye with various contact times (30 min to 24 h) and temperatures (room temperature to 70 °C). A list of the protocols used in the final optimization is summarized in Table\_5.2\_A. 2.

The final optimized staining protocol, based on successful staining of PE, both before and post Fenton application, was subsequently tested on all five polymers as well as PS microspheres in order to ensure that they all achieved a satisfactory fluorescence intensity after applying the Fenton reaction. However, using Fenton as a post treatment did not prove successful for PE, as it lost the majority of its fluorescence regardless of staining optimizations, making the brightness insufficient for real sample detection. Therefore, Fenton was eventually relegated to a pretreatment role for sludge samples to pre-digest organic matter before staining.

This meant that there was a risk of co-staining natural particles which needed to be investigated and solved via alternative post-treatments. These alternative post treatments were: methanol, sodium hypochlorite as well as hydrogen peroxide. Details are shown below and in Table 10.

#### *5.2.2.3. Minimizing co-staining of organic matter and background interference*

As mentioned briefly in the previous section, in order to stain and detect microplastics directly in wastewater samples, it is essential to minimize the interference resulting from co-staining natural particles which otherwise leads to false positives or prevents the identification of microplastic particles due to elevated background brightness/interference. Therefore, a post-staining sample treatment is required. Fenton has proved unsuitable for post-treatment in the previous step. So, it was relegated to pre-treatment role to remove the bulk of organic contaminants before the staining process. This leaves open the need for a suitable post-staining treatment.

Therefore, the developed sample preparation and staining protocols were applied and tested in various combinations (from here on termed workflows). The aim was to obtain a final workflow that produced the least amount of background contamination for blank



sludge samples (i.e. not spiked with polymers) while retaining the dye on the microplastic particles in control and test samples.

First, an initial round of experiments was conducted to gain a better understanding of the effectiveness of possible workflows on 0.5 mL sludge samples (blanks) (Table\_5.2\_A. 3). This round showed the absolute necessity to utilize post-staining treatments to digest the excess dye and remove interference as much as possible.

Therefore, a second round of experiments was conducted to further optimize the workflows and to ensure that the staining on the surrogate polymer PE would survive the suggested alternative treatments. Thus, workflows based on the results obtained from the previous Fenton experiments were further optimized and tested on the surrogate polymer PE with UPW and no sludge (control samples). The second round of protocols were subsequently again tested on 0.5 mL blank sludge samples to ensure minimal background interference. The tested workflows are summarized in Table 10.

*Table 10. Workflow development to increase the remaining brightness on PE particles after treatment. RT: room temperature*

No.	Tested Workflows with UPW samples**
I	PE → Staining → Fenton
II	PE → Staining → H <sub>2</sub> O <sub>2</sub> (30% for 1 h and 2 h @ RT)
III	PE → Staining → Methanol (10 min, 30 min, 1 h @ RT)
IV	PE → Staining → NaClO (14% for 30 min, 1hr and 2 h @ RT)

\*\* These workflows did not include a Fenton digestion prior to the staining process because those were pure PE samples without organic contaminants. Fenton digestion before staining (Pretreatment Fenton) had no impact on the staining performance as explained below.

Experiments showed a slight positive difference (Figure\_5.2\_A. 5) in the staining performance to microplastics if Fenton was applied prior to the staining (Pretreatment Fenton) compared to pristine PE samples (without Fenton pre-treatment). These changes could be due to induced roughness and polarity changes to the surface of the particles to alter the absorbance characteristic of the dye onto the particles' surface. To test for worst case scenarios and to save time and material, Fenton pre-treatment was not included in any experiments not containing sludge matter (such as the ones described in Table 10). However, when sludge samples were investigated,

the workflows always included a Fenton pretreatment to remove the natural organic matter before staining.

The staining protocol used in each of the aforementioned four workflows (Table 10) was selected from the experiments in the previous section (Section 5.2.2.2). The Fenton protocol was adopted from Al-Azzawi et al. with a selected scaling factor (so called K factor as defined by Al-Azzawi et al.) of 10 mL [57]. Sodium hypochlorite bleaching was performed by submerging the sample in 10 mL of 14% of NaClO for 30 min, 1 hr and 2 hrs at room temperatures. Methanol was also used where samples were submerged in 10 mL for 10 min, 30 min as well as 1 hr at room temperature.

After each step in the workflows, the samples were filtered and the contents of the filters were extracted as follows: The filters were submerged in 4 mL of the reagent required for the next step and placed in an ultrasound bath for 5 minutes to loosen up the filtered materials from the surface. The filters were then carefully taken out of the vials and gently rubbed against the glass walls to remove the rest of the matter still adhered to them. The filters were then rinsed using 6 mL of the reagent to bring the total volume in the vials up to 10 mL. Finally, staining steps were always followed by 5 seconds of rinsing with methanol during vacuum filtration to remove excess and precipitated dye particles.

The workflow, which produced the least amount of background contamination (darkest filter background) and the least number of fluorescence interference in non-spiked (blank) sludge samples while at the same time not degrading the staining performance on PE, was selected as the best overall workflow. Analyses were made by imaging 10 individual PE particles as well as 3 general images using a Zeiss LSM 510-META confocal microscope (Carl Zeiss, Germany), using Cy3 channel (Ex:650 nm, Em:670 nm) with an exposure time of 300 ms. Image capturing was performed using Zen Blue 3.0 software. 10 - 20 images of single particles were taken using the 10x objective. Particle brightness were analyzed using ImageJ (for the programmed script please refer to the appendix, chapter 9.6.3)

The schematic overview of the experimental plan is illustrated in Figure 24. The final selected workflow based on successful staining of PE and reduction of matrix interference, was then tested on seven microplastic types (PE, PS, PA, PLA, PVC, PET, PP) to ensure they can all light up.

These experiments were performed with a Leica LMD 7 fluorescence microscope (Leica, Germany), using an automated stage and stitching function to image the entire surface of the 25 mm PCET filters (Carl Roth Germany). Experimental parameters were as follows: A cyan laser with 482-498 nm excitation wavelengths and a 1.25x objective was used. Exposure was 300 ms and a sensitivity of 1 without pixel binning. The pixel cutoff was chosen to be 10 pixels to avoid noise from the background, resulting in a minimum detectable particle size of 18.51  $\mu\text{m}$ , images were captured using a color camera (DFC7000T) at 12 bits. The analysis was done using LASX image analysis suite from Leica using the stitched images. Particles were segmented using the maximum entropy algorithm with color and intensity parameter that were adjusted individually to each image to avoid selecting the background as much as possible. Some particles were green in color which made separating them from the red background easier when dealing with NR treated samples that hasn't been digested yet. Further, a fill holes algorithm was utilized to avoid noise and finally a watershed algorithm with a strength of 30% was applied to separate touching particles and small agglomerates.

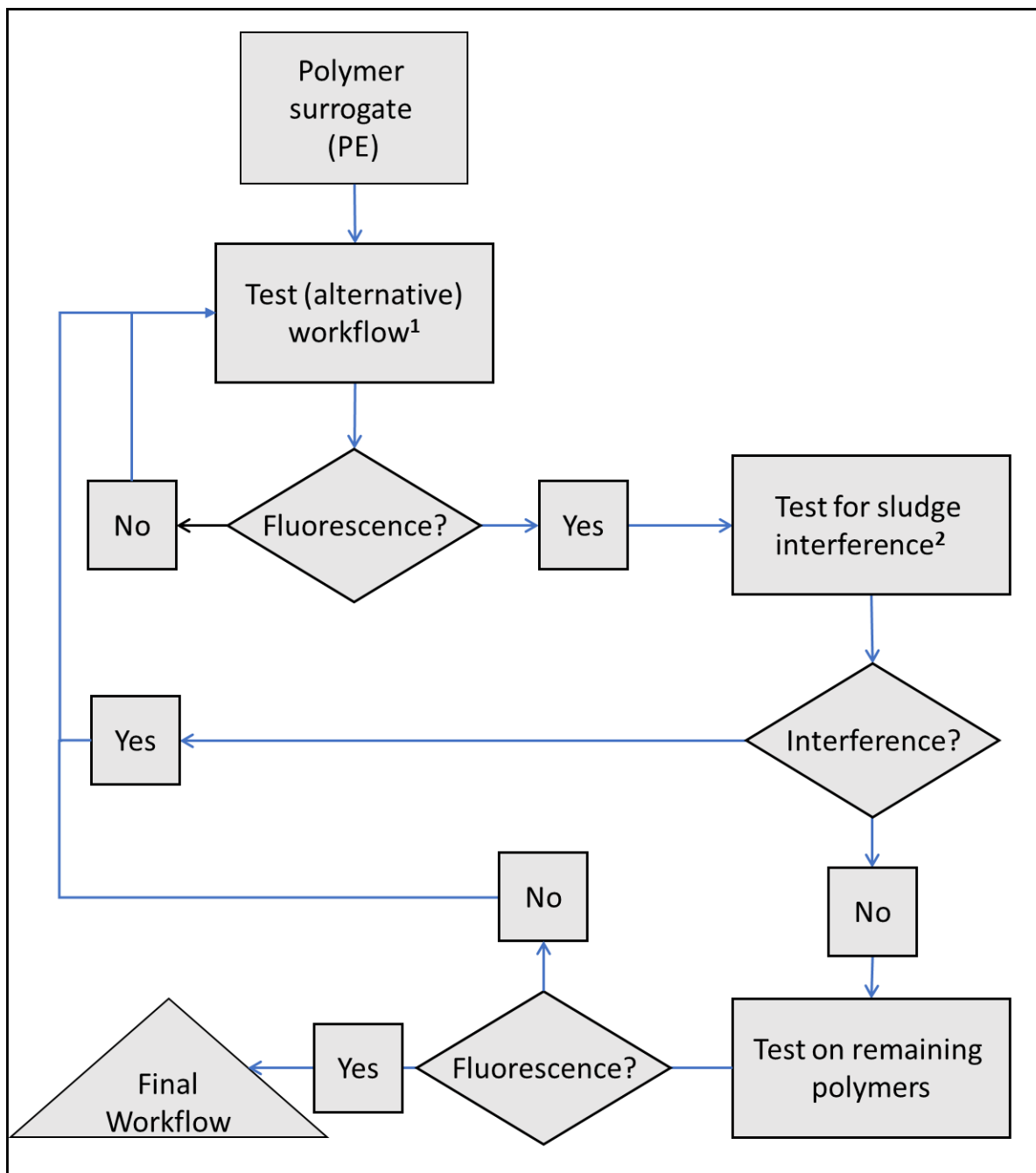


Figure 24. Schematic of the experimental plan to develop a final workflow to detect microplastics within environmental samples. <sup>1</sup> The workflows involving fluorescence method development utilized UPW samples that did not require sample preparation using Fenton pretreatment prior to staining, thus Fenton pretreatment was omitted in these cases as discussed. <sup>2</sup> Samples with sludge utilized Fenton-Pretreatment to remove organic matter constituents from sludge before staining was conducted.

#### 5.2.2.4. Recovery validation

After development of the final workflow for both dyeing the microplastic particles, as well as reducing the background contamination in control samples containing single polymers and blank sludge samples, the recovery performance for a mix of polymers was investigated inside of synthetic environmental samples.

This was achieved by preparing blank samples containing non-spiked sludge samples, containing 0.5 mL of well mixed return activated sludge samples. Control samples were then prepared as a polymer mix (PS, PE, PA, PLA, PVC and PET). The mix was prepared by weighing 2 mg from each polymer then mixing them in a suspension of 10 mL 0.1% (v/v) of Tween 20 then pipetting 0.5 mL for each mixed sample. Finally, spiked sludge samples were prepared by mixing 0.5 mL sludge with 0.5 mL of the six polymers, which was then well mixed and filtered on a 25 mm diameter 0.2  $\mu\text{m}$  PCET filter (Carl Roth, Germany). All the samples and blanks were prepared in triplicates using the final workflow and analyzed using the Leica LMD 7 fluorescence microscope. The microscope had an automated stage and image stitching function to capture the entire filter surface.

Experimental parameters for the recovery phase were as follows: Using a cyan laser with 482-498 nm excitation wavelengths and 1.25x objective. Exposure was 300 ms and a sensitivity of 5 without pixel binning. Images were captured using a DFC7000GT black and white camera at 16 bits. The pixel cutoff was chosen to be 3 to avoid noise, resulting in a minimum detectable particle size of 10.139  $\mu\text{m}$ . The analysis was done using LASX image analysis suite from Leica using the stitched images. Particles were segmented using the maximum threshold method with a lower threshold of 20,000 (out of 65,535 grey values for the 16-bit images). A fill-holes algorithm was also utilized to avoid noise and finally a watershed algorithm with a strength of 30% was applied to separate touching particles and small agglomerates. The reason the final recovery experiments were conducted in black and white rather using the color camera is that most of the polymers as well as the background lit up in red. PE and some PP particles did light up in green and could be easily separated from the background (Figure\_5.2\_A. 7 & Figure\_5.2\_A. 10), but that was in general not a problem because the particles were much brighter than the background. Furthermore, the color shift to green with PE and PP was only observed on the Leica microscope using the specific wavelengths and cutoff filters provided. Using other microscopes with similar but not exact the same setups did not result in this color distinction. Therefore, the reliance on color was omitted in order to create a more generalized workflow that could be easily followed by other labs using different microscopic setups.

#### 5.2.2.5. Cross-validation via $\mu$ FTIR

Triplicate spiked sludge samples as well as one blank (non-spiked sludge) sample were prepared as described above for the selected workflow. The samples were then filtered and rinsed into glass vials via 1% (v/v) Tween 20 in UPW. The glass vials were covered with an aluminum foil and sealed pending analysis by the Bavarian Environmental Agency (LfU) laboratory.

Cross-validation was conducted by both fluorescence microscopy and Fourier-transform infrared microspectroscopy ( $\mu$ FTIR) using focal plane array (FPA). Samples were first filtered on a 25 mm Anodisc™ (Whatman™, PP-Enforced, 0.2  $\mu$ m membrane filters) then left in an exicator for 6 days in a dark room in order to dry to avoid interference with FTIR.

Fluorescence microscopy was performed as a first step prior to  $\mu$ FTIR-analysis as it only took a few minutes and because of the light sensitive nature of fluorescence dyes. Analysis was performed using a Zeiss Axio Imager Z2 microscope with a 5x lens, using 555 nm excitation wavelength with 100% intensity, 161 ms exposure time, and a resolution of 0.9  $\mu$ m. The final scanned area was 13 mm x 13 mm. The particle detection was performed automatically via the software based on the brightness difference of Nile red dyed particles and their background.

Immediately after the fluorescence microscopy, the samples were covered and taken to be analyzed via  $\mu$ FTIR. Samples were placed on a CaF<sub>2</sub> window (25 mm diameter and 2 mm thickness) and analyzed using a Bruker Hyperion 3000 FTIR microscope with Bruker Tensor 27 FTIR spectrometer using a 64x64 Pixel FPA detector. The used IR lens was 3.5x and was operated in transmission mode with 32 scans and a wavelength of 1,250 – 3,600 cm<sup>-1</sup>. Measurements of the whole filtration area were run with a resolution of 11  $\mu$ m. Particle analysis was performed using the siMPle 1.01 software.

To exclude particle moving or loss during transport from fluorescence microscope to  $\mu$ FTIR spectroscopy, fluorescence microscope measurement was repeated immediately after  $\mu$ FTIR measurement.

### 5.2.3. Results and Discussion

#### *5.2.3.1. Initial staining protocol development*

None of the investigated solvents exhibited any detectable deviation in size from the control groups. Therefore, all tested solvents as well as any lower concentrations of them were deemed suitable for treatment of microplastics for the purposes of this study.

The results for the selection of a base staining protocol are shown in the Appendix (Figure\_5.2\_A. 1). It can be observed that acetone- and acetonitrile-based protocols produced brighter particles than the rest. The best performing protocol in these experiments was 1 mg/L Nile red in 10% acetonitrile for 30 minutes at room temperature. This protocol was able to dye all the five microplastic fragments and PS microspheres with an average grey value (14-bit images) for all polymers of 7,890 [-].

#### *5.2.3.2. Optimizing staining resiliency*

After applying Fenton to the stained microplastics, it was observed that PS, PLA, and PA lost 70% of their brightness. Whereas PET fragments and PS microspheres lost 50% and 90% of their brightness, respectively. However, all those polymers were still visible under the microscope, even after this large reduction in brightness. In contrast, PE was the only polymer type that lost all of its brightness and became invisible when viewed under the fluorescence microscope. Thus, a new optimized staining protocol was needed to improve dye retention on PE after Fenton treatment.

To optimize the staining resiliency, an additional round of experiments was conducted. These experiments revealed that using elevated temperature (70 °C) aided in the adsorption of the dye onto the polymer's surface. However, using very long contact times proved counterproductive as the brightness tended to be lower after 24 hours than after 2 hours. This phenomena was also reported by Maes et al. who investigated contact times up to 66 hours and determined a cutoff point after which the brightness starts to decrease as the dye desorbs from the particle surface and starts adsorbing on filters and glass walls [51]. The best performing protocol for these conditions was 10 mg/L Nile red in 10% acetonitrile for 2 hours at 70 °C. This protocol allowed the stained PE particles to remain visible even upon applying the subsequent Fenton reaction. Though, the brightness of PE post Fenton had an average grey value (14-bit

image) of around 200 [-]. This is a very low brightness value. It was enough to visually distinguish and separate the PE particles from the filter's background only when the sample was pure (controls), but not when mixed with a sludge sample (test spiked samples). Therefore, the staining and sample preparation workflows had to be optimized further in order to obtain a higher brightness (grey value) from the microplastic particles while reducing background interference. This additional step included omitting the use of Fenton as a post-treatment after applying the dye and limiting its role to sample pretreatment to digest the organic matter before applying staining. This is further discussed in the next section. This final staining protocol was tested using PA, PET, PLA, and PS fragments as well as PS microspheres. All polymers showed higher brightness levels compared to PE after applying Fenton with a brightness value of >1,000 [-] in all cases.

Finally, the 2 hours contact time was reduced to 30 minutes to increase throughput and there was no noticeable reduction of fluorescence intensity and results were comparable to the 2-hr samples. Therefore, the finally selected staining protocol was submerging the samples in 10 mL solution of 10 mg/L of Nile red dissolved in 10% acetonitrile working solution for 30 minutes at 70 °C. The samples were always suspended in 0.1% v/v Tween 20 to avoid agglomerates. Tests between Tween 20 based working solutions and ultrapure water (UPW) showed no recognizable difference in the staining performance.

#### *5.2.3.3. Minimizing co-staining and background interference*

Applying Nile red directly to sludge samples produced highly contaminated samples where no particles could be distinguished from the bright filter background. Applying Fenton helped to digest and remove the organic matter. However, the order in which the sample preparation and staining is performed (workflow) was crucial; for example, the workflow 'Sample → Fenton → NR staining' still produced very high levels of background interference that made it impossible to recognize particles (Figure 25 A).



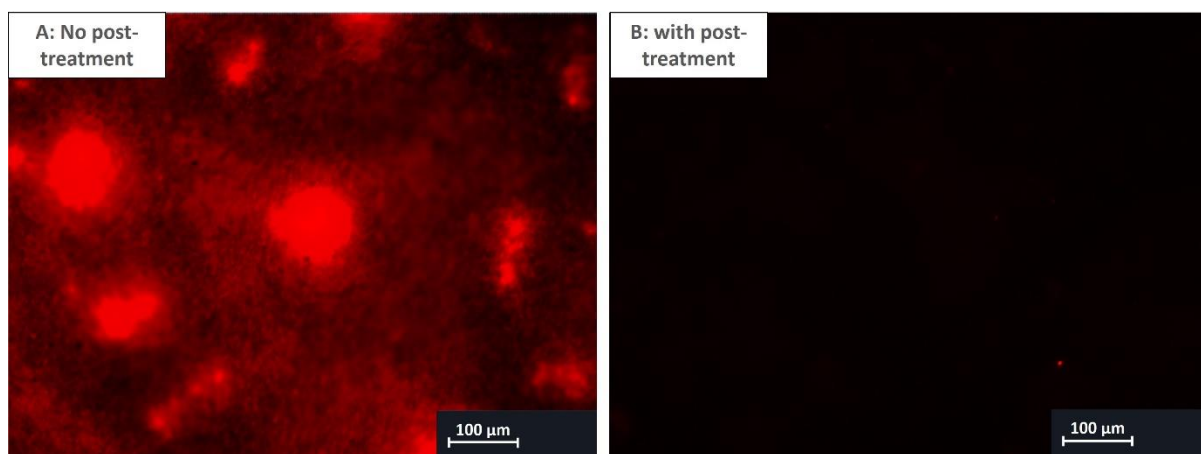


Figure 25. Non-spiked sludge sample image of the background fluorescence brightness for the workflows: A. No post-treatment: Sample → Fenton → NR staining, and B. with post-treatment using the best performing workflow: Sample → Fenton → NR staining → NaClO (30 minutes). The interference due to background co-staining is too high in image A. Thus, no particles can be distinguished without post-treatment.

All other workflows, where the staining step was followed by sample post-treatment, provided a noticeable improvement with a filter background that was much darker for non-spiked sludge samples. However, using Fenton as a post-treatment resulted in dark PE particles that were nearly impossible to distinguish in treated sludge samples. Therefore, it was decided that Fenton should proceed the staining step (Fenton pretreatment). However, to prevent excess dye from interfering with microplastic identification (Figure 25 A), an alternative post-treatment that is not as destructive to the dye as Fenton was needed.

For this purpose, the best performing workflow was found to be ‘Sample → Fenton → NR staining (ACN 10% 10 mg/L for 30 min @ 70 °C) → NaClO (14% for 30 min @ RT)’. Results for all tested workflows are listed in the Appendix, Chapter 6.2. An example for NaClO post-treatment is provided in Figure 25 B.

This final workflow was additionally tested for seven polymers (PA, PS, PP, PE, PET, PVC, and PLA) as well as blanks (non-spiked sludge) and it showed very clean filters with the blank samples as well as bright, clearly identifiable microplastic particles in the controls. The results for the brightness of polymers before applying the bleaching step are presented in Figure 26. The polymers showed on average 42% loss of brightness after applying the selected workflow (i.e. after the bleaching step) compared to no post-treatment. Nevertheless, all polymers were easily distinguished from the background, even PE and PP, which showed the lowest brightness of any

polymer. Example images for each of the polymers are presented in the Appendix, Chapter 9.6.4. Note that Fenton Pretreatment was not included in the workflows performed here as the samples contained no sludge or other contaminants. However, experiments showed a slight positive effect (Figure\_5.2\_A. 5) on the uptake of dye by the polymers if preceded by a Fenton pretreatment as explained in Section 5.2.2.3.

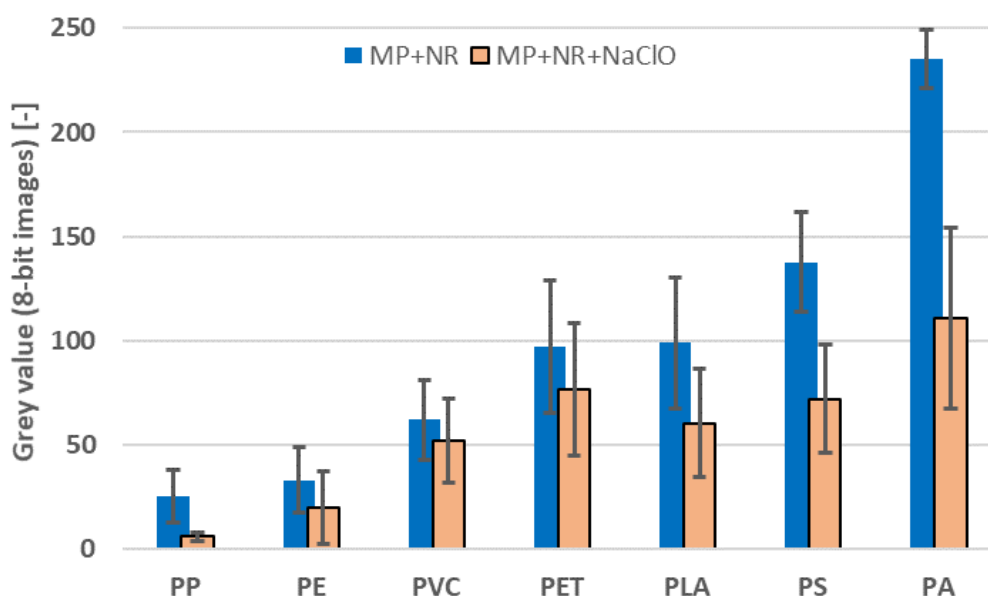


Figure 26. Comparison of microplastic brightness after applying NR staining (MP+NR) and after applying the final workflow (MP+NR+NaClO). Particle brightness are sorted from largest to smallest. Note that Fenton is not included in the workflow here as discussed above.

#### 5.2.3.4. Recovery validation using Fluorescence microscopy

The attempt to perform a recovery validation was unsuccessful for the simple fact that it was very difficult to achieve a consistent number of particles across 6 or more samples. The mixed polymer (PS, PE, PA, PLA, PVC, and PET) samples were suspended in 10 mL 0.1% (v/v) Tween 20, but pipetting 0.5 mL of this mixture for each sample could not deliver consistent number of particles regardless of various attempts to optimize the process. Running an ANOVA test between many of the control samples revealed they were significantly different from each other. Therefore, this approach could not be considered a recovery validation. Nevertheless, it showed the viability of this analytical approach as blank (non-spiked) sludge samples exhibited very little interference when compared to the control and spiked samples.

It was observed that 82% and 95% of particle sizes in the blank sludge samples were under 25  $\mu\text{m}$  and 40  $\mu\text{m}$ , respectively. This means that utilizing this technique could be feasible, since it focuses on a similar particle size range as  $\mu\text{FTIR}$  spectroscopy (particles  $>20 \mu\text{m}$ ) [113]. The comparison between the various samples is presented in Figure 27 for 10  $\mu\text{m}$ , 25  $\mu\text{m}$  and 40  $\mu\text{m}$  cutoffs.

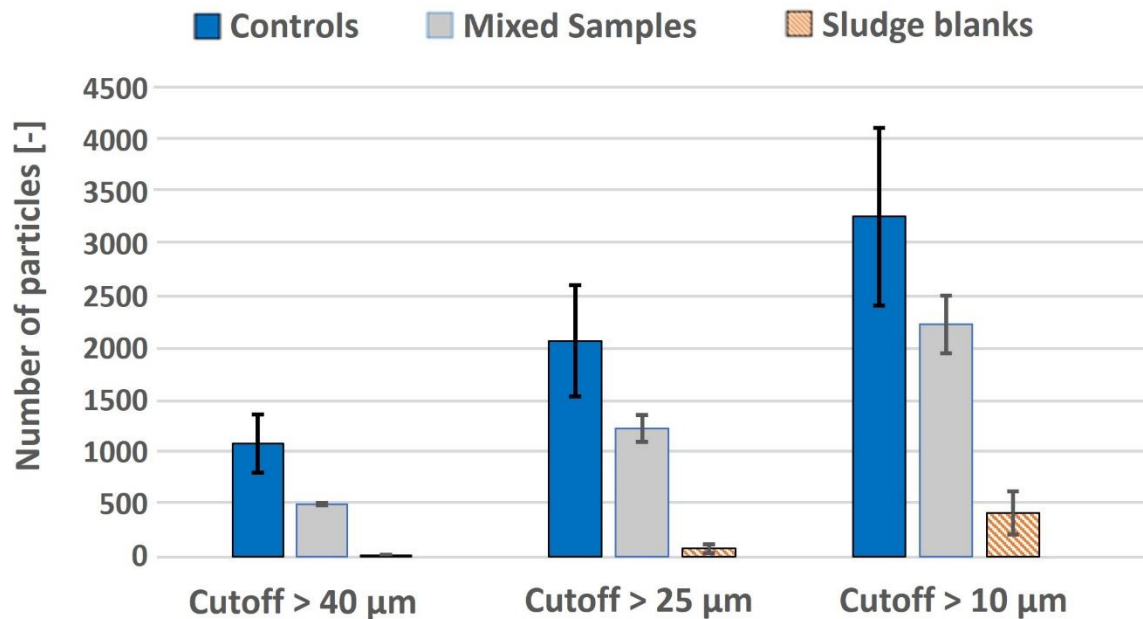


Figure 27. Comparison of controls, mixed samples and sludge blanks for particles  $>40 \mu\text{m}$  (left side),  $>25 \mu\text{m}$  (middle), and  $>10 \mu\text{m}$  (right side).

The sludge blanks only have 13 fluorescence particles on average that are larger than 40  $\mu\text{m}$ , making it very promising for further validation and use under field conditions. The effectiveness of this method in sludge samples is also very evident when looking directly at the obtained images from the Leica microscope, such as the example presented in Figure 28.

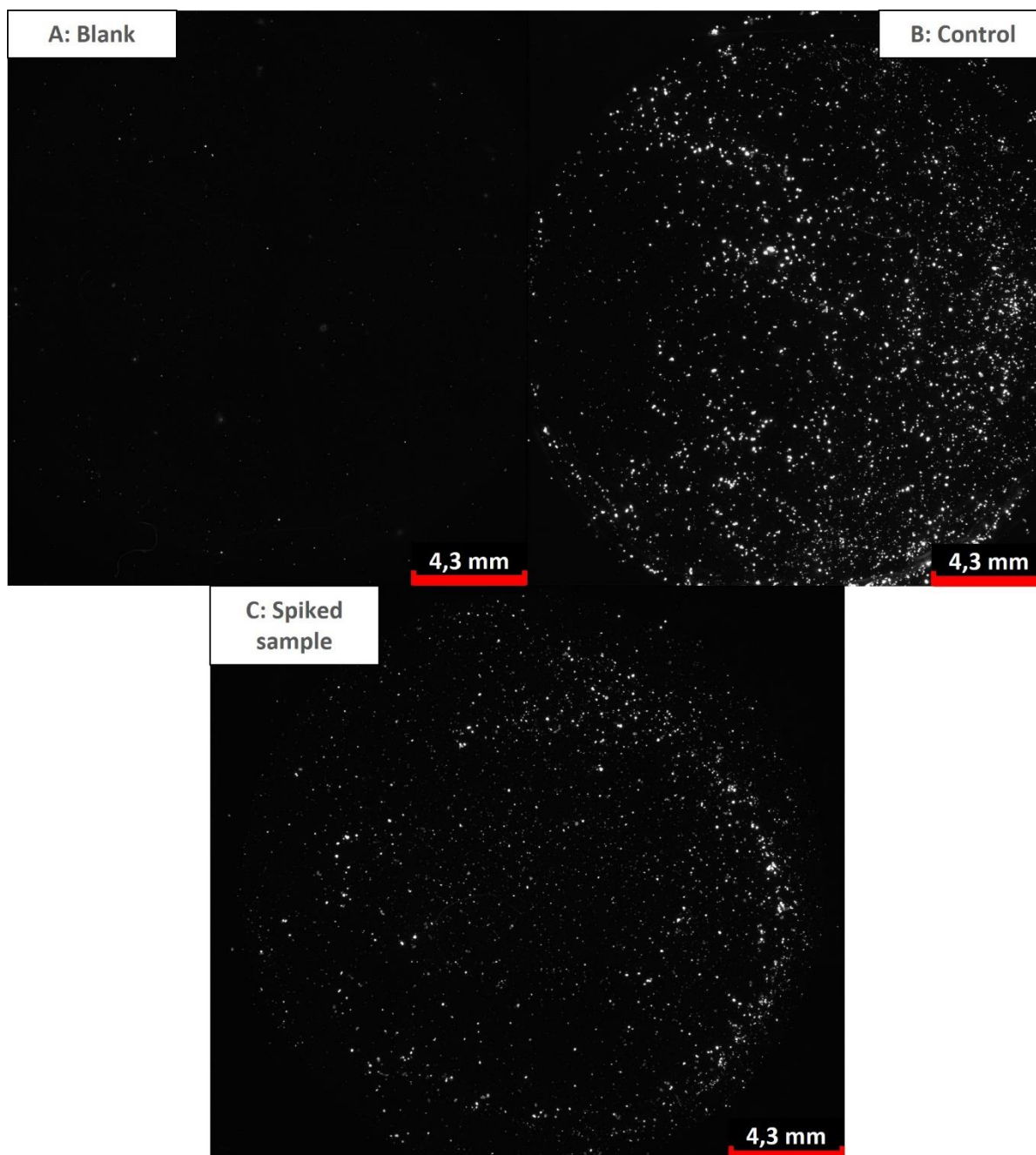


Figure 28. Comparison images of A: non-spike sludge (blank), B: polymer mix (Control), and C: Spiked sludge samples. All samples were treated with the same workflow (Sample → Fenton → NR → NaClO 30 min).

Since PE exhibited only weak fluorescence after applying the final workflow, it was tested again individually by spiking 2 mg of PE in 0.5 mL sludge. This was to ascertain that the weak brightness of PE (Figure 26) was sufficient to separate it from the background within a real sludge matrix. Results are presented in Figure 29 and Figure 30 and confirm that PE could be easily separated from the background. Here, it was again observed that the sludge contains most of the interfering particles at sizes

smaller than 25  $\mu\text{m}$  and almost all are smaller than 40  $\mu\text{m}$ . Therefore, it is recommended to investigate particles larger than 40  $\mu\text{m}$  as this region provides very little interference from sludge.

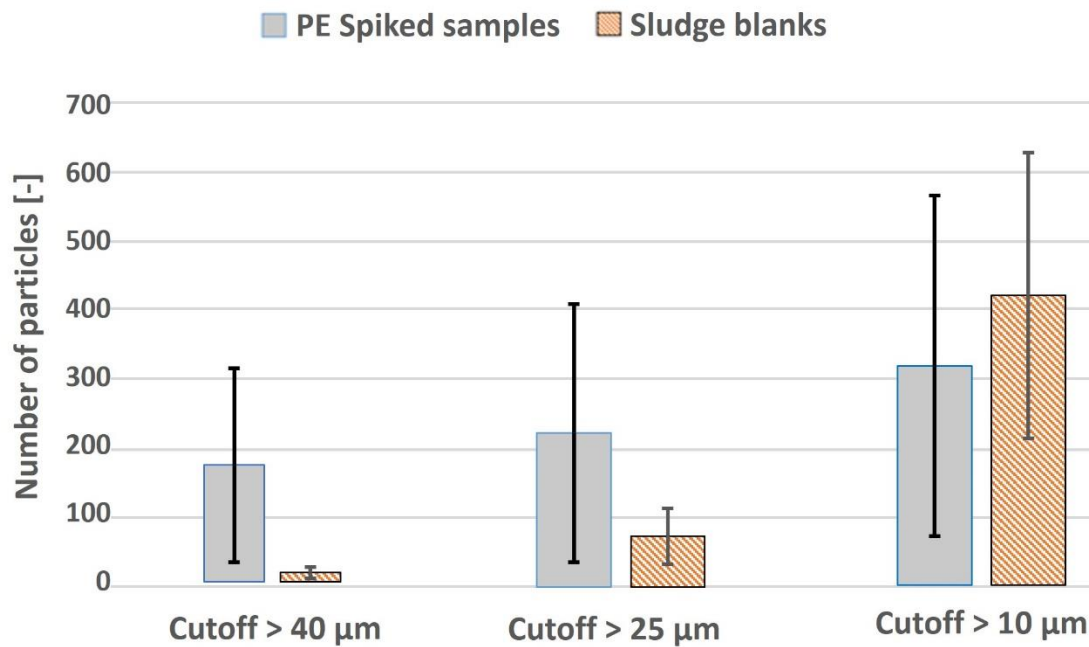


Figure 29. Comparison of PE-spiked samples and blanks for particles >40  $\mu\text{m}$  (left side), >25  $\mu\text{m}$  (middle), and >10  $\mu\text{m}$  (right side).

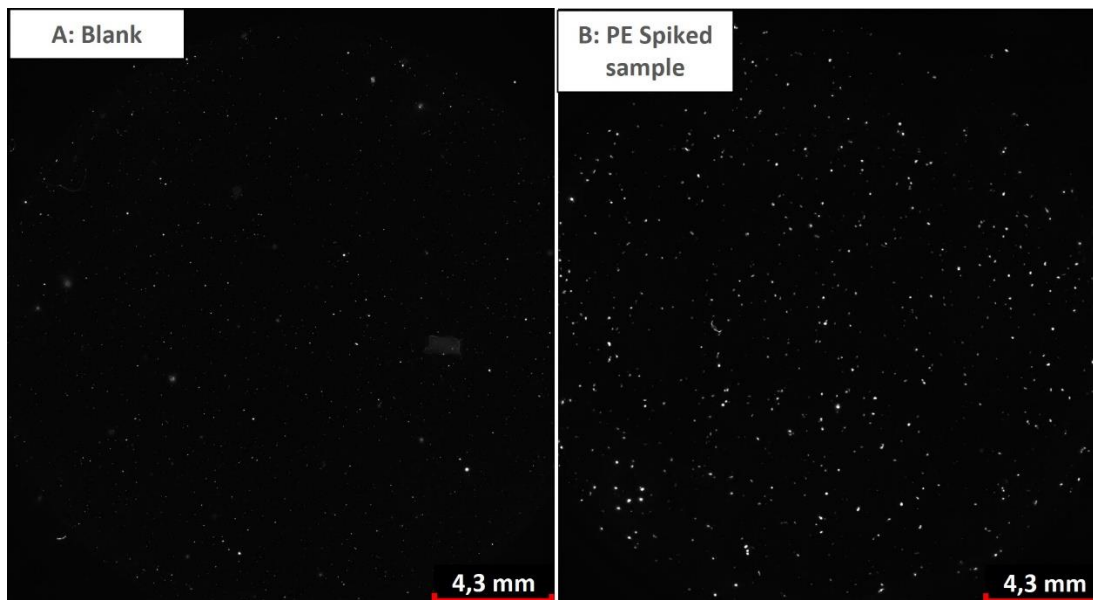


Figure 30. Comparison images of A: non-spike sludge (blank) and B: PE-spiked sludge sample. All samples were treated with the final workflow 'Sample  $\rightarrow$  Fenton  $\rightarrow$  NR  $\rightarrow$  NaClO 30 min'.

#### 5.2.3.5. Cross-validation using $\mu$ FTIR spectroscopy

FTIR spectroscopy operates in the infrared (IR) range, which should render it unsusceptible to interference from fluorescence [26]. Moreover, Maes et al. reported in their study a successful cross-validation of Nile red treated particles using FTIR spectroscopy, without reports of interference [51]. Therefore, this was the assumption for this part of the investigation. Nevertheless, attempting to cross-validate the stained microplastic particles in this study using  $\mu$ FTIR spectroscopy proved unsuccessful due to the garbled microplastic spectra as a possible result of NR and Tween 20 interferences. Samples of these spectra can be seen in the supporting material in the appendix, chapter 9.6.5.

When attempting to update the FTIR library to include reference particles treated with NR as well as Tween 20, no systematic pattern was recognized for the interferences. The new reference particles did not have any significant pattern that could be used as a fingerprint. Nevertheless, an attempt was made to create a new database using the same dyed polymers as reference particles. That proved unsuccessful, increasing the recognition rate for PLA by merely 27% in the reference sample. Whereas in the spiked sludge sample this new database resulted in only two new particles being recognized (out of an expected 250-500 particles). The rest of the polymers showed similarly poor recoveries, with PVC showing zero new particles. These results suggest that further research is needed in the future to investigate the nature of this interference.

#### 5.2.4. Conclusion

The proposed workflow used Fenton pretreatment to reduce natural organic matter in sludge before staining the sample, followed by bleaching the co-stained particles and excess dye using sodium hypochlorite, which was effective at reducing interferences to a minimum. Fenton protocol has been previously validated by the authors to be an effective sample treatment method that does not induce major adverse effects on the microplastics down to 1  $\mu$ m [57, 213]. This workflow shows great promise for wastewater and sludge samples especially in the size range larger than 25  $\mu$ m (or 40  $\mu$ m for worst case scenarios), which would make it an excellent choice to supplement  $\mu$ FTIR analysis. It can even be combined with TED-GC/MS to obtain details regarding numbers and size distribution while TED-GC/MS provides the

identification and chemical composition of the sample. Unfortunately, the experiments to cross-validate the workflow against  $\mu$ FTIR did not yield usable results due to extreme interference with the FTIR spectra. Thus, the proposed method needs further validation via real field samples and a cross-analytical study as suggested previously by Al-Azzawi et al. [214], in order to ascertain the robustness of this method compared to  $\mu$ FTIR spectroscopy.

### *Acknowledgement*

This work represents the culmination of over three years of research that was only made possible by the support of two students at the Chair of Urban Water Systems Engineering at the Technical University of Munich, Sami Fanger and Simran Chauhan.

### *Funding sources*

The presented scientific work was funded by the German Federal Ministry of Education and Research (BMBF) [grant numbers 02WPL1443A, 02WPL1443C] and the Bavarian Research Foundation [grant number: 1258-16]

## 6. Research outcome and discussion

The goals set in this dissertation were to investigate and establish holistic best practices for microplastic analytical approaches in monitoring aquatic environments, especially WWTP effluents. To this end, all relevant aspects of monitoring were investigated, and the knowledge gaps were explored regarding sampling, sample preparation and sample analysis.

### Sampling

The knowledge gaps identified in Chapter 1.1.1, such as the need to sample large volumes and capture smaller particles simultaneously, and to optimize a harmonized workflow in the field, including field blank samples and contamination prevention, as well as workarounds were all addressed in this dissertation. Chapter 3 introduced a pressure driven cascade filtration system that was used to sample secondary and tertiary effluents of three full-scale WWTPs. It also demonstrated the benefits of utilizing sealed cartridge cascade filtration sampling, namely the ability to sample large volumes of water while simultaneously capturing smaller microplastics. This combined the knowledge obtained from studies utilizing non-pressurized cascade filtration systems, such as Bannick et al., with the benefits of sealed cartridge filtration (single sieve filtration) from studies like Lenz et al. [22, 200]. Both of these studies struggled to achieve sampling volumes beyond 1 m<sup>3</sup>, which are not sufficient for sampling larger, more scarce microplastic particles [200]. By combining these two approaches in the current study, much larger volumes were successfully sampled on the larger sieves (up to 7 m<sup>3</sup>) and particles down to 10 µm were collected on the smallest sieve.

In Chapter 5.2, this system was again tested and validated using spectroscopic and thermo-analytical techniques. Here, it was shown that cascade filtration was not reliable for size fractioning of a sample to estimate size classes. This limitation was caused by cake filtration build-up, which trapped smaller particles on larger sieves, as well as sieve wear during use, which compromised the mesh in some areas of the sieve, allowing larger particles to be collected on the smaller sieves. Therefore, it is not recommended to use the cascade filtration in combination with a thermo-analytical method if the information about size fractions is needed. In particular this is an issue as the presence of a few larger particles can overshadow many smaller (but lighter) microplastic particles when using thermo-analytical methods. This was important to



validate as it was suggested that cascade filtration might be used as a quick estimate for size distribution using only thermo-analytical techniques, which is now proven to be error-prone in this dissertation [22].

Finally, Chapter 5.2. also investigated the sampling of field blanks and suggested sampling from larger depths in order to circumvent air pollution and the need to sample those kinds of blanks. This sampling system was already proposed in a previous study by Funck et al. [32]. Therefore, this phase was not associated with the testing of any hypothesis. Instead, Chapter 3 served to introduce the proposed sampling system and investigate its benefits via deploying it in multiple field sampling campaigns at different WWTPs and treatment conditions.

### **Sample preparation**

Sample preparation methods are far from harmonized in literature and as stated in Chapter 1.1.2, this represents a major challenge when trying to compare the results of different authors. Not to mention the complete lack of validation for smaller microplastics ( $\leq 10 \mu\text{m}$ ) in the peer-reviewed literature.

Therefore, sample preparation methods based on Fenton and hydrogen peroxide protocols were first optimized and validated for sludge samples and common polymers in the size range of 80 – 300  $\mu\text{m}$  in Chapter 4.1. These protocols were then further validated for adverse effects on smaller microplastics in the size  $\leq 10 \mu\text{m}$  in Chapter 4.2. Fenton protocols was also harmonized, and two types of previously undiscussed Fenton reaction types were identified, aptly named Fenton type I and type II reactions. Thereby clarifying the discrepancies that existed in literature regarding Fenton reactions. Chapter 4 dealt with the testing of **Hypotheses 1 and 2** (details at the end of the chapter).

### **Sample analysis**

The synergies between different spectroscopic and thermo-analytical techniques were investigated and elaborated on in Chapter 5.1. This also included a discussion about best practices regarding the entire analytical process, starting from sampling and ending with sample analysis. The study was performed and validated in the field using

the cascade filtration system introduced in Chapter 3 and several analytical techniques ( $\mu$ FTIR,  $\mu$ Raman, TED-GC/MS). Subsequently, the knowledge gap regarding the validation of fluorescence microscopy analytical techniques was addressed. Especially regarding its use as an alternative to the lengthy, cost intensive chemical analysis techniques mentioned above. This meant combining an optimized fluorescence staining protocol with the Fenton protocol from Chapter 4.1 as well as sodium hypochlorite (bleach) treatment in order to produce clearly tagged microplastic particles while minimizing false positives due to natural matter interference from the wastewater matrix. Chapter 5.2 dealt with this topic and included testing **hypothesis 3** (details at the end of the chapter).

### **Hypotheses testing**

Following is a summary of the hypotheses and the outcome of their testing:

*“**Hypothesis (1a)** A sample preparation method can be developed that will not reduce the size of microplastic particle which are  $\geq 200 \mu\text{m}$  by more than 10% while also not compromising the identification of microplastics using FTIR spectroscopy or TD-Pyr-GC-MS”*

In Chapter 4.1, two oxidative sample preparation methods were successfully developed and validated (Fenton and hydrogen peroxide). The methods did not cause a decrease in the size distribution of seven common polymers (PS, PE, PET, PP, PA, PLA, and PVC) with an average size of 80 – 300  $\mu\text{m}$ . The method caused a size increase in some cases like PLA, but that was the result for agglomerations as the laser diffraction analytical technique used for the analysis was sensitive to larger particles. Furthermore, no changes were observed in the spectra or pyrograms of any of the microplastic particles after treatment. Since the 80 – 300  $\mu\text{m}$  size range covers sizes both smaller and larger than 200  $\mu\text{m}$ , **hypothesis 1a can be accepted as valid**, as larger microplastics are generally less reactive, and thus less susceptible to chemical reagents than their smaller counterparts due to their smaller surface area to volume ratios.

*“**Hypothesis (1b)** Fenton reactions can be used without cooling to rapidly reduce organic matter content in sludge samples (>90%), without compromising the identification of*

*microplastics using FTIR spectroscopy or TD-Pyr-GC-MS or the size distribution of microplastics by more than 10%”*

Results presented in Chapter 4.1 demonstrated that it is possible to use Fenton reaction (type I, as defined in Chapter 4.1) without any cooling to obtain a rapid and complete removal of organic matter from return activate sludge samples. This method was the same one validated for hypothesis 1(a). Hence, it is validated not to have a significant effect on the size of microplastics, nor their identifiability using FTIR or TD-Pyr-GC/MS. Therefore, this **hypothesis can also be accepted as valid**.

*“Hypothesis (2) The size distribution of sub-microplastics ( $\leq 10 \mu\text{m}$ ) is reduced by more than 10% after directly applying the selected sample preparation methods based on hydrogen peroxide and Fenton as specified for Hypothesis 1”*

Findings presented in Chapter 4.2 showed a validation of the effects of the previously developed sample preparation methods (Fenton and hydrogen peroxide) on small microplastics ( $\leq 10 \mu\text{m}$ ) and nanoplastics ( $< 1 \mu\text{m}$ ). In this case, it was determined that nanoplastics were affected the most and interfered with the average changes for the entire distribution due to their large numbers. The analysis used was fluorescence microscopy as the previous laser scattering technique used for hypothesis 1a wasn't sensitive enough in this case. However, the fluorescence dye was not very stable on very small particles due to their increased surface area to volume ratio and associated reactivity, - possibly causing under reporting of their numbers after sample preparation. Therefore, the results for the nanoplastics could not be relied on and had to be excluded.

The results for the 1 – 10  $\mu\text{m}$  size range were calculated and mostly showed no major changes after sample preparation. However, a few polymers exhibited a change in their average size distribution by more than 10%. Some of those changes were observed as an increase of over 10% in the average size after treatment with Fenton, such as the case for PA and PVC which increased by  $20\% \pm 4\%$  and  $14\% \pm 8\%$ , respectively. Due to the way microscopic image analysis works and the fact that the average sizes were compared, this kind of increase in size is possible in one of two ways: (1) via agglomeration of particles, for example as a result of high temperatures, i.e., actual size increase, or (2) loss of smaller particles as a result of either a reduction in their size below 1  $\mu\text{m}$  or a loss of the dye on the smallest particles. i.e., indicated

average size increase as a result of loss of the smallest particles. The average (mean of the distribution) was selected as the main variable for two reasons; (a) to keep it in line with the testing of hypothesis 1a and (b) to place slightly more importance on the larger particles in these heavily right skewed size distributions.

It is worth noting that only PA and PP had significantly reduced number of particles after treatment than when compared to the control samples, especially for Fenton; PA just showed in general less smaller particles (Figure\_4.2\_SI. 2), whereas PP had very dim images that the autofocus mechanism could not obtain a focus on the smaller microplastics, giving it a cloudy appearance (Figure\_4.2\_SI. 1). Therefore, PP could not really show any significant changes after Fenton due to the large measurement errors (Figure 16). On the other hand, laboratory experiments with PA and staining indicated that it tended to absorb the Nile red dye quite well and did not lose too much color after sample preparation (chapter 5.2). While this cannot be used 1:1 for smaller microplastics and especially not for nanoplastics, it can still be argued that the likelihood is high that such a sensitive polymer like PA might actually lose the smallest particles rather than just lose their staining. Whereas for PP it was clear that the smallest particles were still there but appeared very faint (Figure\_4.2\_SI. 1) and it was difficult to perform an automated analysis with autofocus. Both of these observations are in line with the findings of Li et al. who after performing a principle component analysis showed that PA is one of the most sensitive polymers, whereas PP was the least sensitive to sample treatment [107].

Assuming that the loss of PA and PVC is not attributed just to loss of the Nile red dye, the loss of smallest particles can be observed from the size distribution parts of Figure\_4.2\_SI. 2 and Figure\_4.2\_SI. 6, where the size distribution for Fenton is slightly shifted to the left for both PA and PVC (size decrease) starting around 3  $\mu\text{m}$  and 2  $\mu\text{m}$ , respectively, when compared to the control and hydrogen peroxide samples. This behavior does not exist for the other polymers except PP, where the smallest particles were so dim after Fenton treatment (Figure\_4.2\_SI. 1).

There was also a single incident of the average size reduction by more than 10% in the case of PLA after hydrogen peroxide treatment, which was reduced by  $11\% \pm 2\%$  for the size range of 1 – 10  $\mu\text{m}$ . However, this change was more extreme when nanoplastics were included with a reduction of  $46\% \pm 15\%$  in average size for PLA. Such a reduction can again indicate one of two things: (1) a reduction in size of the

larger particles as a result of melting or (2) the breaking up of agglomerates causing an increase in the count of smaller particles.

Since the reduction in case of PLA was larger when nanoplastics were included in the analysis, this indicates that the reduction came through an apparent increase in the number of smaller particles (i.e., fractioning of larger particles or agglomerates into smaller particles. Furthermore, looking at Figure\_4.2\_SI. 4, PLA exhibited both a large increase in the percentage of smaller (<2  $\mu\text{m}$ ) particles after sample treatment and a reduction of the percentage of particles which are larger than 2  $\mu\text{m}$ . This then is likely a mix of agglomerates breaking up as well as melting of larger particles.

In summary, PA, PLA and PVC showed signs of a size decrease for the smallest particles. With PLA after hydrogen peroxide showing a directly measurable average size decrease across the target size range ( $\leq 10 \mu\text{m}$ ) of  $11\% \pm 2\%$ . Thus, **hypothesis 2 can be partially accepted as valid** for hydrogen peroxide and PLA since it displayed a reduction over the entire range ( $\leq 10 \mu\text{m}$ ). The hypothesis cannot be accepted for Fenton reactions as the results did not indicate a clear reduction of size across the range. For example, when using Fenton with PA and PVC, it could be argued that there was a loss of very small particles (<3  $\mu\text{m}$ ) as a result of size reduction after sample preparation. However, it is impossible to say with certainty using the current setup, if the loss of some of the smaller particles was due to the loss of small particles (<3  $\mu\text{m}$  and <2  $\mu\text{m}$  for PVC and PA, respectively) or the loss of the dye.

*“Hypothesis (3) Hydrophobic fluorescence dyes can be used in conjunction with sample preparation to establish an affordable, rapid quantitative analysis for microplastic particles larger than 40  $\mu\text{m}$  in WWTP effluents. This approach can quantify microplastics with an accuracy of  $\geq 70\%$  compared to  $\mu\text{FTIR}$ ”*

Findings presented in Chapter 5.2 revealed the possibility to use fluorescence staining to detect microplastics in wastewater effluent samples. The method development succeeded in producing a protocol that combines sample preparation using Fenton to remove the organic matrix from samples and subsequently staining the remaining matrix as well as the microplastics in the sample with Nile red. Finally, bleach (sodium hypochlorite) treatment is used to gently remove the excess dye that adsorbed on the rest of the natural matrix as well as the filter, thereby reducing background brightness

which would interfere with the segmentation of the images and identification of particles.

The recovery experiments using spiking with a mix of microplastic particles (>10  $\mu\text{m}$ ) of different polymers (PS, PE, PA, PLA, PVC, and PET) showed that blank sludge samples (no spiking) exhibited very little fluorescence and only very few particles (5% of the total particle count) >40  $\mu\text{m}$ . On the other hand, the spiked samples clearly showed the microplastic particles that were added. Unfortunately, there was no reliable way to count the particle before spiking them, thereby no recovery ratio could be determined.

Moreover, the goal of the hypothesis is to validate fluorescence microscopy against  $\mu\text{FTIR}$ . Unfortunately, due to the difficulties in establishing new libraries to avoid the unexpected interference from the Nile red dye, no  $\mu\text{FTIR}$  analysis could be performed as indicated in Chapter 5.2. Therefore, by definition this hypothesis could not be tested, and it can neither be accepted nor rejected.

## 7. Research outlook

In this dissertation, the basic stepping stones of microplastic monitoring in environmental samples were established. The sampling devices to be utilized and their advantages and limitations, the testing and validation of sample preparation methods, and finally the investigation of existing sample analysis methods and the development of cost-effective alternatives were addressed.

However, the road ahead should continue in the direction of streamlining microplastic monitoring and making it more effective and comparable via means of standardization. Something which was recommended throughout the dissertation but in order for this to happen, a high degree of harmonization and standardization needs to be established to clearly define the best practices depending on the investigated matrix and the information needed. In addition, there is a need for investigations and standardization of monitoring strategies with defined time intervals and sampling requirements that could ultimately gain further insights of microplastic contamination in the environment.

Further investigations regarding sample preparation of nanoparticles are needed. For example, an interesting experiment was conducted at the Institut für Energie- und Umwelttechnik (IUTA) utilizing scanning electron microscopy (SEM). In this study, researchers used PS micro- and nanospheres (1.4  $\mu\text{m}$ , 750 nm, 100 nm) which were then exposed to the Fenton and hydrogen peroxide protocols developed in Chapter 4.1 of this dissertation. It was revealed that for PS, the surfaces of the particles were roughened quite a bit when viewed at that scale (Figure 31). Furthermore, there seems to be melting and agglomeration forming after Fenton and a total loss of the 100 nm particles after hydrogen peroxide. Therefore, it is important that when nanoparticles are to be analyzed in environmental samples, there is still a need to optimize and validate appropriate sample preparation methods.

This leads into the next point and that is the need for more research into analytical techniques capable of detecting smaller microplastics and nanoplastics, which is currently not feasible with existing methods, for example, by further developing the fluorescence analysis technique discussed in Chapter 5.2. Especially this is needed for smaller particles of  $\leq 10 \mu\text{m}$  as those are most often overlooked in environmental samples due to the long analysis times (via  $\mu\text{Raman}$ ) or lack of sufficient concentration

of mass (in case of thermoanalytical methods), despite being the most abundant particles in terms of numbers and the most relevant for toxicological studies. The results obtained in Chapter 5.2 of this dissertation indicated the viability of using fluorescence for wastewater effluent samples, but more validation and field experiments are needed, where the fluorescence analytical technique is compared against  $\mu$ FTIR and  $\mu$ Raman spectroscopy.

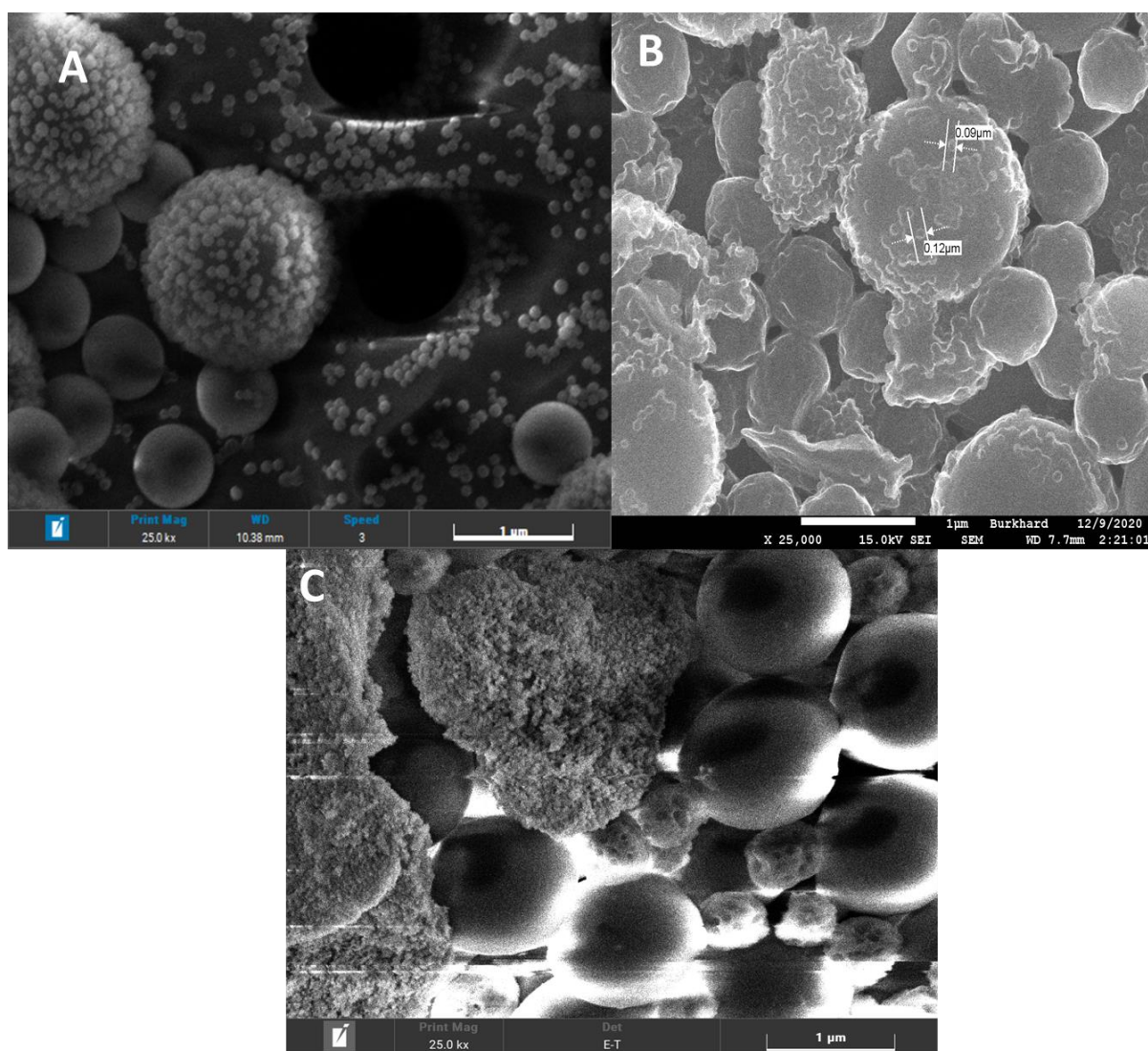


Figure 31. Micrograph of PS particles of different sizes (100 nm, 750 nm, and 1.4  $\mu$ m). A. Control, B. after Fenton, C. after hydrogen peroxide. Micrograph courtesy of M.Sc. Kevin Guerrero from IUTA.

Future research should also focus on investigating the interference to  $\mu$ FTIR spectra caused by staining agents like Nile red, which was previously not discussed in literature, or even downright dismissed, as fluorescence was presumed to have an impact only on  $\mu$ Raman which works in the visible range [26]. This can also be



generalized to include all kinds of additives and dyes commonly used on plastics that are likely to end up in the environment. Otherwise, the accuracy of these analyses will always be best for lab-scale studies where the microplastics used are carefully selected to be free of dyes and additives.

## 8. References

- [1] PlasticsEurope. Plastics-the Facts 2021 An Analysis of European Plastics Production, Demand and Waste Data.
- [2] Hahladakis, J. N.; Iacovidou, E. Closing the Loop on Plastic Packaging Materials: What Is Quality and How Does It Affect Their Circularity? *Sci. Total Environ.*, **2018**, *630*, 1394–1400. <https://doi.org/10.1016/J.SCITOTENV.2018.02.330>.
- [3] Kranzinger, L.; Pomberger, R.; Schwabl, D.; Flachberger, H.; Bauer, M.; Lehner, M.; Hofer, W. Output-Oriented Analysis of the Wet Mechanical Processing of Polyolefin-Rich Waste for Feedstock Recycling. *Waste Manag. Res.*, **2018**, *36* (5), 445–453. <https://doi.org/10.1177/0734242X18764294>.
- [4] Cruz Sanchez, F. A.; Boudaoud, H.; Camargo, M.; Pearce, J. M. Plastic Recycling in Additive Manufacturing: A Systematic Literature Review and Opportunities for the Circular Economy. *J. Clean. Prod.*, **2020**, *264*, 121602. <https://doi.org/10.1016/J.JCLEPRO.2020.121602>.
- [5] Auta, H. S.; Emenike, C. U.; Fauziah, S. H. Distribution and Importance of Microplastics in the Marine Environment: A Review of the Sources, Fate, Effects, and Potential Solutions. *Environ. Int.*, **2017**, *102*, 165–176. <https://doi.org/10.1016/J.ENVINT.2017.02.013>.
- [6] Lassen, C.; Steffen Foss, H.; Kerstin, M.; Nanna B., H.; Pernille, R. J.; Torkel Gissel, N.; Anna, B. Microplastics: Occurrence, Effects and Sources of Releases to the Environment in Denmark. *Danish Environ. Prot. Agency*, **2015**. <https://doi.org/http://mst.dk/service/publikationer/publikationsarkiv/2015/nov/rapport-om-mikroplast>.
- [7] Thompson, R. C.; Olsen, Y.; Mitchell, R. P.; Davis, A.; Rowland, S. J.; John, A. W. G.; McGonigle, D.; Russell, A. E. Lost at Sea: Where Is All the Plastic? *Science* (80-. ), **2004**, *304* (5672), 838–838. <https://doi.org/10.1126/science.1094559>.
- [8] Underwood, A. J.; Chapman, M. G.; Browne, M. A. Some Problems and Practicalities in Design and Interpretation of Samples of Microplastic Waste. *Anal. Methods*, **2017**, *9* (9), 1332–1345. <https://doi.org/10.1039/c6ay02641a>.
- [9] Hartmann, N. B.; Hüffer, T.; Thompson, R. C.; Hassellöv, M.; Verschoor, A.; Daugaard, A. E.; Rist, S.; Karlsson, T.; Brennholt, N.; Cole, M.; et al. Are We Speaking the Same Language? Recommendations for a Definition and Categorization Framework for Plastic Debris. *Environ. Sci. Technol.*, **2019**, *53* (3), 1039–1047. <https://doi.org/10.1021/acs.est.8b05297>.
- [10] Anderson, A.; Andrady, A.; Arthur, C.; Baker, J.; Bouwman, H.; Gall, S.; Hidalgo-Ruz, V.; Köhler, A.; Lavender Law, K.; Leslie, H.; et al. *Sources, Fate and Effects of Microplastics in the Marine Environment: A Global Assessment*; Kershaw, P., Ed.; IMO/FAO/UNESCO-IOC/UNIDO/WMO/IAEA/UN/UNEP/UNDP Joint Group of Experts on the Scientific Aspects of Marine Environmental Protection, **2015**. [https://doi.org/https://ec.europa.eu/environment/marine/good-environmental-status/descriptor-10/pdf/GESAMP\\_microplastics%20full%20study.pdf](https://doi.org/https://ec.europa.eu/environment/marine/good-environmental-status/descriptor-10/pdf/GESAMP_microplastics%20full%20study.pdf).
- [11] Braun, U.; Jekel, M.; Gerdt, G.; Ivleva, N. P.; Jens, R. *Microplastics Analytics Sampling, Preparation and Detection Methods*; **2018**. <https://doi.org/https://bmbf-plastik.de/en/publication/discussion-paper->

- microplastics-analytics.
- [12] ISO. ISO - ISO/TR 21960:2020 - Plastics — Environmental Aspects — State of Knowledge and Methodologies. 2020.
- [13] Jambeck, J. R.; Geyer, R.; Wilcox, C.; Siegler, T. R.; Perryman, M.; Andrady, A.; Narayan, R.; Law, K. L. Marine Pollution. Plastic Waste Inputs from Land into the Ocean. *Science*, **2015**, *347* (6223), 768–771. <https://doi.org/10.1126/science.1260352>.
- [14] Sana, S. S.; Dogiparthi, L. K.; Gangadhar, L.; Chakravorty, A.; Abhishek, N. Effects of Microplastics and Nanoplastics on Marine Environment and Human Health. *Environ. Sci. Pollut. Res.* **2020**, *27* (36), 44743–44756. <https://doi.org/10.1007/S11356-020-10573-X>.
- [15] Reichert, J.; Schellenberg, J.; Schubert, P.; Wilke, T. Responses of Reef Building Corals to Microplastic Exposure. *Environ. Pollut.*, **2018**, *237*, 955–960. <https://doi.org/10.1016/J.ENVPOL.2017.11.006>.
- [16] Prata, J. C.; da Costa, J. P.; Lopes, I.; Duarte, A. C.; Rocha-Santos, T. Environmental Exposure to Microplastics: An Overview on Possible Human Health Effects. *Sci. Total Environ.*, **2020**, *702*, 134455. <https://doi.org/10.1016/J.SCITOTENV.2019.134455>.
- [17] Pabortsava, K.; Lampitt, R. S. High Concentrations of Plastic Hidden beneath the Surface of the Atlantic Ocean. *Nat. Commun.*, **2020**, *11* (1), 1–11. <https://doi.org/10.1038/s41467-020-17932-9>.
- [18] Cózar, A.; Echevarría, F.; González-Gordillo, J. I.; Irigoien, X.; Úbeda, B.; Hernández-León, S.; Palma, Á. T.; Navarro, S.; García-de-Lomas, J.; Ruiz, A.; et al. Plastic Debris in the Open Ocean. *Proc. Natl. Acad. Sci. U. S. A.*, **2014**, *111* (28), 10239–10244. <https://doi.org/10.1073/pnas.1314705111>.
- [19] Carr, S. A.; Liu, J.; Tesoro, A. G. Transport and Fate of Microplastic Particles in Wastewater Treatment Plants. *Water Res.*, **2016**, *91*, 174–182. <https://doi.org/10.1016/j.watres.2016.01.002>.
- [20] Ziajahromi, S.; Neale, P. A.; Rintoul, L.; Leusch, F. D. L. Wastewater Treatment Plants as a Pathway for Microplastics: Development of a New Approach to Sample Wastewater-Based Microplastics. *Water Res.*, **2017**, *112*, 93–99. <https://doi.org/10.1016/J.WATRES.2017.01.042>.
- [21] Michielssen, M. R.; Michielssen, E. R.; Ni, J.; Duhaime, M. B. Fate of Microplastics and Other Small Anthropogenic Litter (SAL) in Wastewater Treatment Plants Depends on Unit Processes Employed. *Environ. Sci. Water Res. Technol.*, **2016**, *2* (6), 1064–1073. <https://doi.org/10.1039/C6EW00207B>.
- [22] Bannick, C. G.; Szewzyk, R.; Ricking, M.; Schniegler, S.; Obermaier, N.; Barthel, A. K.; Altmann, K.; Eisentraut, P.; Braun, U. Development and Testing of a Fractionated Filtration for Sampling of Microplastics in Water. *Water Res.*, **2019**, *149*, 650–658. <https://doi.org/10.1016/j.watres.2018.10.045>.
- [23] Braun, U.; Stein, U.; Schritt, H.; Altmann, K.; Bannick, C. G.; Becker, R.; Bitter, H.; Boschow, M.; Diekers, G.; Enders, K.; et al. *Analysis of Microplastics - Sampling, Preparation and Detection Methods | Plastik in Der Umwelt*, **2020**.
- [24] Gy, P. Sampling of Discrete Materials - A New Introduction to the Theory of Sampling: I. Qualitative Approach. In *Chemometrics and Intelligent Laboratory Systems*; Elsevier, **2004**; Vol. 74, pp 7–24. <https://doi.org/10.1016/j.chemolab.2004.05.012>.
- [25] Funck, M.; Al-Azzawi, M. S. M.; Yildirim, A.; Knoop, O.; Schmidt, T. C. T. C.; Drewes, J. E. J. E.; Tuerk, J. Release of Microplastic Particles to the Aquatic Environment via Wastewater Treatment Plants: The Impact of Sand Filters as

- Tertiary Treatment. *Chem. Eng. J.*, **2021**, *426*, 130933. <https://doi.org/10.1016/J.CEJ.2021.130933>.
- [26] Ivleva, N. P. Chemical Analysis of Microplastics and Nanoplastics: Challenges, Advanced Methods, and Perspectives. *Chem. Rev.*, **2021**, *121* (19), 11886–11936. <https://doi.org/10.1021/ACS.CHEMREV.1C00178>.
- [27] Ou, H.; Zeng, E. Y. Occurrence and Fate of Microplastics in Wastewater Treatment Plants. *Microplastic Contam. Aquat. Environ. An Emerg. Matter Environ. Urgency*, **2018**, 317–338. <https://doi.org/10.1016/B978-0-12-813747-5.00010-2>.
- [28] Dyachenko, A.; Mitchell, J.; Arsem, N. Extraction and Identification of Microplastic Particles from Secondary Wastewater Treatment Plant (WWTP) Effluent. *Anal. Methods*, **2017**, *9* (9), 1412–1418. <https://doi.org/10.1039/c6ay02397e>.
- [29] Talvitie, J.; Mikola, A.; Setälä, O.; Heinonen, M.; Koistinen, A. How Well Is Microlitter Purified from Wastewater? - A Detailed Study on the Stepwise Removal of Microlitter in a Tertiary Level Wastewater Treatment Plant. *Water Res.*, **2017**, *109*, 164–172. <https://doi.org/10.1016/j.watres.2016.11.046>.
- [30] Okoffo, E. D.; O'Brien, S.; O'Brien, J. W.; Tscharke, B. J.; Thomas, K. V. Wastewater Treatment Plants as a Source of Plastics in the Environment: A Review of Occurrence, Methods for Identification, Quantification and Fate. *Environ. Sci. Water Res. Technol.*, **2019**, *5* (11), 1908–1931. <https://doi.org/10.1039/c9ew00428a>.
- [31] Koelmans, A. A.; Mohamed Nor, N. H.; Hermsen, E.; Kooi, M.; Mintenig, S. M.; De France, J. Microplastics in Freshwaters and Drinking Water: Critical Review and Assessment of Data Quality. *Water Res.*, **2019**, *155*, 410–422. <https://doi.org/10.1016/j.watres.2019.02.054>.
- [32] Funck, M.; Yildirim, A.; Nickel, C.; Schram, J.; Schmidt, T. C.; Tuerk, J. Identification of Microplastics in Wastewater after Cascade Filtration Using Pyrolysis-GC–MS. *MethodsX*, **2020**, *7*, 100778. <https://doi.org/10.1016/j.mex.2019.100778>.
- [33] Hurley, R. R.; Lusher, A. L.; Olsen, M.; Nizzetto, L. Validation of a Method for Extracting Microplastics from Complex, Organic-Rich, Environmental Matrices. *Environ. Sci. Technol.*, **2018**, *52* (13), 7409–7417. <https://doi.org/10.1021/acs.est.8b01517>.
- [34] Dümichen, E.; Barthel, A.-K.; Braun, U.; Bannick, C. G.; Brand, K.; Jekel, M.; Senz, R. Analysis of Polyethylene Microplastics in Environmental Samples, Using a Thermal Decomposition Method. *Water Res.*, **2015**, *85*, 451–457. <https://doi.org/10.1016/j.watres.2015.09.002>.
- [35] Prata, J. C.; da Costa, J. P.; Girão, A. V.; Lopes, I.; Duarte, A. C.; Rocha-Santos, T. Identifying a Quick and Efficient Method of Removing Organic Matter without Damaging Microplastic Samples. *Sci. Total Environ.*, **2019**, *686*, 131–139. <https://doi.org/10.1016/j.scitotenv.2019.05.456>.
- [36] Dehaut, A.; Cassone, A.-L.; Frère, L.; Hermabessiere, L.; Himber, C.; Rinnert, E.; Rivière, G.; Lambert, C.; Soudant, P.; Huvet, A.; et al. Microplastics in Seafood: Benchmark Protocol for Their Extraction and Characterization. *Environ. Pollut.*, **2016**, *215*, 223–233. <https://doi.org/10.1016/J.ENVPOL.2016.05.018>.
- [37] Catarino, A. I.; Thompson, R.; Sanderson, W.; Henry, T. B. Development and Optimization of a Standard Method for Extraction of Microplastics in Mussels by Enzyme Digestion of Soft Tissues. *Environ. Toxicol. Chem.*, **2017**, *36* (4), 947–

951. <https://doi.org/10.1002/etc.3608>.
- [38] Munno, K.; Helm, P. A.; Jackson, D. A.; Rochman, C.; Sims, A. Impacts of Temperature and Selected Chemical Digestion Methods on Microplastic Particles. *Environ. Toxicol. Chem.*, **2018**, *37* (1), 91–98. <https://doi.org/10.1002/etc.3935>.
- [39] Foekema, E. M.; De Grijter, C.; Mergia, M. T.; Van Franeker, J. A.; Murk, A. J.; Koelmans, A. A. Plastic in North Sea Fish. *Environ. Sci. Technol.*, **2013**, *47* (15), 8818–8824. <https://doi.org/10.1021/es400931b>.
- [40] Herrera, A.; Garrido-Amador, P.; Martínez, I.; Samper, M. D.; López-Martínez, J.; Gómez, M.; Packard, T. T. Novel Methodology to Isolate Microplastics from Vegetal-Rich Samples. *Mar. Pollut. Bull.*, **2018**, *129* (1), 61–69. <https://doi.org/10.1016/j.marpolbul.2018.02.015>.
- [41] Cole, M.; Webb, H.; Lindeque, P. K.; Fileman, E. S.; Halsband, C.; Galloway, T. S. Isolation of Microplastics in Biota-Rich Seawater Samples and Marine Organisms. *Sci. Rep.*, **2014**, *4* (1), 1–8. <https://doi.org/10.1038/srep04528>.
- [42] Masura, J.; Baker, J. E.; Foster, G. D.; Arthur, C.; Herring, C.; Masura, L.; Baker, J. E.; Foster, G. D.; Arthur, C. Laboratory Methods for the Analysis of Microplastics in the Marine Environment: Recommendations for Quantifying Synthetic Particles Inwaters and Sediments. *NOAA Tech. Memo. NOS-OR&R-48*, **2015**. [https://doi.org/https://marinedebris.noaa.gov/sites/default/files/publications-files/noaa\\_microplastics\\_methods\\_manual.pdf](https://doi.org/https://marinedebris.noaa.gov/sites/default/files/publications-files/noaa_microplastics_methods_manual.pdf).
- [43] Tagg, A. S.; Harrison, J. P.; Ju-Nam, Y.; Sapp, M.; Bradley, E. L.; Sinclair, C. J.; Ojeda, J. J. Fenton's Reagent for the Rapid and Efficient Isolation of Microplastics from Wastewater. *Chem. Commun.*, **2017**, *53* (2), 372–375. <https://doi.org/10.1039/C6CC08798A>.
- [44] Karami, A.; Golieskardi, A.; Choo, C. K.; Romano, N.; Ho, Y. Bin; Salamatinia, B. A High-Performance Protocol for Extraction of Microplastics in Fish. *Sci. Total Environ.*, **2017**, *578*, 485–494. <https://doi.org/10.1016/J.SCITOTENV.2016.10.213>.
- [45] Avio, C. G.; Gorbí, S.; Regoli, F. Experimental Development of a New Protocol for Extraction and Characterization of Microplastics in Fish Tissues: First Observations in Commercial Species from Adriatic Sea. *Mar. Environ. Res.*, **2015**, *111*, 18–26. <https://doi.org/10.1016/j.marenvres.2015.06.014>.
- [46] Nuelle, M.-T. M. T.; Dekiff, J. H.; Remy, D.; Fries, E. A New Analytical Approach for Monitoring Microplastics in Marine Sediments. *Environ. Pollut.*, **2014**, *184*, 161–169. <https://doi.org/10.1016/j.envpol.2013.07.027>.
- [47] Sujathan, S.; Kniggendorf, A.-K.; Kumar, A.; Roth, B.; Rosenwinkel, K.-H.; Nogueira, R. Heat and Bleach: A Cost-Efficient Method for Extracting Microplastics from Return Activated Sludge. *Arch. Environ. Contam. Toxicol.*, **2017**, *73*. <https://doi.org/10.1007/s00244-017-0415-8>.
- [48] Naidoo, T.; Goordiyal, K.; Glassom, D. Are Nitric Acid (HNO<sub>3</sub>) Digestions Efficient in Isolating Microplastics from Juvenile Fish? *Water. Air. Soil Pollut.*, **2017**, *228* (12), 1–11. <https://doi.org/10.1007/s11270-017-3654-4>.
- [49] Claessens, M.; Van Cauwenberghe, L.; Vandegehuchte, M. B.; Janssen, C. R. New Techniques for the Detection of Microplastics in Sediments and Field Collected Organisms. *Mar. Pollut. Bull.*, **2013**, *70* (1–2), 227–233. <https://doi.org/10.1016/j.marpolbul.2013.03.009>.
- [50] Tagg, A. S.; Sapp, M.; Harrison, J. P.; Jesús, J.; Ojeda, J. J. Identification and Quantification of Microplastics in Wastewater Using Focal Plane Array-Based

- Reflectance Micro-FT-IR Imaging. *Anal. Chem.*, **2015**, *87* (12), 6032–6040. <https://doi.org/10.1021/acs.analchem.5b00495>.
- [51] Maes, T.; Jessop, R.; Wellner, N.; Haupt, K.; Mayes, A. G. A Rapid-Screening Approach to Detect and Quantify Microplastics Based on Fluorescent Tagging with Nile Red. *Sci. Rep.*, **2017**, *7* (1), 44501. <https://doi.org/10.1038/srep44501>.
- [52] Stock, F.; Kochleus, C.; Bänisch-Baltruschat, B.; Brennholt, N.; Reifferscheid, G. Sampling Techniques and Preparation Methods for Microplastic Analyses in the Aquatic Environment – A Review. *TrAC Trends Anal. Chem.*, **2019**, *113*, 84–92. <https://doi.org/10.1016/J.TRAC.2019.01.014>.
- [53] Renner, G.; Schmidt, T. C.; Schram, J. Characterization and Quantification of Microplastics by Infrared Spectroscopy. *Compr. Anal. Chem.*, **2017**, *75*, 67–118. <https://doi.org/10.1016/bs.coac.2016.10.006>.
- [54] Zhang, H.; Heung, J. C.; Huang, C. P. Optimization of Fenton Process for the Treatment of Landfill Leachate. *J. Hazard. Mater.*, **2005**, *125* (1–3), 166–174. <https://doi.org/10.1016/j.jhazmat.2005.05.025>.
- [55] Flotron, V.; Delteil, C.; Padellec, Y.; Camel, V. Removal of Sorbed Polycyclic Aromatic Hydrocarbons from Soil, Sludge and Sediment Samples Using the Fenton's Reagent Process. *Chemosphere*, **2005**, *59* (10), 1427–1437. <https://doi.org/10.1016/j.chemosphere.2004.12.065>.
- [56] Aramyan, S. M. Advances in Fenton and Fenton Based Oxidation Processes for Industrial Effluent Contaminants Control-A Review. *Int. J. Environ. Sci. Nat. Resour.*, **2017**, *2* (4). <https://doi.org/10.19080/ijesnr.2017.02.555594>.
- [57] Al-Azzawi, M. S. M.; Kefer, S.; Weißer, J.; Reichel, J.; Schwaller, C.; Glas, K.; Knoop, O.; Drewes, J. E. Validation of Sample Preparation Methods for Microplastic Analysis in Wastewater Matrices—Reproducibility and Standardization. *Water*, **2020**, *12* (9), 2445. <https://doi.org/10.3390/w12092445>.
- [58] Dümichen, E.; Eisentraut, P.; Celina, M.; Braun, U. Automated Thermal Extraction-Desorption Gas Chromatography Mass Spectrometry: A Multifunctional Tool for Comprehensive Characterization of Polymers and Their Degradation Products. *J. Chromatogr. A*, **2019**, *1592*, 133–142. <https://doi.org/10.1016/j.chroma.2019.01.033>.
- [59] Käßler, A.; Fischer, D.; Oberbeckmann, S.; Schernewski, G.; Labrenz, M.; Eichhorn, K.-J.; Voit, B. Analysis of Environmental Microplastics by Vibrational Microspectroscopy: FTIR, Raman or Both? *Anal. Bioanal. Chem.*, **2016**, *408* (29), 8377–8391. <https://doi.org/10.1007/s00216-016-9956-3>.
- [60] Cabernard, L.; Roscher, L.; Lorenz, C.; Gerdts, G.; Primpke, S. Comparison of Raman and Fourier Transform Infrared Spectroscopy for the Quantification of Microplastics in the Aquatic Environment. *Environ. Sci. Technol.*, **2018**, *52* (22), 13279–13288. <https://doi.org/10.1021/acs.est.8b03438>.
- [61] Ivleva, N. P.; Wiesheu, A. C.; Niessner, R. *Microplastic in Aquatic Ecosystems*; John Wiley & Sons, Ltd, **2016**; Vol. 56, pp 1720–1739. <https://doi.org/10.1002/anie.201606957>.
- [62] Mallow, O.; Spacek, S.; Schwarzböck, T.; Fellner, J.; Rechberger, H. A New Thermoanalytical Method for the Quantification of Microplastics in Industrial Wastewater. *Environ. Pollut.*, **2020**, *259*, 113862. <https://doi.org/10.1016/j.envpol.2019.113862>.
- [63] Käßler, A.; Fischer, M.; Scholz-Böttcher, B. M.; Oberbeckmann, S.; Labrenz, M.; Fischer, D.; Eichhorn, K. J.; Voit, B. Comparison of  $\mu$ -ATR-FTIR Spectroscopy and Py-GCMS as Identification Tools for Microplastic Particles and Fibers Isolated from River Sediments. *Anal. Bioanal. Chem.*, **2018**, *410* (21),

- 5313–5327. <https://doi.org/10.1007/S00216-018-1185-5>.
- [64] Essel, R.; Engel, L.; Carus, M.; Heinrich Ahrens, R. Sources of Microplastics Relevant to Marine Protection in Germany. **2015**.
- [65] Simon, M.; van Alst, N.; Vollertsen, J. Quantification of Microplastic Mass and Removal Rates at Wastewater Treatment Plants Applying Focal Plane Array (FPA)-Based Fourier Transform Infrared (FT-IR) Imaging. *Water Res.*, **2018**, *142*, 1–9. <https://doi.org/10.1016/j.watres.2018.05.019>.
- [66] Yakovenko, N.; Carvalho, A.; ter Halle, A. Emerging Use Thermo-Analytical Method Coupled with Mass Spectrometry for the Quantification of Micro(Nano)Plastics in Environmental Samples. *TrAC - Trends Anal. Chem.*, **2020**, *131*. <https://doi.org/10.1016/J.TRAC.2020.115979>.
- [67] Primpke, S.; Fischer, M.; Lorenz, C.; Gerds, G.; Scholz-Böttcher, B. M. Comparison of Pyrolysis Gas Chromatography/Mass Spectrometry and Hyperspectral FTIR Imaging Spectroscopy for the Analysis of Microplastics. *Anal. Bioanal. Chem.*, **2020**, *412* (30), 8283–8298. <https://doi.org/10.1007/s00216-020-02979-w>.
- [68] Elert, A. M.; Becker, R.; Duemichen, E.; Eisentraut, P.; Falkenhagen, J.; Sturm, H.; Braun, U. Comparison of Different Methods for MP Detection: What Can We Learn from Them, and Why Asking the Right Question before Measurements Matters? *Environ. Pollut.*, **2017**, *231*, 1256–1264. <https://doi.org/10.1016/j.envpol.2017.08.074>.
- [69] Shim, W. J.; Hong, S. H.; Eo, S. E. Identification Methods in Microplastic Analysis: A Review. *Analytical Methods*. Royal Society of Chemistry March 7, 2017, pp 1384–1391. <https://doi.org/10.1039/c6ay02558g>.
- [70] Liu, F.; Vianello, A.; Vollertsen, J. Retention of Microplastics in Sediments of Urban and Highway Stormwater Retention Ponds. *Environ. Pollut.*, **2019**, *255*, 113335. <https://doi.org/10.1016/J.ENVPOL.2019.113335>.
- [71] Primpke, S.; Christiansen, S. H.; Cowger, W.; De Frond, H.; Deshpande, A.; Fischer, M.; Holland, E. B.; Meyns, M.; O'Donnell, B. A.; Ossmann, B. E.; et al. Critical Assessment of Analytical Methods for the Harmonized and Cost-Efficient Analysis of Microplastics. *Appl. Spectrosc.*, **2020**, *74* (9), 1012–1047. <https://doi.org/10.1177/0003702820921465>.
- [72] Renner, G.; Schmidt, T. C.; Schram, J. Automated Rapid & Intelligent Microplastics Mapping by FTIR Microscopy: A Python-Based Workflow. *MethodsX*, **2020**, *7*, 100742. <https://doi.org/10.1016/J.MEX.2019.11.015>.
- [73] Cole, M. A Novel Method for Preparing Microplastic Fibers. *Sci. Rep.*, **2016**, *6* (1), 34519. <https://doi.org/10.1038/srep34519>.
- [74] Prata, J. C.; Reis, V.; Matos, J. T. V.; da Costa, J. P.; Duarte, A. C.; Rocha-Santos, T. A New Approach for Routine Quantification of Microplastics Using Nile Red and Automated Software (MP-VAT). *Sci. Total Environ.*, **2019**, *690*, 1277–1283. <https://doi.org/10.1016/j.scitotenv.2019.07.060>.
- [75] Song, Y. K.; Shim, W. J.; Jang, M.; Hong, S. H.; Han, G. M. A Nile Red Staining Method for Microplastic Identification and Quantification. *한국분석과학회 학술대회*, **2014**, 143–143. [https://doi.org/http://www.dbpia.co.kr/journal/articleDetail?nodeId=NODE02429533&language=ko\\_KR](https://doi.org/http://www.dbpia.co.kr/journal/articleDetail?nodeId=NODE02429533&language=ko_KR).
- [76] Joon Shim, W.; Kyoung Song, Y.; Hee Hong, S.; Jang, M. Identification and Quantification of Microplastics Using Nile Red Staining. **2016**. <https://doi.org/10.1016/j.marpolbul.2016.10.049>.

- [77] Tamminga, Matthias Hengstmann, E.; Fischer, E. Nile Red Staining as a Subsidiary Method for Microplastic Quantification: A Comparison of Three Solvents and Factors Influencing Application Reliability. *SDRP J. Earth Sci. Environ. Stud.*, **2017**, 2 (2). <https://doi.org/10.25177/JESES.2.2.1>.
- [78] Erni-Cassola, G.; Gibson, M. I.; Thompson, R. C.; Christie-Oleza, J. A. Lost, but Found with Nile Red: A Novel Method for Detecting and Quantifying Small Microplastics (1 Mm to 20 Mm) in Environmental Samples. *Environ. Sci. Technol.*, **2017**, 51 (23), 13641–13648. <https://doi.org/10.1021/acs.est.7b04512>.
- [79] Lv, L.; Qu, J.; Yu, Z.; Chen, D.; Zhou, C.; Hong, P.; Sun, S.; Li, C. A Simple Method for Detecting and Quantifying Microplastics Utilizing Fluorescent Dyes - Safranin T, Fluorescein Isophosphate, Nile Red Based on Thermal Expansion and Contraction Property. *Environ. Pollut.*, **2019**, 255, 113283. <https://doi.org/10.1016/j.envpol.2019.113283>.
- [80] Dowarah, K.; Patchaiyappan, A.; Thirunavukkarasu, C.; Jayakumar, S.; Devipriya, S. P. Quantification of Microplastics Using Nile Red in Two Bivalve Species *Perna Viridis* and *Meretrix Meretrix* from Three Estuaries in Pondicherry, India and Microplastic Uptake by Local Communities through Bivalve Diet. *Mar. Pollut. Bull.*, **2020**, 153, 110982. <https://doi.org/10.1016/j.marpolbul.2020.110982>.
- [81] Labbe, A. B.; Bagshaw, C. R.; Uttal, L. Inexpensive Adaptations of Basic Microscopes for the Identification of Microplastic Contamination Using Polarization and Nile Red Fluorescence Detection. *J. Chem. Educ.*, **2020**. <https://doi.org/10.1021/acs.jchemed.0c00518>.
- [82] Vermeiren, P.; Muñoz, C.; Ikejima, K. Microplastic Identification and Quantification from Organic Rich Sediments: A Validated Laboratory Protocol. *Environ. Pollut.*, **2020**, 262. <https://doi.org/10.1016/j.envpol.2020.114298>.
- [83] Nguyen, N. B.; Kim, M. K.; Le, Q. T.; Ngo, D. N.; Zoh, K. D.; Joo, S. W. Spectroscopic Analysis of Microplastic Contaminants in an Urban Wastewater Treatment Plant from Seoul, South Korea. *Chemosphere*, **2020**, 263, 127812. <https://doi.org/10.1016/j.chemosphere.2020.127812>.
- [84] Liu, X.; Yuan, W.; Di, M.; Li, Z.; Wang, J. Transfer and Fate of Microplastics during the Conventional Activated Sludge Process in One Wastewater Treatment Plant of China. *Chem. Eng. J.*, **2019**, 362, 176–182. <https://doi.org/10.1016/j.cej.2019.01.033>.
- [85] Hidayaturrahman, H.; Lee, T. G. A Study on Characteristics of Microplastic in Wastewater of South Korea: Identification, Quantification, and Fate of Microplastics during Treatment Process. *Mar. Pollut. Bull.*, **2019**, 146, 696–702. <https://doi.org/10.1016/j.marpolbul.2019.06.071>.
- [86] Talvitie, J.; Mikola, A.; Koistinen, A.; Setälä, O. Solutions to Microplastic Pollution – Removal of Microplastics from Wastewater Effluent with Advanced Wastewater Treatment Technologies. *Water Res.*, **2017**, 123, 401–407. <https://doi.org/10.1016/j.watres.2017.07.005>.
- [87] Bayo, J.; López-Castellanos, J.; Olmos, S. Membrane Bioreactor and Rapid Sand Filtration for the Removal of Microplastics in an Urban Wastewater Treatment Plant. *Mar. Pollut. Bull.*, **2020**, 156, 111211. <https://doi.org/10.1016/j.marpolbul.2020.111211>.
- [88] Mason, S. A.; Garneau, D.; Sutton, R.; Chu, Y.; Ehmann, K.; Barnes, J.; Fink, P.; Papazissimos, D.; Rogers, D. L. Microplastic Pollution Is Widely Detected in US Municipal Wastewater Treatment Plant Effluent. *Environ. Pollut.*, **2016**, 218,



- 1045–1054. <https://doi.org/10.1016/j.envpol.2016.08.056>.
- [89] Ben-David, E. A.; Habibi, M.; Haddad, E.; Hasanin, M.; Angel, D. L.; Booth, A. M.; Sabbah, I. Microplastic Distributions in a Domestic Wastewater Treatment Plant: Removal Efficiency, Seasonal Variation and Influence of Sampling Technique. *Sci. Total Environ.*, **2021**, *752*, 141880. <https://doi.org/10.1016/j.scitotenv.2020.141880>.
- [90] Magnusson, K.; Norén F.; Norén, F. *Screening of Microplastic Particles in and Down-Stream a Wastewater Treatment Plant*; Stockholm, **2014**.
- [91] Mintenig, S. M.; Int-Veen, I.; Löder, M. G. J.; Primpke, S.; Gerdt, G. Identification of Microplastic in Effluents of Waste Water Treatment Plants Using Focal Plane Array-Based Micro-Fourier-Transform Infrared Imaging. *Water Res.*, **2017**, *108*, 365–372. <https://doi.org/10.1016/j.watres.2016.11.015>.
- [92] Horton, A. A.; Cross, R. K.; Read, D. S.; Jürgens, M. D.; Ball, H. L.; Svendsen, C.; Vollertsen, J.; Johnson, A. C. Semi-Automated Analysis of Microplastics in Complex Wastewater Samples. *Environ. Pollut.*, **2021**, *268*, 115841. <https://doi.org/10.1016/j.envpol.2020.115841>.
- [93] Talvitie, J.; Mikola, A.; Koistinen, A.; Setälä, O. Solutions to Microplastic Pollution - Removal of Microplastics from Wastewater Effluent with Advanced Wastewater Treatment Technologies. *Water Res.*, **2017**, *123*, 401–407. <https://doi.org/10.1016/j.watres.2017.07.005>.
- [94] Löder, M. G. J.; Gerdt, G.; Löder, M. G. J.; Gerdt, G.; Helgoland, A.; Wegener, A. Methodology Used for the Detection and Identification of Microplastics—A Critical Appraisal. *Mar. Anthropog. Litter*, **2015**, 201–227. [https://doi.org/10.1007/978-3-319-16510-3\\_8](https://doi.org/10.1007/978-3-319-16510-3_8).
- [95] Hidalgo-Ruz, V.; Gutow, L.; Thompson, R. C.; Thiel, M. Microplastics in the Marine Environment: A Review of the Methods Used for Identification and Quantification. *Environ. Sci. Technol.*, **2012**, *46* (6), 3060–3075. <https://doi.org/10.1021/es2031505>.
- [96] Van Cauwenberghe, L.; Claessens, M.; Vandegehuchte, M. B.; Mees, J.; Janssen, C. R. Assessment of Marine Debris on the Belgian Continental Shelf. *Mar. Pollut. Bull.*, **2013**, *73* (1), 161–169. <https://doi.org/10.1016/j.marpolbul.2013.05.026>.
- [97] Reisser, J.; Slat, B.; Noble, K.; Du Plessis, K.; Epp, M.; Proietti, M.; De Sonneville, J.; Becker, T.; Pattiaratchi, C. The Vertical Distribution of Buoyant Plastics at Sea: An Observational Study in the North Atlantic Gyre. *Biogeosciences*, **2015**, *12* (4), 1249–1256. <https://doi.org/10.5194/bg-12-1249-2015>.
- [98] Cózar, A.; Sanz-Martín, M.; Martí, E.; González-Gordillo, J. I.; Ubeda, B.; Gálvez, J. Á.; Irigoien, X.; Duarte, C. M. Plastic Accumulation in the Mediterranean Sea. *PLoS One*, **2015**, *10* (4), e0121762. <https://doi.org/10.1371/journal.pone.0121762>.
- [99] Eriksen, M.; Mason, S.; Wilson, S.; Box, C.; Zellers, A.; Edwards, W.; Farley, H.; Amato, S. Microplastic Pollution in the Surface Waters of the Laurentian Great Lakes. *Mar. Pollut. Bull.*, **2013**, *77* (1–2), 177–182. <https://doi.org/10.1016/J.MARPOLBUL.2013.10.007>.
- [100] Klein, S.; Dimzon, I. K.; Eubeler, J.; Knepper, T. P. Analysis, Occurrence, and Degradation of Microplastics in the Aqueous Environment. *Handb. Environ. Chem.*, **2018**, *58*, 51–67. [https://doi.org/10.1007/978-3-319-61615-5\\_3](https://doi.org/10.1007/978-3-319-61615-5_3).
- [101] Dris, R.; Gasperi, J.; Rocher, V.; Saad, M.; Renault, N.; Tassin, B. Microplastic Contamination in an Urban Area: A Case Study in Greater Paris. *Environ.*

- Chem.*, **2015**, *12* (5), 592–599. <https://doi.org/10.1071/EN14167>.
- [102] Ng, K. L.; Obbard, J. P. Prevalence of Microplastics in Singapore's Coastal Marine Environment. *Mar. Pollut. Bull.*, **2006**, *52* (7), 761–767. <https://doi.org/10.1016/J.MARPOLBUL.2005.11.017>.
- [103] Gustavsson, B.; Luthbom, K.; Lagerkvist, A. Comparison of Analytical Error and Sampling Error for Contaminated Soil. *J. Hazard. Mater.*, **2006**, *138* (2), 252–260. <https://doi.org/10.1016/J.JHAZMAT.2006.01.082>.
- [104] Fenton, H. J. H. LXXIII. - Oxidation of Tartaric Acid in Presence of Iron. *Journal of the Chemical Society, Transactions*. The Royal Society of Chemistry January 1, 1894, pp 899–910. <https://doi.org/10.1039/CT8946500899>.
- [105] Schymanski, D.; Oßmann, B. E.; Benismail, N.; Boukerma, K.; Dallmann, G.; von der Esch, E.; Fischer, D.; Fischer, F.; Gilliland, D.; Glas, K.; et al. Analysis of Microplastics in Drinking Water and Other Clean Water Samples with Micro-Raman and Micro-Infrared Spectroscopy: Minimum Requirements and Best Practice Guidelines. *Analytical and Bioanalytical Chemistry*. Analytical and Bioanalytical Chemistry 2021, pp 5969–5994. <https://doi.org/10.1007/s00216-021-03498-y>.
- [106] Witzig, C. S.; Földi, C.; Wörle, K.; Habermehl, P.; Pittroff, M.; Müller, Y. K.; Lauschke, T.; Fiener, P.; Dierkes, G.; Freier, K. P.; et al. When Good Intentions Go Bad—False Positive Microplastic Detection Caused by Disposable Gloves. *Environ. Sci. Technol.*, **2020**, *54* (19), 12164–12172. <https://doi.org/10.1021/ACS.EST.0C03742>.
- [107] Li, X.; Chen, L.; Ji, Y.; Li, M.; Dong, B.; Qian, G.; Zhou, J.; Dai, X. Effects of Chemical Pretreatments on Microplastic Extraction in Sewage Sludge and Their Physicochemical Characteristics. *Water Res.*, **2020**, *171*, 115379. <https://doi.org/10.1016/J.WATRES.2019.115379>.
- [108] Renner, G.; Schmidt, T. C.; Schram, J. Analytical Methodologies for Monitoring Micro(Nano)Plastics: Which Are Fit for Purpose? *Curr. Opin. Environ. Sci. Heal.*, **2018**, *1*, 55–61. <https://doi.org/10.1016/j.coesh.2017.11.001>.
- [109] Salzer, R.; Siesler, H. W. Infrared and Raman Spectroscopic Imaging. *Infrared Raman Spectrosc. Imaging*, **2009**, 1–510. <https://doi.org/10.1002/9783527628230>.
- [110] Primpke, S.; Dias, P. A.; Gerdts, G. Automated Identification and Quantification of Microfibres and Microplastics. *Anal. Methods*, **2019**, *11* (16), 2138–2147. <https://doi.org/10.1039/C9AY00126C>.
- [111] Löder, M. G. J.; Kuczera, M.; Mintenig, S.; Lorenz, C.; Gerdts, G.; Löder, M. G. J.; Kuczera, M.; Mintenig, S.; Lorenz, C.; Gerdts, G. Focal Plane Array Detector-Based Micro-Fourier-Transform Infrared Imaging for the Analysis of Microplastics in Environmental Samples. *Environ. Chem.*, **2015**, *12* (5), 563–581. <https://doi.org/10.1071/EN14205>.
- [112] Mintenig, S. M.; Löder, M. G. J.; Primpke, S.; Gerdts, G. Low Numbers of Microplastics Detected in Drinking Water from Ground Water Sources. *Sci. Total Environ.*, **2019**, *648*, 631–635. <https://doi.org/10.1016/J.SCITOTENV.2018.08.178>.
- [113] Vinay Kumar, B. N.; Löschel, L. A.; Imhof, H. K.; Löder, M. G. J.; Laforsch, C. Analysis of Microplastics of a Broad Size Range in Commercially Important Mussels by Combining FTIR and Raman Spectroscopy Approaches. *Environ. Pollut.*, **2021**, *269*, 116147. <https://doi.org/10.1016/J.ENVPOL.2020.116147>.
- [114] Peeken, I.; Primpke, S.; Beyer, B.; Gütermann, J.; Katlein, C.; Krumpfen, T.; Bergmann, M.; Hehemann, L.; Gerdts, G. Arctic Sea Ice Is an Important

- Temporal Sink and Means of Transport for Microplastic. *Nat. Commun.* 2018 91, **2018**, 9 (1), 1–12. <https://doi.org/10.1038/s41467-018-03825-5>.
- [115] Johnson, A. C.; Ball, H.; Cross, R.; Horton, A. A.; Jürgens, M. D.; Read, D. S.; Vollertsen, J.; Svendsen, C. Identification and Quantification of Microplastics in Potable Water and Their Sources within Water Treatment Works in England and Wales. *Environ. Sci. Technol.*, **2020**, *54* (19), 12326–12334. [https://doi.org/10.1021/ACS.EST.0C03211/SUPPL\\_FILE/ES0C03211\\_SI\\_001.PDF](https://doi.org/10.1021/ACS.EST.0C03211/SUPPL_FILE/ES0C03211_SI_001.PDF).
- [116] Lorenz, C.; Roscher, L.; Meyer, M. S.; Hildebrandt, L.; Prume, J.; Löder, M. G. J.; Primpke, S.; Gerds, G. Spatial Distribution of Microplastics in Sediments and Surface Waters of the Southern North Sea. *Environ. Pollut.*, **2019**, *252*, 1719–1729. <https://doi.org/10.1016/J.ENVPOL.2019.06.093>.
- [117] Tagg, A. S.; Sapp, M.; Harrison, J. P.; Sinclair, C. J.; Bradley, E.; Ju-Nam, Y.; Ojeda, J. J. Microplastic Monitoring at Different Stages in a Wastewater Treatment Plant Using Reflectance Micro-FTIR Imaging. *Front. Environ. Sci.*, **2020**, *8*, 145. <https://doi.org/10.3389/FENVS.2020.00145/BIBTEX>.
- [118] Käßler, A.; Windrich, F.; Löder, M. G. J.; Malanin, M.; Fischer, D.; Labrenz, M.; Eichhorn, K. J.; Voit, B. Identification of Microplastics by FTIR and Raman Microscopy: A Novel Silicon Filter Substrate Opens the Important Spectral Range below 1300  $\text{cm}^{-1}$  for FTIR Transmission Measurements. *Anal. Bioanal. Chem.*, **2015**, *407* (22), 6791–6801. <https://doi.org/10.1007/s00216-015-8850-8>.
- [119] von der Esch, E.; Lanzinger, M.; Kohles, A. J.; Schwaferts, C.; Weisser, J.; Hofmann, T.; Glas, K.; Elsner, M.; Ivleva, N. P. Simple Generation of Suspensible Secondary Microplastic Reference Particles via Ultrasound Treatment. *Front. Chem.*, **2020**, *8* (169). <https://doi.org/10.3389/fchem.2020.00169>.
- [120] Raman, C. V.; Krishnan, K. S. The Production of New Radiations by Light Scattering. —Part I. *Proc. R. Soc. London. Ser. A, Contain. Pap. a Math. Phys. Character*, **1929**, *122* (789), 23–35. <https://doi.org/10.1098/rspa.1929.0002>.
- [121] Anger, P. M.; von der Esch, E.; Baumann, T.; Elsner, M.; Niessner, R.; Ivleva, N. P. Raman Microspectroscopy as a Tool for Microplastic Particle Analysis. *TrAC - Trends in Analytical Chemistry*. Elsevier B.V. December 1, 2018, pp 214–226. <https://doi.org/10.1016/j.trac.2018.10.010>.
- [122] Weber, F.; Kerpen, J.; Wolff, S.; Langer, R.; Eschweiler, V. Investigation of Microplastics Contamination in Drinking Water of a German City. *Sci. Total Environ.*, **2021**, *755*, 143421. <https://doi.org/10.1016/J.SCITOTENV.2020.143421>.
- [123] Wolff, S.; Kerpen, J.; Prediger, J.; Barkmann, L.; Müller, L. Determination of the Microplastics Emission in the Effluent of a Municipal Waste Water Treatment Plant Using Raman Microspectroscopy. *Water Res. X*, **2019**, *2*, 100014. <https://doi.org/10.1016/j.wroa.2018.100014>.
- [124] Enders, K.; Käßler, A.; Biniash, O.; Feldens, P.; Stollberg, N.; Lange, X.; Fischer, D.; Eichhorn, K. J.; Pollehne, F.; Oberbeckmann, S.; et al. Tracing Microplastics in Aquatic Environments Based on Sediment Analogies. *Sci. Reports 2019 91*, **2019**, *9* (1), 1–15. <https://doi.org/10.1038/s41598-019-50508-2>.
- [125] Sobhani, Z.; Zhang, X.; Gibson, C.; Naidu, R.; Megharaj, M.; Fang, C. Identification and Visualisation of Microplastics/Nanoplastics by Raman Imaging (i): Down to 100 Nm. *Water Res.*, **2020**, *174*, 115658.

- <https://doi.org/10.1016/J.WATRES.2020.115658>.
- [126] Gillibert, R.; Balakrishnan, G.; Deshoules, Q.; Tardivel, M.; Magazzù, A.; Donato, M. G.; Maragò, O. M.; Lamy De La Chapelle, M.; Colas, F.; Lagarde, F.; et al. Raman Tweezers for Small Microplastics and Nanoplastics Identification in Seawater. *Environ. Sci. Technol.*, **2019**, *53* (15), 9003–9013. [https://doi.org/10.1021/ACS.EST.9B03105/SUPPL\\_FILE/ES9B03105\\_SI\\_004.AVI](https://doi.org/10.1021/ACS.EST.9B03105/SUPPL_FILE/ES9B03105_SI_004.AVI).
- [127] Li, D.; Shi, Y.; Yang, L.; Xiao, L.; Kehoe, D. K.; Gun'ko, Y. K.; Boland, J. J.; Wang, J. J. Microplastic Release from the Degradation of Polypropylene Feeding Bottles during Infant Formula Preparation. *Nat. Food* **2020**, *1* (11), 746–754. <https://doi.org/10.1038/s43016-020-00171-y>.
- [128] Van Cauwenberghe, L.; Devriese, L.; Galgani, F.; Robbins, J.; Janssen, C. R. Microplastics in Sediments: A Review of Techniques, Occurrence and Effects. *Mar. Environ. Res.*, **2015**, *111*, 5–17. <https://doi.org/10.1016/J.MARENRES.2015.06.007>.
- [129] Trainic, M.; Flores, J. M.; Pinkas, I.; Pedrotti, M. L.; Lombard, F.; Bourdin, G.; Gorsky, G.; Boss, E.; Rudich, Y.; Vardi, A.; et al. Airborne Microplastic Particles Detected in the Remote Marine Atmosphere. *Commun. Earth Environ.* **2020**, *1* (1), 1–9. <https://doi.org/10.1038/s43247-020-00061-y>.
- [130] Collard, F.; Gilbert, B.; Eppe, G.; Parmentier, E.; Das, K. Detection of Anthropogenic Particles in Fish Stomachs: An Isolation Method Adapted to Identification by Raman Spectroscopy. *Arch. Environ. Contam. Toxicol.* **2015**, *69* (3), 331–339. <https://doi.org/10.1007/S00244-015-0221-0>.
- [131] Enders, K.; Lenz, R.; Stedmon, C. A.; Nielsen, T. G. Abundance, Size and Polymer Composition of Marine Microplastics  $\geq 10$  Mm in the Atlantic Ocean and Their Modelled Vertical Distribution. *Mar. Pollut. Bull.*, **2015**, *100* (1), 70–81. <https://doi.org/10.1016/J.MARPOLBUL.2015.09.027>.
- [132] Frère, L.; Paul-Pont, I.; Moreau, J.; Soudant, P.; Lambert, C.; Huvet, A.; Rinnert, E. A Semi-Automated Raman Micro-Spectroscopy Method for Morphological and Chemical Characterizations of Microplastic Litter. *Mar. Pollut. Bull.*, **2016**, *113* (1–2), 461–468. <https://doi.org/10.1016/J.MARPOLBUL.2016.10.051>.
- [133] Von Der Esch, E.; Kohles, A. J.; Anger, P. M.; Hoppe, R.; Niessner, R.; Elsner, M.; Ivleva, N. P. TUM-ParticleTyper: A Detection and Quantification Tool for Automated Analysis of (Microplastic) Particles and Fibers. *PLoS One*, **2020**, *15* (6 June), e0234766. <https://doi.org/10.1371/journal.pone.0234766>.
- [134] Brandt, J.; Bittrich, L.; Fischer, F.; Kanaki, E.; Tagg, A.; Lenz, R.; Labrenz, M.; Brandes, E.; Fischer, D.; Eichhorn, K. J. High-Throughput Analyses of Microplastic Samples Using Fourier Transform Infrared and Raman Spectrometry. *Appl. Spectrosc.*, **2020**, *74* (9), 1185–1197. <https://doi.org/10.1177/0003702820932926>.
- [135] Schwaferts, C.; Schwaferts, P.; von der Esch, E.; Elsner, M.; Ivleva, N. P. Which Particles to Select, and If Yes, How Many?: Subsampling Methods for Raman Microspectroscopic Analysis of Very Small Microplastic. *Anal. Bioanal. Chem.*, **2021**, *413* (14), 3625–3641. <https://doi.org/10.1007/S00216-021-03326-3/FIGURES/7>.
- [136] Brandt, J.; Fischer, F.; Kanaki, E.; Enders, K.; Labrenz, M.; Fischer, D. Assessment of Subsampling Strategies in Microspectroscopy of Environmental Microplastic Samples. *Front. Environ. Sci.*, **2021**, *8*, 288. <https://doi.org/10.3389/FENVS.2020.579676/BIBTEX>.
- [137] Picó, Y.; Barceló, D. Pyrolysis Gas Chromatography-Mass Spectrometry in

- Environmental Analysis: Focus on Organic Matter and Microplastics. *TrAC Trends Anal. Chem.*, **2020**, *130*, 115964. <https://doi.org/10.1016/J.TRAC.2020.115964>.
- [138] Mintenig, S. M.; Bäuerlein, P. S.; Koelmans, A. A.; Dekker, S. C.; van Wezel, A. P. Closing the Gap between Small and Smaller: Towards a Framework to Analyse Nano- and Microplastics in Aqueous Environmental Samples. *Environ. Sci. Nano*, **2018**, *5* (7), 1640–1649. <https://doi.org/10.1039/C8EN00186C>.
- [139] Ter Halle, A.; Jeanneau, L.; Martignac, M.; Jardé, E.; Pedrono, B.; Brach, L.; Gigault, J. Nanoplastic in the North Atlantic Subtropical Gyre. *Environ. Sci. Technol.*, **2017**, *51* (23), 13689–13697. <https://doi.org/10.1021/acs.est.7b03667>.
- [140] Watteau, F.; Dignac, M. F.; Bouchard, A.; Revallier, A.; Houot, S. Microplastic Detection in Soil Amended With Municipal Solid Waste Composts as Revealed by Transmission Electronic Microscopy and Pyrolysis/GC/MS. *Front. Sustain. Food Syst.*, **2018**, *2*, 81. <https://doi.org/10.3389/FSUFS.2018.00081/BIBTEX>.
- [141] Ceccarini, A.; Corti, A.; Erba, F.; Modugno, F.; La Nasa, J.; Bianchi, S.; Castelvetro, V. The Hidden Microplastics: New Insights and Figures from the Thorough Separation and Characterization of Microplastics and of Their Degradation Byproducts in Coastal Sediments. *Environ. Sci. Technol.*, **2018**, *52* (10), 5634–5643. <https://doi.org/10.1021/acs.est.8b01487>.
- [142] Dierkes, G.; Lauschke, T.; Becher, S.; Schumacher, H.; Földi, C.; Ternes, T. Quantification of Microplastics in Environmental Samples via Pressurized Liquid Extraction and Pyrolysis-Gas Chromatography. *Anal. Bioanal. Chem.* **2019**, *411* (26), 6959–6968. <https://doi.org/10.1007/S00216-019-02066-9>.
- [143] Goßmann, I.; Halbach, M.; Scholz-Böttcher, B. M. Car and Truck Tire Wear Particles in Complex Environmental Samples – A Quantitative Comparison with “Traditional” Microplastic Polymer Mass Loads. *Sci. Total Environ.*, **2021**, *773*, 145667. <https://doi.org/10.1016/J.SCITOTENV.2021.145667>.
- [144] Eisentraut, P.; Dümichen, E.; Ruhl, A. S.; Jekel, M.; Albrecht, M.; Gehde, M.; Braun, U. Two Birds with One Stone---Fast and Simultaneous Analysis of Microplastics: Microparticles Derived from Thermoplastics and Tire Wear. *Environ. Sci. Technol. Lett.*, **2018**, *5* (10), 608–613. <https://doi.org/10.1021/acs.estlett.8b00446>.
- [145] Klöckner, P.; Reemtsma, T.; Eisentraut, P.; Braun, U.; Ruhl, A. S.; Wagner, S. Tire and Road Wear Particles in Road Environment – Quantification and Assessment of Particle Dynamics by Zn Determination after Density Separation. *Chemosphere*, **2019**, *222*, 714–721. <https://doi.org/10.1016/j.chemosphere.2019.01.176>.
- [146] Braun, U.; Altmann, K.; Herper, D.; Knefel, M.; Bednarz, M.; Bannick, C. G. Smart Filters for the Analysis of Microplastic in Beverages Filled in Plastic Bottles. *Food Addit. Contam. - Part A Chem. Anal. Control. Expo. Risk Assess.*, **2021**, *38* (4), 691–700. <https://doi.org/10.1080/19440049.2021.1889042>.
- [147] Lin, Y.; Huang, X.; Liu, Q.; Lin, Z.; Jiang, G. Thermal Fragmentation Enhanced Identification and Quantification of Polystyrene Micro/Nanoplastics in Complex Media. *Talanta*, **2020**, *208*, 120478. <https://doi.org/10.1016/J.TALANTA.2019.120478>.
- [148] Fuller, S.; Gautam, A. A Procedure for Measuring Microplastics Using Pressurized Fluid Extraction. <https://doi.org/10.1021/acs.est.6b00816>.
- [149] Zhang, Y.; Wang, X.; Shan, J.; Zhao, J.; Zhang, W.; Liu, L.; Wu, F. Hyperspectral

- Imaging Based Method for Rapid Detection of Microplastics in the Intestinal Tracts of Fish. *Environ. Sci. Technol.*, **2019**, *53* (9), 5151–5158. [https://doi.org/10.1021/ACS.EST.8B07321/SUPPL\\_FILE/ES8B07321\\_SI\\_001.PDF](https://doi.org/10.1021/ACS.EST.8B07321/SUPPL_FILE/ES8B07321_SI_001.PDF).
- [150] Materić, D.; Kasper-Giebl, A.; Kau, D.; Anten, M.; Greilinger, M.; Ludewig, E.; Van Sebille, E.; Röckmann, T.; Holzinger, R. Micro- and Nanoplastics in Alpine Snow: A New Method for Chemical Identification and (Semi)Quantification in the Nanogram Range. *Environ. Sci. Technol.*, **2020**, *54* (4), 2353–2359. [https://doi.org/10.1021/ACS.EST.9B07540/SUPPL\\_FILE/ES9B07540\\_SI\\_005.ZIP](https://doi.org/10.1021/ACS.EST.9B07540/SUPPL_FILE/ES9B07540_SI_005.ZIP).
- [151] Imhof, H. K.; Laforsch, C.; Wiesheu, A. C.; Schmid, J.; Anger, P. M.; Niessner, R.; Ivleva, N. P. Pigments and Plastic in Limnetic Ecosystems: A Qualitative and Quantitative Study on Microparticles of Different Size Classes. *Water Res.*, **2016**, *98*, 64–74. <https://doi.org/10.1016/j.watres.2016.03.015>.
- [152] Mason, S. A.; Welch, V. G.; Neratko, J. Synthetic Polymer Contamination in Bottled Water. *Front. Chem.*, **2018**, *6*, 407. <https://doi.org/10.3389/FCHEM.2018.00407/BIBTEX>.
- [153] Kang, H.; Park, S.; Lee, B.; Ahn, J.; Kim, S. Modification of a Nile Red Staining Method for Microplastics Analysis: A Nile Red Plate Method. *Water 2020, Vol. 12, Page 3251*, **2020**, *12* (11), 3251. <https://doi.org/10.3390/W12113251>.
- [154] Catarino, A. I.; Macchia, V.; Sanderson, W. G.; Thompson, R. C.; Henry, T. B. Low Levels of Microplastics (MP) in Wild Mussels Indicate That MP Ingestion by Humans Is Minimal Compared to Exposure via Household Fibres Fallout during a Meal. *Environ. Pollut.*, **2018**, *237*, 675–684. <https://doi.org/10.1016/J.ENVPOL.2018.02.069>.
- [155] Imhof, H. K.; Ivleva, N. P.; Schmid, J.; Niessner, R.; Laforsch, C. Contamination of Beach Sediments of a Subalpine Lake with Microplastic Particles. *Curr. Biol.*, **2013**, *23* (19), R867–R868. <https://doi.org/10.1016/j.cub.2013.09.001>.
- [156] Gewert, B.; Plassmann, M. M.; Macleod, M. Pathways for Degradation of Plastic Polymers Floating in the Marine Environment. *Environ. Sci. Process. Impacts*, **2015**, *17* (9), 1513–1521. <https://doi.org/10.1039/c5em00207a>.
- [157] Thompson, R. C.; Swan, S. H.; Moore, C. J.; Vom Saal, F. S. Our Plastic Age. *Philos. Trans. R. Soc. Lond. B. Biol. Sci.*, **2009**, *364* (1526), 1973–1976. <https://doi.org/10.1098/rstb.2009.0054>.
- [158] PlasticsEurope; PlasticsEurope AISBL; Plastics Europe. Plastics-the Facts 2019: An Analysis of European Plastics Production, Demand and Waste Data. **2019**. [https://doi.org/https://www.plasticseurope.org/application/files/9715/7129/9584/FINAL\\_web\\_version\\_Plastics\\_the\\_facts2019\\_14102019.pdf](https://doi.org/https://www.plasticseurope.org/application/files/9715/7129/9584/FINAL_web_version_Plastics_the_facts2019_14102019.pdf).
- [159] Ribeiro, F.; O'Brien, J. W.; Galloway, T.; Thomas, K. V. Accumulation and Fate of Nano- and Micro-Plastics and Associated Contaminants in Organisms. *TrAC - Trends Anal. Chem.*, **2019**, *111*, 139–147. <https://doi.org/10.1016/j.trac.2018.12.010>.
- [160] Triebkorn, R.; Braunbeck, T.; Grummt, T.; Hanslik, L.; Huppertsberg, S.; Jekel, M.; Knepper, T. P.; Kraus, S.; Müller, Y. K.; Pittroff, M.; et al. Relevance of Nano- and Microplastics for Freshwater Ecosystems: A Critical Review. *TrAC Trends Anal. Chem.*, **2018**. <https://doi.org/10.1016/j.trac.2018.11.023>.
- [161] Andrady, A. L. Microplastics in the Marine Environment. *Mar. Pollut. Bull.*, **2011**, *62* (8), 1596–1605. <https://doi.org/10.1016/j.marpolbul.2011.05.030>.
- [162] Ryan, P. G.; Moore, C. J.; van Franeker, J. A.; Moloney, C. L. Monitoring the

- Abundance of Plastic Debris in the Marine Environment. *Philos. Trans. R. Soc. Lond. B. Biol. Sci.*, **2009**, 364 (1526), 1999–2012. <https://doi.org/10.1098/rstb.2008.0207>.
- [163] Barnes, D. K. A.; Galgani, F.; Thompson, R. C.; Barlaz, M. Accumulation and Fragmentation of Plastic Debris in Global Environments. *Philos. Trans. R. Soc. B Biol. Sci.*, **2009**, 364 (1526), 1985–1998. <https://doi.org/10.1098/rstb.2008.0205>.
- [164] Moore, C. J. Synthetic Polymers in the Marine Environment: A Rapidly Increasing, Long-Term Threat. *Environ. Res.*, **2008**, 108 (2), 131–139. <https://doi.org/10.1016/j.envres.2008.07.025>.
- [165] Huerta Lwanga, E.; Gertsen, H.; Gooren, H.; Peters, P.; Salánki, T.; van der Ploeg, M.; Besseling, E.; Koelmans, A. A.; Geissen, V. Incorporation of Microplastics from Litter into Burrows of *Lumbricus Terrestris*. *Environ. Pollut.*, **2017**, 220 (Pt A), 523–531. <https://doi.org/10.1016/j.envpol.2016.09.096>.
- [166] Gatidou, G.; Arvaniti, O. S.; Stasinakis, A. S. Review on the Occurrence and Fate of Microplastics in Sewage Treatment Plants. *J. Hazard. Mater.*, **2019**, 367, 504–512. <https://doi.org/10.1016/j.jhazmat.2018.12.081>.
- [167] Li, X.; Chen, L.; Mei, Q.; Dong, B.; Dai, X.; Ding, G.; Zeng, E. Y. Microplastics in Sewage Sludge from the Wastewater Treatment Plants in China. *Water Res.*, **2018**, 142, 75–85. <https://doi.org/10.1016/j.watres.2018.05.034>.
- [168] Gies, E. A.; LeNoble, J. L.; Noël, M.; Etemadifar, A. Bishay, F.; Hall, E. R.; Ross, P. S. Retention of Microplastics in a Major Secondary Wastewater Treatment Plant in Vancouver, Canada. *Mar. Pollut. Bull.*, **2018**, 133, 553–561. <https://doi.org/10.1016/j.marpolbul.2018.06.006>.
- [169] Bretas Alvim, C.; Mendoza-Roca, J. A.; Bes-Piá, A. Wastewater Treatment Plant as Microplastics Release Source - Quantification and Identification Techniques. *J. Environ. Manage.*, **2020**, 255, 109739. <https://doi.org/10.1016/j.jenvman.2019.109739>.
- [170] Lares, M.; Ncibi, M. C.; Sillanpää, M.; Sillanpää, M. Occurrence, Identification and Removal of Microplastic Particles and Fibers in Conventional Activated Sludge Process and Advanced MBR Technology. *Water Res.*, **2018**, 133, 236–246. <https://doi.org/10.1016/j.watres.2018.01.049>.
- [171] Murphy, F.; Ewins, C.; Carbonnier, F.; Quinn, B. Wastewater Treatment Works (WwTW) as a Source of Microplastics in the Aquatic Environment. *Environ. Sci. Technol.*, **2016**, 50 (11), 5800–5808. <https://doi.org/10.1021/acs.est.5b05416>.
- [172] Freeman, S.; Booth, A. M.; Sabbah, I.; Tiller, R.; Dierking, J.; Klun, K.; Rotter, A.; Ben-David, E.; Javidpour, J.; Angel, D. L. Between Source and Sea: The Role of Wastewater Treatment in Reducing Marine Microplastics. *Journal of Environmental Management*. Academic Press July 15, 2020, p 110642. <https://doi.org/10.1016/j.jenvman.2020.110642>.
- [173] Bayo, J.; Olmos, S.; López-Castellanos, J. Microplastics in an Urban Wastewater Treatment Plant: The Influence of Physicochemical Parameters and Environmental Factors. *Chemosphere*, **2020**, 238, 124593. <https://doi.org/10.1016/j.chemosphere.2019.124593>.
- [174] Vollertsen, J.; Anna, A. *Microplastic in Danish Wastewater: Sources, Occurrences and Fate*; Vollertsen, J. and Hansen, A. A., Ed.; The Danish Environmental Protection Agency: Copenhagen, Denmark, **2017**.
- [175] Ó Briain, O.; Marques Mendes, A. R.; McCarron, S.; Healy, M. G.; Morrison, L. The Role of Wet Wipes and Sanitary Towels as a Source of White Microplastic

- Fibres in the Marine Environment. *Water Res.*, **2020**, 182. <https://doi.org/10.1016/J.WATRES.2020.116021>.
- [176] Gerba, C. P.; Pepper, I. L. Municipal Wastewater Treatment. In *Environmental and Pollution Science*; Mark L. Brusseau, Ian L. Pepper, Charles P. Gerba, Ed.; Elsevier, **2019**; pp 393–418. <https://doi.org/10.1016/B978-0-12-814719-1.00022-7>.
- [177] Leslie, H. A.; Brandsma, S. H.; van Velzen, M. J. M.; Vethaak, A. D. Microplastics En Route: Field Measurements in the Dutch River Delta and Amsterdam Canals, Wastewater Treatment Plants, North Sea Sediments and Biota. *Environ. Int.*, **2017**, 101, 133–142. <https://doi.org/10.1016/j.envint.2017.01.018>.
- [178] Raju, S.; Carbery, M.; Kuttykattil, A.; Senathirajah, K.; Subashchandrabose, S. R.; Evans, G.; Thavamani, P. Transport and Fate of Microplastics in Wastewater Treatment Plants: Implications to Environmental Health. *Rev. Environ. Sci. Bio/Technology*, **2018**, 17 (4), 637–653. <https://doi.org/10.1007/s11157-018-9480-3>.
- [179] Tchobanoglous, G.; Burton, F. L.; Stensel, H. D. *Wastewater Engineering: Treatment and Reuse*. Metcalf & Eddy, Inc.; **2003**; Vol. 4.
- [180] Schwaferts, C.; Niessner, R.; Elsner, M.; Ivleva, N. P. *Methods for the Analysis of Submicrometer- and Nanoplastic Particles in the Environment*, **2019**; Vol. 112, pp 52–65.
- [181] Rocha-Santos, T.; Duarte, A. C. A Critical Overview of the Analytical Approaches to the Occurrence, the Fate and the Behavior of Microplastics in the Environment. *TrAC - Trends in Analytical Chemistry*. Elsevier B.V. February 1, 2015, pp 47–53. <https://doi.org/10.1016/j.trac.2014.10.011>.
- [182] Qiu, Q.; Tan, Z.; Wang, J.; Peng, J.; Li, M.; Zhan, Z. Extraction, Enumeration and Identification Methods for Monitoring Microplastics in the Environment. *Estuarine, Coastal and Shelf Science*. Academic Press July 5, 2016, pp 102–109. <https://doi.org/10.1016/j.ecss.2016.04.012>.
- [183] Zhao, S.; Zhu, L.; Li, D. Microplastic in Three Urban Estuaries, China. *Environ. Pollut.*, **2015**, 206 (Supplement C), 597–604. <https://doi.org/10.1016/j.envpol.2015.08.027>.
- [184] Gewert, B.; Ogonowski, M.; Barth, A.; MacLeod, M. Abundance and Composition of near Surface Microplastics and Plastic Debris in the Stockholm Archipelago, Baltic Sea. *Mar. Pollut. Bull.*, **2017**, 120 (1), 292–302. <https://doi.org/10.1016/j.marpolbul.2017.04.062>.
- [185] Van Cauwenberghe, L.; Vanreusel, A.; Mees, J.; Janssen, C. R. Microplastic Pollution in Deep-Sea Sediments. *Environ. Pollut.*, **2013**, 182 (Supplement C), 495–499. <https://doi.org/10.1016/j.envpol.2013.08.013>.
- [186] Niederhauser, Livia Cabernard; Edith, Durisch-Kaiser; Jean-Claude, Vogel; Daniel, R. *Mikroplastik in Abwasser Und Gewässern*; **2016**.
- [187] ISO - ISO 13320:2009 - Particle Size Analysis — Laser Diffraction Methods; **2009**.
- [188] Ochiai, N.; Sasamoto, K.; Kanda, H.; Yamagami, T.; David, F.; Tienpont, B.; Sandra, P. Optimization of a Multi-Residue Screening Method for the Determination of 85 Pesticides in Selected Food Matrices by Stir Bar Sorptive Extraction and Thermal Desorption GC-MS. *J. Sep. Sci.*, **2005**, 28 (9–10), 1083–1092. <https://doi.org/10.1002/jssc.200500017>.
- [189] DIN 38409-1 - 1987-01 , German Standard Methods for the Examination of Water, Waste Water and Sludge; Parameters Characterizing Effects and



- Substances (Group H); Determination of Total Dry Residue, Filtrate Dry Residue and Residue on Ignition (H 1); 1987.*
- [190] Kühn, S.; van Werven, B.; van Oyen, A.; Meijboom, A.; Bravo Rebolledo, E. L.; van Franeker, J. A. The Use of Potassium Hydroxide (KOH) Solution as a Suitable Approach to Isolate Plastics Ingested by Marine Organisms. *Mar. Pollut. Bull.*, **2017**, *115* (1–2), 86–90. <https://doi.org/10.1016/j.marpolbul.2016.11.034>.
- [191] Lunt, J. Large-Scale Production, Properties and Commercial Applications of Poly Lactic Acid Polymers. *Polym. Degrad. Stab.*, **1998**, *59* (1–3), 145–152. [https://doi.org/10.1016/s0141-3910\(97\)00148-1](https://doi.org/10.1016/s0141-3910(97)00148-1).
- [192] Zhang, H.; Rankin, A.; Ward, I. M. Determination of the End-Group Concentration and Molecular Weight of Poly(Ethylene Naphthalene-2,6-Dicarboxylate) Using Infra-Red Spectroscopy. *Polymer (Guildf.)*, **1996**, *37* (7), 1079–1085. [https://doi.org/10.1016/0032-3861\(96\)80832-9](https://doi.org/10.1016/0032-3861(96)80832-9).
- [193] Myungwan, H. Chemical Depolymerization Of Pet Bottles Via Methanolysis And Hydrolysis Myungwan Han. Recycling of Polyethylene Terephthalate Bottles; Sabu, T., Ajay, V. R., Krishnan, K., Abitha, V., Martin, G. T., Eds.; **2018**.
- [194] Hwang, J.; Choi, D.; Han, S.; Jung, S. Y.; Choi, J.; Hong, J. Potential Toxicity of Polystyrene Microplastic Particles. *Sci. Reports 2020 101*, **2020**, *10* (1), 1–12. <https://doi.org/10.1038/s41598-020-64464-9>.
- [195] Al-Sabagh, A. M.; Yehia, F. Z.; Eshaq, G.; Rabie, A. M.; ElMetwally, A. E. Greener Routes for Recycling of Polyethylene Terephthalate. *Egypt. J. Pet.*, **2016**, *25* (1), 53–64. <https://doi.org/10.1016/J.EJPE.2015.03.001>.
- [196] Castro-Aguirre, E.; Iñiguez-Franco, F.; Samsudin, H.; Fang, X.; Auras, R. Poly(Lactic Acid)—Mass Production, Processing, Industrial Applications, and End of Life. *Adv. Drug Deliv. Rev.*, **2016**, *107*, 333–366. <https://doi.org/10.1016/J.ADDR.2016.03.010>.
- [197] Imhof, H. K.; Schmid, J.; Niessner, R.; Ivleva, N. P.; Laforsch, C. A Novel, Highly Efficient Method for the Separation and Quantification of Plastic Particles in Sediments of Aquatic Environments. *Limnol. Oceanogr. Methods*, **2012**, *10* (7), 524–537. <https://doi.org/10.4319/lom.2012.10.524>.
- [198] Jambeck, J. R.; Geyer, R.; Wilcox, C.; Siegler, T. R.; Perryman, M.; Andrady, A.; Narayan, R.; Law, K. L. Plastic Waste Inputs from Land into the Ocean. *Science* (80-. ), **2015**, *347* (6223), 768–771. <https://doi.org/10.1126/science.1260352>.
- [199] Jung, S.; Cho, S. H.; Kim, K. H.; Kwon, E. E. Progress in Quantitative Analysis of Microplastics in the Environment: A Review. *Chem. Eng. J.*, **2021**, *422*, 130154. <https://doi.org/10.1016/J.CEJ.2021.130154>.
- [200] Lenz, R.; Labrenz, M. Small Microplastic Sampling in Water: Development of an Encapsulated Filtration Device. *Water*, **2018**, *10* (8), 1055. <https://doi.org/10.3390/w10081055>.
- [201] Pittroff, M.; Müller, Y. K.; Witzig, C. S.; Scheurer, M.; Storck, F. R.; Zumbülte, N. Microplastic Analysis in Drinking Water Based on Fractionated Filtration Sampling and Raman Microspectroscopy. *Environ. Sci. Pollut. Res. Int.*, **2021**, *28* (42), 59439–59451. <https://doi.org/10.1007/S11356-021-12467-Y>.
- [202] Kohles, A. J.; Von der Esch, E.; Phillip, M. A.; Hoppe, R.; Reinhard, N.; Elsner, M.; Ivleva, P. N. *TUM-ParticleTyper: Software and Documentation*; **2020**.
- [203] Dittmar, S.; Zietzschmann, F.; Mai, M.; Worch, E.; Jekel, M.; Ruhl, A. S. Simulating Effluent Organic Matter Competition in Micropollutant Adsorption onto Activated Carbon Using a Surrogate Competitor. *Environ. Sci. Technol.*,

- 2018**, 52 (14), 7859–7866. <https://doi.org/10.1021/ACS.EST.8B01503>.
- [204] Nel, H. A.; Chetwynd, A. J.; Kelleher, L.; Lynch, I.; Mansfield, I.; Margenat, H.; Onoja, S.; Goldberg Oppenheimer, P.; Sambrook Smith, G. H.; Krause, S. Detection Limits Are Central to Improve Reporting Standards When Using Nile Red for Microplastic Quantification. *Chemosphere*, **2021**, 263, 127953. <https://doi.org/10.1016/J.CHEMOSPHERE.2020.127953>.
- [205] Nel, H. A.; Dalu, T.; Wasserman, R. J.; Hean, J. W. Colour and Size Influences Plastic Microbead Underestimation, Regardless of Sediment Grain Size. *Sci. Total Environ.*, **2019**, 655, 567–570. <https://doi.org/10.1016/J.SCITOTENV.2018.11.261>.
- [206] Andrady, A. . Using Flow Cytometry to Detect Micro- and Nano-Scale Polymer Particles. In *Proceedings of the Second Research Workshop on Microplastic Marine Debris*; **2012**.
- [207] Jee, A. Y.; Park, S.; Kwon, H.; Lee, M. Excited State Dynamics of Nile Red in Polymers. *Chem. Phys. Lett.*, **2009**, 477 (1–3), 112–115. <https://doi.org/10.1016/J.CPLETT.2009.06.088>.
- [208] Fox, D. M.; Trulove, P. C.; De Long, H. C.; Gilman, J. W.; Maupin, P. H. Nonaqueous Solvatochromic Behavior of Nile Blue A Perchlorate in Imidazolium-Exchanged Clays and Its Implication Toward Exfoliation in Polymeric Composites \*. <https://doi.org/10.1149/1.3159318>.
- [209] Jose, J.; Burgess, K. Benzophenoxazine-Based Fluorescent Dyes for Labeling Biomolecules. **2006**. <https://doi.org/10.1016/j.tet.2006.08.056>.
- [210] Stanton, T.; Johnson, M.; Nathanail, P.; Gomes, R. L.; Needham, T.; Burson, A. Exploring the Efficacy of Nile Red in Microplastic Quantification: A Costaining Approach. *Environ. Sci. Technol. Lett.*, **2019**, 6 (10), 606–611. [https://doi.org/10.1021/ACS.ESTLETT.9B00499/SUPPL\\_FILE/EZ9B00499\\_SI\\_001.PDF](https://doi.org/10.1021/ACS.ESTLETT.9B00499/SUPPL_FILE/EZ9B00499_SI_001.PDF).
- [211] Asamoah, B. O.; Uurasjärvi, E.; Rätty, J.; Koistinen, A.; Roussey, M.; Peiponen, K. E. Towards the Development of Portable and In Situ Optical Devices for Detection of Micro-and Nanoplastics in Water: A Review on the Current Status. *Polym. 2021, Vol. 13, Page 730*, **2021**, 13 (5), 730. <https://doi.org/10.3390/POLYM13050730>.
- [212] Nguyen, B.; Tufenkji, N. Single Particle-Resolution Fluorescence Microscopy of Nanoplastics. *bioRxiv*, **2022**, 2020.08.25.267443. <https://doi.org/10.1101/2020.08.25.267443>.
- [213] Al-Azzawi, M. S. M.; Knoop, O.; Drewes, J. E. Validation of Sample Preparation Methods for Small Microplastics ( $\leq 10$  Mm) in Wastewater Effluents. *Chem. Eng. J.*, **2022**, 446, 137082. <https://doi.org/10.1016/J.CEJ.2022.137082>.
- [214] Al-Azzawi, M. S. M.; Funck, M.; Kunaschk, M.; der Esch, E. Von; Jacob, O.; Freier, K. P.; Schmidt, T. C.; Elsner, M.; Ivleva, N. P.; Tuerk, J.; et al. Microplastic Sampling from Wastewater Treatment Plant Effluents: Best-Practices and Synergies between Thermoanalytical and Spectroscopic Analysis. *Water Res.*, **2022**, 219, 118549. <https://doi.org/10.1016/J.WATRES.2022.118549>.
- [215] Napotnik, J. A.; Baker, D.; Jellison, K. L. Effect of Sand Bed Depth and Medium Age on Escherichia Coli and Turbidity Removal in Biosand Filters. *Environ. Sci. Technol.*, **2017**, 51 (6), 3402–3409. <https://doi.org/10.1021/acs.est.6b05113>.
- [216] Primpke, S.; Cross, R. K.; Mintenig, S. M.; Simon, M.; Vianello, A.; Gerdt, G.; Vollertsen, J. Toward the Systematic Identification of Microplastics in the Environment: Evaluation of a New Independent Software Tool (SiMPle) for Spectroscopic Analysis. *Appl. Spectrosc.*, **2020**, 74 (9), 1127–1138.

- <https://doi.org/10.1177/0003702820917760>.
- [217] Liu, F.; Olesen, K. B.; Borregaard, A. R.; Vollertsen, J. Microplastics in Urban and Highway Stormwater Retention Ponds. *Sci. Total Environ.*, **2019**, *671*, 992–1000. <https://doi.org/10.1016/j.scitotenv.2019.03.416>.
- [218] Primpke, S.; Wirth, M.; Lorenz, C.; Gerdts, G. Reference Database Design for the Automated Analysis of Microplastic Samples Based on Fourier Transform Infrared (FTIR) Spectroscopy. *Anal. Bioanal. Chem.* *2018 41021*, **2018**, *410* (21), 5131–5141. <https://doi.org/10.1007/S00216-018-1156-X>.

## 9. Appendix

### 9.1. Supplementary Material for Chapter 3

#### Materials and Methods

##### 9.1.1. Sampling Volumes

Table\_3\_SI. 1. Volumes filtered during sampling at WWT A, B and C for each respective basket filter size. The volumes filtered before the sand filter (B.S.F.) and after the sand filter (A.S.F.) for WWTP A and B as well as the effluent of the old sand filter cell (O.S.F. cell) and renewed sand filter cell (R.S.F. cell) of WWTP A are presented.

WWTP	Sampling site	Sampling number	Basket size filter		
			100 $\mu\text{m}$	50 $\mu\text{m}$	10 $\mu\text{m}$
A	Before sand filter	1	3.2 m <sup>3</sup>	3.2 m <sup>3</sup>	0.2 m <sup>3</sup>
		2	3.1 m <sup>3</sup>	3.1 m <sup>3</sup>	0.2 m <sup>3</sup>
		3	2.6 m <sup>3</sup>	2.6 m <sup>3</sup>	0.2 m <sup>3</sup>
A	After sand filter	1	7.5 m <sup>3</sup>	7.5 m <sup>3</sup>	0.4 m <sup>3</sup>
		2	8.2 m <sup>3</sup>	8.2 m <sup>3</sup>	0.2 m <sup>3</sup>
		3	10.1 m <sup>3</sup>	10.1 m <sup>3</sup>	0.3 m <sup>3</sup>
A	Old sand filter cell	1	5.7 m <sup>3</sup>	5.7 m <sup>3</sup>	0.3 m <sup>3</sup>
	New sand filter cell	1	6.1 m <sup>3</sup>	6.1 m <sup>3</sup>	0.5 m <sup>3</sup>
B	Before sand filter	1	4.3 m <sup>3</sup>	4.3 m <sup>3</sup>	0.3 m <sup>3</sup>
		2	3.8 m <sup>3</sup>	3.8 m <sup>3</sup>	0.3 m <sup>3</sup>
B	After sand filter	1	9.5 m <sup>3</sup>	9.5 m <sup>3</sup>	0.4 m <sup>3</sup>
		2	8.7 m <sup>3</sup>	8.7 m <sup>3</sup>	0.5 m <sup>3</sup>
C	effluent	1	3.5 m <sup>3</sup>	3.5 m <sup>3</sup>	0.2 m <sup>3</sup>
		2	3.0 m <sup>3</sup>	3.0 m <sup>3</sup>	0.2 m <sup>3</sup>
		3	3.1 m <sup>3</sup>	3.1 m <sup>3</sup>	0.2 m <sup>3</sup>

### 9.1.2. Volumes extracted from basket filters and aliquots

Table\_3\_Sl. 2. Extracted volumes of the field blanks and samples obtained from the respective basket filters from sampling campaigns at WWTP A. Tween 20 ( $c / 1 \text{ g L}^{-1}$ ) was used transferring the field blanks or samples into glass flask. And the aliquots used for analysis in TED-GC-MS are given.

WWTP	Sampling site	Sampling number	Extracted volumes [mL], (Aliquot [%])		
			100 $\mu\text{m}$	50 $\mu\text{m}$	10 $\mu\text{m}$
A	Before sand filter	1	175, (100)	150, (100)	165, (100)
		2	150, (30)	165, (30)	175, (30)
		3	165, (100)	175, (100)	185, (100)
		Blanks 1	100, (100)	100, (100)	100, (100)
		Blanks 2	100, (30)	120, (30)	125, (30)
		Blanks 3	150, (100)	125, (100)	135, (100)
	After sand filter	1	150, (100)	125, (100)	150, (100)
		2	275, (30)	225, (30)	225, (30)
		3	225, (100)	215, (100)	200, (100)
		Blanks 1	100, (100)	100, (1000)	1005, (100)
		Blanks 2	125, (30)	150, (30)	125, (30)
		Blanks 3	100, (100)	100, (100)	125, (100)
A	Old sand filter cell	1	175, (30)	125, (30)	175, (30)
		Blank 1	175, (30)	175, (30)	125, (30)
	New sand filter cell	1	175, (30)	175, (30)	175, (30)
		Blank 1	175, (30)	175, (30)	125, (30)

Table\_3\_Sl. 3. Extracted volumes of the field blanks and samples obtained from the respective basket filters from sampling campaigns at WWTP B and C. Tween 20 ( $c / 1 \text{ g L}^{-1}$ ) was used transferring the field blanks or samples into glass flask. And the aliquots used for analysis in TED-GC-MS are given.

WWTP	Sampling site	Sampling number	Extracted volumes [mL], (Aliquot [%])		
			100 $\mu\text{m}$	50 $\mu\text{m}$	10 $\mu\text{m}$
B	Before sand filter	1	175, (30)	150, (30)	125, (30)
		2	175, (100)	225, (100)	150, (100)
		Blank 1	125, (30)	150, (30)	125, (30)
		Blank 2	100, (100)	175, (100)	175, (100)
	After sand filter	1	175, (30)	175, (30)	150, (30)
		2	225, (100)	175, (100)	175, (100)
		Blank1	100, (30)	75, (30)	100, (30)
		Blank 2	150, (100)	175, (100)	225, (100)
C	Secondary effluent	1	250, (100)	250, (100)	250, (100)
		2	225, (100)	175, (100)	175, (100)
		3	175, (100)	225, (100)	165, (100)
		Blank 1	150, (100)	150, (100)	100, (100)
		Blank 2	125, (100)	100, (100)	75, (100)
		Blank 3	75, (100)	150, (100)	100, (100)

### 9.1.3. Polymer calibrations

The Attributes of the calibration curves for PE, PS, PP, and PET, respectively, are shown in Table\_3\_Sl. 4. Duplicates were executed, and the calibration ranged between 1 µg - 240 µg in nine points for each respective polymer. Detailed masses can be taken from each figure caption. Quality control samples which consisted of all polymers were measured: One before (20 µg), in between (40 µg) and after (80 µg) the measurements. Calibrations were performed before measurements to ensure accurate reporting of mass for the polymers.

Table\_3\_Sl. 4. Attributes of the calibrations for PE, PS PP and PET.

Polymer	R <sup>2</sup>	Slope	Intercept
		Calibration 1	
PS	0.9969	77303	-13607
PE	0.9975	870	692
PET	0.9985	31002	-37180
PP	0.9985	3323	-3381
		Calibration 2	
PS	0.9997	51667	-52570
PE	0.9991	1379	-238
PET	0.9974	38125	25434
PP	0.9984	2845	1671

Table\_3\_Sl. 5. Selected pyrolysis products for PE, PS, PP and PET identification in TED-GC-MS. Characteristic fragment ions and retention times for each pyrolysis product are presented with characteristic fragment ions and the respective intensity ratios.

Polyme r	Pyrolysis product name	Characteristic fragment ions <i>m/z (i.r.)</i>	Retention time (min)
PS	PS 1 Styrene	51 (18%); 78 (41%); 104 (100%)	8.49
	PS 2 2,4-Diphenyl-1-butene	91 (100%); 104 (24%); 130 (18%); 208 (22%)	27.84
	PS 3 2,4,6-Triphenyl-1-hexene	91 (100%); 117 (30%); 194 (16%); 207 (23%)	42.42
PE	PE 1 1,12-Tridecadiene	55 (100%); 81 (84%); 67 (74%); 95 (52%)	21.52
	PE 2 1,13-Tetradecadiene	81 (78%); 95 (55%); 109 (27%)	24.22
	PE 3 1,14-Pentadecadiene	55 (100%); 81 (82%); 95 (58%); 109 (29%)	26.75
PP	PP 1 2,4,6-Trimethylnon-1-ene	43 (89); 69 (100); 111 (32); 125 (12)	11.90
	PP 2 2,4,6,8-Tetramethylundec-1-ene	69 (100); 83 (52); 111 (52); 125 (14); 154 (10)	18.01
	PP 3 2,4,6,8-Tetramethylundec-1-ene	69 (100); 83 (53); 111 (56); 125 (14); 154 (13)	18.20
PET	PET 1 Vinyl benzoate	77 (48); 51 (14); 105 (100)	12.50
	PET 2 Ethyl benzoate	77 (46); 105 (100); 122 (23); 150 (20)	14.00



PET 3	1,1 Biphenyl	76 (7); 154 (100)	19.00
----------	--------------	-------------------	-------

For quantification of PS, PS 2 was used. The quantification of PE was executed with PE 2. PP was quantified by using PP 3 and PET was quantified by determining PET 2.

The detection limit (LOD) and quantification limit (LOQ) were determined using the signal to noise ratio (S/N) of 3 and 10. The noise is an average taken before and after the respective polymer peaks.

*Table\_3\_Sl. 6. LODs and LOQs for the polymers PE, PS, PP and PET. The values are given in µg-absolute.*

Polyme r	Signal Noise	/ Mass (µg)	LOD (µg)	absolute LOQ (µg)	absolute
PS	64	6.0	0.3	0.9	
PE	17	6.5	1.1	3.8	
PP	27	3.0	0.3	1.1	
PET	11	3.5	0.9	3.1	

#### 9.1.4. Sample filtration and processing

After the aliquot has been filtered via a 0.2 µm cellulose-nitrate membrane filter (General Electric, Boston, Massachusetts, USA). It is then rinsed from the filter with 4 x 50 µL of 1 mg/mL Tween 20 in UPW solution. The filter is further wiped against the sides of the glass flask to ensure that the entire filtered material has been transferred to the flask.

This protocol was validated by using three clean membrane filters equilibrated for three consecutive days (72 h) in a dust free room at 20 °C, 40 % relative humidity and at a pressure of 1,014 mbar which are then weighed in the dust free room. These pre-weighed filters were then used to filter real wastewater samples. The filters were subsequently dried in a dust free weighting room at 20 °C, 40 % relative humidity for 72 h, then weighed again to determine the total weight of the filtered material. After which, the rinsing method was employed, and the rinsed filters were again dried in the

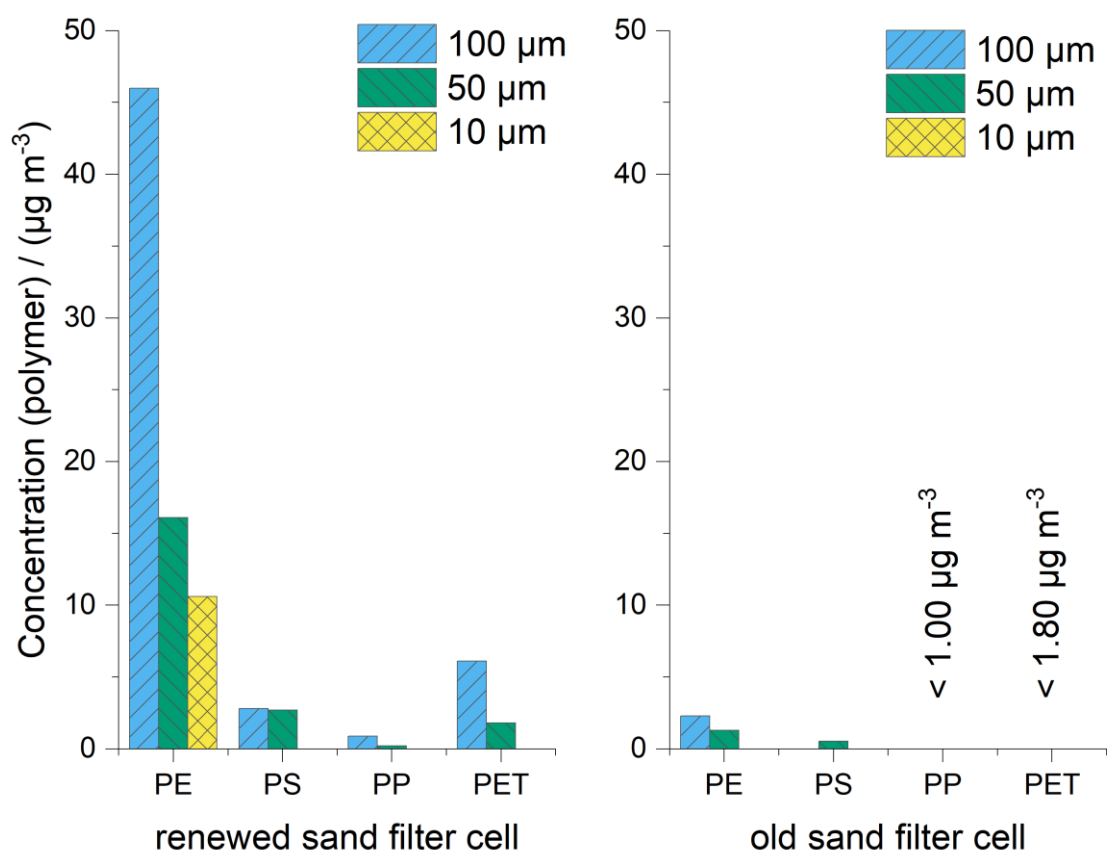
weighing room for 72 h and weighed to determine the remaining filtered material that could not be extracted via the rinsing protocol. The result was an extraction of 90wt% ± 1wt%.

*Table\_3\_Sl. 7. Mean concentrations of the four respective polymers found in the respective basket filters B.SF. and A.SF of WWTPA. For filters in which the polymer concentration ( $\mu\text{g m}^{-3}$ ) was below the LOD, the LOD is divided by the average sample volume and further divided by two.*

<b>WWTP A</b>	<b>Mean concentration PE (<math>\mu\text{g m}^{-3}</math>)</b>	<b>Mean concentration PS (<math>\mu\text{g m}^{-3}</math>)</b>	<b>Mean concentration PP (<math>\mu\text{g m}^{-3}</math>)</b>	<b>Mean concentration PET (<math>\mu\text{g m}^{-3}</math>)</b>
100 $\mu\text{m}$ B.SF.	122.9	7.0	4.9	15.1
50 $\mu\text{m}$ B.SF.	36.7	7.0	1.7	5.2
10 $\mu\text{m}$ B.SF.	3.4	0.8	3.8	5.5
100 $\mu\text{m}$ A.SF.	12.0	1.4	0.2	3.1
50 $\mu\text{m}$ A.SF.	1.3	0.4	<LOD	0.9
10 $\mu\text{m}$ A.SF.	<LOD	0.1	<LOD	(<LOD)
Renewed Sand filter Cell 100 $\mu\text{m}$	46.00	2.80	0.90	6.10
Renewed Sand filter Cell 50 $\mu\text{m}$	16.10	2.70	0.20	1.80
Renewed Sand filter Cell 10 $\mu\text{m}$	10.60	(<LOD)	(<LOD)	(<LOD)
Old Sand filter Cell 100 $\mu\text{m}$	2.30	0.05	0.05	0.35
New Sand filter Cell 50 $\mu\text{m}$	1.30	0.53	(<LOD)	(<LOD)
New Sand filter Cell 10 $\mu\text{m}$	(<LOD)	(<LOD)	(<LOD)	(<LOD)

Table\_3\_Sl. 8. Mean concentrations of the four respective polymers found in the respective basket filters B.SF. and A.SF. of WWTP B. For filters in which the polymer concentration ( $\mu\text{g m}^{-3}$ ) was below the LOD, the LOD is divided by the average sample volume and further divided by two.

WWTP B	Mean concentration PE ( $\mu\text{g m}^{-3}$ )	Mean concentration PS ( $\mu\text{g m}^{-3}$ )	Mean concentration PP ( $\mu\text{g m}^{-3}$ )	Mean concentration PET ( $\mu\text{g m}^{-3}$ )
100 $\mu\text{m}$ B.SF.	58.9	11.1	27.4	39.1
50 $\mu\text{m}$ B.SF.	51.4	3.8	0.7	3.5
10 $\mu\text{m}$ B.SF.	30.1	1.35	(<LOD)	(<LOD)
100 $\mu\text{m}$ A.SF.	39.6	2.6	1.6	9.5
50 $\mu\text{m}$ A.SF.	7.4	1.6	(<LOD)	0.3
10 $\mu\text{m}$ A.SF.	1.4	(<LOD)	(<LOD)	(<LOD)



Figure\_3\_Sl. 1. The results of sampling an old and a renewed sand filter cell from WWTP A are presented in  $\mu\text{g m}^{-3}$  for the polymers PE, PS, PP and PET for each respective sieve fraction (100  $\mu\text{m}$ , 50  $\mu\text{m}$  and 10  $\mu\text{m}$ ). The effluent of each respective cell was sampled. As WWTP A was renewing each sand filter cell only one sampling was possible. Polymers which were below LOD are marked as such. The LOD concentrations were calculated by

*dividing the absolute LOD-value (Table\_3\_SI. 6) by the corresponding average sampling volume taken from Table\_3\_SI. 1.*

FS 1 shows the comparison between the effluent MP concentration of an old (7 years old) and new sand filter cell. The sand filter cell using old sand media, when compared to the sand filter cell using freshly restored media, exhibited 94% and 78% higher removal efficiencies for PE and PS, respectively. Furthermore, no PP or PET were detected in the effluent of the cell using older sand media, whereas those were detected in the effluent of the cell using freshly restored media. However, since only a single point could be sampled due to limited accessibility during the reconstruction, the data presented in Figure\_3\_SI. 1 cannot be considered statistically significant. Nevertheless, it indicated that sand filter cells can effectively retain MP even after years of operation. This might be explained as sand filters maturing with time due to the buildup of biofilms and changing pore space distributions and therefore improving retention efficiency. In comparison, freshly restored sand might need a few weeks to reach a similar condition [215].

## 9.2. Appendix A (Appendix for Chapter 4.1)

Abbreviations for microplastics used in the tables below: Polyethylene (PE), polypropylene (PP), polyvinyl chloride (PVC), polyethylene terephthalate (PET), polyamide (PA), polyurethane (PUR), and polycarbonate (PC), acrylonitrile-butadiene-styrene (ABS), expanded PS (EPS), low-density PE (LDPE), linear LDPE (LLDPE), high-density PE (HDPE), nylon-6 (polyamide-6 or NY6), nylon-66 (polyamide-66 or NY66), cellulose acetate (CA), Poly(methyl methacrylate) (PMMA), Poly(hexamethylene nonanediamide): Nylon 6/9, Poly 1,4-butylene terephthalate (PBT), Nylon12 (NY12, or PA-12), crosslinked polystyrene (PSXL), polytetrafluoroethylene (PTFE), un-plasticized polyvinyl chloride (uPVC), styreneacrylate (SA)

Table\_4.1\_A. 1. Summary of various hydrogen peroxide protocols used in microplastic studies. RT: (Room Temperature)

Protocols	Conditions	Matrix	MPs	Effects on organics	Effects on MP
H <sub>2</sub> O <sub>2</sub> (30 %) [33]	60 °C for *24/12 hr. or 70 °C for *24 hr.	Sludge and soil	PP, LDPE, HDPE, PS, PET, NY66, PC, PMMA	Digestion > 80 % for sludge and >96% for soil	Degradation of NY66 (at 70 °C), PP (at 70 °C). As for PS; less degradation at 60 °C and more at 70 °C
H <sub>2</sub> O <sub>2</sub> (35 %) [44]	50 °C for 96 hr.	Fish	LDPE, HDPE, PP, PS, PET, PVC, NY6, NY66	Digestion of 98 %	Discoloration of PET, loss of NY6 and NY6
H <sub>2</sub> O <sub>2</sub> (30 %) [45]	55 °C for 7 days	Fish	PE, PS	**Extraction efficiency of 70%	No report
Density separation then H <sub>2</sub> O <sub>2</sub> (15 %) [45]	50 °C overnight	Fish	PE, PS	**Extraction efficiency of 95%	No effects
H <sub>2</sub> O <sub>2</sub> (30 %) [46]	RT. For 7 days	Marine sediment	PVC, PET, PA, ABS, PC, PUR, PP, LDPE, LLDPE, HPDE	50% digestion and the rest were discolored	Discoloration or degradation in PA, PC, PP, PET, LLDPE, PVC, PUR, LDPE

H <sub>2</sub> O <sub>2</sub> (35 %) [46]	RT. For 7 days	Marine sediment	PVC, PP, LDPE, PE, HDPE, PET, PUR, PS, PC, PA, ABS, EPS	92% digestion and discoloration	Size reduction PP and PE
H <sub>2</sub> O <sub>2</sub> (30 %) then density separation [47]	70 °C overnight	Sludge	PE	**Extraction efficiency of 78%	No adverse effects reported

\* Contact times in the study of Hurley et al. [7] were not clearly reported. The experiments for the effects on microplastics was 24 hours for all 6 protocols. However, the experiments for organic matter digestion were done separately and the contact time was not specified. Their protocol for H<sub>2</sub>O<sub>2</sub> was based on a protocol by Sujathan et al [47] where the contact time was defined as 12 hours (overnight).

\*\* Extraction efficiency represents only the recovery of microplastics from an environmental matrix, it does not report on the reduction of the matrix.

Table\_4.1\_A. 2. Summary of various Fenton protocols used in microplastic studies. RT: (Room Temperature)

Protocols	Conditions	Matrix	MPs	Effects on organics	Effects on MP
H <sub>2</sub> O <sub>2</sub> (30 %) + 20 g/L FeSO <sub>4</sub> 7H <sub>2</sub> O <sub>2</sub> 1:1 (v/v) [33]	<40 °C (Ice bath) *24 hr./20 min	Sludge and soil	PP, LDPE, HDPE, PS, PET, NY66, PC, PMMA	Digestion 87% for sludge and 106% for soil	No adverse effects
H <sub>2</sub> O <sub>2</sub> (30 %) + 15 g/L FeSO <sub>4</sub> 7H <sub>2</sub> O <sub>2</sub> 1:1 (v/v) [35]	50 °C for 1 hr.	Plant and animal tissues	PE, PP, PS, PET, PVC, CA, PA	Digestion of 72.6% of fish tissue, 100% of algae, 26.3% driftwood, 17.5% paraffin	Degradation of CA

H <sub>2</sub> O <sub>2</sub> (30 %) + 15 g/L FeSO <sub>4</sub> 7H <sub>2</sub> O <sub>2</sub> 1:1 (v/v) [42]	75 °C for >35 min	Water, beach and sediment	None tested	No reports	No reports
H <sub>2</sub> O <sub>2</sub> (30 %) + 20 g/L FeSO <sub>4</sub> 7H <sub>2</sub> O <sub>2</sub> (2:1 v/v) [43]	RT. 10 min (no ice reaction + 10 bath) min cooling	Sludge	PE, PP, PVC, PA	Effective removal (No exact details provided)	No observed effects

\* Contact times in the study of Hurley et al. [7] were not clearly reported. The experiments for the effects on microplastics used 24 hours for all protocols. However, the experiments for organic matter digestion were done separately and the contact time was not specified. Their protocol for Fenton was based on a protocol by Tagg et al. [43], where the contact time was defined as 20 minutes in total.

Table\_4.1\_A. 3. Summary of various acid-based digestions used in microplastic studies. RT: (Room Temperature)

Protocols	Conditions	Matrix	MPs	Effects on organics	Effects on MP
HNO <sub>3</sub> (69 %) [44]	25 °C for 96 hr.	Fish	LDPE, HDPE, PP, PS, PET, PVC, NY6, NY66	Removal >95%	Loss of NY6, NY66. Melting of LDPE, HDPE, PP. Recovery of PVC 69%. Discoloration of others
HNO <sub>3</sub> (55%) [48]	Based on fish size: RT. For 3-10 hr. or 80 °C for 10-20 min	Fish	HDPE, PA, Nylon 6/9, PBT, PVC	Complete digestion of the fish	Tested at room temperature for 1 month. Loss of Nylon within 24 hours, the rest showed no significant changes after 1 month.
HNO <sub>3</sub> (22.5 M) [49]	RT. Overnight then boiling for 2 hr.	Mussels	PS, PA	Good digestion of the tissues	PA fibers (30x200 µm) were lost. PA particles 100x400 µm were 98% recovered. PS particles 30 µm and 10 µm were recovered.

HNO <sub>3</sub> (22.5 M) [49]	60 °C for 1 hr. then 100 °C for 1 hr.	Mussels	PS, PA	Satisfactory digestion of the tissues	PS particles melting together when exposed to the reagent directly. This did not occur when PS was embedded in the tissues. PA was completely lost
HNO <sub>3</sub> (22.5 M) [45]	RT. overnight then boiling for 30 min	Fish	PS, PE	**Extraction efficiency of only 4%	Almost complete loss of PS and PE
HNO <sub>3</sub> (65%) [36]	RT. overnight then 60 °C for 2 hr.	None	LDPE, HDPE, PP, NY12, PS	Not tested due to damaged polymers	Melting of NY12, yellowing of the rest
HNO <sub>3</sub> (35%) [37]	60 °C overnight	Mussels	PET, HDPE, PVC, PA	Complete digestion	Melting together of PET, HDPE, loss of PA
HCL (37%) [44]	25 °C for 96 hr.	Fish	LDPE, HDPE, PP, PS, PET, PVC, NY6, NY66	Digestion efficiency >95%	Loss of NY6, NY66. Melting and clumping of PET
HCL (20%) [46]	RT. for 7 days	Marine sediment	PVC, PET, PA, ABS, PC, PUR, PP, LDPE, LLDPE, HPDE	No complete dissolution of any biogenic organic matter	Not reported

\*\* Extraction efficiency represents only the recovery of microplastics from an environmental matrix, it does not report on the reduction of the matrix.

Table\_4.1\_A. 4. Summary of various alkaline-based digestions used in microplastic studies. RT: (Room Temperature)

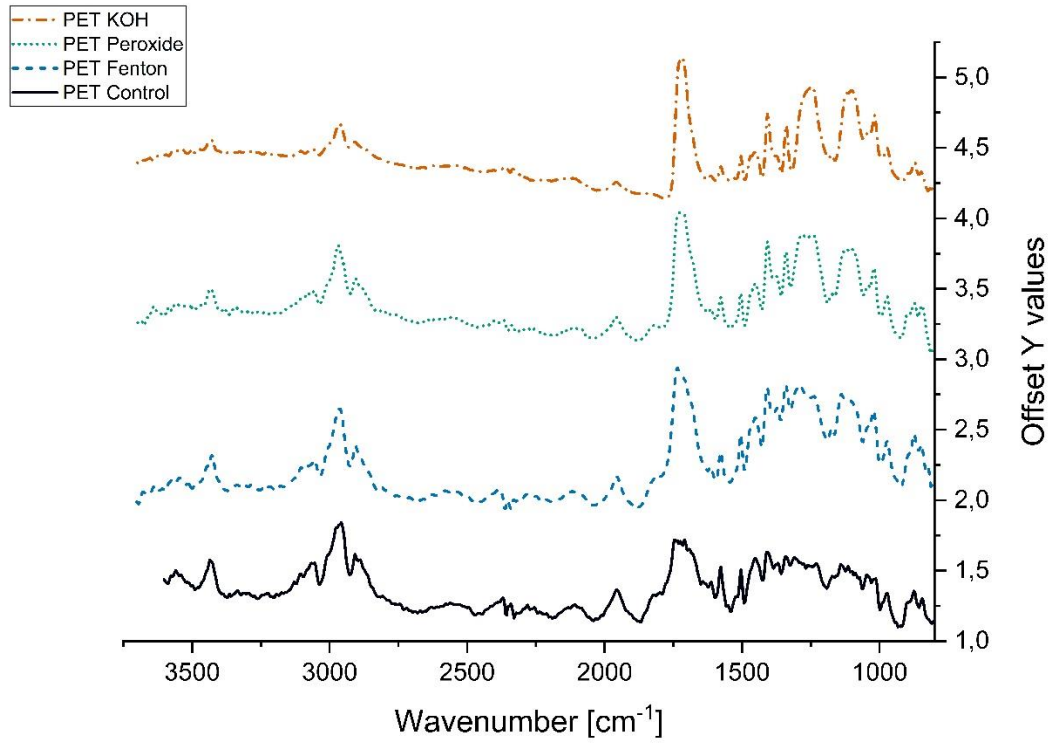
Protocols	Conditions	Matrix	MPs	Effects on organics	Effects on MP
KOH (10%) [33]	60 °C for 24 hr.	Sludge and soil	PP, LDPE, HDPE, PS, PET, NY66, PC, PMMA	Digestion of sludge: 57% And for soil: 35%	A slight weight decrease for PC



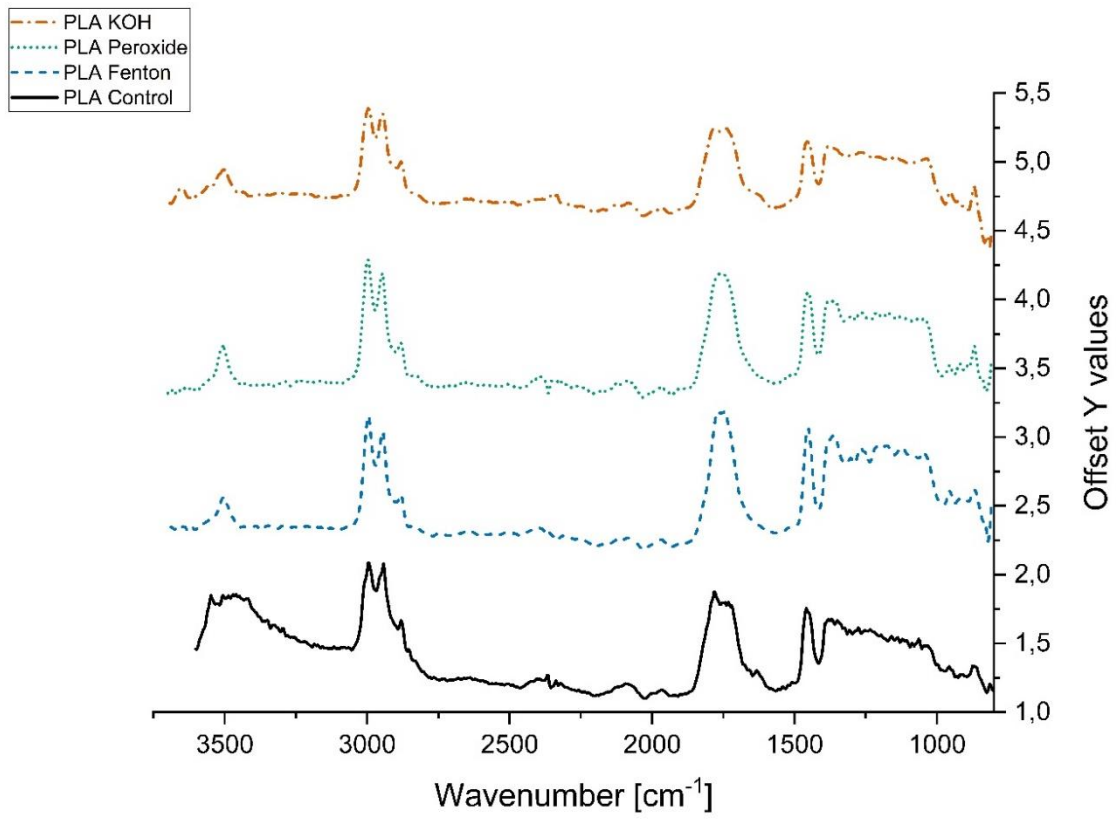
KOH (10%) [44]	25 °C for 96 hr. or 40 °C for 48 hr. or 50 °C for 36 hr. or 60 °C for 24 hr.	Fish	LDPE, HDPE, PP, PS, PET, PVC, NY6, NY66	Removal >95% (all temperatures)	Yellowing of NY66. Reduction of PVC and PET recovery that worsens with increased temperature
KOH (10%) [36]	60 °C for 24 hr.	Mussels, crabs, fish	CA, HDPE, LDPE, NY6, NY12, PC, PET, PMMA, PP, PS, PSXL, PTFE, PUR, uPVC, EPS	Digestion efficiency > 99.5%	Degradation of CA
KOH (56, 224 g/L) [38]	RT. For 14 days	None	Cera Microcrystalline, PE	**Extraction efficiency > 95%	Discoloration of cera microcrystalline and PE (for 224 g/L)
KOH (10%) [39]	RT. For 2-3 weeks	Fish	No spiking: PE, PP, PET, SA	Digestion satisfactory	None tested
KOH (10%) [40]	60 °C for 24 hr.	Vegetal	PP, PE, PVC, PUR, PET, PS	No digestion observed	No effects observed
NaOH (1, 10 M) [33]	60 °C for 24 hr.	Sludge and soil	PP, LDPE, HDPE, PS, PET, NY66, PC, PMMA	Digestion of sludge: 61% (1M) 67% (10M) and soil: 68 % (1 M) 65% (10 M)	Degradation of PET, PC (even more with 10 M)

NaOH (20, 30, 40, 50%) [46]	RT. For 7 days	Marine sediment	PVC, PET, PA, ABS, PC, PUR, PP, LDPE, LLDPE, HPDE	No complete dissolution of any biogenic organic matter. Strongest reaction with NaOH (20%)	Not reported
NaOH (10 M) [36]	60 °C for 24 hr.	None	CA, HDPE, LDPE, NY6, NY12, PC, PET, PMMA, PP, PS, PSXL, PTFE, PUR, uPVC, EPS	Not tested due to damage to polymers	Degradation of CA, PC, PET
NaOH (1 M) [37]	60 °C overnight	Mussels	PET, HDPE, PVC, PA	Complete digestion and extraction efficiency of 93%	No significant effects
NaOH (10 M) [41]	60 °C for 24 hr.	Zooplankton	PS, PA, PET, PE, uPVC	Digestion efficiency of 91%	Partial degradation of PA, clumping of PE, yellowing of uPVC, partial loss of PS
NaOH (10 M) [40]	60 °C for 24 hr.	Vegetal	PP, PE, PVC, PUR, PET, PS	Almost no digestion	Degradation of PET

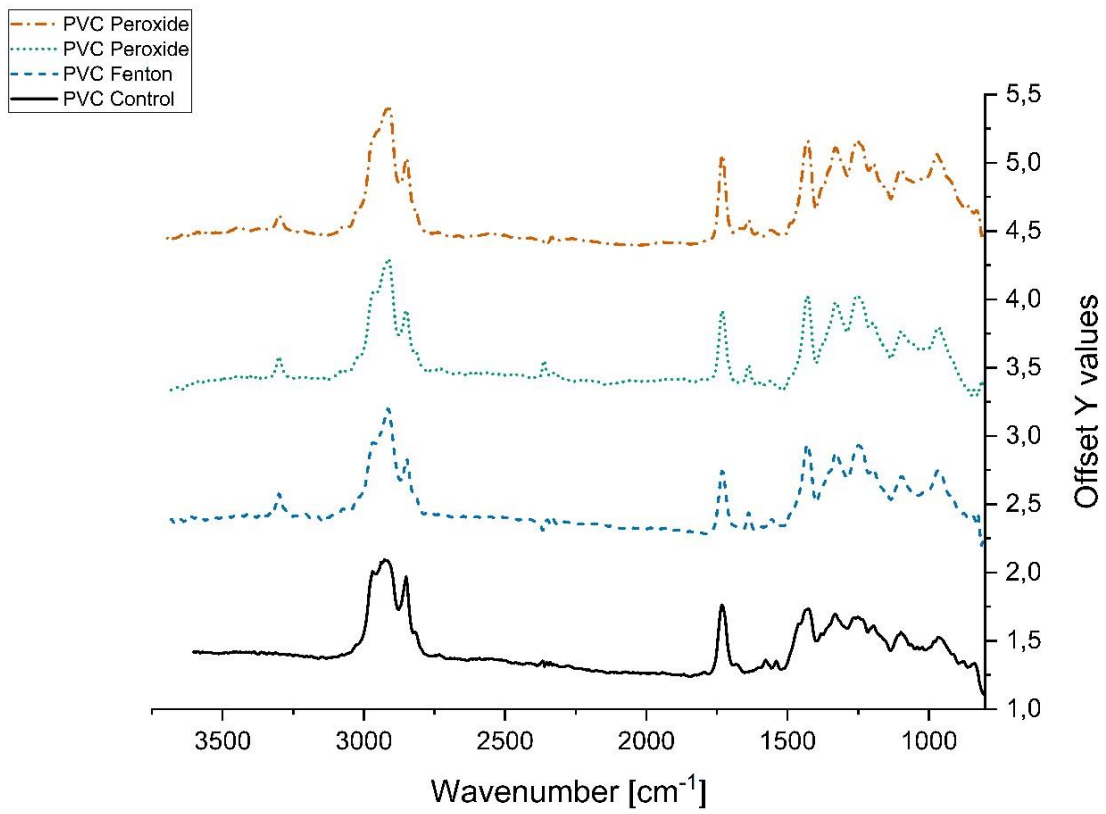
\*\* Extraction efficiency represents only the recovery of microplastics from an environmental matrix, it does not report on the reduction of the matrix.



Figure\_4.1\_A. 1.  $\mu$ FTIR Spectra of PET



Figure\_4.1\_A. 2.  $\mu$ FTIR Spectra of PLA



Figure\_4.1\_A. 3.  $\mu$ FTIR Spectra of PVC

### 9.3. Supplementary Material for Chapter 4.1

#### 9.3.1. Protocols investigated in the study

##### 9.3.1.1. Pre-experiments for protocol selection

After conducting an extensive literature review, ten protocols were identified for a round of pre-selection. The pre-experiments were simplified, using only polystyrene spheres (PS) of size 250  $\mu\text{m}$  (BS-Partikel, Germany) and analyzed using a light microscopy (Axioplan 2, Carl Zeiss AG, Germany) to determine negative effects on the microplastics. The pre-experiments were conducted by weighing 1 mg of PS spheres and letting them react for 24 hours at room temperature with the various reagents Table\_4.1\_Sl. 1. After which, the mixtures were filtered on a 25 mm diameter track etched polycarbonate membrane filter with a pore size of 0.2  $\mu\text{m}$  (Carl Roth, Germany), and rinsed with ultrapure water to remove any remaining reagents from the particles' surface, then the entire filter was scanned by a light microscope to compare changes to the control samples.

Table\_4.1\_Sl. 1. Protocols investigated in the pre-experiments and the literature source they were adopted from.

<b>Protocol</b>	<b>Visual effects on PS-spheres (250 <math>\mu\text{m}</math>)</b>	<b>Details</b>
H <sub>2</sub> O <sub>2</sub> (30%) [33, 47]	-	No obvious effects observed
H <sub>2</sub> O <sub>2</sub> (30%) + H <sub>2</sub> SO <sub>4</sub> (98%) [155]	++	Changes to the surface of particles and melting of particles
Fenton reaction [43]	-	No obvious effect observed
HCL 2 M [41]	++	Changes to the surface of particles and melting of particles
HCL 12M [41]	++	Changes to the surface of particles and melting particles

Ultrasound [41]	+	A large number of fractured particles were found
HNO <sub>3</sub> (65%) [49]	++	Changes to the surface of particles and melting of particles. Formation of small (10 μm) particles/bubbles attached to the originals
NaOH (32%) [41]	++	Roughening of the surface (matt appearance). Plus melting and deep scratches to the surface
NaClO (15%) [19]	-	No obvious effect observed
H <sub>2</sub> SO <sub>4</sub> (98%) [186]	+	Deep scratches to the surface of the particles

(-) No changes, (+) Smaller changes, (++) Obvious changes

Further experiments were performed on granular PE, PA and PLA (90-125 μm) as well as spherical PS (140 μm) using the same approach described above but for 24 hours and 60 °C for both KOH (10%) as well as NaOH (1 M) [33]. The second round of pre-experiments showed roughening of the PS surfaces (matt appearance) for both alkaline treatments, as well as a complete destruction of PLA particles. Changes on PE and PA were hard to quantify using only a microscope due to their non-uniformly shaped particles. Therefore, the results here were only meant as preliminary results and are not robust.

### 9.3.1.2. Fenton protocol

#### Chemicals

1. H<sub>2</sub>O<sub>2</sub> (30%) (ISO, Stabilized, suitable for Fenton Type I reaction as discussed in the main paper)
2. FeSO<sub>4</sub> 7 H<sub>2</sub>O (20 g/L)
3. Polyethylene glycol sorbitan monolaurate, or Polyoxyethylenesorbitan monolaurate (Tween 20) as a surfactant to aid in rinsing glassware and filters.

*Note:* The **K** value in the script is a factor that can be used to scale the procedure up or down, if other volumes of iron sulfate are desired, or when smaller samples are

taken. The recommended dose tested in this study was however **K=10 mL** for 2 mL of return activated sludge (RAS). The K value is recommended to be five times the volume of sample.

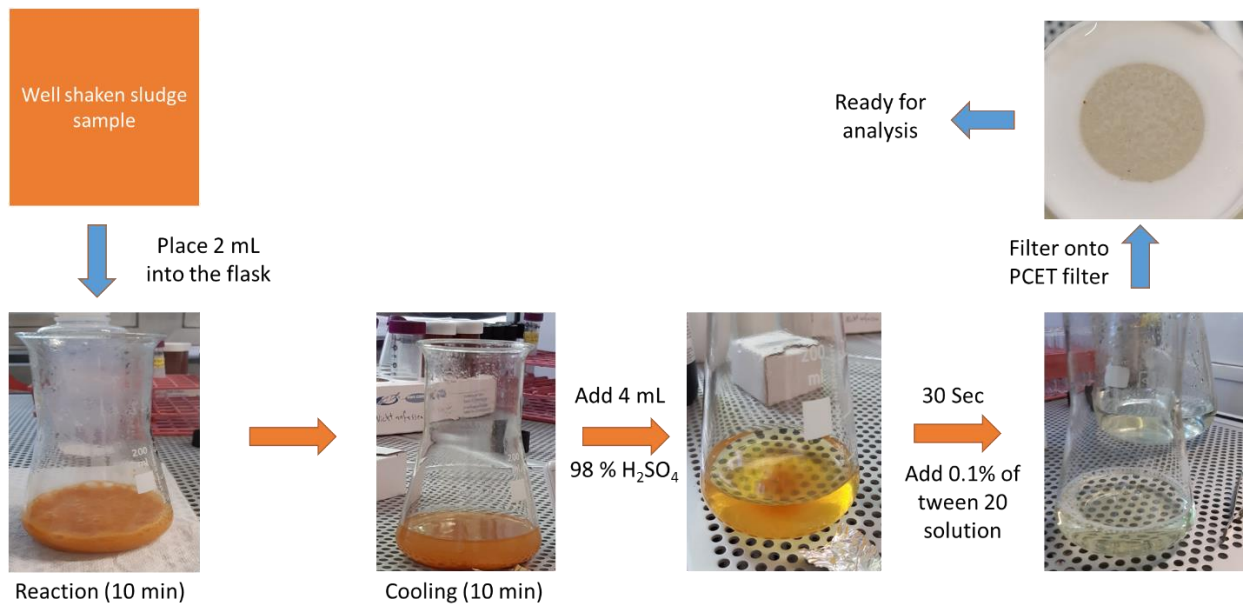
*Procedure:*

1. Iron sulfate solution in a concentration of 20 g/L should be prepared. pH should be then set to 3 using 0.5 M sulfuric acid. Iron sulfate solutions prepared like this can be used up to four days after preparation. But it needs to be visually controlled for precipitated iron particles, as a result of Iron(II) being oxidized to Iron(III). The solution will then show a slight orange tint and microparticles of rust will start to form in it. When this stage is reached, it is advised to prepare a new solution.
2. Two washing bottles are needed (Made of a material that is not the polymers being investigated, Fluorinated ethylene propylene (FEP) was used in this case). One bottle is filled with ultrapure water, whereas the second is filled with ultrapure water with 0.1 % (v/v) of Tween 20. The surfactant bottle helps rinse particles off glass surfaces and the filter membrane.
3. The sludge sample is shaken well to ensure mixing and then 2 mL of sludge is taken with a pipette and placed in a 250 mL conical flask or larger. This provides a safe volume to account for the violent reaction and overflow.
4. Add 10 mL or (**K**) of the Iron sulfate solution prepared in step 1.
5. To start the reaction, 20 ml or (**2 K**) of the Hydrogen peroxide should be added and a timer should be started.
6. after 1 Minute, additional hydrogen peroxide should be added at a rate of 5 ml/min (0.5 **K/Min**) or simply 5 ml (**0.5 K**) at the start of each new minute. This will keep the reaction going.
7. The reaction is exothermic, and the temperature will start to increase in the first minutes, shortly reaching 90 °C. No water bath is needed, and the reaction is violent but controlled. However, wearing a glove that is heat resistant is advised. Shaking or stirring of the flask might be needed if there is foam build up to prevent it from spilling over. In some extreme cases where boiling is to



about to overflow, a washing bottle is used to spray around 1-4 mL of UPW inside the reaction flask to reduce temperatures and bring the boiling under control.

8. At time= 10 minutes, the last 5 ml (**0.5 K**) of peroxide should be added. Then another 10 minutes for cooling is needed. The reaction continues in a weakened state and eventually dies down and cools to below 50 °C.
9. After 20 Minutes has passed, 4 ml (**0.4 K**) of concentrated sulfuric acid (98 %) should be added (That equates to a concentration of 5% in the final reaction volume). The flask should be shaken continuously while adding the acid, this will quickly react with the cloud of Iron (III) particles that have formed during the reaction and clear up the sample within 30 seconds.
10. The solution should now be mostly clear (with a light-yellow color due to dissolved Iron complexes). Quickly adding 10 mL of the surfactant from the washing bottle into the flask to dilute the solution and prevent microplastics from adhering to the glass walls.
11. The content of the flask is then poured into a vacuum filtration unit with a PCTE, 0.2 µm filter. The surfactant bottle can be used here to rinse the contents of the flask into the filtration unit, as well as any particles adhering to the glass walls of the filtration unit.
12. The sample is ready for analysis. Alternatively, it can be stored as a suspension for later, where the same filter from step 11 can be rinsed down into a clean glass test tube using the surfactant bottle and then stored for further analysis or filtration on a different kind of filter.



Figure\_4.1\_SI. 1. An overview of the Fenton protocol for a 2 mL thickened sludge sample.

### 9.3.1.3. Hydrogen Peroxide Protocol

#### Chemicals

1. Hydrogen Peroxide (30%)
2. Polyethylene glycol sorbitan monolaurate, or Polyoxyethylenesorbitan monolaurate (Tween 20) as a surfactant to aid in rinsing glassware and filters.

#### Procedure:

1. Two washing bottles are needed (Made of material that is not the polymers being investigated, Fluorinated ethylene propylene (FEP) was used in this case). One bottle is filled with ultrapure water, whereas the second is filled with ultrapure water with 0.1 % (v/v) of Tween 20. The surfactant bottle helps rinse particles off glass surfaces and the filter membrane.
2. The sludge sample is shaken well to ensure mixing and then 2 mL of sludge is taken with a pipette and placed in a suitable test tube or flask (45 mL). Then 20 mL of 30% Hydrogen peroxide solution or (**10:1 ratio**) is added
3. The test tube is sealed and placed in an oven at 60 °C for 24 ± 1 hours.

4. The tubes are removed from the oven, 10 mL of 0.1 % (v/v) Tween 20 is added to dilute the solution and stop further reactions as well as preventing microplastics from adhering to the glass walls of the tubes. Then the sample is filtered in a vacuum filtration unit with a PCTE, 0.2  $\mu\text{m}$  filter. The surfactant bottle can be used here to rinse the contents of the test tube into the filtration unit, as well as any particles adhering to the glass walls of the filtration unit.
5. The sample is ready for analysis. Alternatively, it can be stored as a suspension for later, where the same filter from step 4 can be washed down into a clean tube using the surfactant bottle and then stored for further analysis or filtration on a different kind of filter.

#### *9.3.1.4. Potassium hydroxide Protocol*

##### *Chemicals:*

1. Potassium hydroxide (10% W/W)
2. Polyethylene glycol sorbitan monolaurate, or Polyoxyethylenesorbitan monolaurate (Tween 20) as a surfactant to aid in rinsing glassware and filters.

##### *Procedure:*

Exactly the same as the hydrogen peroxide protocol

#### *1.5. Contamination mitigation and cleaning protocol*

##### *Material*

1. Polyethylene glycol sorbitan monolaurate, or Polyoxyethylenesorbitan monolaurate (Tween 20) as a surfactant to aid in rinsing glassware and filters.
2. Two Fluorinated ethylene propylene (FEP) washing bottles are used, one with ultrapure water containing 0.1 % Tween 20 (v/v) and the other with ultrapure water
3. Additives free washing liquid
4. Small plastic brush
5. Distilled or tap water at higher flow rates for rinsing

*Procedure:*

1. Using distilled water or tap water, the glassware should be rinsed under running water to remove the visible of the particles (especially if dried up contaminants are found).
2. Using washing liquid and the brush, one should clean the glassware and then rinse them under running water again to remove all visible contaminants.
3. The first and second steps can be eliminated if the glassware in question is free from visible contaminants
4. The final cleaning step uses the Tween 20 washing bottle where the glassware is washed with Tween 20 at least three times and then finally rinsed with the ultrapure water bottle.
5. The glassware can now either be used directly in the next sequence, or it can be dried in an oven at 100 °C and stored till needed.

*9.3.2. Polymers investigated and their characteristics*

*Table\_4.1\_Sl. 2. The reference (control) polymers used for the size distribution analysis.*

<b>Polymer</b>	<b>Mean diameter µm</b>	<b>D10 D(v,0.1) µm</b>
PA	146.9 ± 3.3	70.6 ± 3.4
PE	115.6 ± 4.4	45.7 ± 11.3
PET	130.9 ± 11.8	48.9 ± 11.4
PLA	110.7 ± 1.1	65.9 ± 3.2
PS	80.1 ± 1.6	33.2 ± 0.9
PP (KOH analysis)	334.7 ± N.A	105.6 ± N.A
PP (Rest)	190.5 ± 9.4	45.8 ± 6.5
PVC (H <sub>2</sub> O <sub>2</sub> analysis)	200.1 ± N.A	125.7 ± N.A

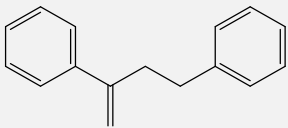
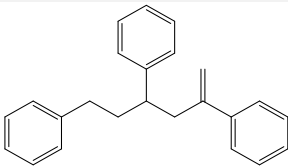

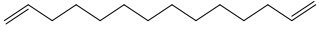
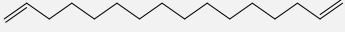
PVC (Rest)	118.8 ± 0.6	54.5 ± 1.8
------------	-------------	------------

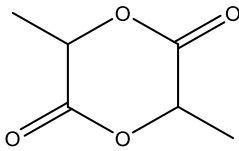
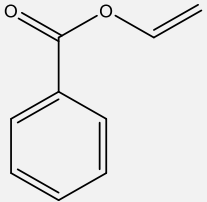
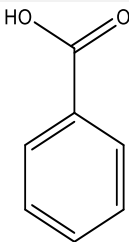
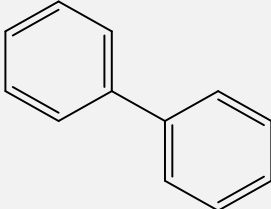
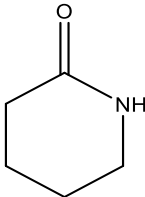
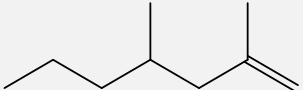
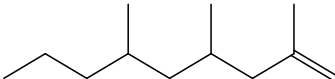
\* There were difficulties in manufacturing PP as well as PVC in the needed quantities. Therefore, two different sizes were used.

### 9.3.3. Results from TD-Pyr-GC-MS

The following characteristic pyrolysis products of the individual polymers were used for identification

Table\_4.1\_Sl. 3. Characteristic pyrolysis products of the selected polymers for identification.

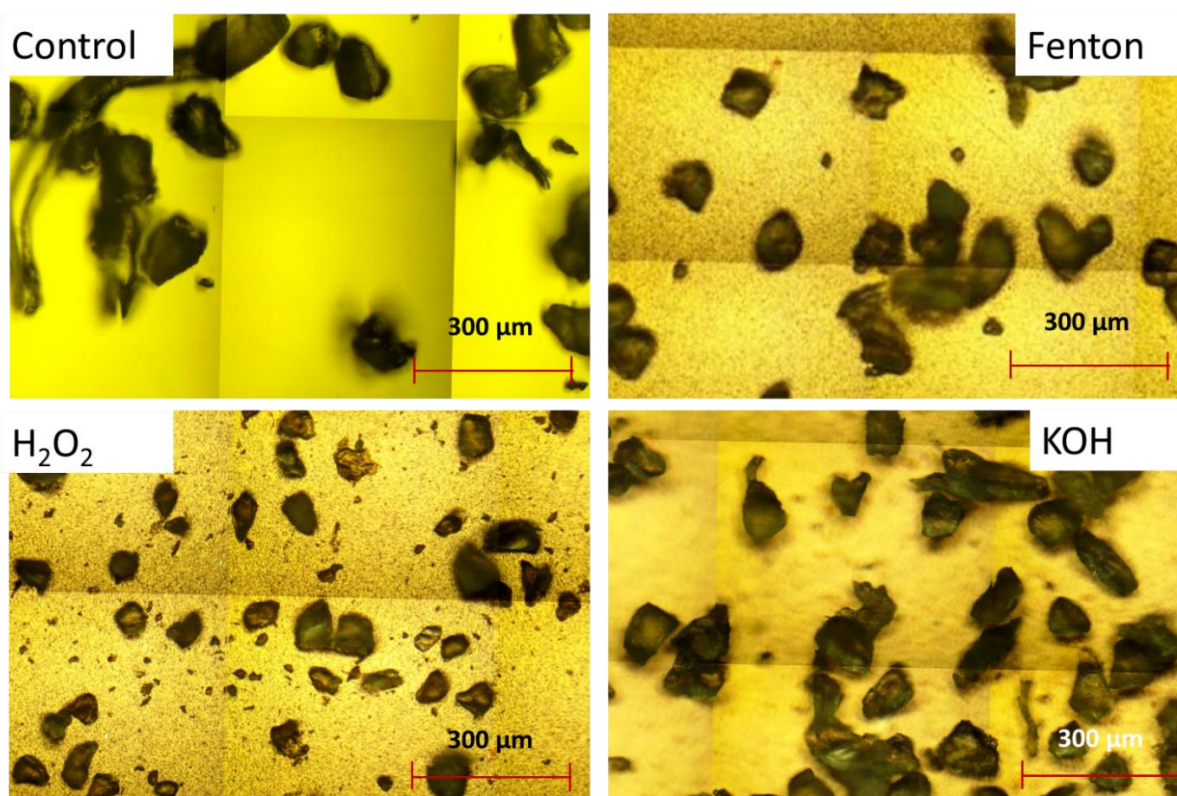
Polymer type	Characteristic pyrolysis products	Formula	m/z (intensity ratio)*	Structure
PS	3-butene-1,3-diyldibenzene (styrene dimer)	C <sub>16</sub> H <sub>16</sub>	91 (100), 104 (27), 130 (24), 208 (31)	
	5-hexene-1,3,5-triyltribenzene (styrene trimer)	C <sub>24</sub> H <sub>24</sub>	91 (95), 117 (31), 194 (19), 207 (27)	
PE	1,12-tridecadiene	C <sub>13</sub> H <sub>24</sub>	55 (52), 81 (44), 67 (38), 95 (26)	
	1,13-tetradecadiene	C <sub>14</sub> H <sub>26</sub>	81 (42), 95 (27), 109 (13)	
	1,15-hexadecadiene	C <sub>16</sub> H <sub>30</sub>	55 (63), 81 (50), 96 (45), 69 (37)	

PLA	Lactide	$C_6H_8O_4$	28(75), 45(34), 56(100), 144(1)	
	Vinyl benzoate	$C_9H_8O_2$	51 (15), 77(62), 105(100)	
PET	Benzoic acid	$C_7H_6O_2$	51(18), 77(57), 105(100), 122(99),	
	1,1-Biphenyl	$C_{12}H_{10}$	28 (100), 76 (12), 154(92)	
PA	Caprolactam	$C_6H_{11}NO$	55 (79), 67 (11), 85 (61), 113 (100)	
	2,4-Dimethylhept-1-ene	$C_9H_{18}$	43 (97), 70 (100), 83 (27), 126 (18)	
PP	2,4,6-trimethyl-1-nonene	$C_{12}H_{24}$	28 (100), 43 (59), 69 (88), 111 (33), 125 (13)	

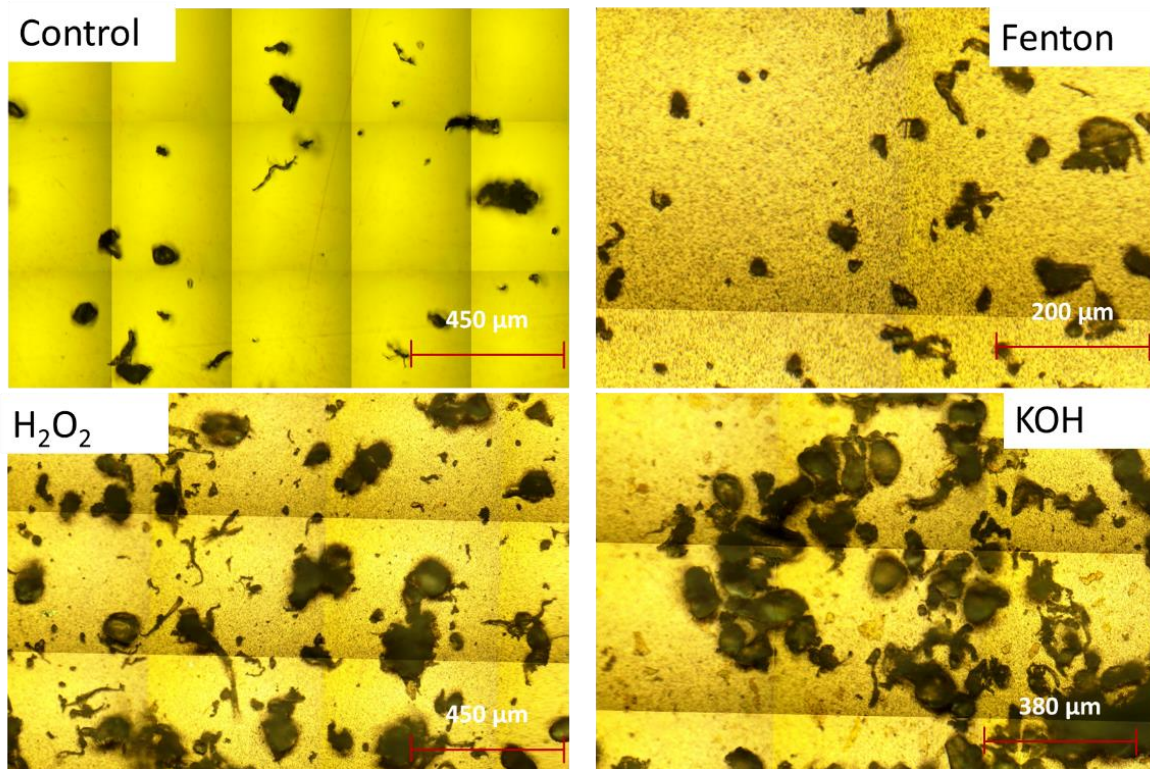
\* Intensity ratio to largest peak in spectra [%]

#### 9.3.4. Images from microscopy

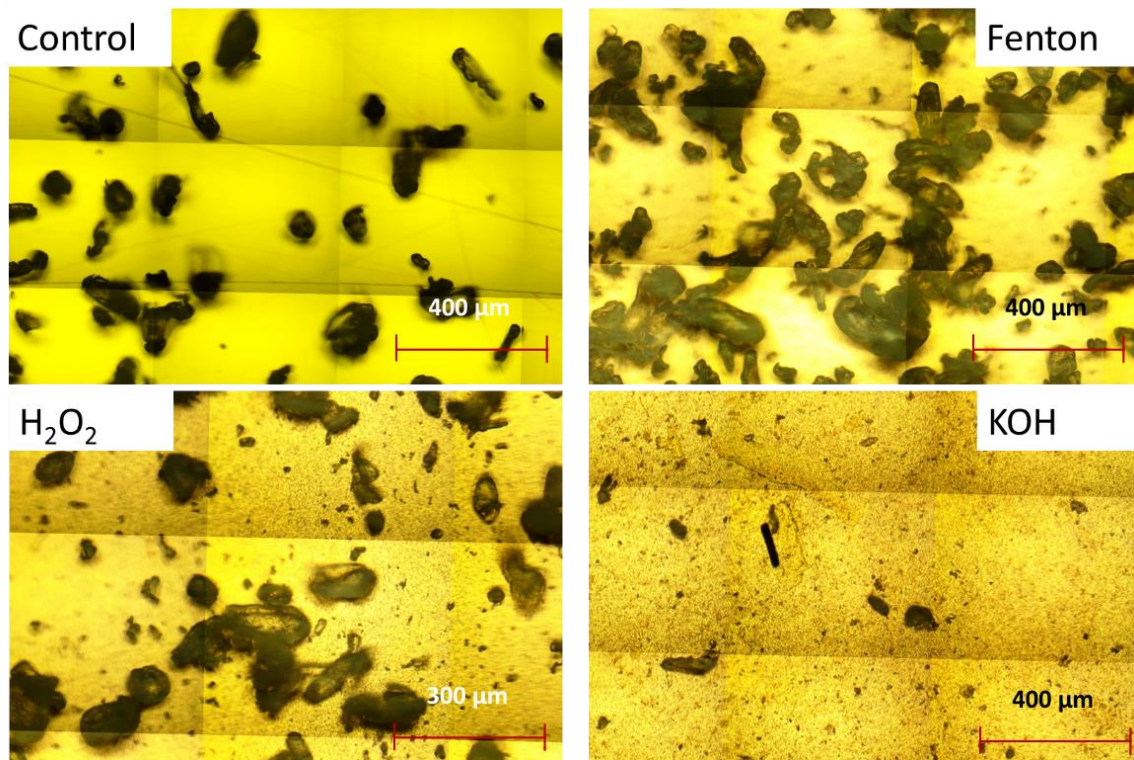
Some of the polymers (especially larger ones like PP) were highly irregularly shaped and determining their sizes only relying on image analysis, especially based on a small number of particles, would be highly error prone. Therefore, this section is meant to only visualize the surface of the particles before and after treatment. For size alterations, please refer to the size distribution analysis.



Figure\_4.1\_Sl. 2. PA: Microscopic images.

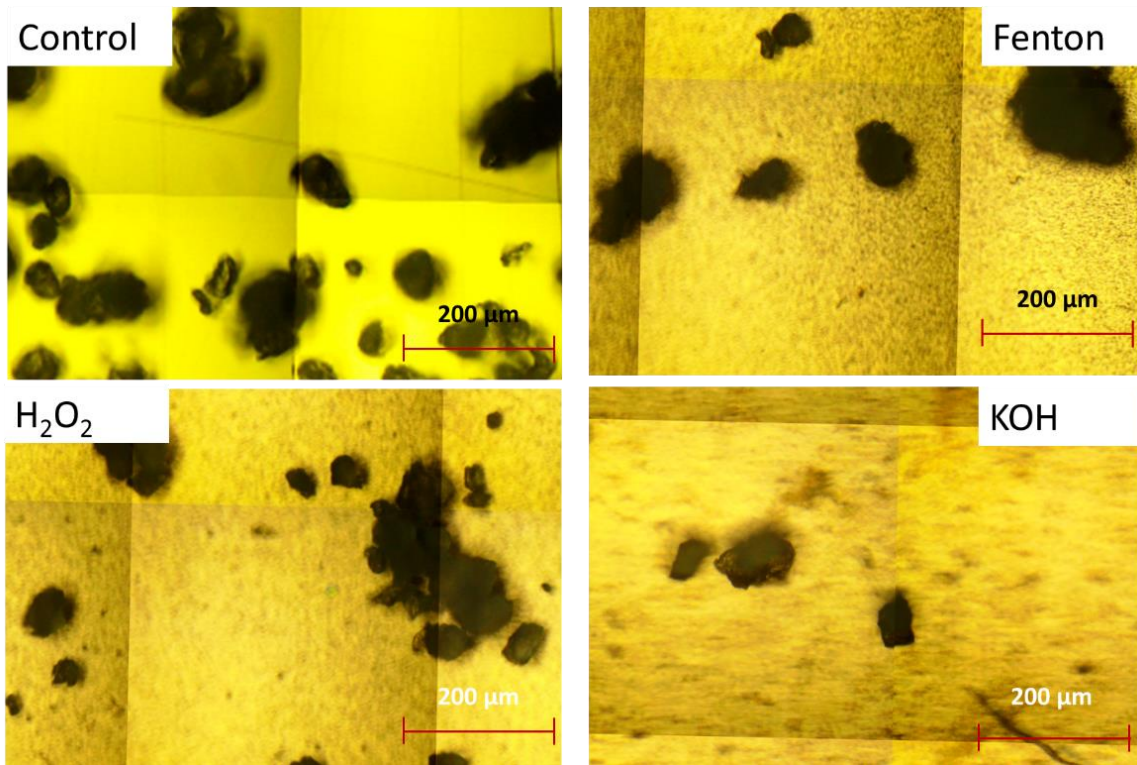


Figure\_4.1\_Sl. 3. PE: Microscopic images

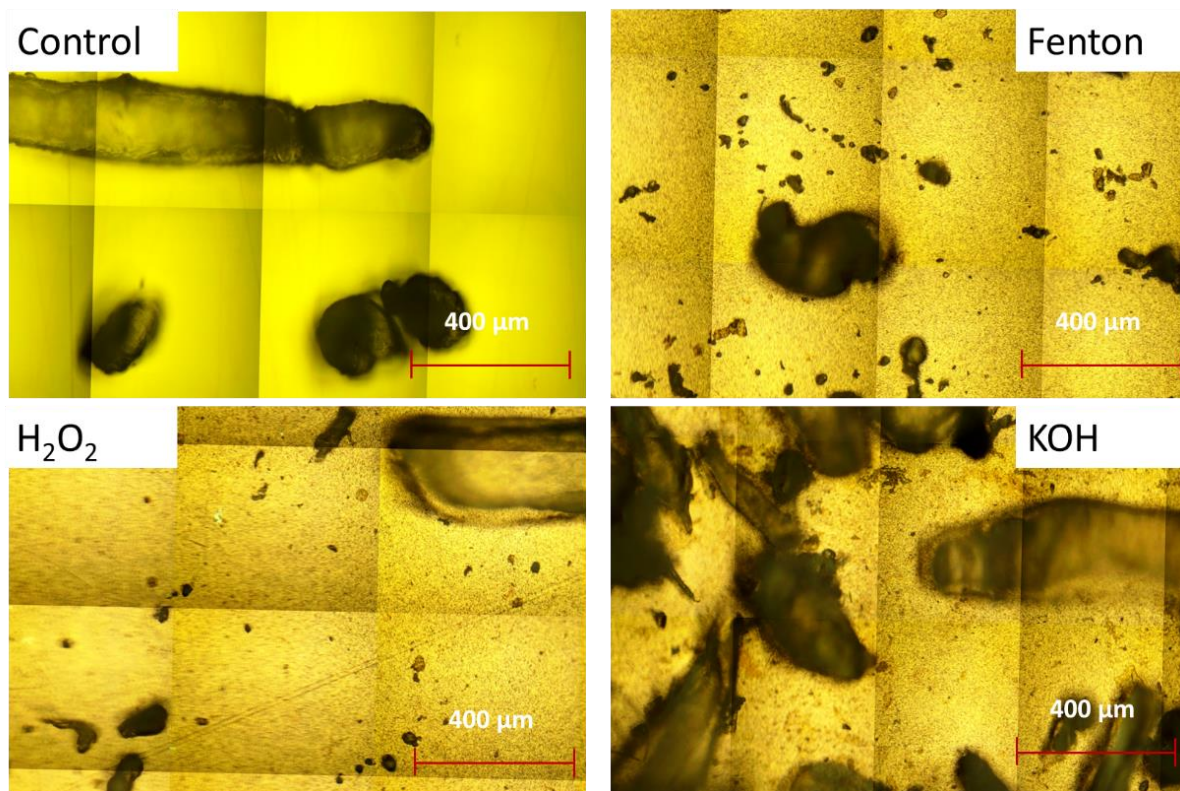


Figure\_4.1\_Sl. 4. PET: Microscopic images. Most of the particles were destroyed after KOH treatment.

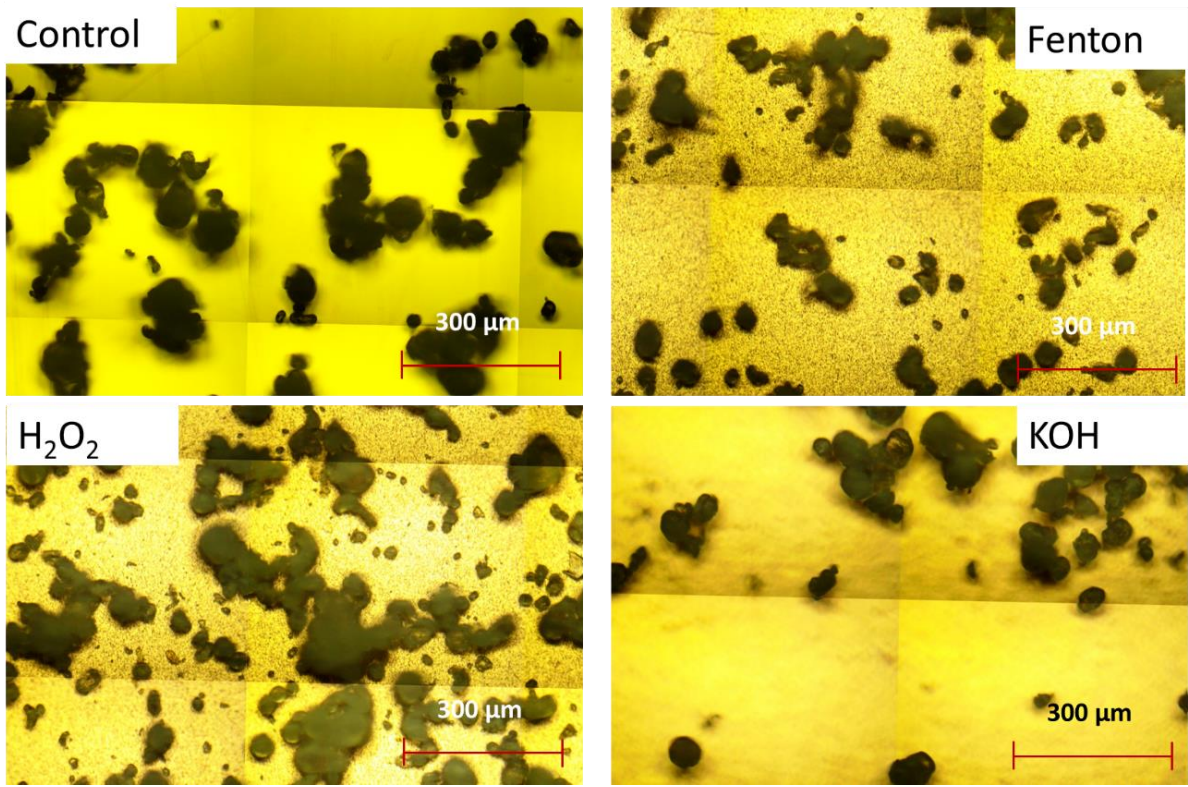




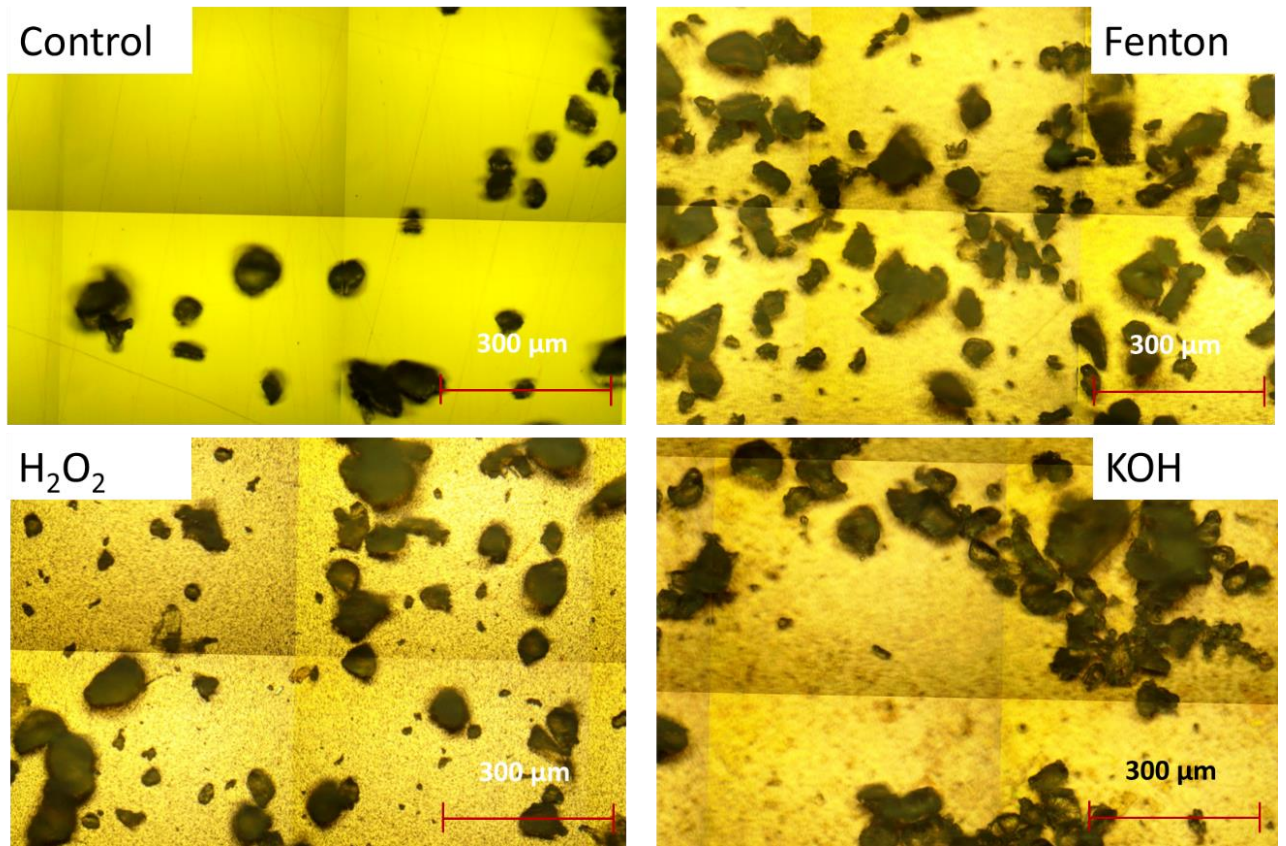
Figure\_4.1\_Sl. 5. PLA: Microscopic images. Most of the particles were destroyed after KOH treatment.



Figure\_4.1\_Sl. 6. PP: Microscopic images.

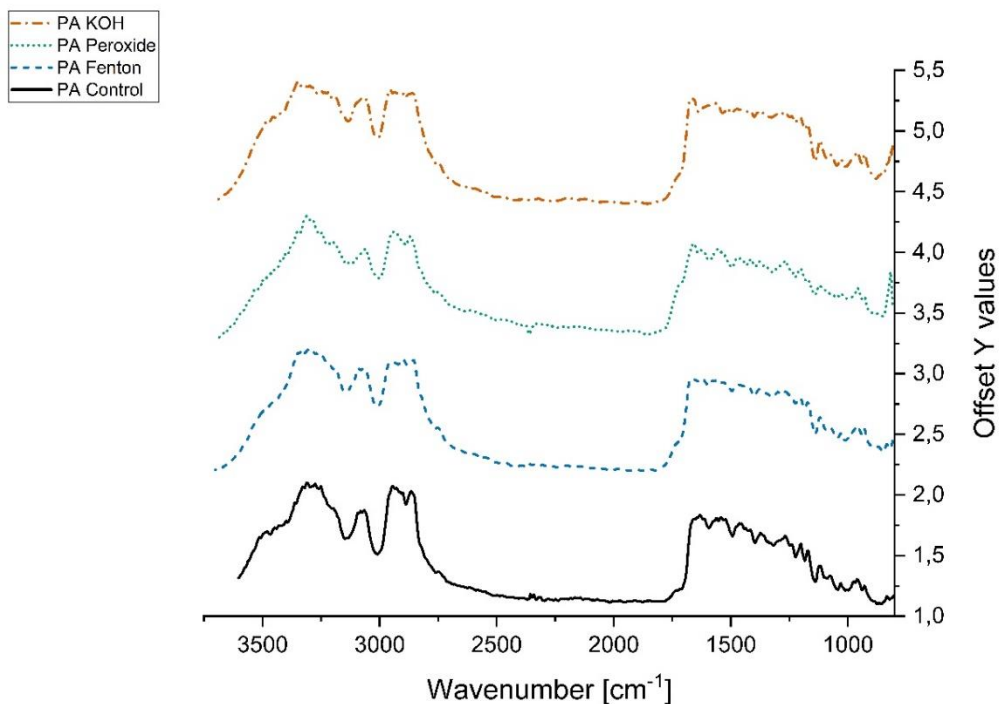


Figure\_4.1\_SI. 7. PS: Microscopic images.

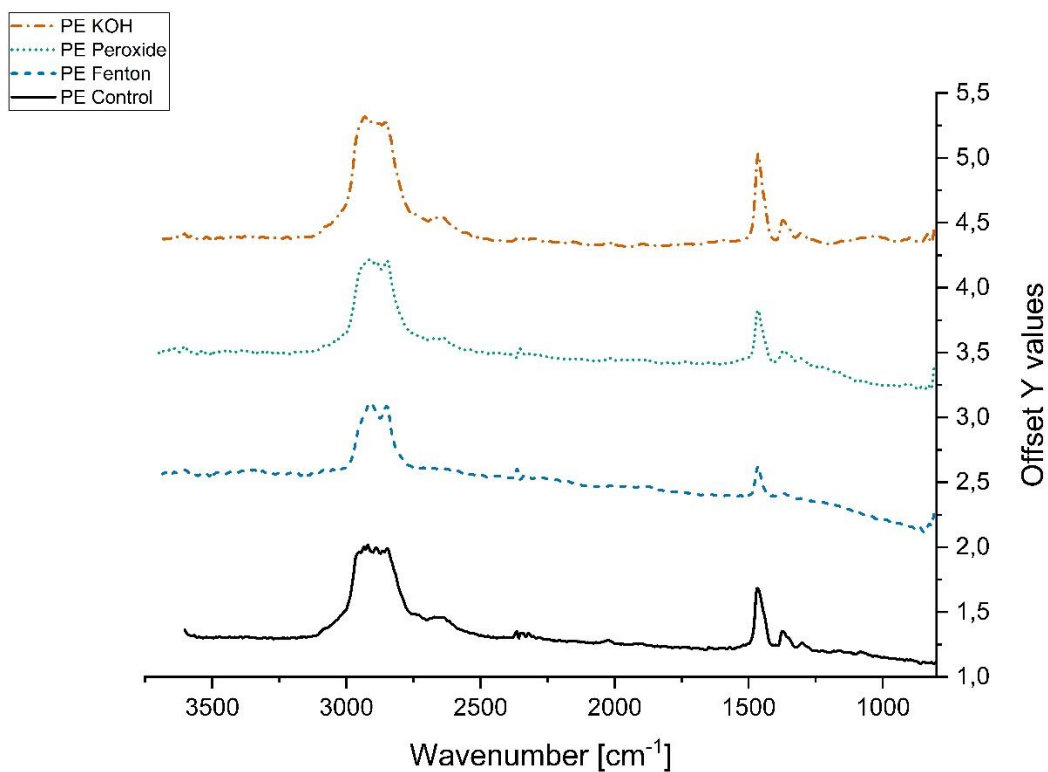


Figure\_4.1\_SI. 8. PVC: Microscopic images.

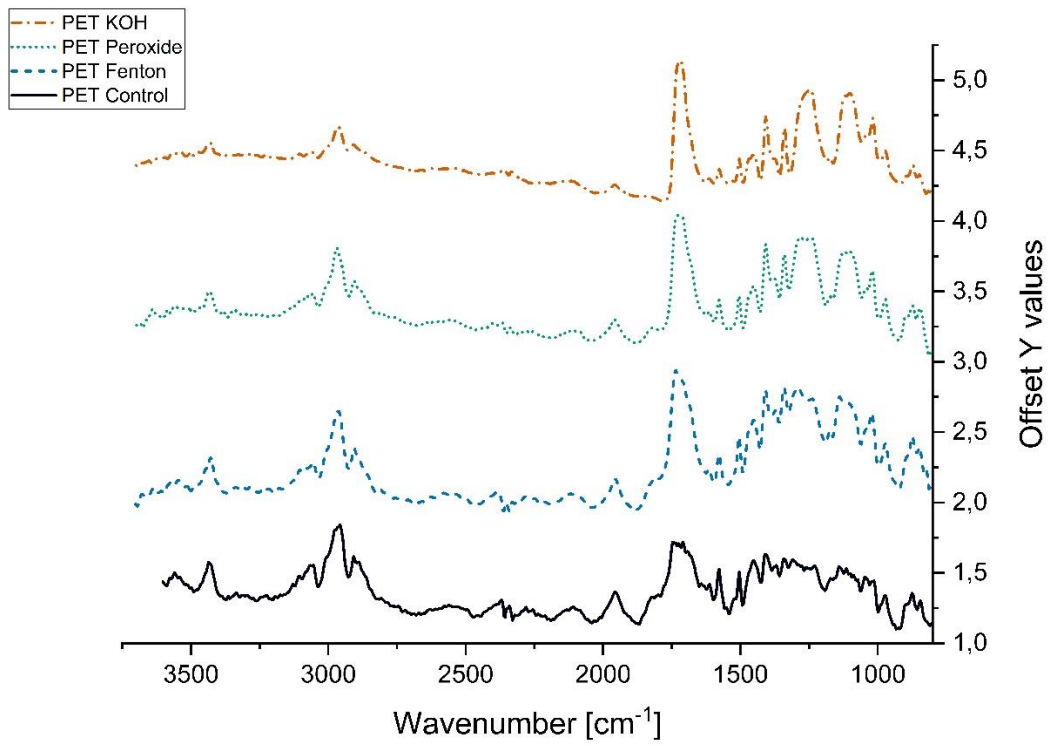
### 9.3.5. $\mu$ FTIR spectra before and after chemical treatments



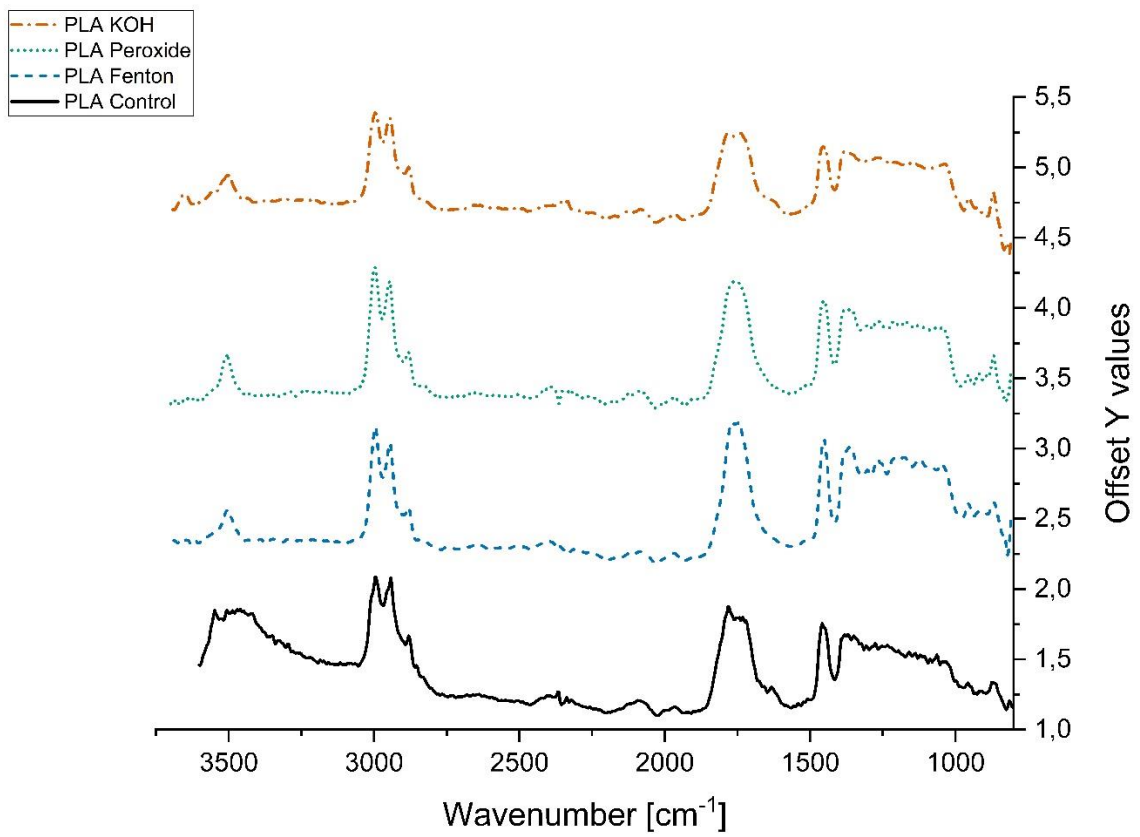
Figure\_4.1\_SI. 9.  $\mu$ FTIR Spectra of PA.



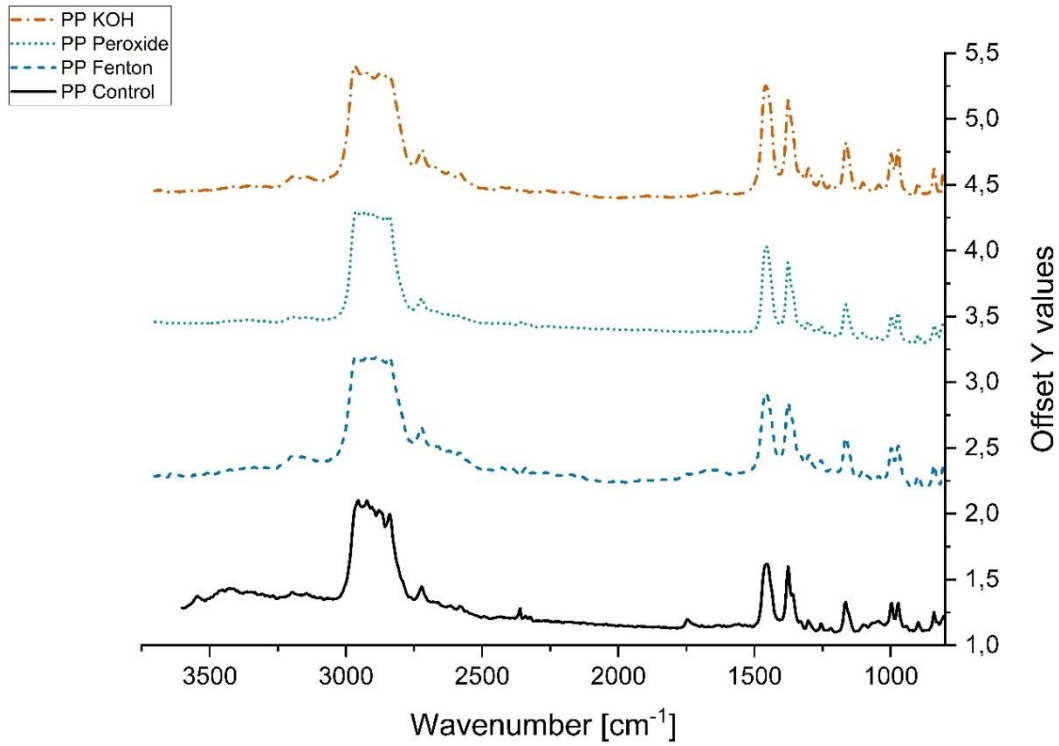
Figure\_4.1\_SI. 10.  $\mu$ FTIR Spectra of PE.



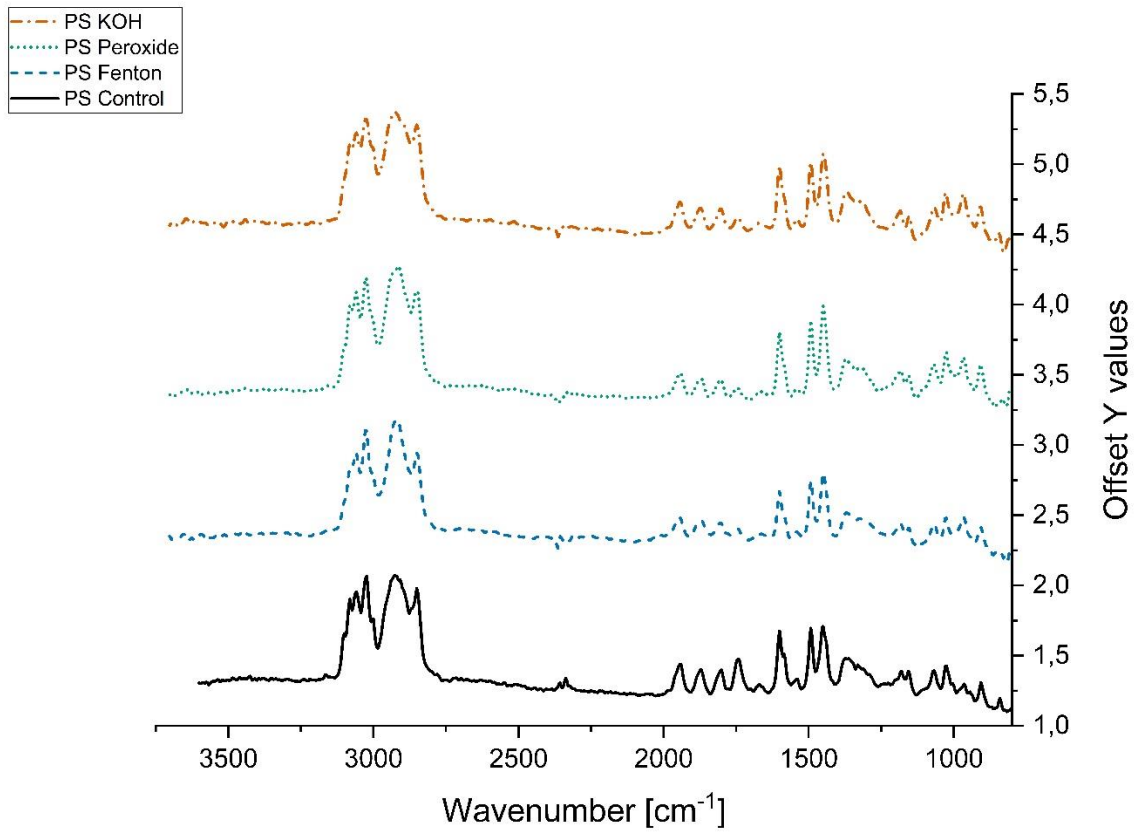
Figure\_4.1\_Sl. 11.  $\mu$ FTIR Spectra of PET.



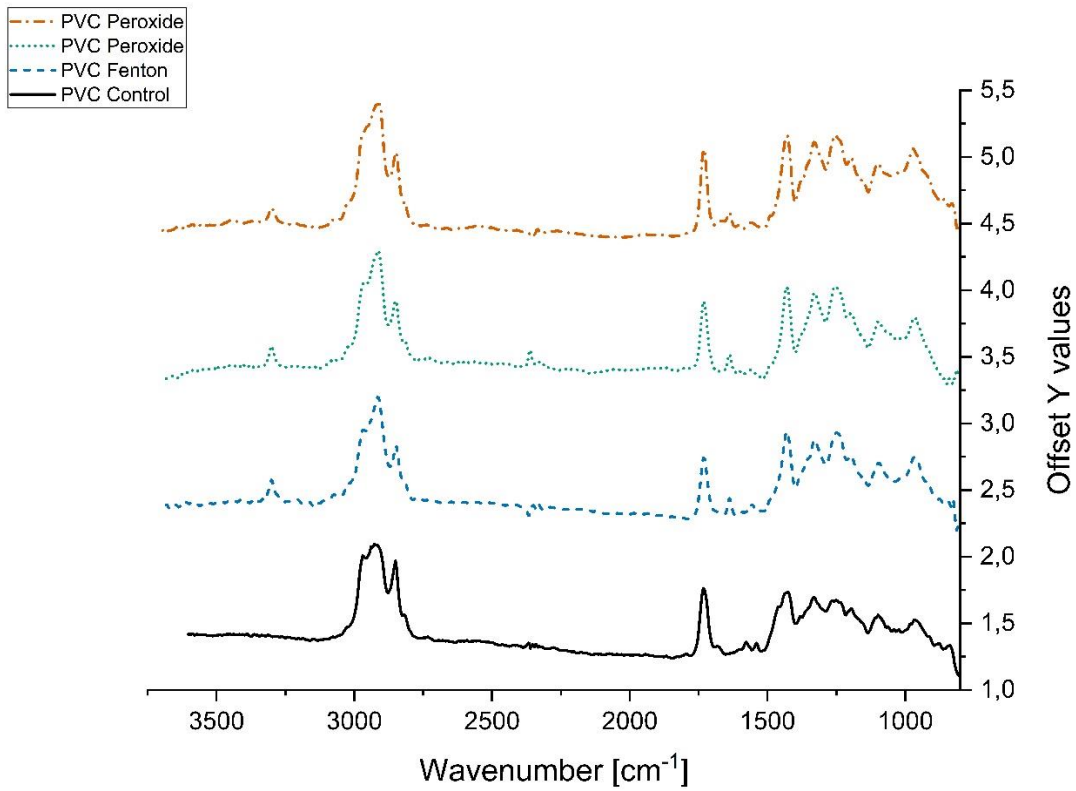
Figure\_4.1\_Sl. 12.  $\mu$ FTIR Spectra of PLA.



Figure\_4.1\_Sl. 13. μFTIR Spectra of PP.

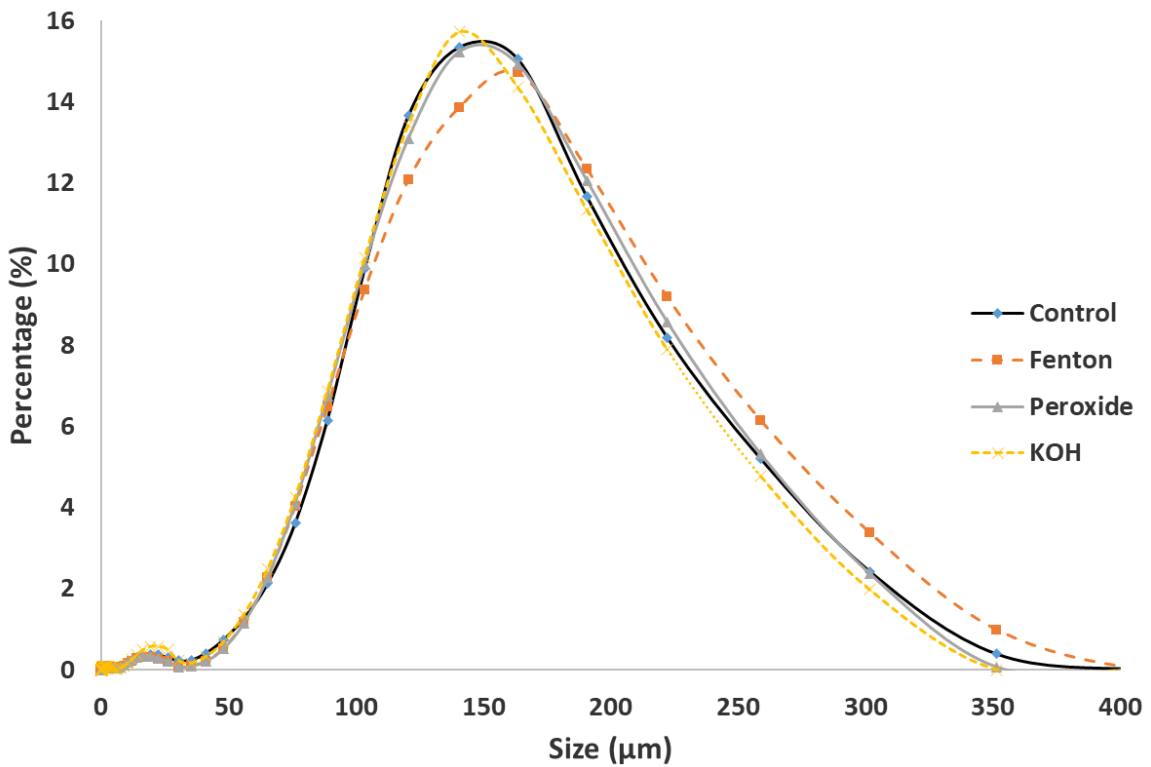


Figure\_4.1\_Sl. 14. μFTIR Spectra of PS.

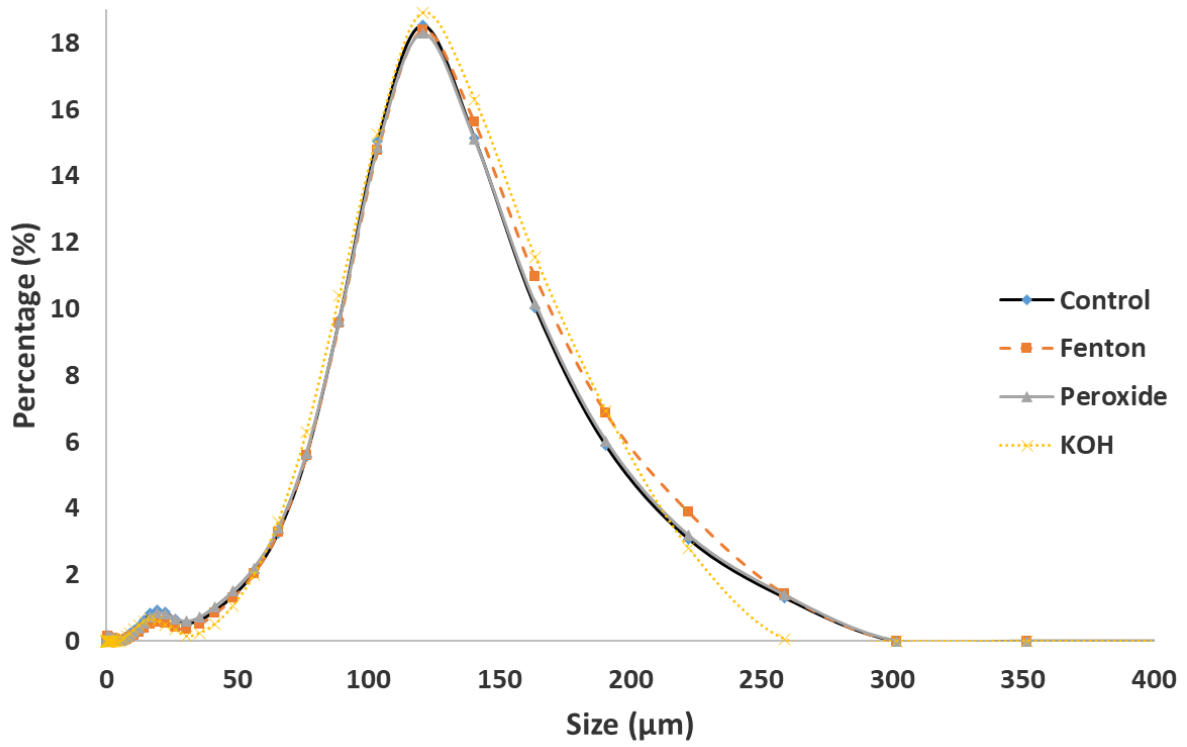


Figure\_4.1\_Sl. 15.  $\mu$ FTIR Spectra of PVC.

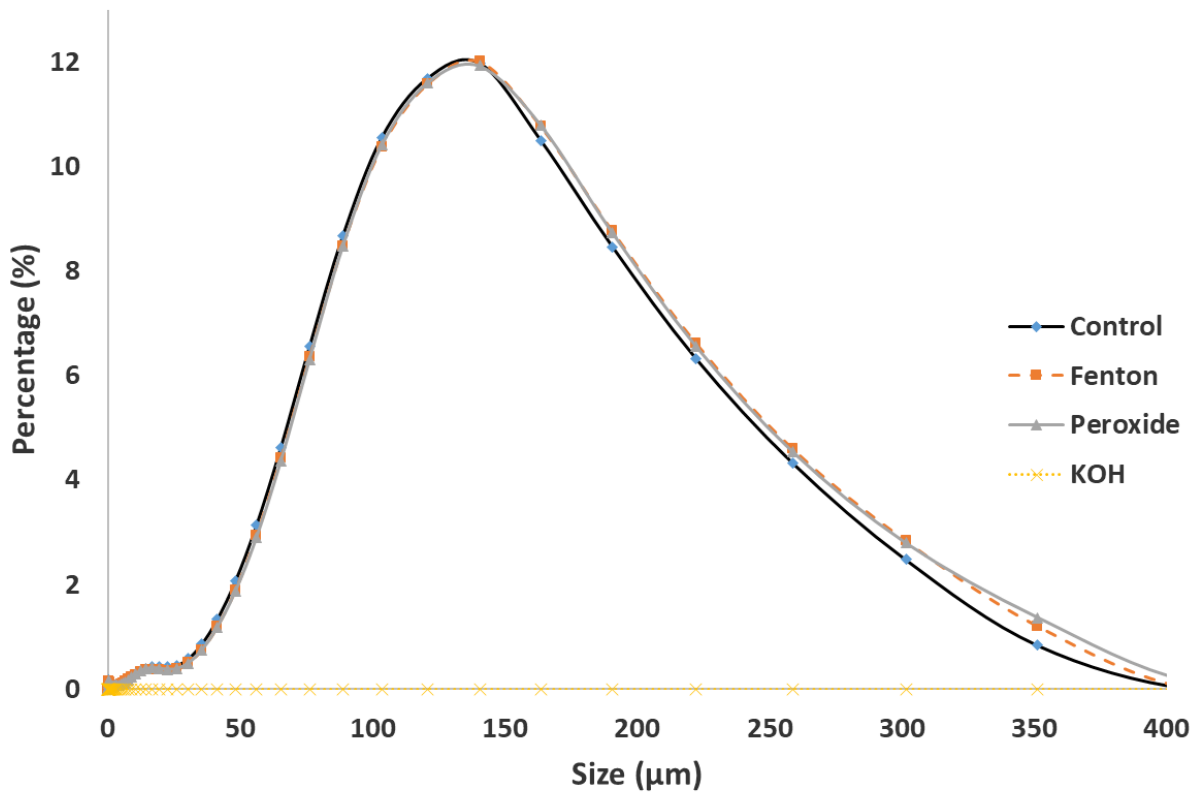
### 9.3.6. Size distribution analysis



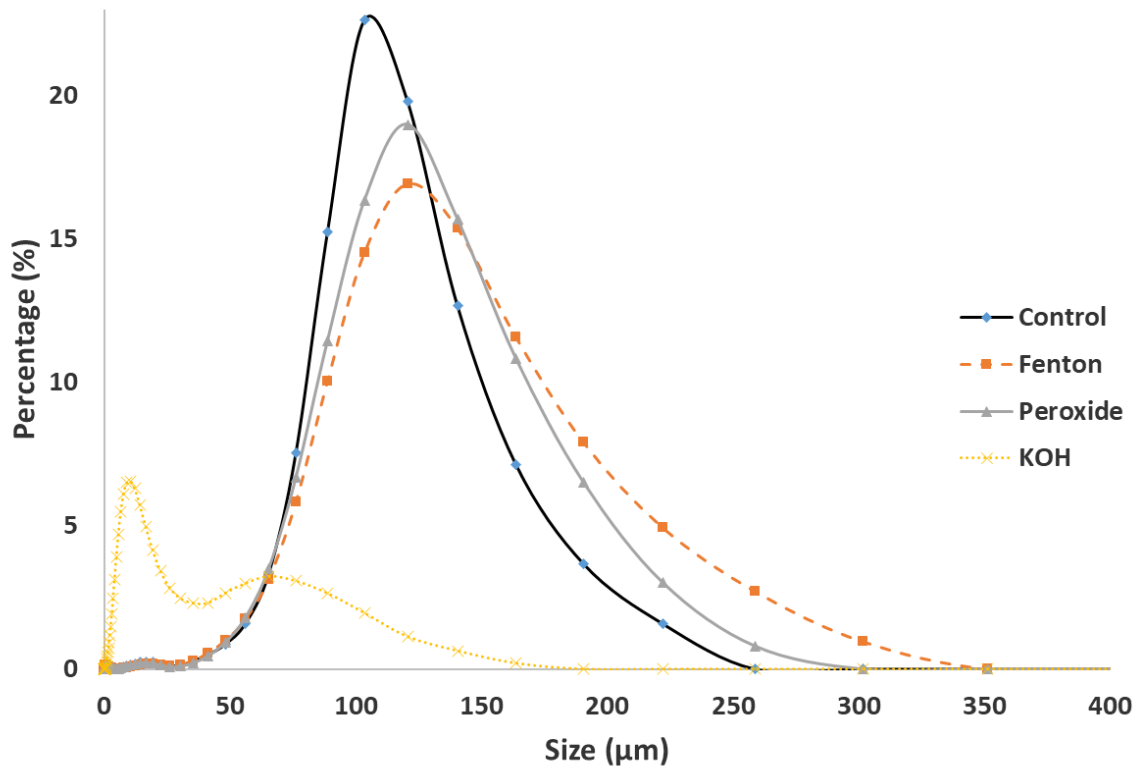
Figure\_4.1\_Sl. 16. Size distribution analysis (PA).



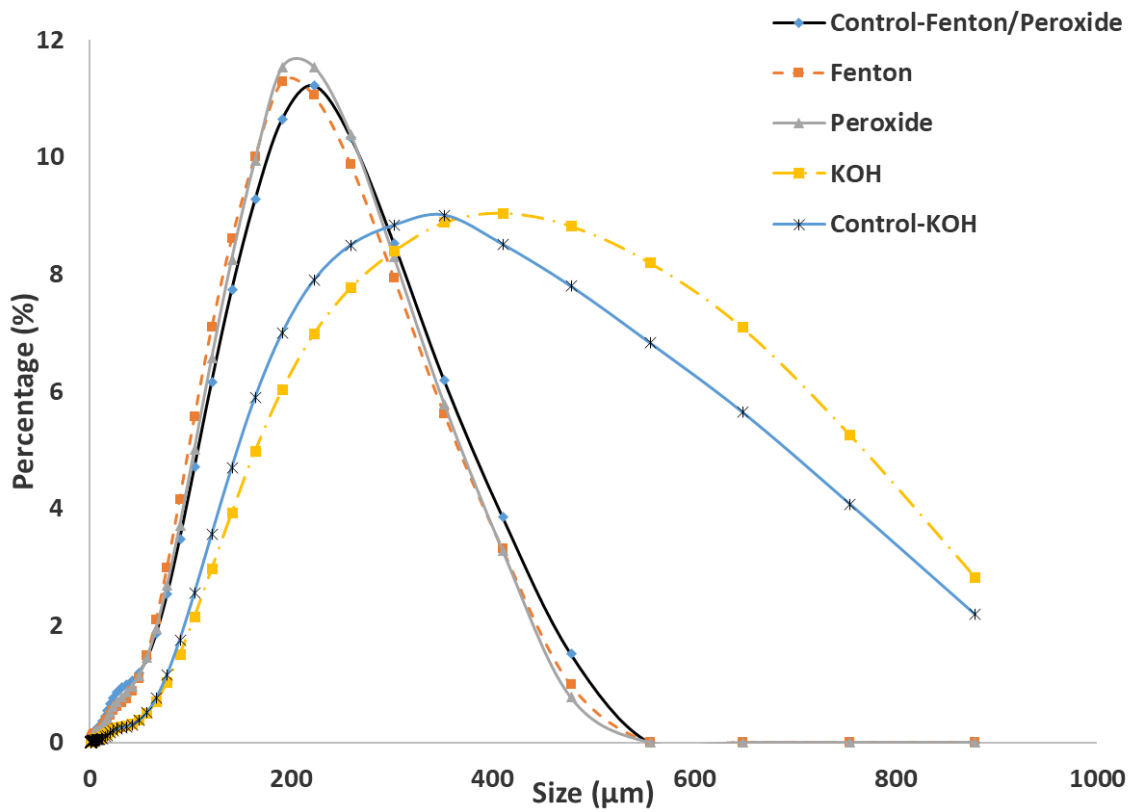
Figure\_4.1\_Sl. 17. Size distribution analysis (PE).



Figure\_4.1\_Sl. 18. Size distribution analysis (PET). KOH completely dissolved the particles during the tests.

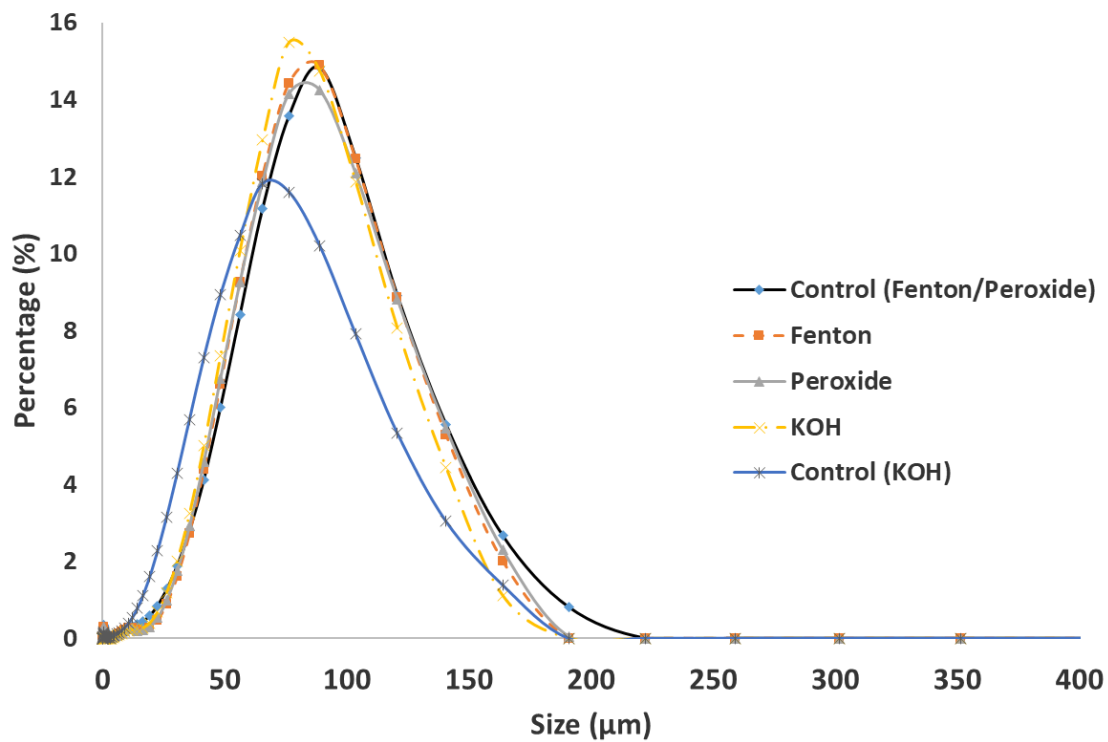


Figure\_4.1\_SI. 19. Size distribution analysis (PLA). KOH completely dissolved the particles during the tests.

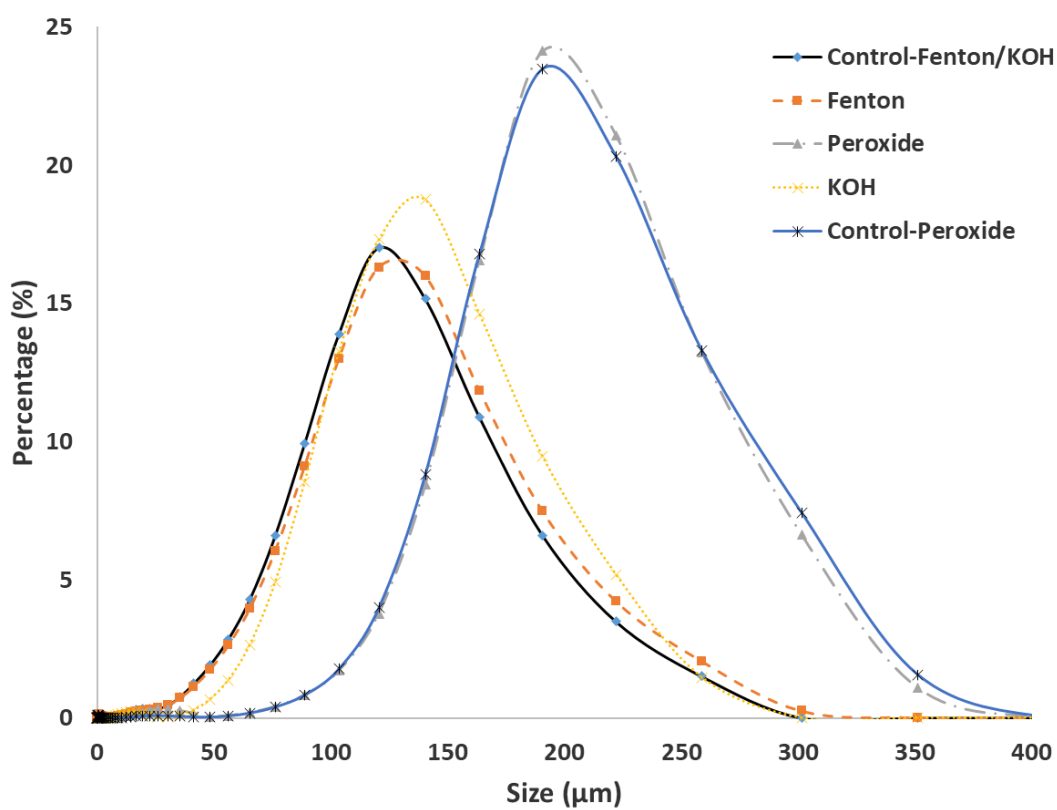


Figure\_4.1\_SI. 20. Size distribution analysis (PP). KOH tests were made with a different particle size due to manufacturing difficulties of the microplastics in the needed quantities.





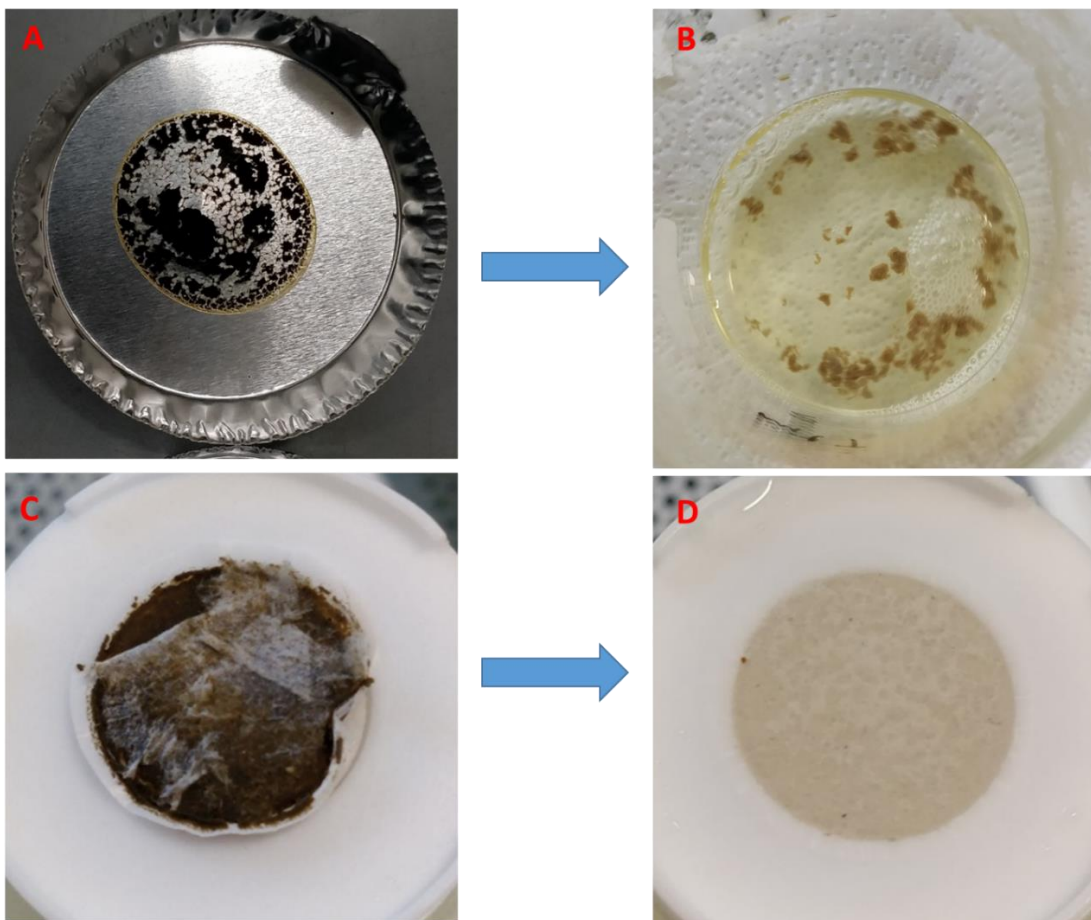
Figure\_4.1\_SI. 21. Size distribution analysis (PS). Tests made for KOH were made using a different batch of microplastics that was 18.3% smaller (mean size) than the controls used for Fenton/Peroxide



Figure\_4.1\_SI. 22. Size distribution analysis (PVC). Peroxide tests were made with a different particle size due to manufacturing difficulties of the microplastics in the needed quantities.

### 9.3.7. Pre-experiments of Organic matter removal efficiency

Figure\_4.1\_Sl. 23 shows how the sludge did not react very well with Fenton due to it being clumped after drying, resulting in very poor removal visually compared to undried samples.



Figure\_4.1\_Sl. 23. The visual difference between drying 1mL of sludge before treatment Vs. No drying. A: Dried sludge before Fenton's reaction. B: Dried sludge after Fenton's reaction. C: Wet sludge (filtered). D: Wet sludge after Fenton reaction.

## 9.4. Supplementary material for Chapter 4.2

### 9.4.1. Fenton Protocol

This Fenton protocol was first introduced by Al-Azzawi et al. [57].

Note: The used hydrogen peroxide must be tested to meet the requirements for Fenton Type I reaction, as defined by Al-Azzawi et al. [57]

#### *Procedure:*

1. Iron sulfate catalyst (20 g/L) is prepared with pH 3 via adding a few drops of 0.5 M sulfuric acid. The solution should be left to dissolve till it is colorless and clear.
2. The sample is placed in a 100 mL flask then 2 mL of the catalyst is added. Fenton reaction is started by adding 4 mL H<sub>2</sub>O<sub>2</sub>.
3. After the end of each minute, 1 mL H<sub>2</sub>O<sub>2</sub> is added till t=10 min. This is followed by 10 min cooling time.
4. After 10 minutes cooling, **0.8** mL of concentrated sulfuric acid (98 %) is added. This helps to dissolve the precipitated iron particles to facilitate analysis. To avoid prolonged contact with the acid, the flask is hand stirred for 30 seconds then quickly filtered.
5. The filter is then rinsed with 100 mL ultrapure water (UPW) to remove remaining acid.
6. Filter is then ready for analysis under the microscope, the filter is removed via tweezers and placed on a wetted glass slide. A cover slip is placed on top and affixed on both end via sticky tape to prevent movement and to flatten the filter for easier analysis.

### 9.4.2. Exposure times used for fluorescence microscopy

Exposure times were selected to set a balance between not overblowing the highlights and keeping the background dark without reducing the intensity of the smallest particles in each sample. Since the brightness of the fluorescent particles depended on the type of polymer as well as the sample preparation method, the brightness

tended to vary widely between samples, thereby necessitating adjustments in the exposure time to normalize brightness across all samples. This may cause a measurement induced error as a result of imperfect normalization. As such, this was included in the error estimation measurement as described in the main paper.

*Table\_4.2.\_SI. 1. The chosen exposure time in order to normalize brightness between samples of the same polymer.*

<b>Sample</b>	<b>Exposure times [ms]</b>
PLA	Controls (5), Samples (75)
PET	Controls (5), Samples (20)
PVC	Controls (25), peroxide (50), Fenton (75)
PS	Controls (15), Peroxide (40), Fenton_1&2 (40), Fenton_3 (20)
PA	Controls (20), peroxide (60), Fenton (100)
PP	Controls (20), Peroxide & Fenton_1 (60), Fenton_2&3 (150)

#### *9.4.3. Thresholding the grey values for segmentation*

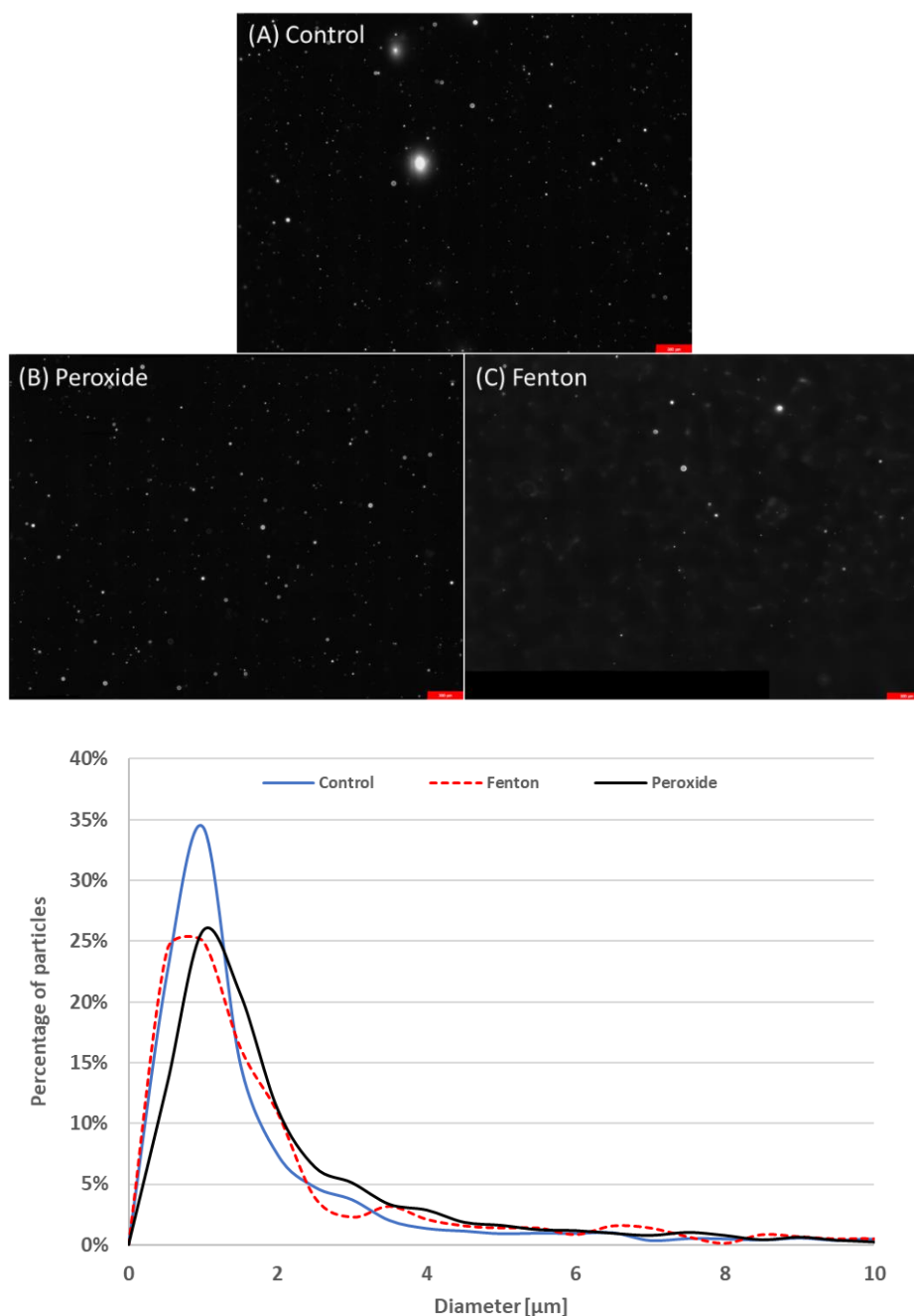
The following are the values used for automatic segmentation using the LASX software suite from Leica. The threshold values are left consistent across all samples per polymer in order to reduce variables.

*Table\_4.2.\_SI. 2. The selected threshold values for each polymer.*

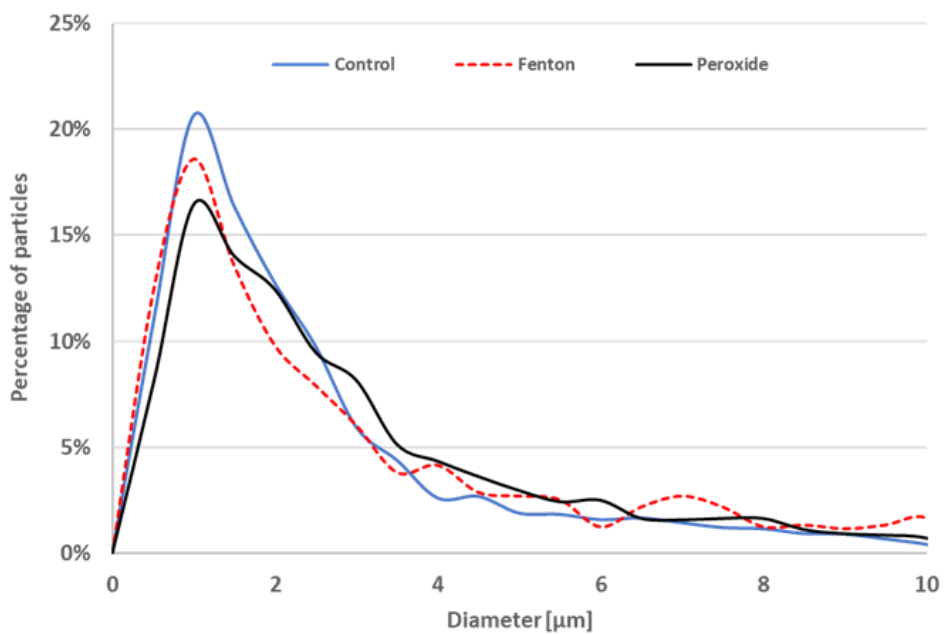
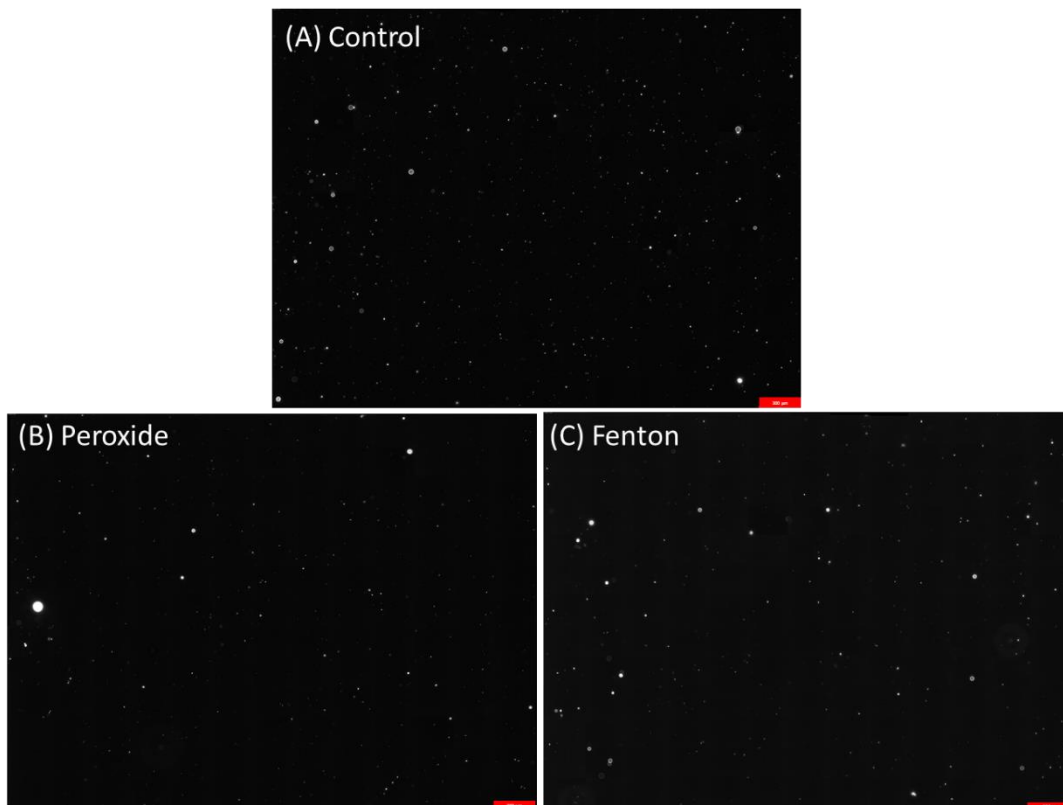
<b>Polymer</b>	<b>Thresholding (grey) value [-]</b>
PLA	$\geq 10,000$
PET	$\geq 20,000$
PVC	$\geq 20,000$
PS	$\geq 20,000$
PA	$\geq 20,000$
PP	$\geq 30,000$

#### 9.4.4. Fluorescence spectroscopy images and resulting size distributions

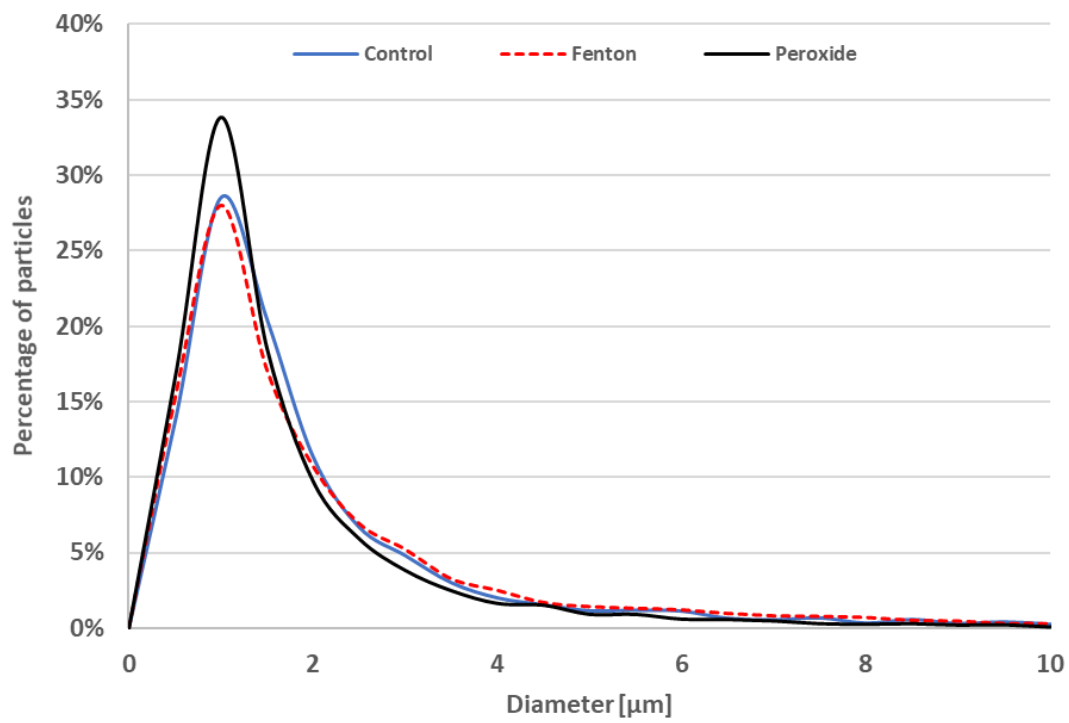
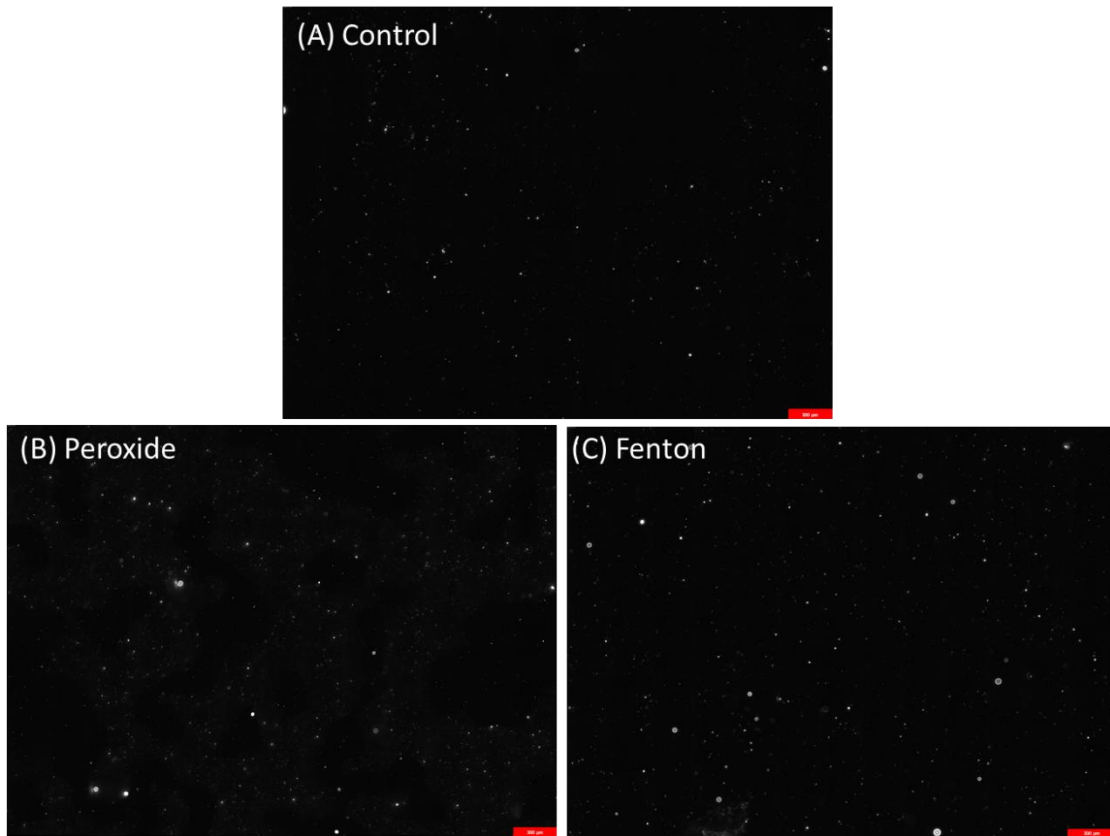
Below are example images from every polymer as well as a size distribution comparison of the combined results for each polymer type. Microplastics over 10  $\mu\text{m}$  were excluded from analyses due to their small numbers, uneven distribution amongst samples and large effect on the results.



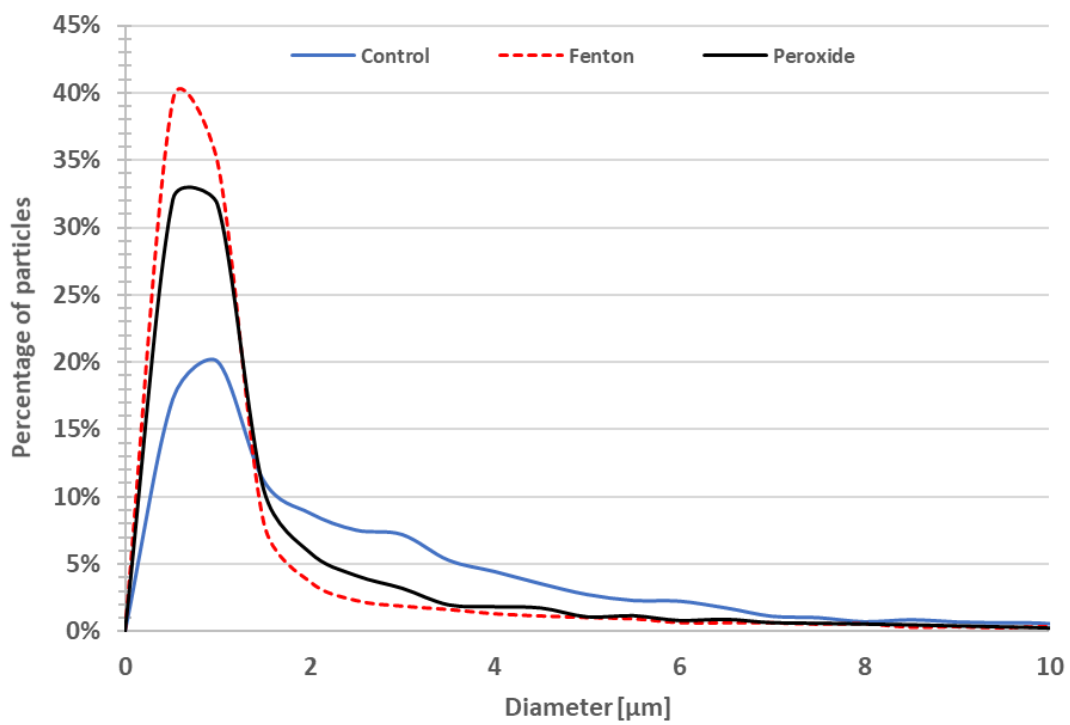
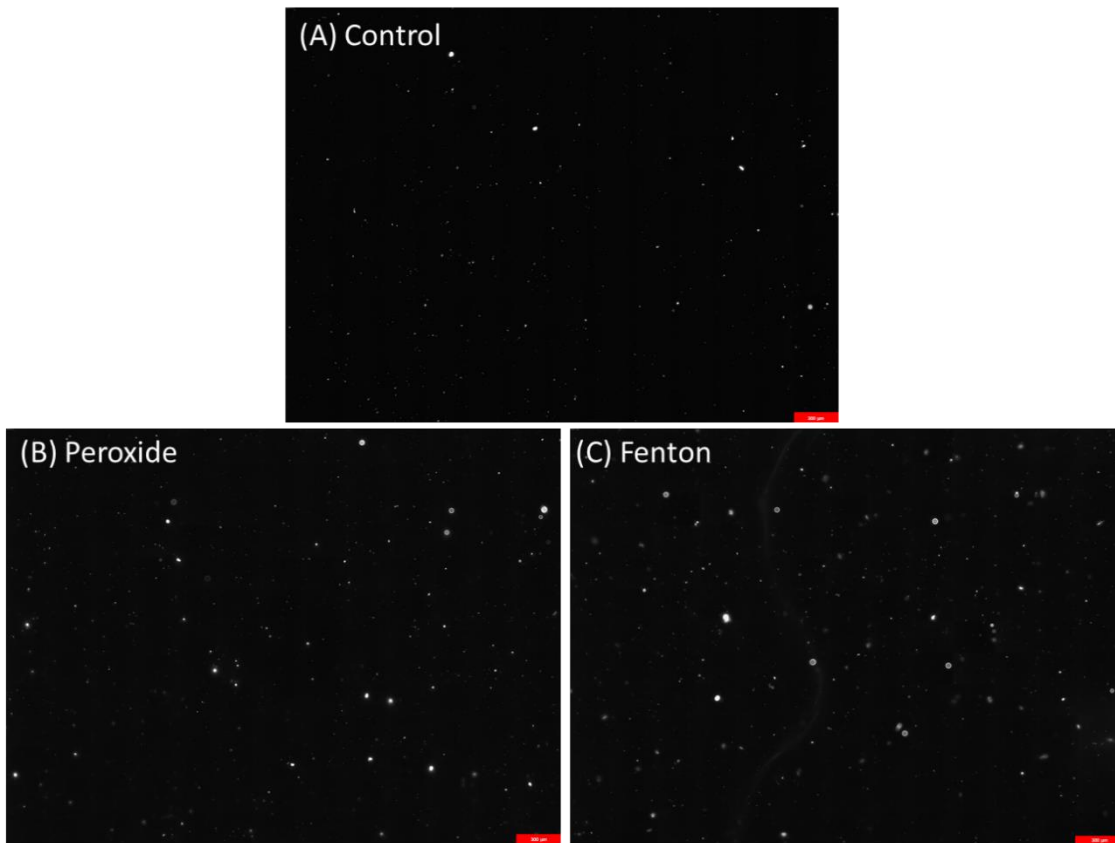
Figure\_4.2\_SI. 1. Above: Three samples of PP under the fluorescence microscope with x400 magnification. Fenton samples were so dim that the autofocus function of the microscope could not focus on small particles. Hence the cloudy appearance. The red scale bars represent 300  $\mu\text{m}$  in length. Below: Size distribution analysis for PP. The values are presented as a ratio to normalize the difference in particle count between the samples.



Figure\_4.2\_SI. 2. Above: Three samples of PA under the fluorescence microscope with x400 magnification. The red scale bars represent 300  $\mu\text{m}$  in length. Below: Size distribution analysis for PA. The values are presented as a ratio to normalize the difference in particle count between the samples.



Figure\_4.2\_SI. 3. Above: Three samples of PET under the fluorescence microscope with x400 magnification. The red scale bars represent 300  $\mu\text{m}$  in length. Below: Size distribution analysis for PET. The values are presented as a ratio to normalize the difference in particle count between the samples.



Figure\_4.2\_SI. 4. Above: Three samples of PLA under the fluorescence microscope with x400 magnification. The red scale bars represent 300  $\mu\text{m}$  in length. Below: Size distribution analysis for PLA. The values are presented as a ratio to normalize the difference in particle count between the samples.



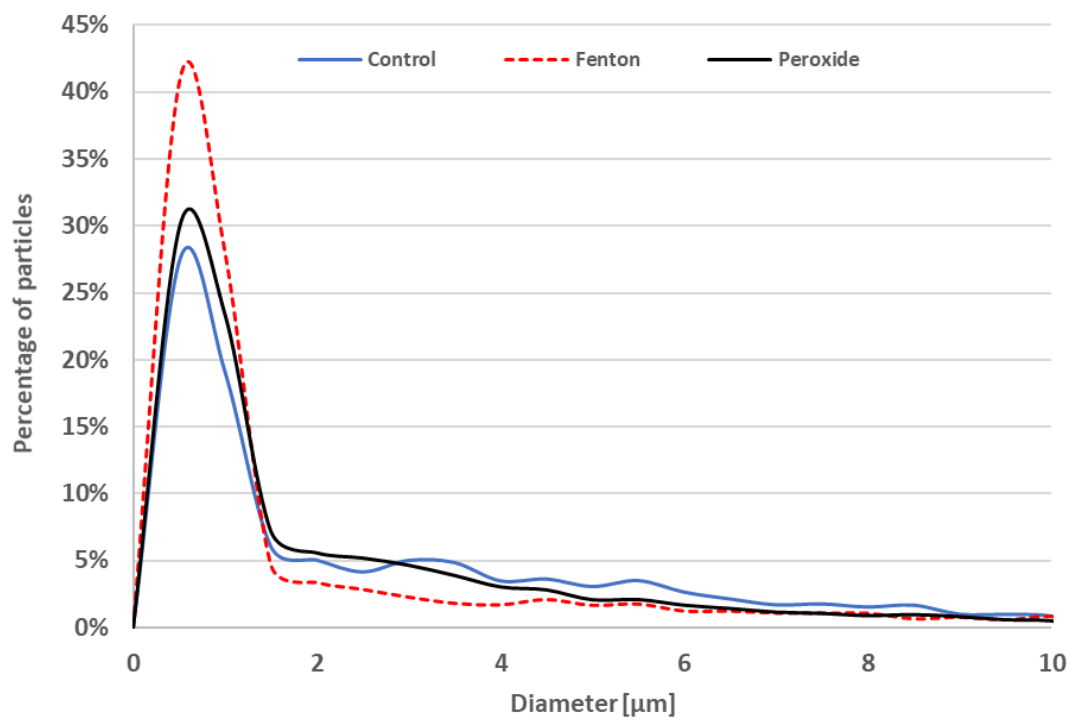
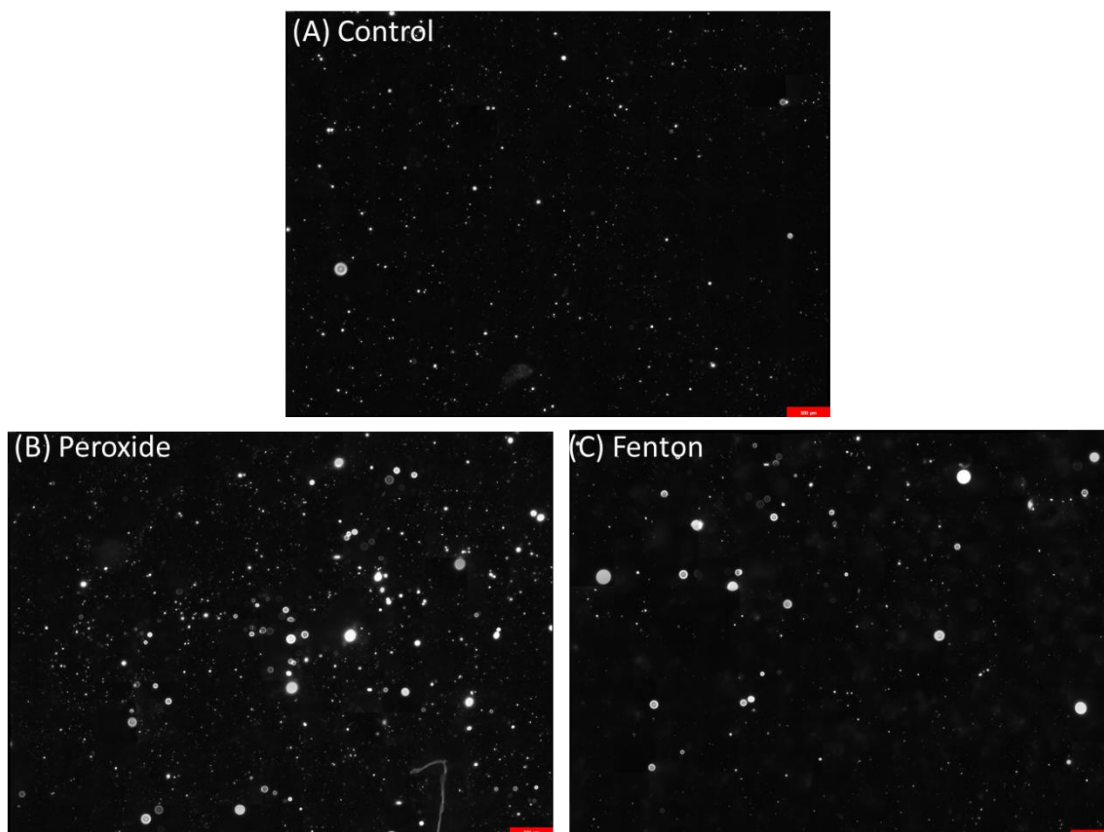
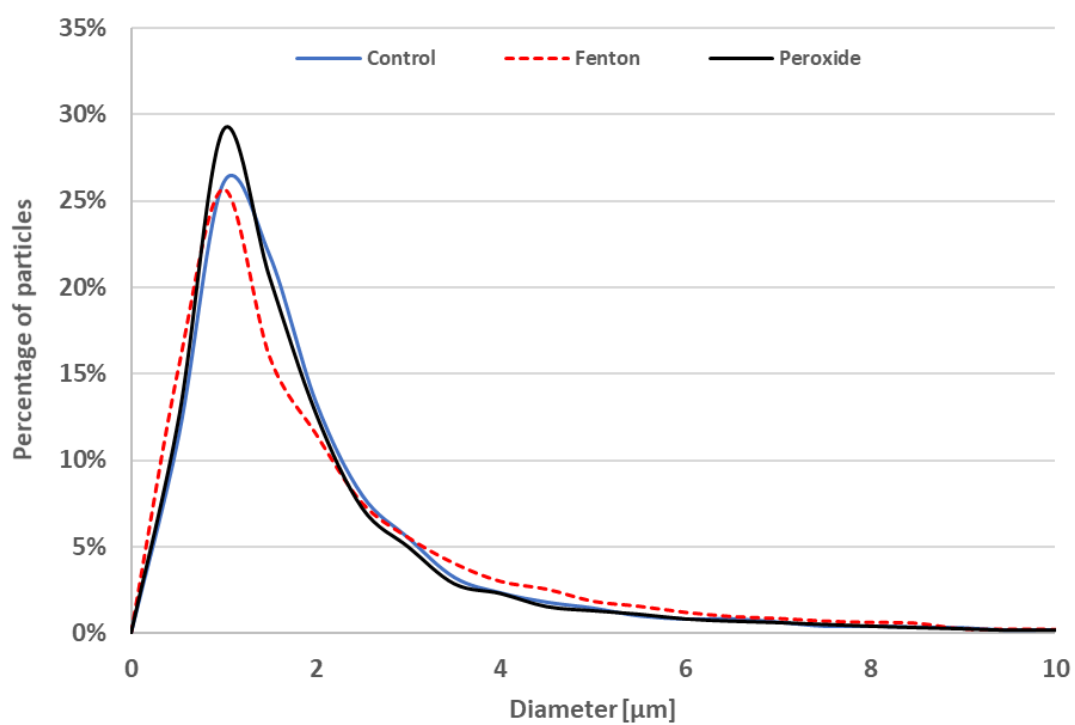
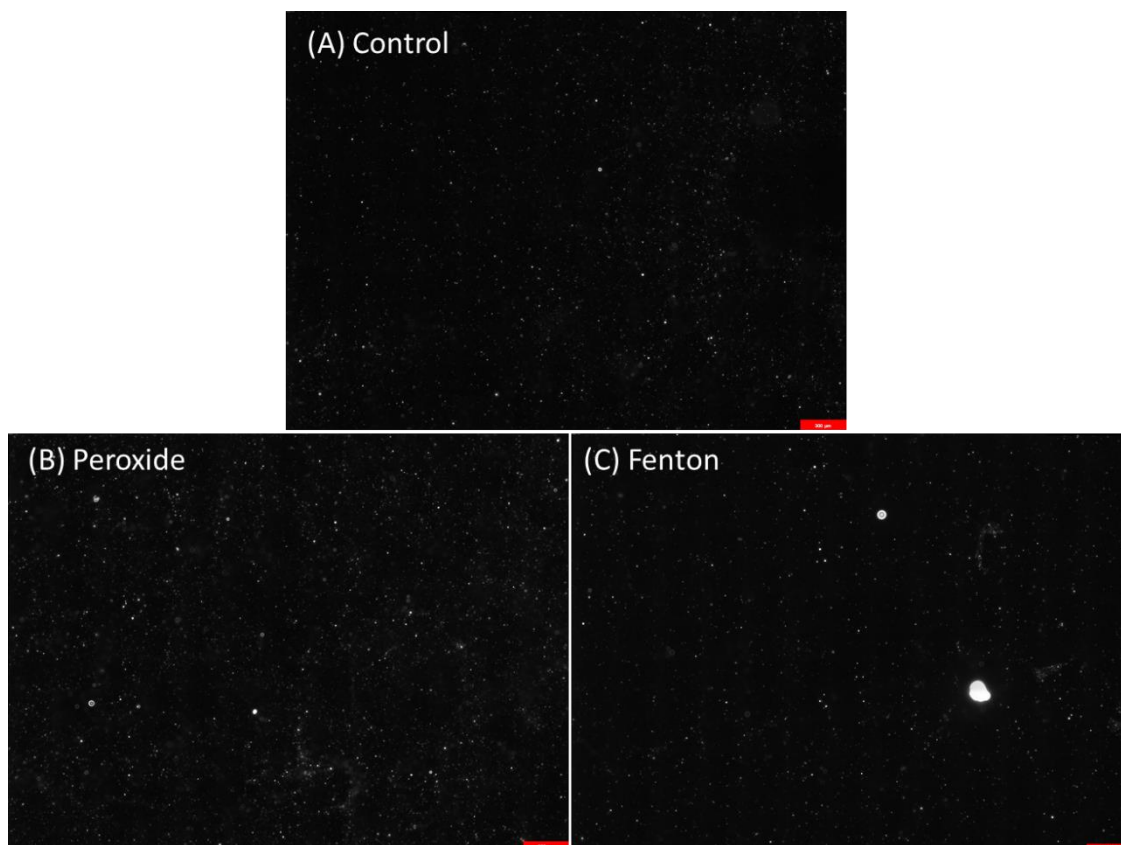


Figure 4.2 SI. 5. Above: Three samples of PS under the fluorescence microscope with x400 magnification. The red scale bars represent 300  $\mu\text{m}$  in length. Below: Size distribution analysis for PS. The values are presented as a ratio to normalize the difference in particle count between the samples.



Figure\_4.2\_SI. 6. Above: Three samples of PVC under the fluorescence microscope with x400 magnification. The red scale bars represent 300  $\mu\text{m}$  in length. Below: Size distribution analysis for PVC. The values are presented as a ratio to normalize the difference in particle count between the samples.

## 9.5. Supplementary Material for Chapter 5.1

### 9.5.1. Sampling campaign information

Table\_5.1\_Sl. 1. Sampling campaign conducted at WWTP A and B during 2019 and 2021. The volumes filtered through each respective basket filter size 100  $\mu\text{m}$ , 50  $\mu\text{m}$  and 10  $\mu\text{m}$  is given before the sand filter (B.S.F.) and after the sand filter (A.S.F.) for WWTP A and B. Additionally, the filtered volume from the effluent of the old sand filter cell (O.S.F. cell) and renewed sand filter cell (R.S.F. cell) of WWTP A are presented.

WWTP	Sampling site	Basket filter			Date
		100 $\mu\text{m}$	50 $\mu\text{m}$	10 $\mu\text{m}$	
A	B.S.F.	4.0 m <sup>3</sup>	4.0 m <sup>3</sup>	0.2 m <sup>3</sup>	05.08.19
	B.S.F.	3.1 m <sup>3</sup>	3.1 m <sup>3</sup>	0.2 m <sup>3</sup>	17.02.20
	B.S.F.	2.9 m <sup>3</sup>	2.9 m <sup>3</sup>	0.5 m <sup>3</sup>	13.04.21
	A.S.F.	7.0 m <sup>3</sup>	7.0 m <sup>3</sup>	0.3 m <sup>3</sup>	05.08.19
	A.S.F.	8.2 m <sup>3</sup>	8.2 m <sup>3</sup>	0.2 m <sup>3</sup>	17.02.20
	A.S.F.	6.4 m <sup>3</sup>	6.4 m <sup>3</sup>	0.8 m <sup>3</sup>	13.04.21
	O.S.F. cell	5.7 m <sup>3</sup>	5.7 m <sup>3</sup>	0.3 m <sup>3</sup>	18.02.19
	R.S.F. cell	6.1 m <sup>3</sup>	6.1 m <sup>3</sup>	0.5 m <sup>3</sup>	18.02.19
	B.S.F.	4.3 m <sup>3</sup>	4.3 m <sup>3</sup>	0.3 m <sup>3</sup>	20.02.20
B	A.S.F.	9.5 m <sup>3</sup>	9.5 m <sup>3</sup>	0.4 m <sup>3</sup>	20.02.20

### 9.5.2. Aliquot information

Table\_5.1\_Sl. 2. Extracted volumes from the 100  $\mu\text{m}$ , 50  $\mu\text{m}$  and 10  $\mu\text{m}$  basket filters from sample campaigns before the sand filter (B.S.F.) and after the sand filter (A.S.F.) for WWTP A. Additionally, the filtered volume from the effluent of the old sand filter cell (O.S.F. cell) and renewed sand filter cell (R.S.F. cell) of WWTP A are presented. Tween 20 solution ( $1 \text{ g L}^{-1}$ ) was used during extraction. Aliquot percentages for TED-GC-MS,  $\mu\text{FTIR}$  and  $\mu\text{Raman}$  analysis are respectively shown for each sample.

WWTP	Sampling Site	Sampling number	Extracted volumes [mL], (Aliquot [%])		
			100 $\mu\text{m}$	50 $\mu\text{m}$	10 $\mu\text{m}$
A	B.S.F.	1	175, (30) <sup>1</sup> (10) <sup>2</sup>	150, (30) <sup>1</sup> (10) <sup>2</sup>	165, (30) <sup>1</sup> (10) <sup>3</sup>
	B.S.F.	2	150, (30) <sup>1</sup> (10) <sup>2</sup>	165, (30) <sup>1</sup> (10) <sup>2</sup>	175, (30) <sup>1</sup>
	B.S.F.	3	100, (30) <sup>1</sup> , (30) <sup>2</sup>	100, (30) <sup>1</sup> , (30) <sup>2</sup>	100, (30) <sup>1</sup> , (30) <sup>2</sup>
	B.S.F.	Blanks 1	, (30) <sup>1</sup> (10) <sup>2</sup>	, (30) <sup>1</sup> (10) <sup>2</sup>	, (30) <sup>1</sup> (10) <sup>3</sup>
	B.S.F.	Blanks 2	100, (30) <sup>1</sup> (10) <sup>2</sup>	120, (30) <sup>1</sup> (10) <sup>2</sup>	125, (30) <sup>1</sup>
	B.S.F.	Blanks 3	100, (30) <sup>1</sup> , (30) <sup>2</sup>	100, (30) <sup>1</sup> , (30) <sup>2</sup>	100, (30) <sup>1</sup> , (30) <sup>2</sup>
	A.S.F.	1	, (30) <sup>1</sup> (10) <sup>2</sup>	, (30) <sup>1</sup> (10) <sup>2</sup>	, (30) <sup>1</sup> (10) <sup>3</sup>
	A.S.F.	2	275, (30) <sup>1</sup> (10) <sup>2</sup>	225, (30) <sup>1</sup> (10) <sup>2</sup>	225, (30) <sup>1</sup>
	A.S.F.	3	100, (30) <sup>1</sup> , (30) <sup>2</sup>	100, (30) <sup>1</sup> , (30) <sup>2</sup>	100, (30) <sup>1</sup> , (30) <sup>2</sup>
	A.S.F.	Blanks 1	, (30) <sup>1</sup> (10) <sup>2</sup>	, (30) <sup>1</sup> (10) <sup>2</sup>	, (30) <sup>1</sup> (10) <sup>3</sup>
	A.S.F.	Blanks 2	125, (30) <sup>1</sup> (10) <sup>2</sup>	150, (30) <sup>1</sup> (10) <sup>2</sup>	125, (30) <sup>1</sup>

<b>A</b>	A.S.F.	Blanks 3	100, (30) <sup>1</sup> , (30) <sup>2</sup>	100, (30) <sup>1</sup> , (30) <sup>2</sup>	100, (30) <sup>1</sup> , (30) <sup>2</sup>	(30) <sup>1</sup> ,
	O.S.F.	1	175, (30) <sup>1</sup> (10) <sup>2</sup>	125, (30) <sup>1</sup> (10) <sup>2</sup>	175, (30) <sup>1</sup> (10) <sup>3</sup>	(30) <sup>1</sup>
	O.S.F.	Blank 1	175, (30) <sup>1</sup> (10) <sup>2</sup>	175, (30) <sup>1</sup> (10) <sup>2</sup>	125, (30) <sup>1</sup> (10) <sup>3</sup>	(30) <sup>1</sup>
	R.S.F.	1	175, (30) <sup>1</sup> (10) <sup>2</sup>	175, (30) <sup>1</sup> (10) <sup>2</sup>	175, (30) <sup>1</sup> (10) <sup>3</sup>	(30) <sup>1</sup>
	R.S.F.	Blank 1	175, (30) <sup>1</sup> (10) <sup>2</sup>	175, (30) <sup>1</sup> (10) <sup>2</sup>	125, (30) <sup>1</sup> (10) <sup>3</sup>	(30) <sup>1</sup>

<sup>1</sup>TED-GC-MS aliquot; <sup>2</sup>μFTIR aliquot; <sup>3</sup>μRaman aliquot

*Table\_5.1\_Sl. 3. Extracted volumes from the 100 μm, 50 μm and 10 μm basket filters from sample campaigns before the sand filter (B.S.F.) and after the sand filter (A.S.F.) for WWTP B. Tween 20 solution (1 g L<sup>-1</sup>) was used during extraction. Aliquot percentages for TED-GC-MS, μFTIR and μRaman analysis are respectively shown for each sample.*

<b>WWTP</b>	<b>Sampling site</b>	<b>Sampling number</b>	<b>Extracted volumes [mL], (Aliquot [%])</b>		
			<b>100 μm</b>	<b>50 μm</b>	<b>10 μm</b>
<b>B</b>	B.S.F.	1	175, (30) <sup>1</sup> (10) <sup>2</sup>	150, (30) <sup>1</sup> (10) <sup>2</sup>	125, (30) <sup>1</sup>
	B.S.F.	Blank 1	125, (30) <sup>1</sup> (10) <sup>2</sup>	150, (30) <sup>1</sup> (10) <sup>2</sup>	125, (30) <sup>1</sup>
	A.S.F.	1	175, (30) <sup>1</sup> (10) <sup>2</sup>	175, (30) <sup>1</sup> (10) <sup>2</sup>	150, (30) <sup>1</sup>
	A.S.F.	Blank1	100, (30) <sup>1</sup> (10) <sup>2</sup>	75, (30) <sup>1</sup> (10) <sup>2</sup>	100, (30) <sup>1</sup>

<sup>1</sup>TED-GC-MS aliquot; <sup>2</sup>μFTIR aliquot; <sup>3</sup>μRaman aliquot

### 9.5.3. Sample preparation for spectroscopic analysis: Fenton

The sample preparation used here is a slightly modified version of the sample preparation protocol suggested by Al-Azzawi et al. (2020). It utilizes an extra step to reduce the water content of samples via filtration, and then extract them from the filters. Water content otherwise can interfere with the effectiveness of Fenton as a sample preparation step or prevent the reaction from reaching its critical temperature [57].

#### Chemical reagents needed:

1. H<sub>2</sub>O<sub>2</sub> (30%) stabilized, (Perhydrol®) EMSURE® ISO analytical reagent, Supelco® (Merck, Germany) (Other variants can be used as well as long as they meet the definition for Fenton Type I reaction, as defined in Al-Azzawi et al. (2020).
2. FeSO<sub>4</sub> x 7 H<sub>2</sub>O (20 g/L) (Merck, Germany)
3. Polyoxyethylenesorbitan monolaurate (Tween 20) (Merck, Germany).
4. Sulfuric acid (98%) and 0.5 M (VWR, Germany)

Note: K is as a scaling factor defined by Al-Azzawi et al. (2020). The **K** factor value used in this work was **10 mL**

#### Step by step procedure:

7. Preparation of catalyst (Iron sulfate) solution (20 g/L) should be prepared. pH is adjusted to 3 via 0.5 M sulfuric acid. The solution should be left to dissolve till it is colorless and clear.
8. The aliquot is filtered on a Whatman™ cellulose nitrate membrane filter (45 mm diameter, 0.2 μm pore size) (GE Healthcare Life Sciences, Chalfont ST Giles, GB). This is performed to remove most of the water content which as explained, can interfere with the reaction otherwise. The filter is then wiped against the glass walls of the reaction flask (at least 250 mL flask) with a clean finger (either using new nitrile gloves, or thoroughly rinsing bare finger with 0.1% tween 20 solution) and rinsed down with **K** mL of the catalyst. If the filter becomes visibly clean afterwards, it is taken out with a tweezer and rinsed with **2K** mL of H<sub>2</sub>O<sub>2</sub> which would help remove any remaining sample from the filter as well as start the reaction. This will be referred to as the filter wet extraction protocol (Fi-WEPE).

If the filter does not become clear due to the mechanical rubbing action, then the filter is left in the reaction flask and the Fenton reaction is started by adding **2K** mL H<sub>2</sub>O<sub>2</sub>. This filter is then either removed after a few minutes as the Fenton reaction will help loosen the particles. Or is left till the end at the expense of possibly generating more cellulose particles from membrane degradation.

9. After Fenton reaction starts, add **0.5K** mL of hydrogen peroxide at the end of each minute till t=10 min. This is followed by 10 min cooling time.
10. A bottle filled with UPW should be kept nearby in case the reaction foams and is about to spill over. This can sometimes happen as the reaction is exothermic and not cooled. In such extreme cases, spraying a few milliliters of UPW inside the reaction flask helps to cool it down just enough to prevent spilling.
11. After 20 minutes, **0.4K** mL of concentrated sulfuric acid (98 %) is added to dissolve the precipitated iron species that would otherwise cover the sample and prevent analysis. The flask should be hand shaken gently for 30 seconds then quickly filtered.
12. The filter is rinsed with 100 mL UPW to remove any acid residue that might damage the plastic particles in the long term.
13. Filter can either be analyzed as is or the filter can be cleaned as per Fi-WEP using Tween 20 solution to rinse it instead of the Fenton reagents. The suspension can then be stored for transport. Tween 20 solutions act as a surfactant to prevent particle agglomeration.

Note: The Fi-WEP protocol showed 83% ± 2% recovery rate (chapter 6 below).

#### *9.5.4. $\mu$ FTIR analysis*

After transport Fenton treated suspensions (as described in SI Section 3) were filtered on 25 mm Anodiscs<sup>TM</sup> (Whatman<sup>TM</sup>, PP-supported, 0.2  $\mu$ m pore size) and subsequently analyzed via focal plane array (FPA-)  $\mu$ FTIR spectroscopy. A Bruker Hyperion 3000 FTIR microscope with a 64x64 pixel FPA detector and Bruker Tensor 27 FTIR spectrometer was used for imaging in transmission mode. The Filters were placed on CaF<sub>2</sub> windows (25 mm diameter, 2 mm thickness, Korth Kristalle, Germany). The entire surface of the filter was scanned using a 15x IR objective.

Spectra were collected using a co-addition of 6 scans at a resolution of 8 cm<sup>-1</sup> and a measuring range between 1 250 and 3 600 cm<sup>-1</sup>. Additional 4×4 binning resulted in pixel sizes of the measured data of 11 μm. Imaging data were then compared against a reference database using siMPle (v. 1.0.1) [216]. The reference data contained spectra of two polymer databases [217, 218], as well as the substance spectra of stearates, surfactants and waxes as described by [106] to avoid false positive PE detection.

#### 9.5.5. *μRaman analysis*

The particles within the sample (aqueous suspension, as described at number 7 of the step by step procedure in section 3) were collected on the filter (gold-coated track etched filter made from polycarbonate, Analytische Produktions-, Steuerungs- und Controllgeräte GmbH, Germany) through vacuum filtration (Filtration device, Sartorius AG, Germany), and analyzed with a Raman microscope alpha 300 applying the following steps: (1) image acquisition of the entire filter (20× objective with N.A. = 0.4, 3 [db] Gain, 3% top illumination, 1/10 fps, 16 000 μm × 16 000 μm, 8 000 pixel × 8 000 pixel, 30 μm z-stacking, by custom image stitching). (2) Localization and morphological characterization of all particles on the filter surface using TUM-ParticleTyper [133, 202]: The entire filter area in which particles can be located due to the restricted accessibility through the filtration process is observed. (3) Raman measurement (3 mW using TruePower, 532 nm laser, 2.5 – 20 s measurement time, 20× objective) yields the chemical identity via database match (database search with TrueMatch) of n ~ 7000 randomly selected particles per filter as described [121]. Correlation coefficients (hit quality index, HQI, values 0 – 1, threshold 0.45) between each sample spectrum and all database spectra are calculated to obtain a list of possible materials for each particle, from which the highest ranked is chosen. Only spectral regions of expected high signal variance are respected (590 cm<sup>-1</sup> – 1770 cm<sup>-1</sup> and 2690 cm<sup>-1</sup> – 3300 cm<sup>-1</sup>), appropriate Raman bands of the database spectra belonging to plastic materials as well as their assignments according to the literature are shown in table 5. Additionally, spectra of following non-plastic materials are contained: cellulose, Cu-phthalocyanine, carotenoids, quartz, and soot. Polycarbonate particles are not quantified, as the filter



membrane is made of this material. The combination of the morphological data and chemical identified subsample leads to a compound correlated size distribution for the total number of particles upon extrapolation.

Estimated time for analysis (RM+TUM-ParticleTyper): 48h (RM measurements, 7000 spectra) + 2h (evaluation).

#### *9.5.6. Sample preparation for TED-GC-MS*

The sample preparation for the TED-GC-MS consisted of extracting the sample from the basket filters with a wire brush and Tween 20 solution into a 200 mL glass flask. Afterwards an aliquot or the whole sample was filtered with a Whatman™ cellulose nitrate membrane filter (45 mm diameter, 0.2 µm pore size) (GE Healthcare Life Sciences, Chalfont ST Giles, GB). Thereafter, the filter was rinsed with 1 mL Tween 20 and transferred into a 30 mL ND20 brown screw top vial and capped with aluminum foil. The content of the vial is dried at 50 °C and the residue is transferred with 600 µL pure ethanol into previously weighted crucible. This sample preparation had been validated. While the transfer method from the basket filter was validated by Funck et al. (2020). The recovery rates for the 100 µm basket filter were 87% ± 2%, the 50 µm basket filter showed a recovery rate of 85% ± 2% and the 10 µm basket filter had 88% ± 2% of the particles recovered.

The sample transfer from the cellulose nitrate membrane filter via Fi-WEP to the TED-GC-MS was validated by adding PE onto the filter. Masses of 20 µg, 69 µg and 39 µg were added to three separate filters. Afterwards the particles were transferred as described above and analysed by TED-GC-MS. The results showed a recovery rate of 83% ± 2%.

#### *9.5.7. TED-GC-MS analysis*

Each sample was weighed by the TGA and pyrolyzed from 25 °C to 600 °C, with a heating rate of 10 °C min<sup>-1</sup> and nitrogen (N<sub>2</sub>) purge gas flow of 50 mL min<sup>-1</sup>. The decomposition products were purged through a 240 °C heated coupling unit (Gerstel GmbH & Co KG, Mülheim an der Ruhr, Germany) and sorbed at 50 °C to a Gerstel Twister.

Within the TDU3.5+ unit, the decomposition products on the Gerstel Twister are mobilized from 50 - 200 °C with a heating rate of 40 °C min<sup>-1</sup>, using split-less mode. Helium (He) is used as a carrier with 99.999 mol% purity (Air Liquide Deutschland GmbH, Düsseldorf, Germany) and a flow of 24 mL min<sup>-1</sup>. The decomposition products are injected and cryo-focused at -120 °C for 8.75 min and are subsequently released at -120 °C to 270 °C with a heating rate of 12 °C sec<sup>-1</sup>.

The decomposition products are then introduced into the gas chromatograph (GC7890, Agilent, Santa Clara, California, USA) equipped with a capillary column (HP 5ms Ultra Inert 30 m x 250 µm x 0.25 µm, Hewlett Packard, Palo Alto, California, USA). The chromatographic separation was achieved with a temperature program of 40 - 300 °C at a rate of 5 °C min<sup>-1</sup>, 4 min isothermal at 300 °C with a 1 mL min<sup>-1</sup> He flow. The GC-MS coupling interface heated to 300 °C. The mass spectrometer (5977 B MSD, Agilent) ion source temperature was set to 230 °C, the quadrupole temperature was set to 150 °C and an electron ionization at 70 eV. Scan mode with a range of m/z 35 - 440 was used.

#### 9.5.8. TED-GC-MS calibration and quality control samples

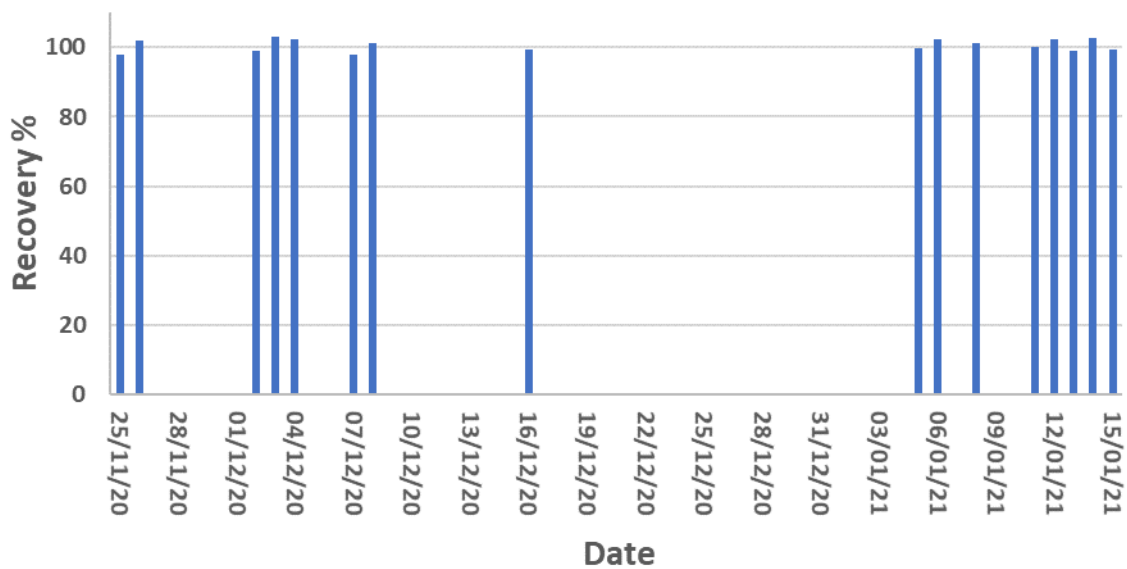
For the TED-GC-MS an external calibration with PS; PE, PP and PET (provided by Bundesanstalt für Materialforschung und -prüfung) was conducted. Additionally, accompanying every measurement sequence quality control sample consisting of PS, PE, PP and PET were measured.

The calibration R<sup>2</sup> are given in the Table\_5.1\_SI. 4. An excerpt of the quality control samples from 22.11.2020 to 18.01.2021 for PE are shown in Figure\_5.1\_SI. 1.

Table\_5.1\_SI. 4. External calibration of PE, PS PP and PET for TED-GC-MS analysis

Polymer	R <sup>2</sup>
PS	0.9969
PE	0.9975

PET	0.9985
PP	0.9985
PS	0.9997
PE	0.9991
PET	0.9974
PP	0.9984



Figure\_5.1\_Sl. 1. Results regarding the recovery of PE in quality control (QC) samples measured by TED-GC-MS. QC sample measurements are shown from 25.11.2020 to 15.01.2021

### 9.5.9. Polymer identification

Table\_5.1\_Sl. 5. Selected identification bonds with wavelengths and pyrolysis products for  $\mu$ FTIR,  $\mu$ Raman and TED-GC-MS.

Polyme r	Pyrolysis product corresponding $m/z$ values	TED-GC- MS with	Bond $\mu$ Raman	Wavelength
<b>PS [10, 11]</b>	Styrene	51; 78; 104	620	Phenyl group, in-plane
			795	C–H out-of-plane deform.
			1000	Ring skeleton bending/stretching
	2,4-Diphenyl-1-butene	91; 104; 130; 208	1031	C–H in-plane deform.
			1155	$\nu(\text{C–C})$
	2,4,6-Triphenyl-1-hexene	91; 117; 194; 207	1582	$\nu(\text{C=C})$
			1602	$\nu(\text{C=C})_{\text{arom}}$
			2852	$\nu_{\text{s}}(\text{CH}_2)$
			2910	$\nu_{\text{as}}(\text{CH}_2)$
			3053	$\nu(\text{C–H})_{\text{arom}}$
<b>PPTA [12]</b>			796	Ring vibrations
			1191, 1284, 1334, 1520, 1619	$\nu(\text{CC})_{\text{arom}}$
			1658	$\nu(\text{C=O})$
<b>PE [13]</b>	1,12-Tridecadiene	55; 81; 67;95	1063	skeletal
			1130	skeletal
	1,13-Tetradecadiene	81; 95; 109	1296	$\nu(\text{CH}_2)$
			1440	$\delta(\text{CH}_2)$
	1,14-Pentadecadiene	55; 81; 95; 109	2849	$\nu_{\text{s}}(\text{CH}_2)$
			2882	$\nu_{\text{as}}(\text{CH}_2)$

PP [14]	2,4,6-Trimethylnon-1-ene	43; 69; 111; 125	810, 843, 974	$\nu(\text{C}-\text{C})$
			997	$\delta(\text{CH}), r(\text{CH}_3)$
	2,4,6,8-Tetramethylundec-1-ene	69; 83; 111; 125; 154	1153	$\delta(\text{C}-\text{C}), \delta(\text{CH}_3), \delta(\text{C}-\text{H})$
			1220	$t(\text{CH}_2)$
			1331	$t(\text{CH}_2), \delta(\text{C}-\text{H})$
			1361	$\delta_s(\text{CH}_3)$
2,4,6,8-Tetramethylundec-1-ene	69; 83; 111; 125; 154	1460	$\delta_{as}(\text{CH}_3)$	
		2842	$\nu_s(\text{CH}_2)$	
		2885	$\nu_s(\text{CH}_3)$	
		2906	$\nu(\text{CH})$	
		2925	$\nu_{as}(\text{CH}_2)$	
		2954	$\nu_{as}(\text{CH}_3)$	
Polymer	Pyrolysis product	TED-GC-MS with	Bond and Wavelength $\mu\text{Raman}$	
			corresponding $m/z$ values	
PET [15]	Vinyl benzoate	77; 51; 105	857	$\nu(\text{CC}), \nu(\text{COO})$
			1094	$\delta(\text{C}-\text{C}), \nu(\text{CC})_{\text{arom}}$
	Ethyl benzoate	77; 105; 122; 150	1111, 1286	$\nu(\text{C}-\text{O})$
			1613	benzene ring vibr.
1,1 Biphenyl	76; 154	1727	$\nu(\text{C}=\text{O})$	
		2967	$\nu(\text{CH}_2)$	
		3077	$\nu(\text{C}-\text{H})_{\text{arom}}$	
Alkyd-Resin	-			

<b>PA</b> <b>[16]</b>	6	-	932	$\nu(\text{C}-\text{CO})$
		-	1080, 1127	$\nu(\text{C}-\text{C})$ (skeletal)
		-	1280, 1305	$\text{t}(\text{CH}_2)$
		-	1444	$\delta(\text{CH}_2)$
		-	1635	$\nu(\text{C}=\text{O})$
		-	2873–2929	$\nu(\text{C}-\text{H})$
<b>POM</b> <b>[17]</b>		-	3296	$\nu(\text{N}-\text{H})$
		-	918	$\nu_{\text{s}}(\text{COC}) - \text{r}(\text{CH}_2)$
		-	1090	$\nu_{\text{as}}(\text{COC}) - \delta(\text{OCO})$
		-	1334	$\text{t}(\text{CH}_2) - \nu_{\text{as}}(\text{COC})$
		-	1490	$\delta(\text{CH}_2)$
		-	2922	$\nu_{\text{s}}(\text{CH}_2)$
<b>PMMA</b> <b>[18]</b>		-	2995	$\nu_{\text{as}}(\text{CH}_2)$
		-	600	$\nu(\text{C}-\text{COO}), \nu_{\text{s}}(\text{C}-\text{C}-\text{O})$
		-	820	$\nu_{\text{s}}(\text{C}-\text{O}-\text{C})$
		-	980	$\text{r}(\text{O}-\text{CH}_3)$
		-	1130–1250	$\nu(\text{C}-\text{O})$ region
		-	1451	$\delta(\text{C}-\text{H})$ ( $\alpha\text{-CH}_3$ )
-	1725	$\nu(\text{C}=\text{O})$ ( $\text{C}-\text{COO}$ )		
-	2842–3000	$\nu(\text{CH}_2)$		

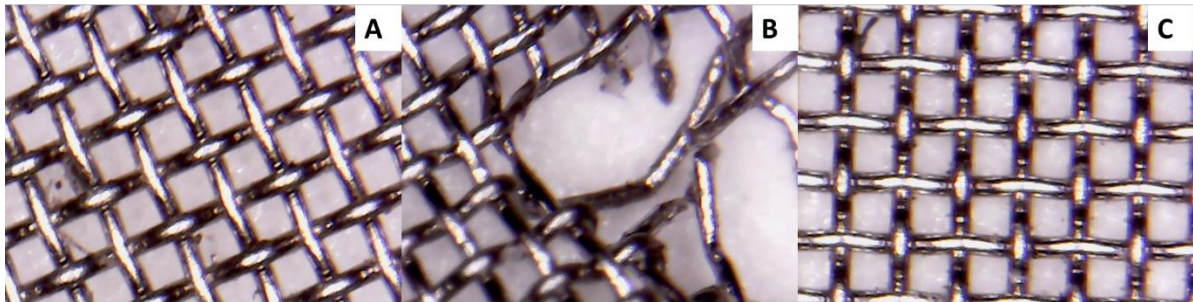
<b>PVC [19]</b>	-	636	$\nu(\text{C}-\text{Cl})$
		1090	$\nu(\text{C}-\text{C}), r(\text{CH}_2), t(\text{CH}_2)$
		1180	$\delta(\text{H}-\text{C}-\text{Cl})$
		1330	$\delta(\text{H}-\text{C}-\text{Cl}), t(\text{CH}_2)$
		1430	$\delta(\text{CH}_2)$
		2915	$\nu_s(\text{CH}_2)$
		2969	$\nu_{as}(\text{CH}_2)$
<b>Polymer</b>	Pyrolysis product TED-GC-MS with corresponding $m/z$ values	Bond and Wavelength $\mu\text{Raman}$	
<b>PLA [20]</b>		874	$\nu(\text{C}-\text{COO})$
		1045	$\nu(\text{C}-\text{CH}_3)$
		1128	$r_{as}(\text{CH}_3)$
		1457	$\delta_{as}(\text{CH}_3)$
		1769	$\nu(\text{C}=\text{O})$
		2946	$\nu_s(\text{CH}_3)$
		3000	$\nu_{as}(\text{CH}_3)$
<b>PC [21]</b>		635	ring deformation (in-plane)
		707	ring deformation (out-of-plane)
		886	$\nu(\text{C}-\text{CH}_3)$
		1110, 1180	$w(\text{CH}_2)$ (in-plane)
		1231	$\nu(\text{C}-\text{O})$
		1603	$\nu(\text{C}=\text{C})_{\text{arom}} / \text{ring stretch}$
		1780	$\nu(\text{C}=\text{O})$
		2938	$\nu(\text{C}-\text{H})$
3072	$\nu(\text{C}-\text{H})_{\text{arom}}$		

<b>PTFE</b> <b>[22]</b>	730	$\nu_x(\text{CF}_2)$
	1215	$\nu_{ax}(\text{CF}_2)$
	1300, 1381	$\nu(\text{C}-\text{C})$
<b>ETFE</b> <b>[23]</b>	605	$r(\text{CF}_2), w(\text{CF}_2)$
	841	$\nu(\text{CF}_2)$
	1048	$\nu(\text{C}-\text{C})$ (skeletal)
	1449	$\delta(\text{CH}_2)$
	2975, 3000	$\nu(\text{CH}_2)$
<b>Silicone</b> <b>rubber</b> <b>[24]</b>	715	$\nu(\text{C}-\text{Si}-\text{C})$
	2914	$\nu_s(\text{CH}_2)$
	2973	$\nu_{as}(\text{CH}_2)$

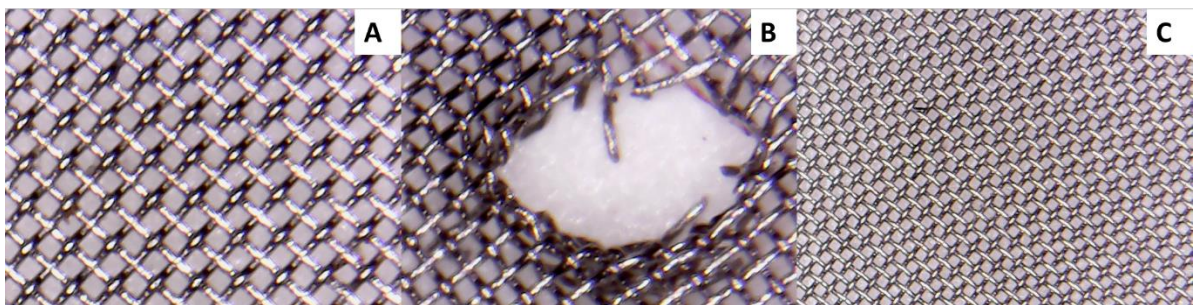


#### 9.5.10. Basket filter sieve integrity evaluation

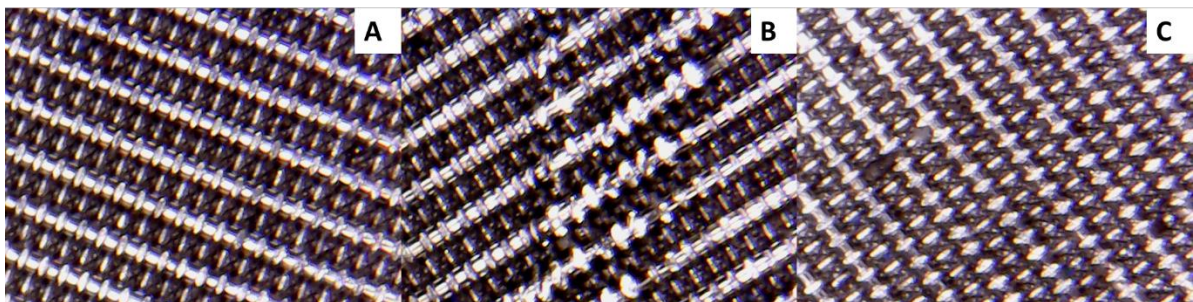
Figure\_5.1\_Sl. 2, 3 and 4 show that treating the filter material with a natural hairbrush leads to no significant change in the filter material.



Figure\_5.1\_Sl. 2. 100  $\mu\text{m}$  basket filters are depicted. Part A depicts an untreated 100  $\mu\text{m}$  basket filter. Part B depicts a 100  $\mu\text{m}$  basket filter treated 3 times with a wire brush showing a hole in the filter material. Part C depicts a 100  $\mu\text{m}$  basket filter treated 3 times with a natural hairbrush showing no significant change in the filter material.



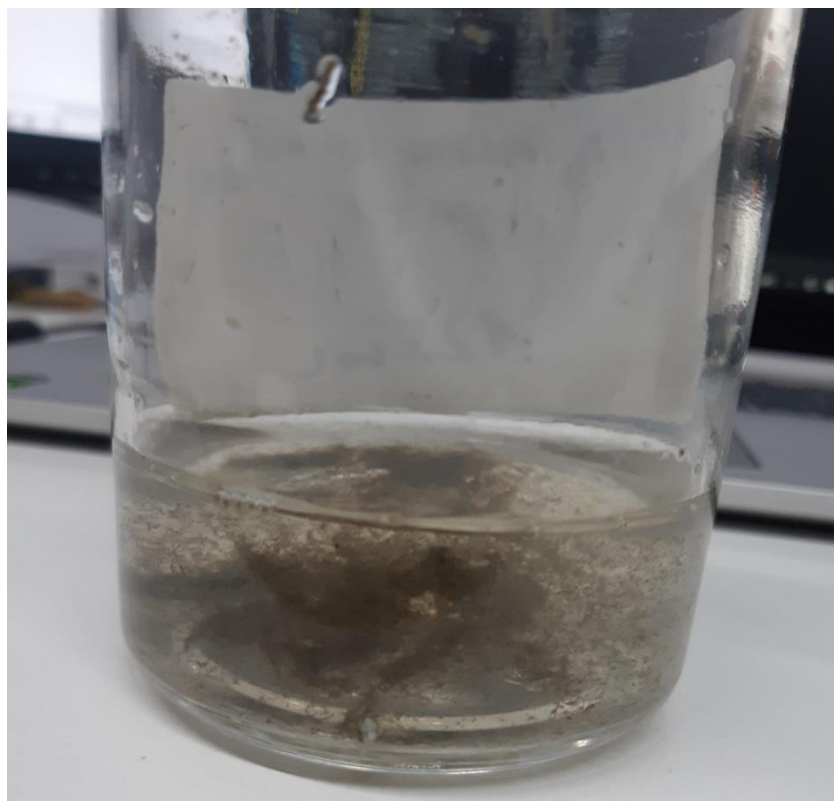
Figure\_5.1\_Sl. 3. 50  $\mu\text{m}$  basket filters are depicted. Part A depicts an untreated 50  $\mu\text{m}$  basket filter. Part B depicts a 50  $\mu\text{m}$  basket filter treated 3 times with a wire brush showing a hole in the filter material. Part C depicts a 50  $\mu\text{m}$  basket filter treated 3 times with a natural hairbrush showing no significant change in the filter material.



Figure\_5.1\_Sl. 4. 10  $\mu\text{m}$  basket filters are depicted. Part A depicts an untreated 10  $\mu\text{m}$  basket filter. Part B depicts a 10  $\mu\text{m}$  basket filter treated 3 times with a wire brush showing scratches in the filter material. Part C depicts a 10  $\mu\text{m}$  basket filter treated 3 times with a natural hairbrush showing no significant change in the filter material.

### 9.5.11. Picture of algae in extracted samples

Figure\_5.1\_SI. 5 showed that the 5 mm intake filter at the cascadic MP filtration plant does not block algae from accumulating in the respective filters. Therefore, cake filtration occurs within the filters, which is why smaller particles < 100 µm accumulate in e.g., the 100 µm basket filter.



Figure\_5.1\_SI. 5. The figure shows algae in a sample extracted from a 100 µm basket filter. Despite the 5 mm filter at the intake of the cascadic microplastic filtration plant algae get sucked in.

### 9.5.12. Reduced flow sampling campaign

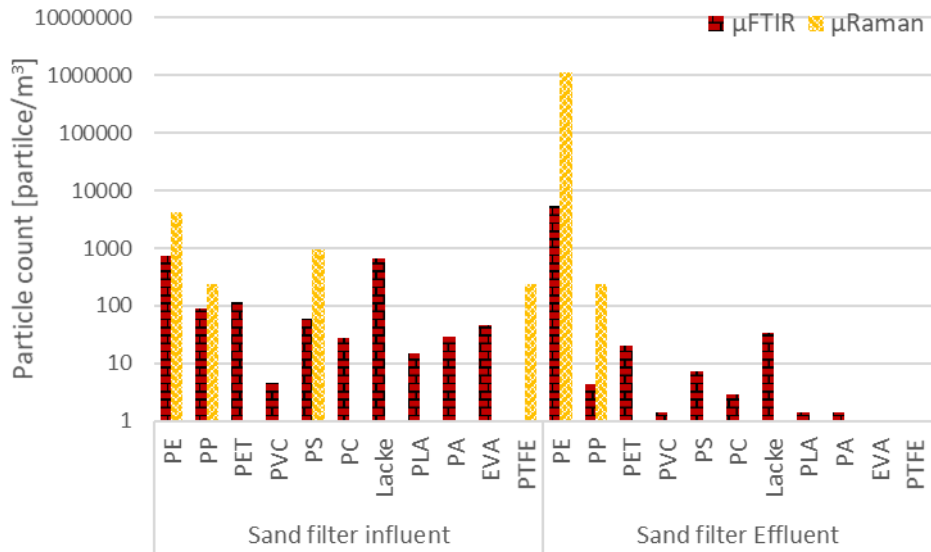
Table\_5.1\_SI. 6. Analysis of WWTP A before sand filter with TED-GC-MS for the polymers PS, PE, PP and PET. For the experiments three flow rates are compared: 3000 L h<sup>-1</sup> (standard sampling flow rate) and 375 L h<sup>-1</sup> (8-hour sampling). The sampling dates are stated. The results for each basket filter are given in µg m<sup>-3</sup> with respective LOD's for each polymer in dependence of the filtered volume.

WWTP A B.S.F.		Polymers				
Date	Flow rate L h <sup>-1</sup>	Basket filter	PS (µg m <sup>-3</sup> )	PE (µg m <sup>-3</sup> )	PP (µg m <sup>-3</sup> )	PET (µg m <sup>-3</sup> )
17.02.2020	3000 (1h)	100 µm	5	95	4	16
		50 µm	4	43	< LOD 0.4	4

		10 µm	< LOD 0.3	29	< LOD 0.4	3
<b>18.02.2020</b>	375 (8h)	100 µm	< LOD 0.3	< LOD 1.3	< LOD 0.4	< LOD 0.6
		50 µm	< LOD 0.3	< LOD 1.3	< LOD 0.4	< LOD 0.6
		10 µm	< LOD 0.3	< LOD 1.3	< LOD 0.4	< LOD 0.6
<b>13.04.2021</b>	3000 (1h)	100 µm	< LOD 0.3	94	18	9
		50 µm	< LOD 0.3	24	6	2
		10 µm	< LOD 0.3	< LOD 1.3	< LOD 0.4	< LOD 0.6
<b>13.04.2021</b>	375 (8h)	100 µm	< LOD 0.3	< LOD 1.3	< LOD 0.4	< LOD 0.6
		50 µm	< LOD 0.3	< LOD 1.3	< LOD 0.4	< LOD 0.6
		10 µm	< LOD 0.3	< LOD 1.3	< LOD 0.4	< LOD 0.6
<b>15.04.2021</b>	3000 (1h)	100 µm	< LOD 0.3	154	32	27
		50 µm	< LOD 0.3	74	19	10
		10 µm	< LOD 0.3	5	< LOD 0.4	< LOD 0.6

### 9.5.13. Complementary results from spectroscopic analyses

Below are the results from spectroscopic analytical techniques ( $\mu$ FTIR and  $\mu$ Raman) during the operational anomaly during the 2019 sampling event. The libraries of the two analytical approaches do not match, hence no comparison between most of the polymers could be made. However, using multiple analytical approaches as well as libraries has enabled the authors to analyze more polymer types than if only one technique was utilized.



Figure\_5.1\_Sl. 6. The figure shows all analyzed polymers during the 2019 sampling event, with  $\mu$ FTIR and  $\mu$ Raman. Significantly more PE particles were observed by both instruments after the sand filter.  $\mu$ FTIR results represent the sum of the particles found on the 100  $\mu$ m + 50  $\mu$ m sieves. Whereas the  $\mu$ Raman results represent the particles found on the 10  $\mu$ m sieve. Reason for these results is a not specified operational anomaly in the WWTP.

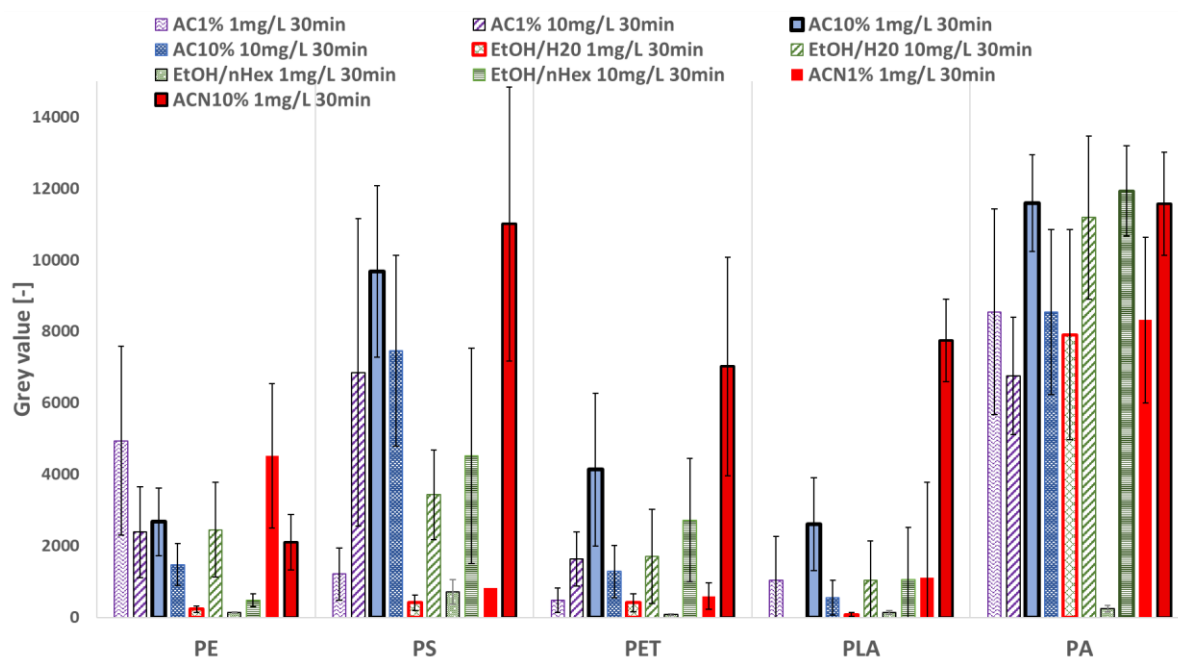
## 9.6. Supplementary material for Chapter 5.2

### 9.6.1. Staining protocol development

Table\_5.2\_A.1. Investigated protocols using five polymers (PE, PS, PET, PLA, PA) during initial protocol screening based on literature. \*All solvents are diluted in UPW, except EtOH/n-Hexane, which were mixed in a 1:1 volume ratio.

Protocol	Nile concentration	red Solvent % in UPW*	Conditions
1	1 mg/L	Acetone 1 %	30 Min @ RT
2	10 mg/L	Acetone 1 %	30 Min @ RT
3	1 mg/L	Acetone 10 %	30 Min @ RT
4	10 mg/L	Acetone 10 %	30 Min @ RT
5	1 mg/L	EtOH/n-Hexane (1:1)	30 Min @ RT
6	10 mg/L	EtOH/n-Hexane (1:1)	30 Min @ RT
7	1 mg/L	EtOH 50%	30 Min @ RT
8	10 mg/L	EtOH 50%	30 Min @ RT
9	1 mg/L	Acetonitrile 1 %	30 Min @ RT
10	1 mg/L	Acetonitrile 10 %	30 Min @ RT

\*Except for ethanol/n-Hexane mixes



Figure\_5.2\_A. 1. First round of protocol development using five polymers and ten protocols. All protocols were performed at room temperature. The grey value represents the weighted average brightness of ten single particles and their standard deviation (14-bit greyscale images in Cy3 channel). Brightness analyses were done using ImageJ. Results for PS microspheres are not shown because they were not quantified in the pre-experiments. Abbreviations used: Ac: Acetone, ACN: Acetonitrile, EtOH: Ethanol, nHex: n-Hexane

Table\_5.2\_A. 2. The investigated protocols for dyeing PE during the final staining protocol optimization round.

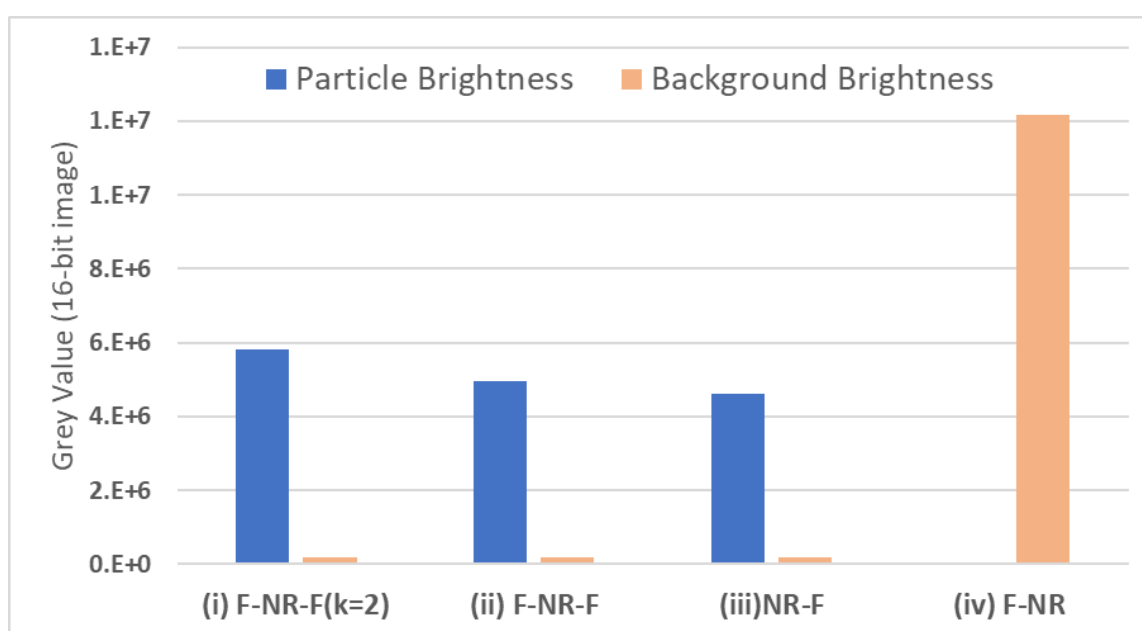
Protocol	Dye	Solvent % in UPW	Conditions
NR_1	Nile red 1 mg/L	Acetonitrile 10 %	30 Min @ RT
NR_2	Nile red 1 mg/L	Acetonitrile 10 %	60 Min @ RT
NR_3	Nile red 1 mg/L	Acetonitrile 10 %	24 Hr. @ RT
NR_4	Nile red 10 mg/L	Acetonitrile 10 %	60 Min @ RT
NR_5	Nile red 10 mg/L	Acetonitrile 20 %	60 Min @ RT
NR_6	Nile red 10 mg/L	Acetonitrile 10 %	24 Hr. @ 70 °C
NR_7	Nile red 10 mg/L	Acetonitrile 10 %	2 Hr. @ 70 °C
NB_1	Nile blue 10 mg/L	Acetonitrile 10 %	30 Min @ RT
NB_2	Nile blue 10 mg/L	Ethanol 10 %	2 Hr. @ 70 °C

### 9.6.2. Workflow protocol optimizations

Initially, different sequences were tested on 0.5 mL sludge sample which were then filtered on PCET filters with 0.2 µm pore size (Carl Roth, Germany) to determine the effects on background interference. Many variants were tested in this stage to gain a better understanding of the behavior of sludge. The list of all tested workflows can be found in (Table\_5.2\_A. 3). Analyses for this phase were made using a Zeiss LSM 510-META confocal microscope (Carl Zeiss, Germany), using Cy3 channel (Ex:650 nm, Em:670 nm) with an exposure time of 300 ms. Image capturing was done using Zen Blue 3.0 software. 10 - 20 images of single particles were taken using the x10 objective.

Table\_5.2\_A. 3. Sequence development to reduce fluorescence interference from 0.5 mL sludge. RT: Room temperature, ACN: acetonitrile. When no k value is mentioned for Fenton, it is assumed to be 10 mL.

No.	Workflows
i	Sludge → Fenton → NR (ACN 10% 10 mg/L for 30 min @ 70 °C) → Fenton (k=2)
ii	Sludge → Fenton → NR (ACN 10% 10 mg/L for 30 min @ 70 °C) → Fenton
iii	Sludge → NR (ACN 10% 10 mg/L for 30 min @ 70 °C) → Fenton
iv	Sludge → Fenton → NR (ACN 10% 10 mg/L for 30 min @ 70 °C)

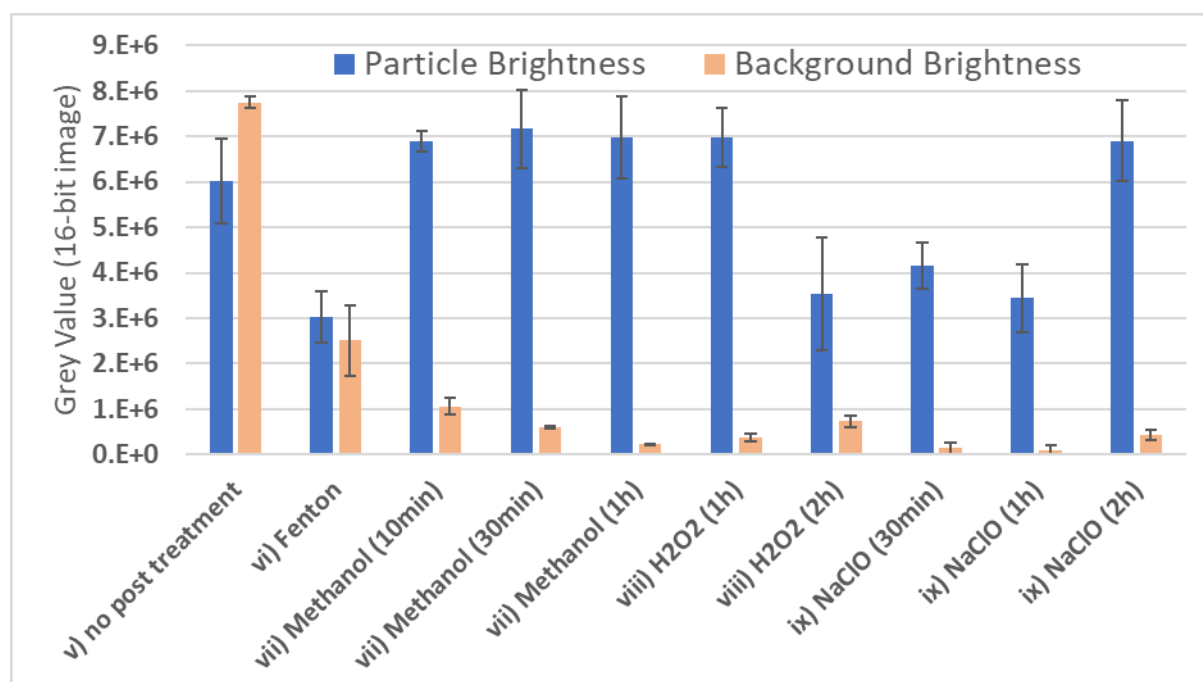


Figure\_5.2\_A. 2. Results for the initial reduction of interference from the organic matrix using organic matrix reduction.

After the first round of development on sludge samples, further workflows were tested on PE to retain the staining on the surface of the particles. The workflows are listed in the table below.

Table\_5.2\_A. 4. Workflow development to increase the brightness of PE after post-treatment. RT: Room temperature, ACN: acetonitrile. When no k value is mentioned for Fenton, it is assumed to be 10 mL.

No.	Workflows
v	PE → NR (ACN 10% 10 mg/L for 30 min @ 70 °C)
vi	PE → NR (ACN 10% 10 mg/L for 30 min @ 70 °C) → Fenton
vii	PE → NR (ACN 10% 10 mg/L for 30 min @ 70 °C) → Methanol (10 min, 30 min, 1 hr @ RT)
viii	PE → NR (ACN 10% 10 mg/L for 30 min @ 70 °C) → H <sub>2</sub> O <sub>2</sub> (30% for 1 hr & 2 hr @ RT)
ix	PE → NR (ACN 10% 10 mg/L for 30 min @ 70 °C) → NaClO (14% for 30 min, 1 hr and 2 hr @ RT)



Figure\_5.2\_A. 3. Sequence optimization to increase the brightness of PE particles after applying post-treatment.



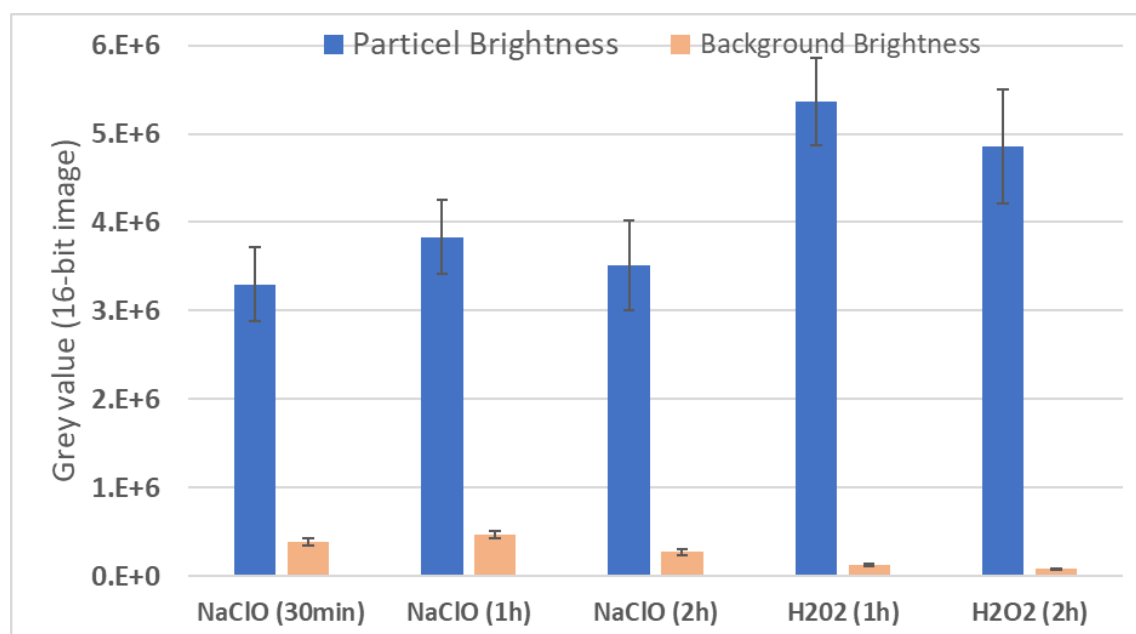
From Figure\_5.2\_A. 3, it could be observed that not using any post treatment resulted in very bright background which impeded identification. Fenton removed the dye in most of the particles. Finally, Methanol tended to stain the filter in a way that produced bright spots that were falsely identified as particles; therefore, both were deemed unsuitable.

H<sub>2</sub>O<sub>2</sub> and NaClO did not produce any such negative results and so were selected as suitable post-treatments that retained enough staining on PE particles as well as managed a dark background in the control samples. Therefore, both protocols were selected for a further round of testing on sludge samples as can be seen below.

Table\_5.2\_A. 5. Workflow development to test the reduction fluorescence interference from 0.5 mL sludge using the successful post-treatment from Table\_5.2\_A. 4. RT: Room temperature, ACN: acetonitrile. When no k value is mentioned for Fenton, it is assumed to be 10 mL.

**No. Workflows**

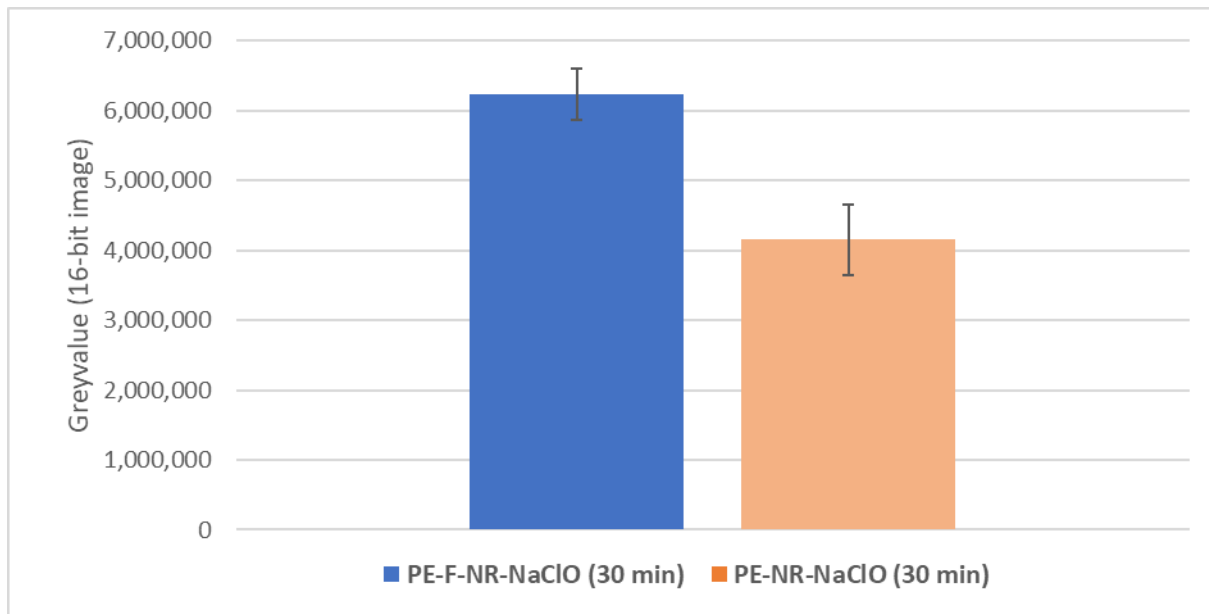
x	Sludge → Fenton → NR (ACN 10% 10 mg/L for 30 min @ 70 °C) → H <sub>2</sub> O <sub>2</sub> (30% for 1 hr & 2 hr @ RT)
xi	Sludge → Fenton → NR (ACN 10% 10 mg/L for 30 min @ 70 °C) → NaClO (14% for 30 min, 1 hr and 2 hr @ RT)



Figure\_5.2\_A. 4. Final round of testing for matrix interference from sludge after applying the best performing workflows from Table\_5.2\_A. 4. After the first round of

development on sludge samples, further workflows were tested on PE to retain the staining on the surface of the particles. The workflows are listed in the table below.

Table\_5.2\_A. 4.



Figure\_5.2\_A. 5. Comparison of the PE particle brightness with and without applying Fenton as pretreatment in the workflow first.

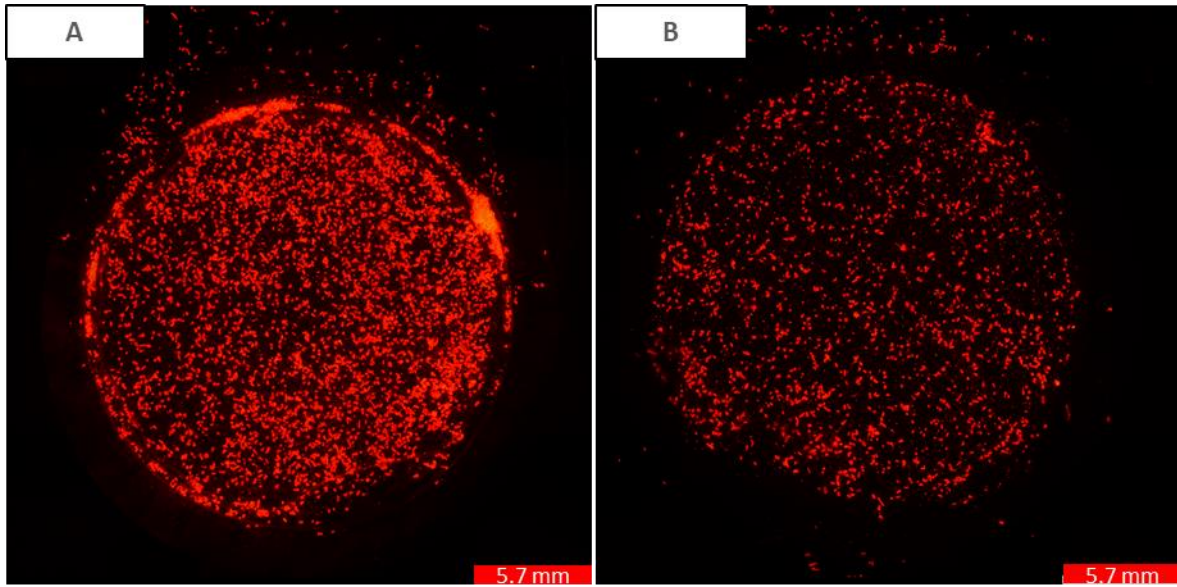
### 9.6.3. Code used to analyze the brightness of particles using ImageJ

```
input=getDirectory("Choose input folder");
output=getDirectory("Choose output folder for the results");

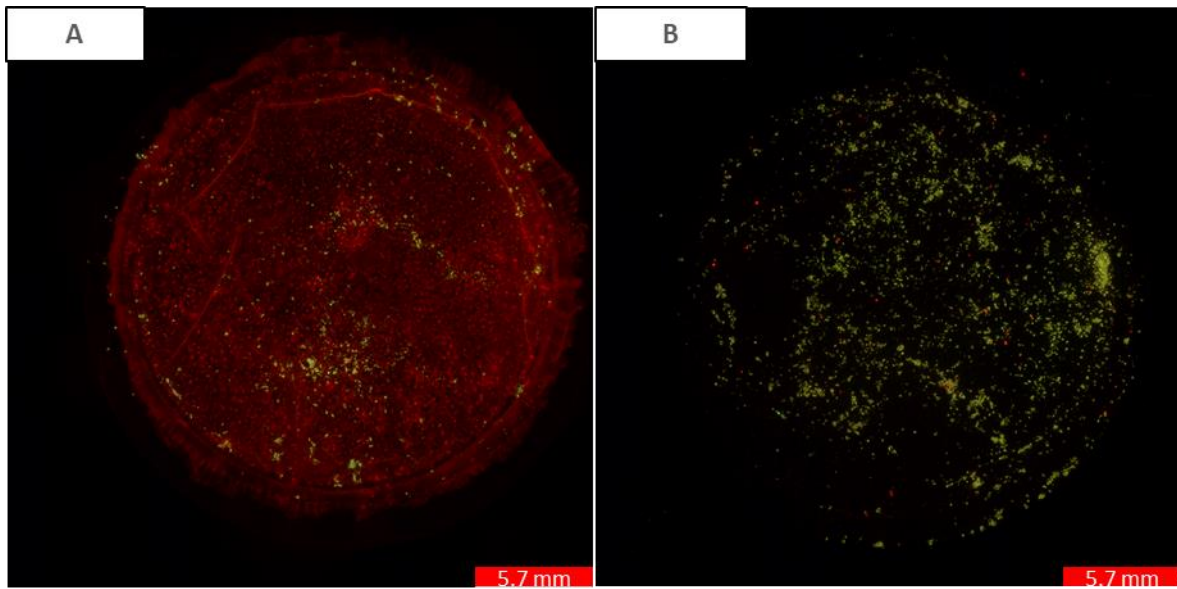
setBatchMode(true);
    list = getFileList(input);
    for (i = 0; i < list.length; i++)
        action(input, output, list[i]);
    selectWindow("Results");
    saveAs("Results", output+"results.csv");
    //save results in .csv file
    run("Close");
    setBatchMode(false);
function action(input, output, list){
path = input + list;
run("Bio-Formats Importer", "open=path color_mode=Colorized view=Hyperstack
stack_order=XYCZT");
makeOval(537, 384, 565, 582);
run("Crop");
//select general area of particle
run("Subtract Background...", "rolling=500");
//remove lokal variances in background signal
run("Set Measurements...", "area mean standard limit redirect=None decimal=0");
setAutoThreshold("Li dark");
//enter desired AutoThreshold function; selects area of interest
run("Measure");
//measures grey value in selected region of interest
setOption("BlackBackground", true);
run("Convert to Mask", "black method=default background=default ");
//generate binary image
saveAs("Jpeg", output+title);
//save binary image
selectWindow(title);
close();
}
```

### 9.6.4. Image of polymer controls using the final workflow

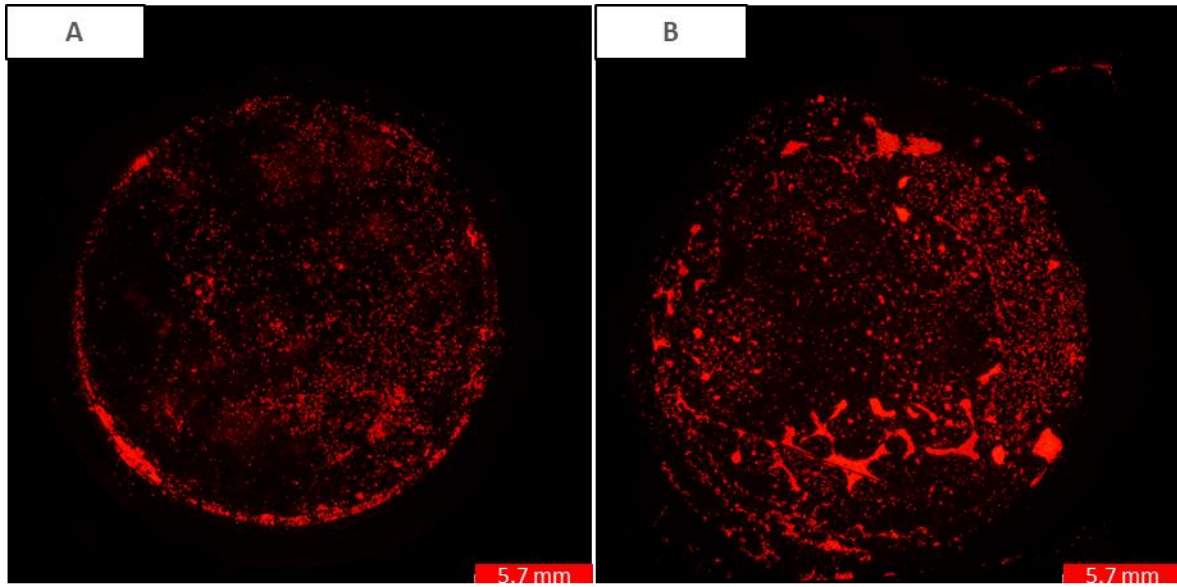
It can generally be observed that the images on the left (A) are brighter, both in terms of the particles as well as the filter background. Both are reduced on the right side (B) where bleaching is applied after staining, thereby reducing background interference without completely losing the staining from the particles.



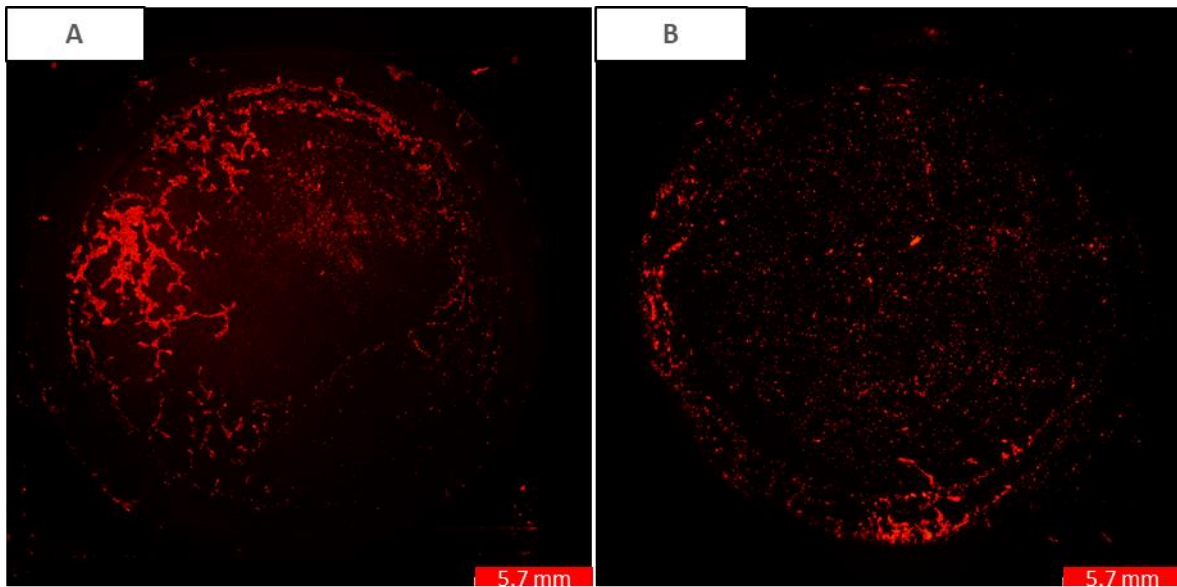
Figure\_5.2\_A. 6. Fluorescence microscopy images of PA. A: After staining only. B: After applying the workflow.



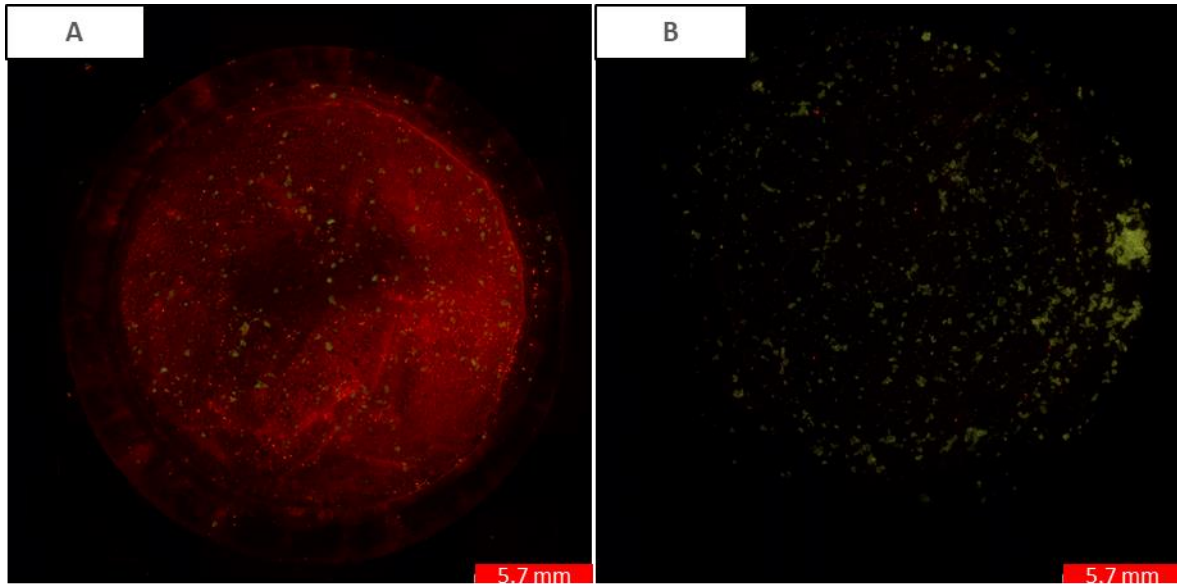
Figure\_5.2\_A. 7. Fluorescence microscopy images of PE. A: After staining only. B: After applying the workflow. Brightness is boosted by 40% and contrast is reduced by 40% to enhance viewing.



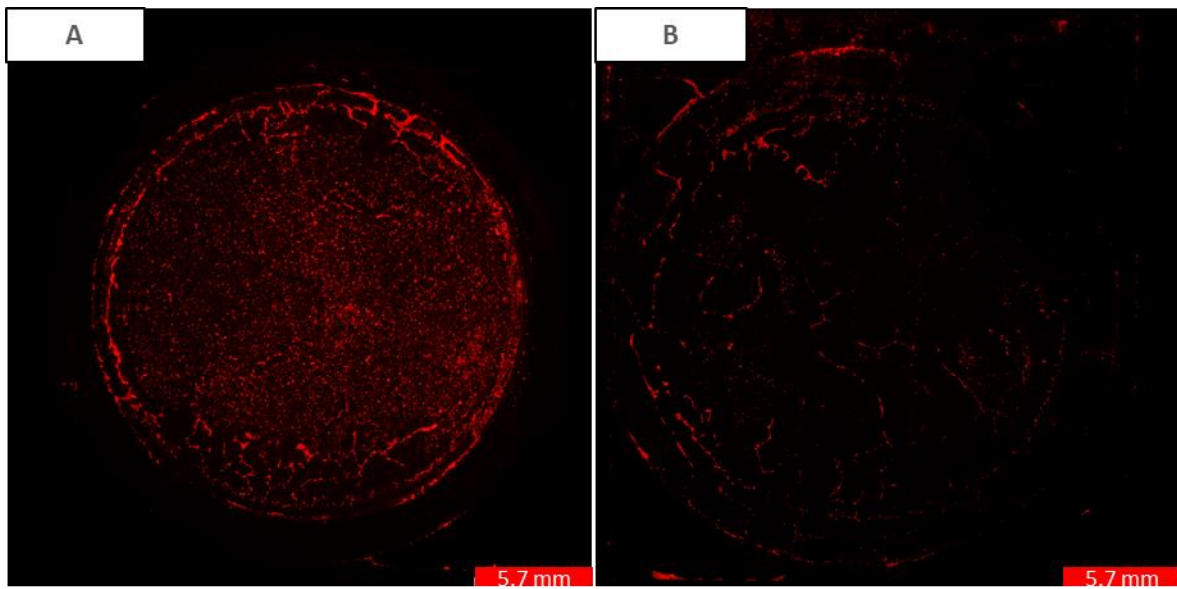
Figure\_5.2\_A. 8. Fluorescence microscopy images of PET. A: After staining only. B: After applying the workflow.



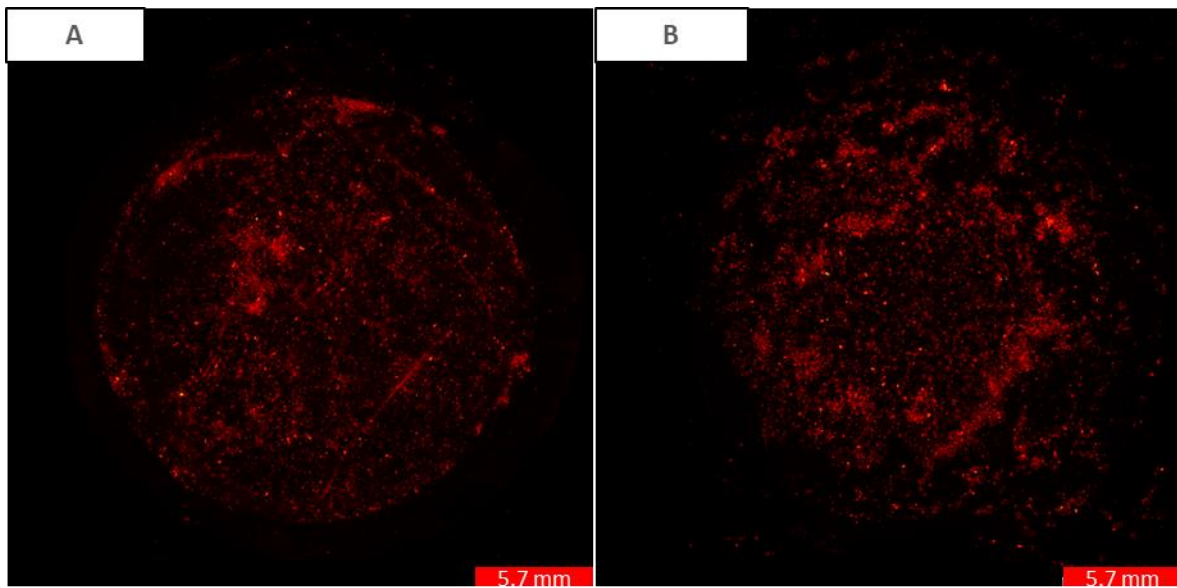
Figure\_5.2\_A. 9. Fluorescence microscopy images of PLA. A: After staining only. B: After applying the workflow.



Figure\_5.2\_A. 10. Fluorescence microscopy images of PP. A: After staining only. B: After applying the workflow. Brightness is boosted by 40% and contrast is reduced by 40% to enhance viewing.

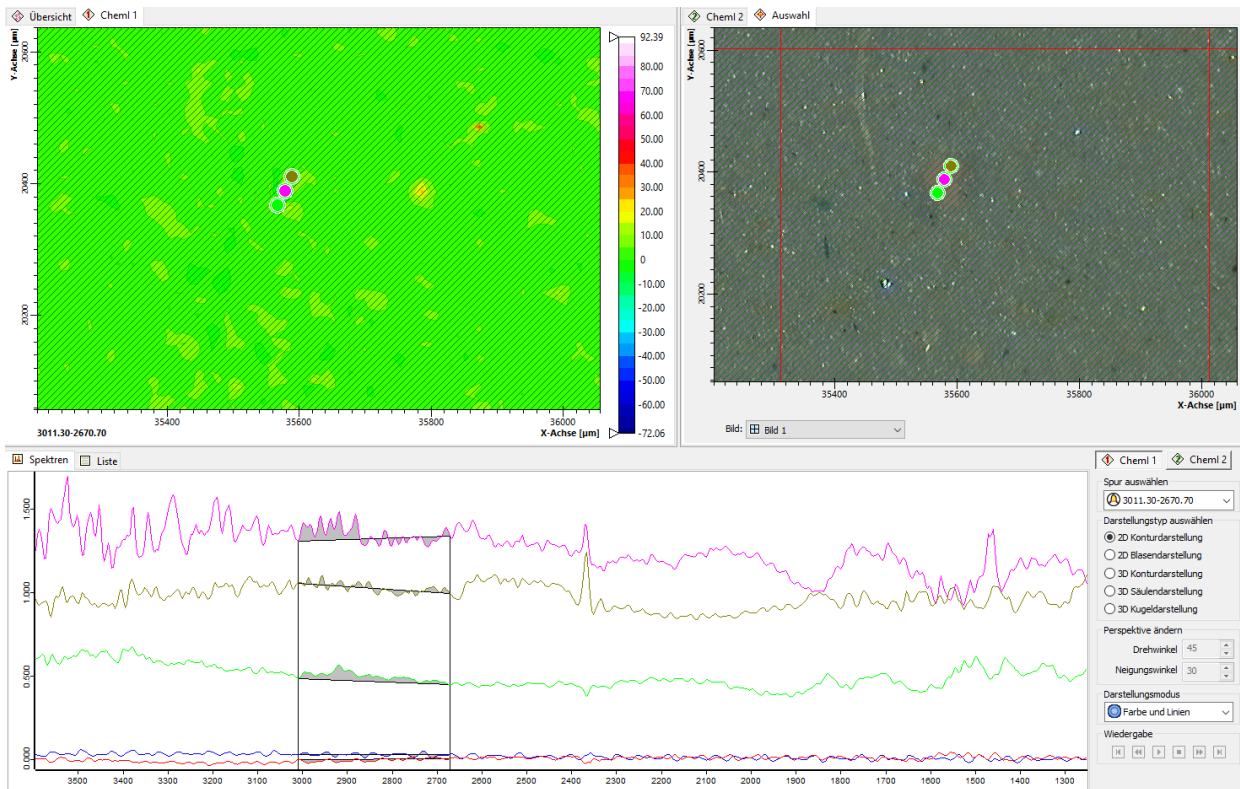


Figure\_5.2\_A. 11. Fluorescence microscopy images of PS. A: After staining only. B: After applying the workflow.



Figure\_5.2\_A. 12. Fluorescence microscopy images of PVC. A: After staining only. B: After applying the workflow protocol.

### 9.6.5. Examples of $\mu$ FTIR spectra



Figure\_5.2\_A. 13. Chemical image (upper left), visual image (upper right) and IR spectra (below) for a large fluorescent particle in a spiked sludge sample. No typical polymer band is present in green and yellow spectra due to high absorption while background is low (blue and red spectra).

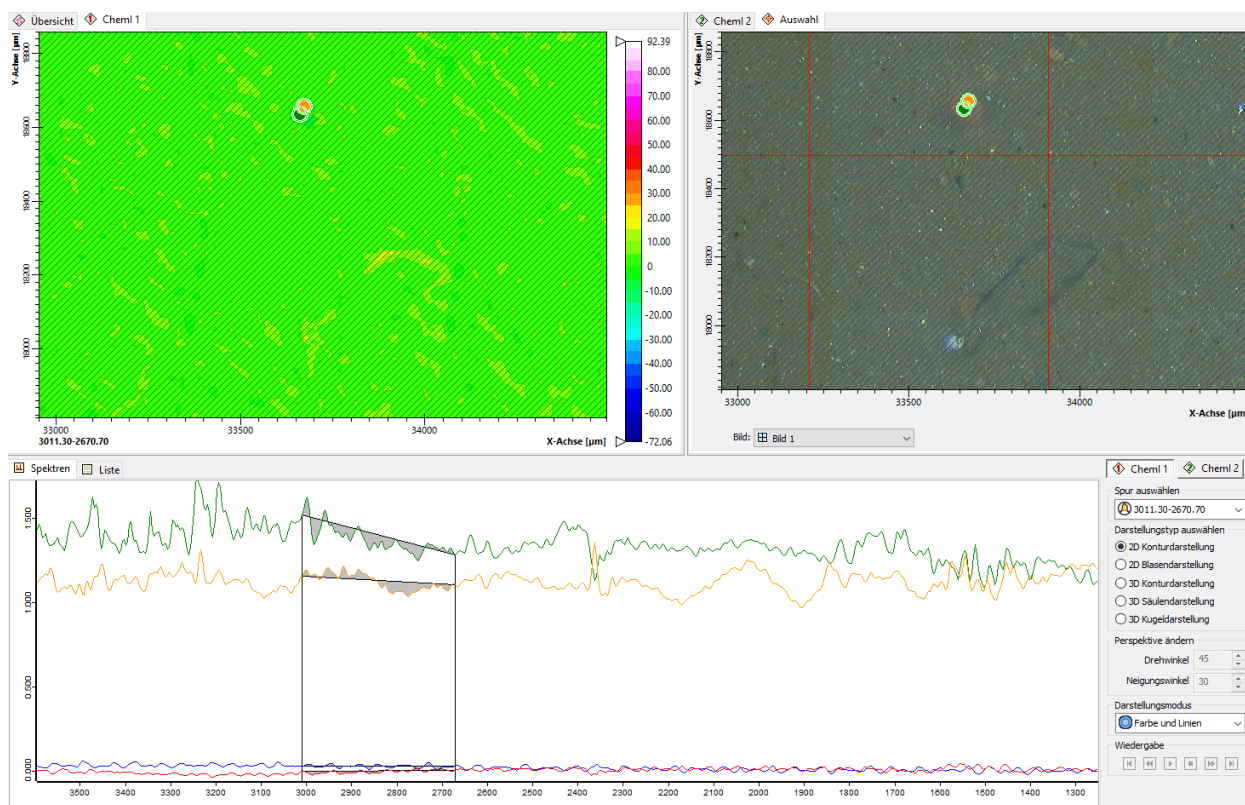
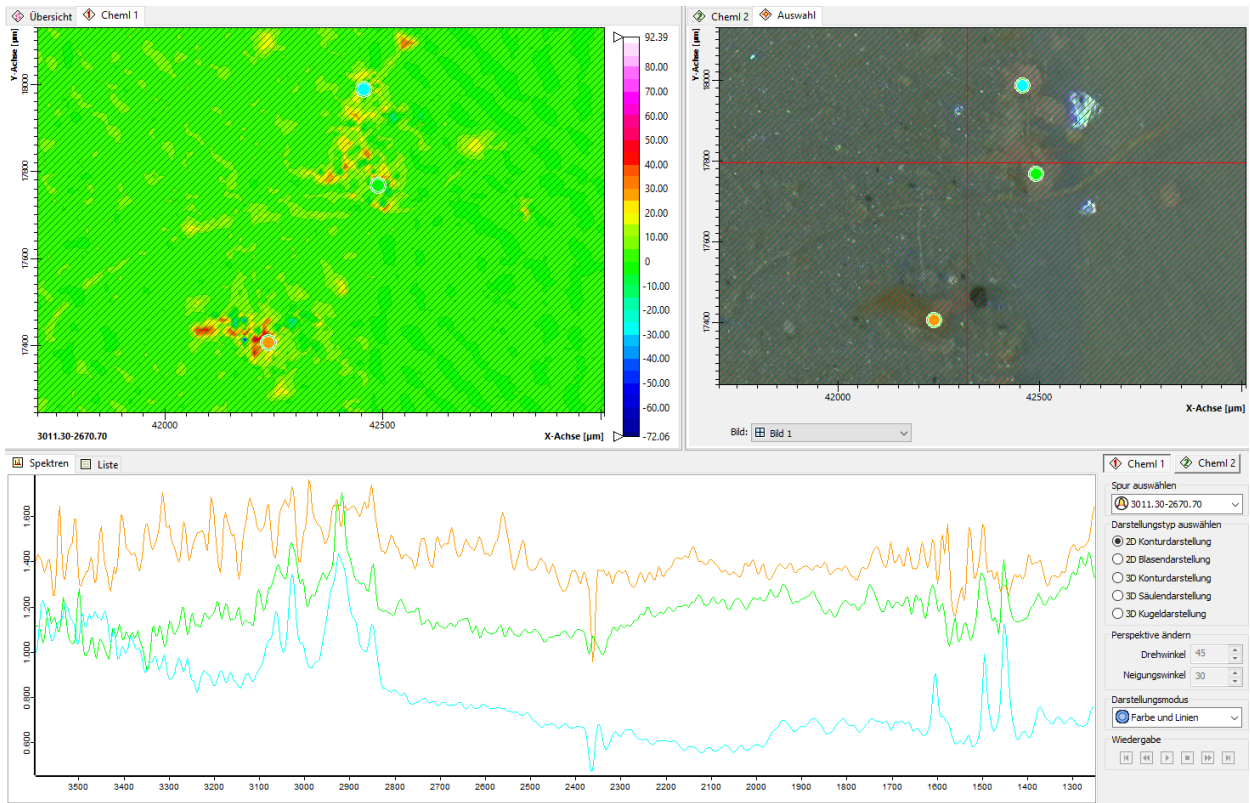
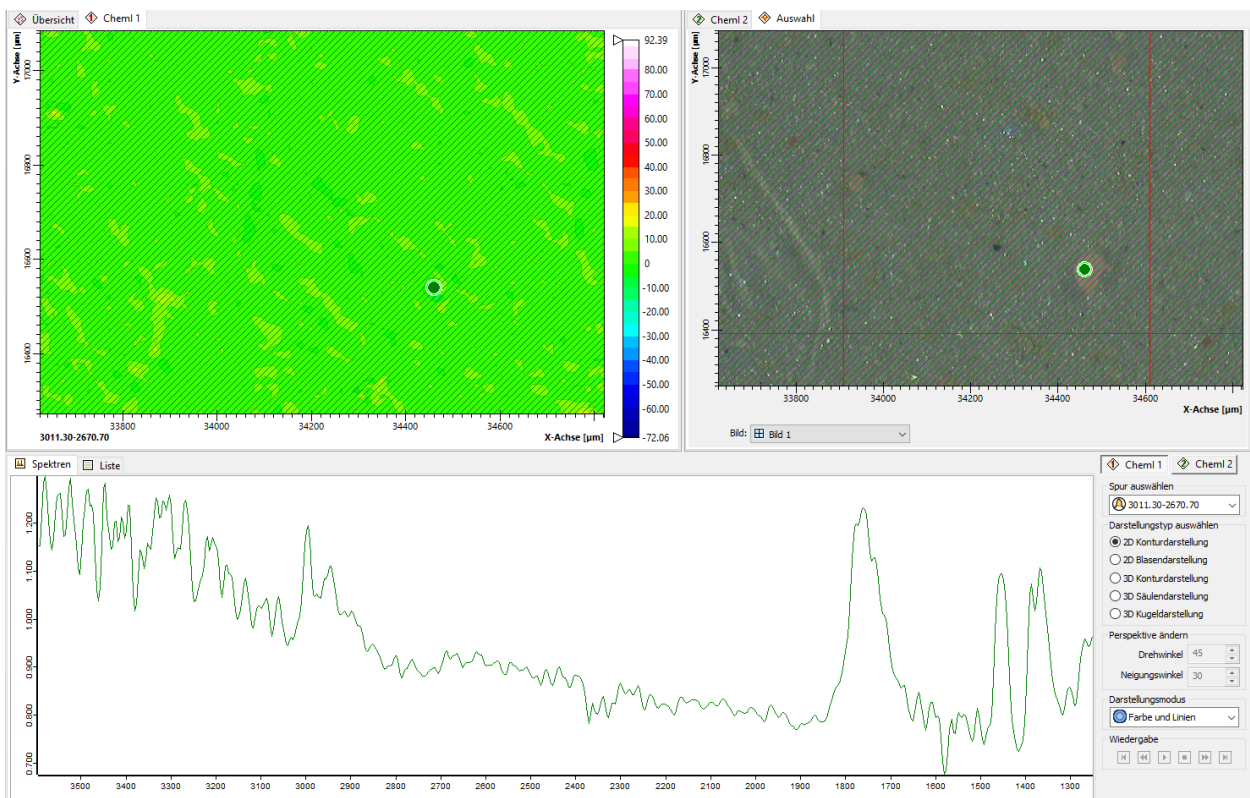


Figure 5.2\_A. 14. Chemical image (upper left), visual image (upper right) and IR spectra (below) for a large fluorescent particle in a spiked sludge sample. No typical polymer band is present in green and yellow spectra due to high absorption while background is low (blue and red spectra).





Figure\_5.2\_A. 15. Chemical image (upper left), visual image (upper right) and IR spectra (below) in a spiked sludge sample for two correctly identified fluorescent PS particles (turquoise and green spectra) as well as a non-identifiable fluorescent particle (orange spectrum).



*Figure\_5.2\_A. 16. Chemical image (upper left), visual image (upper right) and IR spectrum (below) in a spiked sludge sample for an unidentified fluorescent particle. The particle exhibits bands typical for acrylic type polymers, but the total spectrum doesn't allow clear identification of this particle.*